# Characterization of the limit performance in non-cooperative games with imperfect observation : application to 5G

Chao Zhang

université PARIS-SACLAY

CentraleSupélec

UNIVERSITÉ PARIS SUD
Comprendre le monde, construire l'avenir

NNT: 2017SACLS570

# Caractérisation des performances limites des jeux non-coopératifs avec observation imparfaite: application à la téléphonie mobile 5G

Thèse de doctorat de l'Université Paris-Saclay
préparée à l'Université Paris-Sud

École doctorale No. 580 : Sciences et technologie de l'information et de la communication
Spécialité de doctorat : Réseaux, information et communications

Thèse présentée et soutenue à Gif-sur-Yvette, le 21/12/2017, par

**Chao ZHANG**

Composition du Jury :

| | |
|---|---|
| Mérouane Debbah<br>Professeur, Huawei, Paris | Président |
| David Gesbert<br>Professeur, Eurecom, Sophia Antipolis | Rapporteur |
| Eduard Jorswieck<br>Professeur, Technische Universität Dresden | Rapporteur |
| Luca Sanguinetti<br>Professeur associé, Université de Pise | Examinateur |
| Yezekael Hayel<br>Professeur associé, Université d'Avignon | Examinateur |
| E. Veronica Belmega<br>Professeur associé, ENSEA, Cergy-pontoise, | Examinateur |
| Mylène Pischella<br>Professeur associé, CNAM, Paris | Examinateur |
| Samson Lasaulce<br>DR, CNRS, L2S, Gif-sur-Yvette | Directeur de thèse |

Thèse de doctorat

**Université Paris-Saclay**
Espace Technologique / Immeuble Discovery
Route de l'Orme aux Merisiers RD 128 / 91190 Saint-Aubin, France

# Acknowledgement

First and foremost, I would like to express my sincere gratitude to my advisor Prof. Samson Lasaulce for the continuous support of my Ph.D study and related research, for his patience, motivation, and immense knowledge. His guidance helped me in all the time of research and writing of this thesis. I could not have imagined having a better advisor and mentor for my Ph. D study.

Besides my advisor, I would like to express my deep gratitude to the reviewers Prof. David Gesbert and Prof. Eduard Jorswieck, and to the examiners Prof. Mérouane Debbah, Dr. Luca Sanguinetti, Dr. Yezekael Hayel, Dr. E. Veronica Belmega and Dr. Mylène Pischella, for their insightful comments and encouragement, but also for the hard questions which incented me to widen my research from various perspectives.

I would also like to thank the members of Samson's group. Two Indian brothers, Vineeth Varma and Achal Agrawal, thanks for their help to my research, especially for English writing, and also to be the support of video games. Two muslim friends, Sara Berri and Nizar Khalfet, I am very grateful for the numerous collaborations undertaken with them, and also keeping up the ambiance in the office. Two experts in smart grid, Olivier Beaude and Mauricio Gonzalez, who are models for me to follow in terms of efficiency and hard work.

My sincere thanks also goes to all my friends and colleagues from CentraleSupélec for various interesting discussions we had during the last three years : Maryvonne Giron, Frédéric Desprez, Céline Labrude, Laurence Antunes, Delphine Maucherat, Dr. Patrice Brault, Prof. Michel Kieffer, Dr. Benjamin Larrousse, Dr. Mircea Dumitru, Camille Chapdelaine, Amine Hadjyoucef, Alina Meresescu, Dr. Fangchen Feng, Guillaume Revillon, Dr. Faton Maliqi, Dr. Zicheng Liu, Yanqiao Hou, Chen Kang, Dr. Wenjie Li, Shanshan Wang, Jian Song, Xiaojun Xi, Xuewen Qian, Xiaoxia Zhang, Dr. Chi Jin, Weichao Liang, Zhenyu Liao, Peipei Ran, Paulo Prezotti, Sara Berri, Dr. Zheng Chen, Dr. Chao He.

I also deeply thank all my dearest Chinese friends, who have been together with me for already ten years : Dr. Kai Wan, Dr. Yunsong Wang, Dr. Siqi Wang, Yao Liu, Dr. Xin Wang, Nan Guan, Dr. Xiang Liu, Dr. Jie Wei, Mengsu Guo, . No matter where we are in the world I will always remember them forever and always.

Last, but not the least important, I devote this thesis to my family for their patience and understanding. My parents, Changhua Zhang and Hua Tan, I'm very grateful for their endless support, trust and love ! I would like to thank with love to my wife, Dr. Li Wang. Her support and encouragement is the key point to make this dissertation possible.

With regards to numerous questions about my future academic endeavors from friends and family, I shall answer in the words of Sir Winston Churchill : "Now this is not the

end. It is not even the beginning of the end. But it is, perhaps, the end of the beginning."

# Table des matières

# Table des figures

# Liste des tableaux

# 1

# Synthèse en francais

Une grande partie des résultats rapportés dans cette thèse est basée sur une observation qui n'a jamais été faite pour les communications sans fil et le contrôle de puissance en particulier : les niveaux de puissance d'émission et plus généralement les matrices de covariance peuvent être exploitées pour intégrer des informations de coordination. Les échantillons de rétroaction dépendants des interférences peuvent être exploités comme canal de communication. Premièrement, nous montrons que le fameux algorithme itératif de remplissage d'eau n'exploite pas suffisamment l'information disponible en termes d'utilité-somme. En effet, nous montrons que l'information globale d'état de canal peut être acquise à partir de la seule connaissance d'une rétroaction de type SINR. Une question naturelle se pose alors. Est-il possible de concevoir un algorithme de contrôle de puissance distribué qui exploite au mieux les informations disponibles ? Pour répondre à cette question, nous dérivons la caractérisation de la région d'utilité pour le problème considéré et montrons comment exploiter cette caractérisation non seulement pour mesurer globalement l'efficacité, mais aussi pour obtenir des fonctions de contrôle de puissance one-shot globalement efficaces. Motivés par le succès de notre approche sur les réseaux d'interférences mono bande et multibande, nous nous sommes demandé si elle pourrait être exploitée pour les réseaux MIMO. Nous avons identifié au moins un scénario très pertinent. En effet, nous montrons que l'alignement d'interférence opportuniste peut être implémenté en supposant seulement une rétroaction de covariance d'interférence plus bruit à l'émetteur secondaire. Puis, dans le dernier chapitre, nous généralisons le problème de la quantification, la motivation étant donnée par certaines observations faites dans les chapitres précédents. Premièrement, nous supposons que le quantificateur et le déquantificateur sont conçus pour maximiser une fonction d'utilité générale au lieu de la fonction de distorsion classique. Deuxièmement, nous supposons que le quantificateur et le déquantificateur peuvent avoir des fonctions d'utilité différentes. Cela soulève des problèmes techniques non triviaux, notre revendication est de faire un premier pas dans la résolution d'eux.

Dans le Chapitre 2, une nouvelle technique d'estimation est proposée qui permet à chaque émetteur d'acquérir des informations d'état de canal global (CSI) à partir de la

seule connaissance des mesures individuelles de puissance du signal reçu ; ceci rend inutiles les retours d'informations dédiés ou les canaux de signalisation inter-transmetteurs et permet une coordination dans les réglages typiques de contrôle de puissance distribuée. Pour ce faire, nous avons recours à une technique complètement nouvelle dont l'idée clé est d'exploiter les niveaux de puissance d'émission comme des symboles pour intégrer l'information et l'interférence observée comme canal de communication que les émetteurs peuvent exploiter pour échanger des informations de coordination. Selon que le niveau de puissance d'émission est supposé être **discrete** ou **continuous**, deux schémas de modulation de puissance différents sont proposés. Bien que les techniques utilisées permettent à **tout type d'information à faible débit** d'être échangées entre les émetteurs, l'accent est ici mis sur l'échange de CSI local. La technique proposée comprend également une phase qui permet d'estimer le CSI local. Une fois qu'une estimation du CSI global est acquise par les émetteurs, elle peut être utilisée pour optimiser toute fonction d'utilité qui en dépend. Alors que les algorithmes qui utilisent le même type de mesures comme l'algorithme de remplissage d'eau itératif (IWFA) implémentent la dynamique séquentielle de meilleure réponse (BRD) appliquée aux utilitaires individuels, ici, grâce à la disponibilité du CSI global, la BRD peut être , appliqué à l'utilitaire de somme. Lorsque l'on compare la technique proposée à l'IWFA, on constate que des gains significatifs peuvent être obtenus. Par exemple, la somme totale du réseau peut être améliorée de 20-30 % pour les scénarios typiques. Lorsqu'on compare la modulation de puissance discrète et continue (en supposant que les émetteurs peuvent fonctionner dans les deux modes de transmission), il semble que la première, bien que très simple, offre de meilleures performances à condition que le niveau de bruit de retour ne soit pas trop élevé. Il est intéressant de noter que, d'un point de vue technique, la technique d'estimation CSI globale proposée est même adaptée aux scénarios où seule une rétroaction ACK / NACK est disponible. En effet, il peut être vu comme le cas particulier où la puissance du signal reçu ou SINR est quantifiée avec un seul bit.

Le but du Chapitre 3 est de contribuer à la recherche de stratégies de contrôle du pouvoir qui exploitent au mieux les informations disponibles sur l'état global du canal ; les informations disponibles considérées ici pour les scénarios considérés sont principalement locales et peuvent être bruyantes. Différent de la technique proposée dans la dernière section, qui permet d'acquérir des informations d'état de canal globales en utilisant la modulation de puissance, un cadre de contrôle de puissance basé sur des informations locales est proposé ici. Comme une façon appropriée de mesurer l'efficacité globale d'un schéma de contrôle de puissance est d'utiliser la région d'utilité moyenne, nous abordons d'abord le problème de la caractérisation de la région d'utilité réalisable. Nous fournissons la caractérisation de la région d'utilité moyenne pour tout problème de contrôle de puissance pour lequel l'état du canal est i.i.d. et la structure d'observation est sans mémoire. Deuxièmement, le théorème correspondant est exploité pour obtenir un algorithme itératif qui fournit des stratégies de contrôle de puissance sans mémoire et stationnaires (les stratégies se résument donc à des fonctions de décision **one-shot**). Bien que l'algorithme proposé ne soit pas optimal en termes d'utilité-somme pondérée, de nombreuses simulations montrent qu'il fonctionne très bien pour des fonctions d'utilité classiques (par exemple, l'énergie-efficacité totale, la somme-débit, la somme-bénéfice). En plus des politiques de **team power control**, nous proposons également un système de contrôle de puissance égoïste. En effet nous étudions un réseau d'interférences multi-bandes en présence de multiples fonctions utilitaires. L'une des idées clés que nous avons trouvées est que restreindre les choix en termes de vecteurs d'allocation de puissance au-

torisés pour les émetteurs peut être bénéfique pour la performance individuelle et celle du réseau, ce qui prouve un paradoxe de Braess. Ce résultat justifie a posteriori que l'utilisation d'espaces d'action discrets au lieu d'espaces d'action continue peut être un meilleur choix pour la performance. Cela justifie également en partie pourquoi l'algorithme itératif que nous proposons pour calculer les fonctions de décision en une seule fois suppose des ensembles d'actions discrètes. Cet argument vient s'ajouter à d'autres arguments donnés dans des travaux précédents tels que le contrôle de puissance binaire qui montre que l'utilisation de petits alphabets pourrait induire une perte d'optimalité nulle ou faible par rapport aux alphabets continus.

Au chapitre 4, nous montrons comment les mesures du domaine de puissance peuvent être exploitées pour deux techniques bien connues de traitement de domaine de signal, à savoir l'alignement d'interférence opportuniste et l'estimation de canal de domaine de signal basé sur la formation. En ce qui concerne l'alignement des interférences, nous considérons la version opportuniste proposée dans [9]. Dans [9], les auteurs supposent que l'émetteur primaire choisit sa matrice de précodage pour maximiser son débit de transmission individuel tandis que l'émetteur secondaire exploite les opportunités spatiales disponibles. Pour cela, l'émetteur secondaire aligne son signal pour garantir une interférence nulle au niveau du récepteur primaire et a besoin d'informations d'état de canal global (CSI). Un problème de problème crucial avec cette technique est que les auteurs n'ont fourni aucune technique pour acquérir les informations requises sur les différents canaux, sachant que les auteurs recommandent que les CSI globaux soient disponibles. Dans ce chapitre, nous montrons que le CSI global n'est pas requis pour implémenter l'alignement d'interférence opportuniste de [9]. En effet, nous prouvons que la seule connaissance de la rétroaction de la matrice de covariance interférence-bruit à l'émetteur secondaire est suffisante pour mettre en œuvre la technique considérée ; cette hypothèse a été faite, par exemple, pour dériver la version MIMO de l'algorithme itératif de remplissage d'eau [15]. En ce qui concerne l'estimation des canaux basés sur la formation, nous montrons que les mesures de puissance reçues peuvent être utilisées comme priors pour améliorer significativement le niveau de précision de l'estimation des canaux. Plus précisément, nous proposons de nouveaux estimateurs MMSE et MAP qui intègrent ces connaissances antérieures. L'erreur quadratique moyenne d'estimation peut être diminuée d'environ 50 % dans des scénarios typiques en termes de SNR et même en supposant un nombre relativement petit de mesures de puissance reçues.

Dans la première partie du chapitre 5, nous revenons sur le problème de la quantification en considérant un choix arbitraire pour la fonction d'utilité au lieu du critère de performance classique, à savoir la distorsion ou l'erreur quadratique moyenne. Cette manière nouvelle et générale d'aborder le problème de quantification est pertinente, par exemple, pour des scénarios où le récepteur doit quantifier des informations d'état de canal (CSI) et signaler cette version imparfaite du canal à l'émetteur qui doit maximiser une certaine fonction utilitaire. L'opération de maximisation correspondante est nécessairement sous-optimale car la connaissance parfaite du canal n'est pas disponible à l'émetteur, d'où notre motivation à rendre la perte d'optimalité correspondante aussi faible que possible. Implicitement, nous supposons que le quantificateur et le déquantificateur ont le même objectif, c'est-à-dire maximiser la fonction d'utilité considérée. Les simulations montrent que l'utilisation du quantificateur orienté utilitaires permet de réduire la perte d'optimalité globale de 5% au lieu de 40% en utilisant l'algorithme classique de Lloyd-Max. Dans la deuxième partie du chapitre 5, nous supposons que l'émetteur et le récepteur

ont des fonctions d'utilité non alignées, c'est-à-dire que leur intérêt peut être divergent. Dans les simulations, nous montrons l'influence du biais en termes d'utilités sur la performance d'équilibre de l'émetteur et du récepteur. Nous avons identifié un scénario de communication qui apparaît dans le domaine des réseaux intelligents pour lequel ce cadre est pleinement pertinent. Lorsqu'un consommateur doit révéler des informations sur ses besoins en termes d'énergie, son intérêt peut être différent de celui de l'agrégateur, du fournisseur d'énergie ou de l'opérateur. Par exemple, le consommateur peut vouloir satisfaire complètement son besoin énergétique alors que l'opérateur peut aussi vouloir gérer le réseau électrique ou prendre en compte certaines contraintes liées au niveau de production d'énergie. Cela engendre un biais en termes de fonctions d'utilité et constitue donc un scénario de communication en présence d'intérêts divergents. Pour de tels scénarios, nous fournissons quelques résultats préliminaires pour comprendre l'impact du biais sur la communication. Certes, beaucoup d'efforts doivent être faits pour comprendre ce scénario de communication délicat mais nos résultats constituent un premier pas vers cet objectif difficile.

# 2 Introduction

In this thesis, we mainly investigate resource allocation problems in distributed interference networks in which the transmitting-receiving pair can communicate over several orthogonal channels. Apart from that, we study quantizations scheme with the objective of maximizing a common utility function, or diverging utility functions.

## 2.1 Context of the thesis

Wireless networks in which transmitters have to take decisions on how to use radio resources in an autonomous manner is of increasing interest to the communications community. We will refer to this type of wireless networks as distributed or decentralized wireless networks. An example of such a network is given by small cell networks (SCNs) [1]. Indeed, one way of boosting data rates in cellular networks is to deploy a large number of small base stations that cannot be controlled by a single central entity, and therefore have to be nearly autonomous in terms of managing radio resources. Another important example of such networks is WiFi networks in which each access point has to select the operating channel, or band without the assistance of a central entity. In this manuscript, we consider wireless interference networks that are distributed both decision-wise and information-wise. More specifically, each transmitter has to perform a power control or resource allocation task by itself, having only access to partial information of the network state.

When inspecting the literature on distributed power control (see e.g., [2][3]), one can conclude that while the derived power control scheme is effectively distributed decision-wise and information-wise, it is not globally efficient. A natural and important question arises : are such schemes inefficient because the considered power control schemes are not good enough, or does it stem from intrinsic limitations such as information availability ? To the best of our knowledge, this question has not been addressed formally. In this manuscript, we will propose two different novel approaches to tackle this issue.

The first way is to exploit the available feedback signal to implement coordination. In most of the literature on coordination among autonomous decision-makers, like team decision problems (see e.g., [4]), the typical assumption is that decision-makers have access to dedicated channels to coordinate their actions. These dedicated channels allow the decision-makers to signal or communicate with each other without affecting the objective or utility function [5]. Typically, in an interference network, when there is no direct line of communication between the transmitters ; the transmitters use a distributed or selfish strategy, e.g. the iterative water-filling algorithm (IWFA)[6][7], and work at a sub-optimal level of performance. One important message of the work is to show that IWFA-like distributed algorithms do not exploit the available feedback signal efficiently. In the exploration phase, instead of using several time-slots (and their associated signal to interference plus noise ratio (SINR) realizations) to allow the transmitters to converge to a Nash point, the feedback signal realizations can be used to acquire global channel state information (CSI). The merit of the proposed technique is the potential to cope with the global inefficiency issue. The key ideas of the first approach is that information feedback, such as an SINR feedback or received signal strength indicator (RSSI) feedback, can be used both to estimate local CSI and to exchange it through an appropriate power modulation scheme.

However, in some wireless networks, reconstructing the global CSI can be prohibitive due to a lack of a suitable feedback channel. This motivates us to develop our second approach in which, we provide a framework that allows one to derive the limiting performance of power control with partial information, and therefore allowing us to measure the efficiency of a given power control scheme. One of the key ideas of the second approach is to exploit the recent theorem derived in [8] to find power control functions which may exploit the available knowledge optimally. We exploit these results to characterize the limiting performance in terms of long-term utility region. When it is difficult to exchange local CSI, it is shown in Chapter 3 that the statistics of the global CSI can still be useful in order to bring improvements to the network performance.

Aside from the power control strategy in interference networks, we also investigate the connections between the power domain feedback and signal domain operations, e.g., the interference alignment and channel estimation. We study the way to exploit the power domain feedback in Cognitive multiple-input and multiple-output (MIMO) networks and interference networks. Cognitive networks are initiated by the apparent lack of spectrum under the current spectrum management policies, which aims at allocating the spectrum in a dynamic manner. To avoid the secondary users inducing any significant degradation of the quality of service (QoS), interference alignment (IA) has been recently developed. The technique of IA for cognitive networks was extended for the case of MIMO in [9]. However, limited by the information availability, the opportunistic IA scheme is difficult to be realized. In this work, it is shown that even with partial information, the IA scheme can be reconstructed by exploiting the power domain feedback, namely, the covariance matrix of the received signal. Moreover, it can be also verified that the power domain feedback in a single antenna system, namely received signal strength indicator (RSSI), can improve the estimation accuracy level in interference networks. In the context of interference networks, a precise estimation of the channel can be acquired by sending pilot symbols and estimating the channel with the minimum mean square error (MMSE) estimator [10][11]. Interestingly, with the additional information RSSI feedback, the estimation accuracy level can be still enhanced without any degradation of the network performance.

Finally, a part of the manuscript focuses on quantization schemes. There are a variety

of existing quantizers, e.g., the uniform quantizer or the well-known quantizer based on the Lloyd-Max algorithm (LMA) [12][13] to minimize the distortion, i.e., the mean square error between the source and its reconstructed version. However, note that these designs consider the quantized variable (such as channel gains) itself instead of considering the use of the quantized variable (such as energy efficiency which depends on the channel gains). It turns out that the quantizer design might be improved when measured in terms of the final use of utility function. In Chapter 5, we investigate the utility-oriented quantization in two different scenarios : the utility functions are aligned and its application to power control in wireless communications and, the utility functions are non-aligned and its application to smart grid.

## 2.2 Contributions

The contribution of this manuscript can be summarized based on five main aspects : 1) global CSI acquisition by exploiting power domain feedback without interrupting the regular communication ; 2) provide a framework to derive the expected utility region of power control with partial information and therefore to be able to measure the efficiency of a given power control scheme ; 3) reconstruct the interference alignment scheme with partial information by exploiting the power domain feedback, namely covariance matrix of the received signal ; 4) propose a novel MMSE and maximum a posteriori (MAP) estimate in interference networks when RSSI feedbacks are available at transmitters ; 5) design a novel quantization scheme aiming at minimizing the optimality loss in terms of the utility functions.

We propose a novel technique to estimate local CSI and exchange local CSI in Chapter 2. The main contributions of Chapter 2 are as follows :
▶ We introduce the important and novel idea of communication in the power domain, i.e., encoding the message on the transmit power instead of the signal, and decoding by observing the received signal strength or SINR. We study scenarios with both continuous power levels and discrete power levels. Two different approaches are proposed in this chapter. Both can be used in general to **exchange any kind of low-rate information** and not only CSI.
▶ This allows interfering transmitters to exchange information **without requiring the presence of dedicated signaling channels** (like direct inter-transmitter communication), which may be unavailable in real systems (e.g., in conventional Wifi systems or heterogeneous networks).
▶ Normal (say high-rate) communication can be done even during the proposed learning phase with a sub-optimal power control, i.e., communication during the learning time in the proposed scheme is similar to communication in the convergence time for algorithms like IWFA.
▶ We propose a way to both learn and exchange the local CSI. Global CSI is acquired at every transmitter by observing the RSSI feedback.
▶ The proposed technique accounts for the presence of various noise sources which are non-standard and affect the RSSI measurements (the corresponding modeling is provided in Sec. II). In contrast, apart from a very small fraction of works (such as [7][22][23]), IWFA-like algorithms assume noiseless measurements.
▶ We conduct a detailed performance analysis to assess the benefits of the proposed

approach for the exploitation phase, which aims at optimizing the sum-rate or sum-energy-efficiency. As (imperfect) global CSI is available, globally efficient solutions become attainable.

In Chapter 3, we provide a framework to find power control strategy by exploiting all the available information (e.g. local CSI realization and global CSI statistic). The main contributions of Chapter 3 are as follows :
▶ We propose a framework to derive the limiting performance of power control with partial information.
▶ We exploit the results obtained in [8] to characterize the limiting performance in terms of long-term utility region.
▶ The auxiliary variable is presented to define the Pareto frontier of the long-term utility region and can be helpful to enlarge the utility region when there exist some constraints. The cardinality of the auxiliary variable can be upper bounded.
▶ When considering the selfish spectrally efficient power allocation, we provide some conditions, under which allowing individual rate-maximizing transmitters to spread their power over the entire spectrum, as opposed to using a single band, may result in sum-rate performance losses.

In chapter 4, we further explore how power domain feedback can be exploited to enhance signal domain operations. We have discovered two relevant situations and techniques that achieve this, which are summarized as follows :
▶ In MIMO cognitive networks, it is shown that the interference alignment scheme proposed by [9] can be reconstructed without knowing the global CSI by exploiting the covariance matrix of the received signal.
▶ By exploiting the RSSI, a novel MMSE estimate is proposed and is proved to outperform the classical MMSE in terms of the distortion.
▶ By exploiting the RSSI, a novel MAP estimate is proposed. In contrast with classical MAP, it can be shown by simulations that the novel MAP reduces the distortion when the SNR is not low.

We propose different quantization schemes when the two agents have aligned utility functions or non-aligned utility functions in Chapter 5. The main contributions of Chapter 5 are as follows :
▶ Instead of considering the distortion or minimum mean square error to design the quantizer, the final use (utility) of the quantized parameters is considered.
▶ The benefit from implementing the proposed utility-oriented quantization approach is illustrated with the problem of energy-efficient and spectrally efficient power control problem.
▶ In smart grid networks, when the consumer and the aggregator have non-aligned utility functions, we propose an algorithm to obtain the novel quantization scheme and provide several sufficient conditions for the convergence of the algorithm.

## 2.3 Publications during Ph.D

### Journal Papers :

- **C. Zhang**, V. Varma, S. Lasaulce, and R. Visoz, "Interference coordination via power domain channel estimation", IEEE Transactions on Wireless Communications, Vol. 16, No. 10, Oct. 2017.
- **C. Zhang**, S. Lasaulce, and V. Varma, "Using continuous power modulation for exchanging local channel state information", IEEE Communications Letters, Vol. 21, No. 5, pp. 1187-1190, Jan. 2017.
- **C. Zhang**, A. Agrawal, S. Lasaulce, and R. Visoz, "A framework for distributed power control with partial channel state information", IEEE Transactions on Wireless Communications, submitted.
- **C. Zhang**, S. Berri, S. Lasaulce, "Implementing opportunistic interference alignment in MIMO cognitive networks with partial channel state information", IEEE Signal Processing Letters, submitted.
- **C. Zhang**, V. Varma, S. Lasaulce, "Improving channel estimation via power domain feedback", IEEE Communication Letters, submitted.
- O. Beaude, **C. Zhang**, B. Larrousse, and S. Lasaulce, "Strategic communications in smart grids", IEEE Transactions on Signal Processing, to be submitted.

### Conference Papers :

- **C. Zhang**, S. Lasaulce, and E. V. Belmega, "Using more channels can be detrimental to the global performance in interference networks", IEEE International Conference on Communications (ICC), London, UK, June 2015.
- V. Varma, S. Lasaulce, **C. Zhang**, and R. Visoz, "Power Modulation : Application to Inter-Cell Interference Coordination", IEEE Proc. of the EUSIPCO conference, Nice, France, Aug.-Sep. 2015, invited paper.
- **C. Zhang**, V. Varma, and S. Lasaulce, "Robust power modulation for channel state information exchange", Springer Proc. of the 9th International Conference on NETwork Games, COntrol and OPtimization (NETGCOOP), Avignon, France, Nov. 2016, invited paper.
- **C. Zhang**, N. Khalfet, S. Lasaulce, V. Varma, and S. Tarbouriech, "Payoff-oriented quantization and application to power control", 15th IEEE International Symposium on Modeling and Optimization in Mobile, Ad Hoc, and Wireless Networks (WiOpt), Paris, France, 2017.
- **C. Zhang**, S. Berri, S. Lasaulce, V. Varma, and S. Tarbouriech, "Quantification orientée objectif et application au contrêle de puissance", Gretsi conference, Juan-les-Pins, France, Sep. 2017.

# 3

# Interference Coordination via Power Domain Channel Estimation

In this chapter, a novel estimation technique is proposed which enables each transmitter to acquire global channel state information (CSI) from the sole knowledge of individual received signal power measurements; this makes dedicated feedback or inter-transmitter signaling channels unnecessary and enables coordination in typical distributed power control settings. To make this possible, we resort to a completely new technique whose key idea is to exploit the transmit power levels as symbols to embed information and the observed interference as a communication channel the transmitters can exploit to exchange coordination information. Depending on whether the transmit power level is assumed to be **discrete** or **continuous**, two different power modulation schemes are proposed. Although the used techniques allow **any kind of low-rate information** to be exchanged among the transmitters, the focus here is to exchange local CSI. The proposed technique also comprises a phase which allows local CSI to be estimated. Once an estimate of global CSI is acquired by the transmitters, it can be used to optimize any utility function which depends on it. While algorithms which use the same type of measurements such as the iterative water-filling algorithm (IWFA) implement the sequential best-response dynamics (BRD) applied to individual utilities, here, thanks to the availability of global CSI, the BRD can be e.g., applied to the sum-utility. When comparing the proposed technique to IWFA, it is seen that significant gains can be obtained. For instance, the network sum-rate can be improved by 20-30% for typical scenarios. When comparing discrete and continuous power modulation (by assuming that the transmitters can operate in both transmission modes), it appears that the former, although very simple, provides better performance provided that the feedback noise level is not too high. Interestingly, from the technical aspect, the proposed global CSI estimation technique is even suitable to scenarios where only an ACK/NACK feedback is available. Indeed, it can be seen as the special case where the received signal power or SINR is quantized with a single bit.

| Acronym | Meaning | Definition |
|---|---|---|
| ALMA | advanced Lloyd-Max algorithm | (3.20),(3.21) |
| CPM | continuous power modulation | |
| CSI | channel state information | |
| DPM | discrete power modulation | |
| EE | energy-efficiency | |
| ESNR | estimation signal-to-noise ratio | (3.35) |
| ISD | inter site distance | |
| IWFA | iterative water-filling algorithm | [6] |
| LMA | conventional Lloyd-Max algorithm | [12][13] |
| LSPD | least squares estimator in power domain | (3.5) |
| MEQ | maximum entropy quantizer | (4.55),(4.56) |
| MMSEPD | minimum mean square error estimator in power domain | (3.12) |
| MS | mobile station | |
| SBS | small base station | |
| Team BRD | team best response dynamics | (3.34),(3.37) |

TABLE 3.1 – Acronyms used in Chapter 3

## 3.1 Motivation and state of the art

Interference networks are wireless networks which are largely distributed decision-wise or information-wise. In the case of distributed power allocation over interference networks with multiple bands, the iterative water-filling algorithm (IWFA) is considered to be one of the well-known state-of-the art distributed techniques [6][7][15]. IWFA-like distributed algorithms have at least two attractive features : they only rely on local knowledge e.g., the individual signal-to-interference plus noise ratio (SINR), making them distributed information-wise ; the involved computational complexity is typically low. On the other hand, one drawback of IWFA and many other distributed iterative and learning algorithms (see e.g., [16][17]) is that convergence is not always ensured [7] and, when converging, it leads to a Nash point which is globally inefficient.

One of the key messages of the chapter is to show that it is possible to exploit the available feedback signal more efficiently than IWFA-like distributed algorithms do. In the exploration phase [1], instead of using local observations (namely, the individual feedback) to allow the transmitters to converge to a Nash point, one can use them to acquire global channel state information (CSI). This allows coordination to be implemented, and

1. IWFA operates over a period which is less than the channel coherence time and it does so in two steps : an exploration phase during which the transmitters update in a round robin manner their power allocation vector ; an exploitation phase during which the transmitters keep their power vector constant at the values obtained at the end of the exploration phase. As for IWFA, unless mentioned otherwise, we will assume the number of time-slots of the exploitation phase to be much larger than that of the exploration phase, making the impact of the exploration phase on the average performance negligible.

more precisely global performance criteria or network utility to be optimized during the exploitation phase. As for complexity, it has to be managed by a proper choice of the network utility function which has to be maximized.

To obtain global CSI, one of the key ideas of this work is to exploit the transmit power levels as information symbols and to exploit the interference observed to decode these information symbols. In the literature of power control and resource allocation, there exist papers where the observation of interference is exploited to optimize a given performance criterion. In this respect, an excellent monograph on power control is [2]. Very relevant references include [18] and [19]. In [18], optimal power control for a reversed network (receivers can transmit) is designed, in which the receiver uses the interference to estimate the cross channel, assuming perfect exchange of information between the transmitters. In [19], the authors estimate local CSI from the received signal but in the signal domain and in a centralized setting. To the best of the authors' knowledge, there is no paper where the interference measurement is exploited as a communication channel the transmitters can utilize to exchange information or local CSI (namely, the channel gains of the links which arrive to a given receiver), as is the case under investigation. In fact, we provide a complete estimation procedure which relies on the sole knowledge of the individual received signal strength indicator (RSSI). The proposed approach is somewhat related to the Shannon-theoretic work on coordination available in [20][21], which concerns two-user interference channels when one master transmitter knows the future realizations of the global channel state.

It is essential to insist on the fact that the purpose of the proposed estimation scheme is not to compete with conventional estimation schemes such as [11] (which are performed in the signal-domain), but rather, to evaluate the performance of an estimation scheme that solely relies on information available in the power-domain. Indeed, one of the key results of the chapter is to prove that global CSI (without phase information) can be acquired from the **sole** knowledge of a **given** feedback which is the SINR or RSSI feedback. The purpose of such a feedback is generally to adjust the power control vector or matrix but, to our knowledge, it has not been shown that it also allows global CSI to be recovered, and additionally, at every transmitter. This sharply contrasts with conventional channel estimation techniques which operate in the **signal** domain and use a **dedicated** channel for estimation.

## 3.2 Problem statement and proposed technique general description

**Channel and communication model** : The system under consideration comprises $K \geq 2$ pairs of interfering transmitters and receivers ; each transmitter-receiver pair will be referred to as a user. Our technique directly applies to the multi-band case, and this has been done in the numerical section. In particular, we assess the performance gain which can be obtained with respect to the IWFA. However, for the sake of clarity and ease of exposition, we focus on the single-band case, and explain in the end of Sec. IV, the modifications required to treat the multi-band case. From this point on, we will therefore assume the single-band case unless otherwise stated.

In the setup under study, the quantities of interest for a transmitter to control its

| Main notations | |
|---|---|
| **Symbol** | **Meaning** |
| $g_{ji}$ | Channel gain from Transmitter $j$ to Receiver $i$ |
| $\widetilde{g}_{ji}$ | Estimate of $g_{ji}$ available at Transmitter $i$ |
| $\widetilde{g}_{ji}^{k}$ | Estimate of $g_{ji}$ available at Transmitter $k \neq i$ |
| $\underline{g}_{i} = (g_{1i}, ..., g_{Ki})^{\mathrm{T}}$ | Local CSI for Receiver $i$ |
| $\underline{\widetilde{g}}_{j}^{i} = (\widetilde{g}_{1j}^{i}, ..., \widetilde{g}_{Kj}^{i})^{\mathrm{T}}$ | Estimate of the local CSI of Receiver $j$ available at Transmitter $i$ |
| $\mathbf{G}$ | Global channel matrix |
| $\widetilde{\mathbf{G}}^{k}$ | Estimate of $\mathbf{G}$ available at Transmitter $k$ |
| $\omega_i(t)$ | The received signal power at Receiver $i$ on time-slot t |
| $\widetilde{\omega}_i(t)$ | The observed received signal power at Transmitter $i$ on time-slot t |
| $\widetilde{\omega}_i^j(t)$ | The observed received signal power at Transmitter $i$ on time-slot t when Transmitter $j$ is active |

TABLE 3.2 – Main notations of Chapter 2

power are given by the channel gains. The channel gain of the link between Transmitter $i \in \{1, ..., K\}$ and Receiver $j \in \{1, ..., K\}$ is denoted by $g_{ij} = |h_{ij}|^2$ (See Table I), where $h_{ij}$ may typically be the realization of a complex Gaussian random variable, if Rayleigh fading is considered. In several places in this chapter we will use the $K \times K$ *channel matrix* $\mathbf{G}$ whose entries are given by the channel gains $g_{ij}$, $i$ and $j$ respectively representing the row and column indices of $\mathbf{G}$. Each channel gain is assumed to obey a classical block-fading variation law. More precisely, channel gains are assumed to be constant over each transmitted data frame. A *frame* comprises $T_{\mathrm{I}}+T_{\mathrm{II}}+T_{\mathrm{III}}$ consecutive time-slots where $T_m \in \mathbb{N}$, $m \in \{\mathrm{I}, \mathrm{II}, \mathrm{III}\}$, corresponds to the number of time-slots of Phase $m$ of the proposed procedure ; these phases are described further. Transmitter $i$, $i \in \{1, ..., K\}$, can update its power from time-slot to time-slot. The corresponding power level is denoted by $p_i$ and is assumed to be subject to power limitation as : $0 \leq p_i \leq P_{\max}$. The $K-$dimensional column vector formed by the transmit power levels will be denoted by $\underline{p} = (p_1, ..., p_K)^{\mathrm{T}}$, T standing for the transpose operator.

**Feedback signal model** : We assume the existence of a feedback mechanism which provides each transmitter, an image or noisy version of the power received at its intended receiver for each time-slot. The power at Receiver $i$ on time-slot $t$ is expressed as

$$\omega_i(t) = g_{ii}p_i(t) + \sigma^2 + \sum_{j \neq i} g_{ji}p_j(t). \tag{3.1}$$

where $\sigma^2$ is the receive noise variance and $p_i(t)$ the power of Transmitter $i$ on time-slot $t$. We assume that the following procedure is followed by the transmitter-receiver pair. Receiver $i$ : measures the received signal (RS) power $\omega_i(t)$ at each time slot and quantizes it with $N$ bits (the *RS power quantizer* is denoted by $\mathcal{Q}_{\mathrm{RS}}$) ; sends the quantized RS power $\widehat{\omega}_i(t)$ as feedback to Transmitter $i$ through a noisy feedback channel. After quantization, we assume that for all $i \in \{1, ..., K\}$, $\widehat{\omega}_i(t) \in W$, where $W = \{\mathrm{w}_1, \mathrm{w}_2, \ldots, \mathrm{w}_M\}$ such that $0 \leq \mathrm{w}_1 < \mathrm{w}_2 < \cdots < \mathrm{w}_M$ and $M = 2^N$. Transmission over the feedback channel and the dequantization operation are represented by a discrete memoryless channel (DMC) whose

*conditional probability* is denoted by $\Gamma$. The distorted and noisy version [2] of $\omega_i(t)$, which is available at Transmitter $i$, is denoted by $\widetilde{\omega}_i(t) \in W$ ; the quantity $\widetilde{\omega}_i(t)$ will be referred to as the *received signal strength indicator (RSSI)*. With these notations, the probability that Transmitter $i$ decodes the symbol $\mathrm{w}_\ell$ given that Receiver $i$ sent the quantized RS power $\mathrm{w}_k$ equals $\Gamma(\mathrm{w}_\ell|\mathrm{w}_k)$.

In contrast with the vast majority of works on power control and especially those related to the IWFA, we assume the feedback channel to be noisy. Note also that these papers typically assume SINR feedback whereas the RSSI is considered here. The reasons for this is fourfold : 1) if Transmitter $i$ knows $p_i(t)$, $g_{ii}(t)$, and has SINR feedback, this amounts to knowing its RS power since $\omega_i(t) = g_{ii}p_i(t)\left(1+\frac{1}{\mathrm{SINR}_i(t)}\right)$ where

$$\mathrm{SINR}_i(t) = \frac{g_{ii}p_i(t)}{\sigma^2 + \sum_{j\neq i} g_{ji}p_j(t)}; \tag{3.2}$$

2) Assuming an RS power feedback is very relevant in practice since some existing wireless systems exploit the RSSI feedback signal (see e.g., [24]) ; 3) The SINR is subject to higher fluctuations than the RS power, which makes SINR feedback less robust to distortion and noise effects and overall less reliable ; 4) As a crucial technical point, it can be checked that using the SINR as the transmitter observation leads to complex estimators [25], while the case of RS power observations leads to a simple and very efficient estimation procedure, as shown further in this chapter.

Note that, here, it is assumed that the RS power is quantized and then transmitted through a DMC, which is a reasonable and common model for wireless communications. Another possible model for the feedback might consist in assuming that the receiver sends directly received signal power over an AWGN channel ; depending on how the feedback channel gain fluctuations may be accounted for, the latter model might be more relevant and would deserve to be explored as well ($\star$).

**Proposed technique general description** : The general power control problem of interest consists in finding, for each realization of the channel gain matrix $\mathbf{G}$, a power vector which maximizes a network utility of the form $u(\underline{p};\mathbf{G})$. For this purpose, each transmitter is assumed to have access to the realizations of its RSSI over a frame. One of the key ideas of this work is to exploit the transmit power levels as information symbols and exploit the observed interference (which is observed through the RSSI or SINR feedback) for inter-transmitter communication. The corresponding implicit communication channel is exploited to acquire global CSI knowledge namely, the matrix $\mathbf{G}$ and therefore to perform operations such as the maximization of $u(\underline{p};\mathbf{G})$. The process of achieving the desired power control vector is divided into three phases (see Fig. 3.1). In Phase I, a sequence of power levels which is known to all the transmitters is transmitted (similar to a training sequence in classical channel estimation but in the power domain), and Transmitter $i$ estimates its own channel gains (i.e., $g_{1i}, g_{2i}, ..., g_{Ki}$) by exploiting the noisy RSSI feedback ; we refer to the corresponding channel gains as *local CSI*. In Phase II, each transmitter informs the other transmitters about its local CSI by using power modulation.

2. Note that, for the sake of clarity, it is assumed here that the RS power quantizer and DMC are independent of the user index, but the proposed approach holds in the general case.

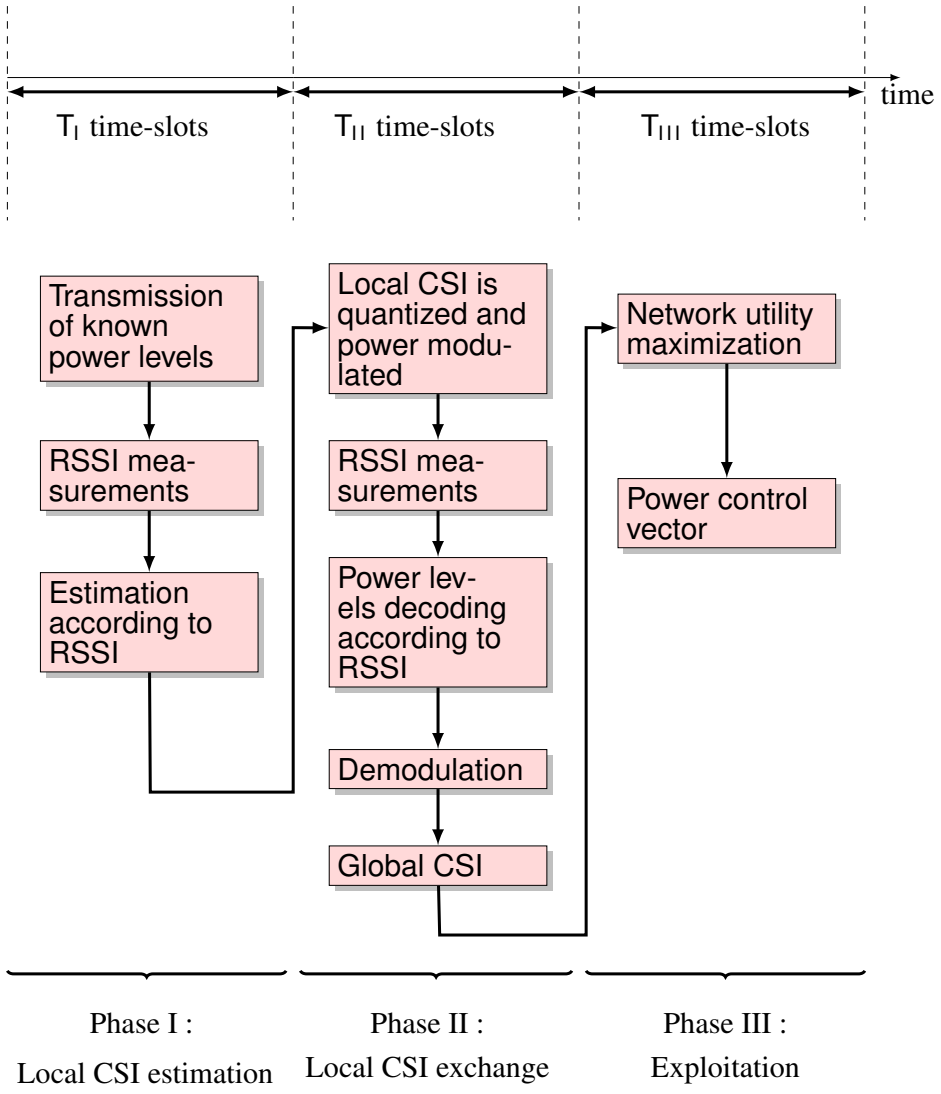


FIGURE 3.1 – The flowchart of the proposed scheme

By decoding the modulated power, each transmitter can estimate the channel gains of the other users and thus, at the end of Phase II each transmitter has its own estimate of the *global CSI* $\mathbf{G}$ ; the situation where transmitters have a non-homogeneous or different knowledge of global CSI is referred to as a distributed CSI scenario in [31]. In Phase III, each transmitter can then exploit global CSI to maximize (possibly in a sub-optimal manner) the network utility of interest. In the numerical part, we make specific and classical choices for the network utility namely, we consider the network sum-rate and network sum-energy-efficiency.

## 3.3 Local CSI estimation with power domain feedback

Phase I comprises $T_{\mathrm{I}}$ time-slots. The aim of Phase I is to allow Transmitter $i$, $i \in \{1, ..., K\}$, to acquire local CSI from the $T_{\mathrm{I}}$ observations $\widetilde{\omega}_i(1), ..., \widetilde{\omega}_i(T_{\mathrm{I}})$ which are available thanks to the feedback channel between Receiver $i$ and Transmitter $i$. Obviously, if local CSI is already available e.g., because another estimation mechanism is available, Phase I can be skipped and one can directly proceed with the local CSI exchange among the transmitters namely, performing Phase II.

For every time-slot of Phase I, each transmitter transmits at a prescribed power level which is assumed to be known to all the transmitters. One of the key observations we make in this chapter is that, when the channel gains are constant over several time-slots, it is possible to recover local CSI from the RSSI or SINR ; this means that, as far as power control is concerned, there is no need for additional signaling from the receiver for local CSI acquisition by the transmitter. Thus, the sequences of power levels in Phase I can be seen as training sequences. Technically, a difference between classical training-based estimation and Phase I is that estimation is performed in the power domain and over several time-slots and not in the symbol domain (symbol duration is typically much smaller than the duration of a time-slot) within a single time-slot. Also note that working in the symbol domain would allow one to have access to $h_{ij}$ but the phase information on the channel coefficients is irrelevant for the purpose of maximizing a utility function of the form $u(\underline{p}; \mathbf{G})$. Another technical difference stems from the fact that the feedback noise is not standard, which is commented more a little further.

By denoting $(p_i(1), ..., p_i(T_{\mathrm{I}}))$, $i \in \{1, ..., K\}$, the sequence of training power levels used by Transmitter $i$, the following training matrix can be defined :

$$\mathbf{P}_{\mathrm{I}} = \begin{pmatrix} p_1(1) & \dots & p_K(1) \\ \vdots & \vdots & \vdots \\ p_1(T_{\mathrm{I}}) & \dots & p_K(T_{\mathrm{I}}) \end{pmatrix}. \tag{3.3}$$

With the above notations, the *noiseless RS power vector* $\underline{\omega}_i = (\omega_i(1), ..., \omega_i(T_{\mathrm{I}}))^{\mathrm{T}}$ can be expressed as :

$$\underline{\omega}_i = \mathbf{P}_{\mathrm{I}} \underline{g}_i + \sigma^2 \underline{1}. \tag{3.4}$$

where $\underline{g}_i = (g_{1i}, .., g_{Ki})^{\mathrm{T}}$ and $\underline{1} = (1, 1, ..., 1)^{\mathrm{T}}$.

To estimate the local CSI $\underline{g}_i$ from the sole knowledge of the *noisy RS power vector or RSSI* $\widetilde{\underline{\omega}}_i$ we propose to use the least-squares (LS) estimator in the power domain (PD),

abbreviated as LSPD, to estimate the local CSI as :

$$\widetilde{\underline{g}}_i^{\mathrm{LSPD}} = \left(\mathbf{P}_{\mathrm{I}}^{\mathrm{T}}\mathbf{P}_{\mathrm{I}}\right)^{-1}\mathbf{P}_{\mathrm{I}}^{\mathrm{T}}\left(\widetilde{\underline{\omega}}_i - \sigma^2\underline{1}\right). \tag{3.5}$$

where $\sigma^2$ is assumed to be known from the transmitters since it can always be estimated through conventional estimation procedures (see e.g., [26]). Using the LSPD estimate for local CSI therefore assumes that the training matrix $\mathbf{P}_{\mathrm{I}}$ is chosen to be pseudo-invertible. A necessary condition for this is that the number of time-slots used for Phase I verifies : $T_{\mathrm{I}} \geq K$. Using a diagonal training matrix allows this condition to be met and to simplify the estimation procedure.

It is known that the LSPD estimate may coincide with the maximum likelihood (ML) estimate. This holds for instance when the observation model of the form $\widetilde{\omega}_i = \omega_i + z$ where $z$ is an independent and additive white Gaussian noise. In the setup under investigation, $z$ represents both the effects of quantization and transmission errors over the feedback channels and does not meet neither the independence nor the Gaussian assumption. However, we have identified a simple and sufficient condition under which the LSPD estimate maximizes the *likelihood* $P(\widetilde{\underline{\omega}}_i|\underline{g}_i)$. This is the purpose of the next proposition.

**Proposition 3.3.1.** *Denote by* $\mathcal{G}_i^{\mathrm{ML}}$ *the set of ML estimates of* $\underline{g}_i$*, then we have*

$$\begin{aligned}
&(i) \quad \mathcal{G}_i^{\mathrm{ML}} = \arg\max_{\underline{g}_i} \prod_{t=1}^{T_{\mathrm{I}}} \Gamma\left(\widetilde{\omega}_i(t) \,\middle|\, Q_{\mathrm{RS}}\left(\underline{e}_t^{\mathrm{T}}\mathbf{P}_{\mathrm{I}}\underline{g}_i + \sigma^2\right)\right);\\
&(ii) \quad \widetilde{\underline{g}}_i^{\mathrm{LSPD}} \in \mathcal{G}_i^{\mathrm{ML}} \text{ when for all } \ell,\ \arg\max_k \Gamma(\mathrm{w}_\ell|\mathrm{w}_k) = \ell;
\end{aligned}$$

*where* $\underline{e}_t$ *is a column vector whose entries are zeros except for the* $t^{\mathrm{th}}$ *entry which equals* 1.

**Proof :** From Sec. 2.2, we have $\widehat{\underline{\omega}}_i \in W$ and $\widetilde{\underline{\omega}}_i \in W$, where $\Omega$ is a discrete set. Therefore, we can rewrite the likelihood probability $\Pr\left(\widetilde{\underline{\omega}}_i|\underline{g}_i\right)$ as follows

$$\begin{aligned}
\Pr\left(\widetilde{\underline{\omega}}_i|\underline{g}_i\right) &\overset{(a)}{=} \sum_{m=1}^{M^{T_{\mathrm{I}}}} \Pr\left(\widetilde{\underline{\omega}}_i|\widehat{\underline{\omega}}_i = \underline{\mathrm{w}}_m\right)\Pr\left(\widehat{\underline{\omega}}_i = \underline{\mathrm{w}}_m|\underline{g}_i\right)\\
&\overset{(b)}{=} \sum_{m=1}^{M^{T_{\mathrm{I}}}} \Pr\left(\widehat{\underline{\omega}}_i = \underline{\mathrm{w}}_m|\underline{g}_i\right)\prod_{t=1}^{T_{\mathrm{I}}}\Gamma\left(\widetilde{\omega}_i(t)\,|\widehat{\omega}_i(t)\right)\\
&\overset{(c)}{=} \prod_{t=1}^{T_{\mathrm{I}}}\Gamma\left(\widetilde{\omega}_i(t)\,|Q_{\mathrm{RS}}\left(\underline{e}_t^{\mathrm{T}}\mathbf{P}_{\mathrm{I}}\underline{g}_i + \sigma^2\right)\right)
\end{aligned} \tag{3.6}$$

where $\underline{e}_t$ is a column vector whose entries are zeros except for the $t^{\mathrm{th}}$. In (3.6), (a) holds as the estimation and feedback process $\underline{g}_i$ to $\widehat{\underline{\omega}}_i$ to $\widetilde{\underline{\omega}}_i$ (represented in Fig. 1) is Markovian, (b) holds because the DMC is separable and (c) holds because $\Pr\left(\widehat{\underline{\omega}}_i|\underline{g}_i\right)$ is a discrete delta function that is zero everywhere except when $Q_{\mathrm{RS}}\left(\mathbf{P}_{\mathrm{I}}\underline{g}_i\right) = \widehat{\underline{\omega}}_i$.

From (3.6), the set of the ML estimators can now be written as

$$\mathcal{G}_i^{\mathrm{ML}} = \left\{\arg\max_{\underline{g}_i}\prod_{t=1}^{T_{\mathrm{I}}}\Gamma\left(\widetilde{\omega}_i(t)\,|Q_{\mathrm{RS}}\left(\underline{e}_t^{\mathrm{T}}\mathbf{P}_{\mathrm{I}}\underline{g}_i + \sigma^2\right)\right)\right\} \tag{3.7}$$

which is the first claim of our proposition. Now, we look at the LS estimator, which is know from (3.5) to be

$$\mathbf{P}_{\mathrm{I}}\underline{g}_i^{\mathrm{LSPD}} + \sigma^2\underline{1} = \underline{\widetilde{\omega}_i} \tag{3.8}$$

or equivalently :

$$\underline{e}_t^{\mathrm{T}}\mathbf{P}_{\mathrm{I}}\underline{g}_i^{\mathrm{LSPD}} + \sigma^2 = \widetilde{\omega}_i\left(t\right) \tag{3.9}$$

If for all $\ell$, $\arg\max_k \Gamma(\mathrm{w}_\ell|\mathrm{w}_k) = \ell$, then the ML set can be evaluated based on (3.7) as

$$\mathcal{G}_i^{\mathrm{ML}} = \left\{\underline{g}_i | \forall t, Q_{\mathrm{RS}}\left(\underline{e}_t^{\mathrm{T}}\mathbf{P}_{\mathrm{I}}\underline{g}_i + \sigma^2\right) = \widetilde{\omega}_i\left(t\right)\right\} \tag{3.10}$$

Therefore, we observe that if $\mathcal{G}_i^{\mathrm{ML}}$ is given as in (3.10), then from (3.9), we have $\underline{g}_i^{\mathrm{LSPD}} \in \mathcal{G}_i^{\mathrm{ML}}$, our second claim. ■

The sufficient condition corresponding to $(ii)$ is clearly met in classical practical scenarios. Indeed, as soon as the probability of correctly decoding the sent quantized RS power symbol (which is sent by the receiver) at the transmitter exceeds 50%, the above condition is verified. It has to be noted that $\mathcal{G}_i^{\mathrm{ML}}$ is not a singleton set in general, which indicates that even if the LSPD estimate maximizes the likelihood, the set $\mathcal{G}_i^{\mathrm{ML}}$ will typically comprise a solution which can perform better e.g., in terms of mean square error.

If some statistical knowledge on the channel gains is available, it is possible to further improve the performance of the channel estimate. Indeed, when the probability of $\underline{g}_i$ is known it becomes possible (up to possible complexity limitations) to minimize the mean square error $\mathbb{E}\|\widehat{\underline{g}}_i - \underline{g}_i\|^2$. The following proposition provides the expression of the minimum mean square error (MMSE) estimate in the power domain (PD) .

**Proposition 3.3.2.** *Assume that* $\forall i \in \{1, ..., K\}$, $\widehat{\underline{\omega}}_i$ *and* $\widetilde{\underline{\omega}}_i$ *belong to the set* $\Omega = \{\underline{\mathrm{w}}_1, ..., \underline{\mathrm{w}}_{M^{T_\mathrm{I}}}\}$, *where* $\underline{\mathrm{w}}_1 = (\mathrm{w}_1, \mathrm{w}_1, ..., \mathrm{w}_1)^{\mathrm{T}}$, $\underline{\mathrm{w}}_2 = (\mathrm{w}_1, \mathrm{w}_1, ..., \mathrm{w}_2)^{\mathrm{T}}$,..., $\underline{\mathrm{w}}_{M^{T_\mathrm{I}}} = (\mathrm{w}_M, \mathrm{w}_M, ..., \mathrm{w}_M)^{\mathrm{T}}$ *(namely, vectors are ordered according to the lexicographic order and have* $T_\mathrm{I}$ *elements each). Define* $\mathcal{G}_m$ *as*

$$\mathcal{G}_m := \left\{\underline{x} \in \mathbb{R}_+^K : \ Q_{\mathrm{RS}}\left(\mathbf{P}_{\mathrm{I}}\underline{x} + \sigma^2\underline{1}\right) = \underline{\mathrm{w}}_m\right\}. \tag{3.11}$$

*Then the MMSE estimator in the power domain expresses as :*

$$\widetilde{\underline{g}}_i^{\mathrm{MMSEPD}} = \frac{\displaystyle\sum_{m=1}^{M^{T_\mathrm{I}}}\prod_{t=1}^{T_\mathrm{I}}\Gamma\left(\widetilde{\omega}_i(t)|\underline{\mathrm{w}}_m(t)\right)\int_{\mathcal{G}_m}\phi_i\left(\underline{g}_i\right)\underline{g}_i \mathrm{d}g_{1i}...\mathrm{d}g_{Ki}}{\displaystyle\sum_{m=1}^{M^{T_\mathrm{I}}}\prod_{t=1}^{T_\mathrm{I}}\Gamma\left(\widetilde{\omega}_i(t)|\underline{\mathrm{w}}_m(t)\right)\int_{\mathcal{G}_m}\phi_i\left(\underline{g}_i\right)\mathrm{d}g_{1i}...\mathrm{d}g_{Ki}}, \tag{3.12}$$

*where* $\phi_i$ *represents the probability density function (p.d.f.) of* $\underline{g}_i$ *and* $\underline{\mathrm{w}}_m(t)$ *is the* $t$*-th element of* $\underline{\mathrm{w}}_m$.

**Proof :** After the RSSI quantization, the $M^{T_\mathrm{I}}$ different levels of $\widehat{\underline{\omega}}_i$ or $\widetilde{\underline{\omega}}_i$ are $\underline{\mathrm{w}}_1, \underline{\mathrm{w}}_2, .., \underline{\mathrm{w}}_{M^{T_\mathrm{I}}}$ forming the set $\Omega$.

Define by $h : \Omega \to G$ which maps the observed RSSI feedback to a channel estimate, where $G := \{\underline{\mathrm{g}}_1, \underline{\mathrm{g}}_2, ..., \underline{\mathrm{g}}_{M^{T_\mathrm{I}}}\}$, such that $h(\underline{\mathrm{w}}_m) = \underline{\mathrm{g}}_m$. That is, when transmitter $i$ observes the RSSI feedback $\widetilde{\underline{\omega}}_i$ to be $\underline{\mathrm{w}}_m$, local channel estimate $\widetilde{\underline{g}}_i$ is $\underline{\mathrm{g}}_m$.

Based on the above definitions, we have that

$$\mathbb{E}\left[|\widetilde{\underline{g}}_i - \underline{g}_i|^2\right] = \sum_{n=1}^{M^{T_\mathrm{I}}} \int_{\underline{x}\in\mathbb{R}^K_{\geq 0}} \Pr\left(\widetilde{\underline{g}}_i = \underline{\mathrm{g}}_n | \underline{g}_i = \underline{x}\right) \phi_i\left(\underline{x}\right) |\underline{\mathrm{g}}_n - \underline{x}|^2 \mathrm{d}\underline{x} \tag{3.13}$$

The term $\Pr\left(\widetilde{\underline{g}}_i = \underline{\mathrm{g}}_n | \underline{g}_i = \underline{x}\right)$ can be further expanded as

$$\begin{aligned}\Pr\left(\widetilde{\underline{g}}_i = \underline{\mathrm{g}}_n | \underline{g}_i = \underline{x}\right) &= \textstyle\sum_{\ell=1}^{M^{T_\mathrm{I}}} \sum_{m=1}^{M^{T_\mathrm{I}}} \Pr\left(\widetilde{\underline{g}}_i = \underline{\mathrm{g}}_n, \widetilde{\underline{\omega}}_i = \underline{\mathrm{w}}_\ell, \widehat{\underline{\omega}}_i = \underline{\mathrm{w}}_m | \underline{g}_i = \underline{x}\right) \\ = \textstyle\sum_{\ell=1}^{M^{T_\mathrm{I}}} \sum_{m=1}^{M^{T_\mathrm{I}}} \Pr\left(\widetilde{\underline{g}}_i = \underline{\mathrm{g}}_n | \widetilde{\underline{\omega}}_i = \underline{\mathrm{w}}_\ell\right) &\Pr\left(\widetilde{\underline{\omega}}_i = \underline{\mathrm{w}}_\ell | \widehat{\underline{\omega}}_i = \underline{\mathrm{w}}_m\right) \Pr\left(\widehat{\underline{\omega}}_i = \underline{\mathrm{w}}_m | \underline{g}_i = \underline{x}\right)\end{aligned} \tag{3.14}$$

Now we know that the mapping $h()$ is deterministic and results in $h(\underline{\mathrm{w}}_m) = \underline{\mathrm{g}}_m$. Therefore, $\Pr\left(\widetilde{\underline{g}}_i = \underline{\mathrm{g}}_n | \widetilde{\underline{\omega}}_i = \underline{\mathrm{w}}_\ell\right) = \delta_{n,\ell}$, where $\delta_{n,\ell}$ is the Kronecker delta function such that $\delta_{n,\ell} = 0$ when $n \neq \ell$ and $\delta_{n,\ell} = 1$ when $n = \ell$. Additionally, we also know that $\Pr\left(\widetilde{\underline{\omega}}_i = \underline{\mathrm{w}}_\ell | \widehat{\underline{\omega}}_i = \underline{\mathrm{w}}_m\right) = \prod_{t=1}^{T_I} \Gamma\left(\underline{\mathrm{w}}_\ell(t) | \underline{\mathrm{w}}_m(t)\right)$ by definition (where $\underline{\mathrm{w}}_m(t)$ is the $t$-th component of $\underline{\mathrm{w}}_m$) . This results in (3.14) being simplified to

$$\Pr\left(\widetilde{\underline{g}}_i = \underline{\mathrm{g}}_n | \underline{g}_i\right) = \sum_{m=1}^{M^{T_\mathrm{I}}} \prod_{t=1}^{T_I} \Gamma\left(\underline{\mathrm{w}}_n(t) | \underline{\mathrm{w}}_m(t)\right) \Pr\left(\widehat{\underline{\omega}}_i = \underline{\mathrm{w}}_m | \underline{g}_i = \underline{x}\right) \tag{3.15}$$

Recall that $\widehat{\underline{\omega}_i} = Q_{\mathrm{RS}}\left(\mathbf{P}_\mathrm{I} \underline{g_i}\right)$ by definition of the quantizer. Define by

$$\mathcal{G}_m := \left\{\underline{x} \in \mathbb{R}^K_{\geq 0} : \; Q_{\mathrm{RS}}\left(\mathbf{P}_\mathrm{I}\underline{x} + \sigma^2 \underline{1}\right) = \underline{\mathrm{w}}_m\right\} \tag{3.16}$$

resulting in

$$\Pr\left(\widehat{\underline{\omega}}_i = \underline{\mathrm{w}}_m | \underline{g}_i = \underline{x}\right) = \begin{cases} 1 & \text{if } \underline{x} \in \mathcal{G}_m \\ 0 & \text{if } \underline{x} \notin \mathcal{G}_m \end{cases} \tag{3.17}$$

Now, we can simplify (3.13) using (3.17) and (3.15) into

$$\begin{aligned}&\mathbb{E}\left[|\widetilde{\underline{g}}_i - \underline{g}_i|^2\right] \\ =&\sum_{n=1}^{M_{T_\mathrm{I}}} \sum_{m=1}^{M_{T_\mathrm{I}}} \prod_{t=1}^{T_1} \Gamma\left(\underline{\mathrm{w}}_n(t) | \underline{\mathrm{w}}_m(t)\right) \int_{\mathcal{G}_m} \phi_i\left(\underline{x}\right) |\underline{\mathrm{g}}_n - \underline{x}|^2 \mathrm{d}\underline{x}\end{aligned} \tag{3.18}$$

For a fixed DMC, we can find the $\underline{g}_i^{\mathrm{MMSE}}$ which will minimize the distortion by taking the derivative of the distortion over $\underline{\mathrm{g}}_n$ :

$$\frac{\partial \mathbb{E}\left[|\widetilde{\underline{g}}_i - \underline{g}_i|^2\right]}{\partial \underline{\mathrm{g}}_n} = 2 \sum_{m=1}^{M_{T_\mathrm{I}}} \prod_{t=1}^{T_1} \Gamma\left(\underline{\mathrm{w}}_n(t) | \underline{\mathrm{w}}_m(t)\right) \int_{\mathcal{G}_m} \phi_i\left(\underline{x}\right) \left(\underline{\mathrm{g}}_n - \underline{x}\right) \mathrm{d}\underline{x} \tag{3.19}$$

To minimize distortion, this derivative should be equal to zero. The $\underline{\mathrm{g}}_n$ minimizing the distortion is by definition, the MMSE of the channel given $\widetilde{\underline{\omega}}_i = \underline{\mathrm{w}}_n$. Therefore by rearranging (3.19), we can find the expression for the MMSE given in the proposition III.2. ■

In Sec. 2.6, we will compare the LSPD and MMSEPD performance in terms of estimation SNR, sum-rate, and sum-energy-efficiency. While the MMSEPD estimate may

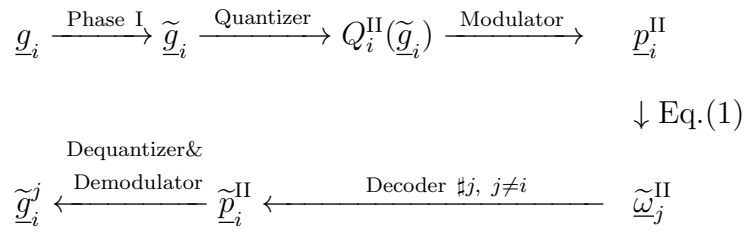


FIGURE 3.2 – The figure summarizes the overall processing chain for the CSI

provide a quite significant gain in terms of MSE over the LSPD estimate, it also has a much higher computational cost. Simulations reported in Sec. V will exhibit conditions under which choosing the LSPD solution may involve a marginal loss w.r.t. the MMSEPD solution e.g., when the performance is measured in terms of sum-rate. Therefore the choice of the estimator can be made based on the computation capability, the choice of utility for the system under consideration, or the required number of time-slots (MMSEPD allows for a number of time-slots which is less than $K$, whereas this is not possible for LSPD). Note that some refinements might be brought to the proposed estimator e.g., by using a low-rank approximation of the channel vector (see e.g., [28]), which is particularly relevant if the channel appears to possess some sparseness.

## 3.4 Local CSI exchange with discrete power levels (Discrete Power Modulation)

Phase II comprises $T_{\mathrm{II}}$ time-slots. The aim of Phase II is to allow Transmitter $i$, $i \in \{1, ..., K\}$, to exchange its knowledge about local CSI with the other transmitters; the corresponding estimate will be merely denoted by $\widetilde{\underline{g}}_i = (\widetilde{g}_{1i}, ..., \widetilde{g}_{Ki})^{\mathrm{T}}$, knowing that it can refer either to the LSPD or MMSEPD estimate. The proposed procedure is as follows and is also summarized in Fig. 3. Transmitter $i$ quantizes the information $\widetilde{\underline{g}}_i$ through a *channel gain quantizer* called $\mathcal{Q}_i^{\mathrm{II}}$ and maps the obtained bits (through a modulator) into the sequence of power levels $\underline{p}_i^{\mathrm{II}} = (p_i(T_{\mathrm{I}}+1), ..., p_i(T_{\mathrm{I}}+T_{\mathrm{II}}))^{\mathrm{T}}$. From the RSSI observations $\widetilde{\underline{\omega}}_j^{\mathrm{II}} = (\widetilde{\omega}_j(T_{\mathrm{I}}+1), ..., \widetilde{\omega}_j(T_{\mathrm{I}}+T_{\mathrm{II}}))^{\mathrm{T}}$, Transmitter $j$ ($j \neq i$) can estimate (through a decoder) the power levels used by Transmitter $i$. To facilitate the corresponding operations, we assume that the used power levels in Phase II have to lie in the *reduced set* $\mathcal{P} = \{P_1, ..., P_L\}$ with $\forall \ell \in \{1, ..., L\}$, $P_\ell \in [0, P_{\max}]$. The estimate Transmitter $j$ has about the channel vector $\underline{g}_i$ will be denoted by $\widetilde{\underline{g}}_i^j = \left(\widetilde{g}_{1i}^j, ..., \widetilde{g}_{Ki}^j\right)^{\mathrm{T}}$. The corresponding *channel matrix estimate* is denoted by $\widetilde{\mathbf{G}}^j$. In what follows, we describe the proposed schemes for the three operations required to exchange local CSI namely, quantization, power modulation, and decoding. The situation where transmitters have different estimates of the same channel is referred to as a distributed CSI scenario in [31]. Assessing analytically the impact of distributed CSI on the sum-rate or sum-energy-efficiency is beyond the scope of this chapter but constitutes a very relevant extension of it ($\star$); only simulations accounting for the distributed CSI effect will be provided here.

It might be noticed that the communication scenario in Phase II is similar to the X-channel scenario in the sense that each transmitter wants to inform the other transmitters

(which play the role of receivers) about its local CSI, and this is done simultaneously. All the available results on the X-channel exploit the channel structure (e.g., the phase information) to improve performance (e.g., by interference alignment [27] or filter design). Therefore, knowing how to exploit the X-channel scenario in the setup under consideration (which is in part characterized by the power domain operation) in this chapter, appears to a relevant extension ($\star$).

**Channel gain quantization operation** $\mathcal{Q}_i^{\mathrm{II}}$ : The first step in Phase II is for each of the transmitters to quantize the $K-$dimensional vector $\underline{\widetilde{g}}_i$. For simplicity, we assume that each element of the real $K-$dimensional vector $\underline{\widetilde{g}}_i$ is quantized by a scalar quantizer into a label of $N_{\mathrm{II}}$ bits. This assumption is motivated by low complexity but also by the fact that the components of $\underline{\widetilde{g}}_i$ are independent in the most relevant scenarios of interest. For instance, if local CSI is very well estimated, the estimated channel gains are close to the actual channel gains, which are typically independent in practice. Now, in the general case of arbitrary estimation noise level, the components of $\underline{\widetilde{g}}_i$ will be independent when the training matrix $\mathbf{P}_{\mathrm{I}}$ is chosen to be diagonal, which is a case of high interest and is motivated further in Sec. V. Under the channel gain (quasi-) independency, vector quantization would bring (almost) no performance improvement. The *scalar quantizer* used by Transmitter $i$ to quantize $\widetilde{g}_{ji}$ is denoted by $\mathcal{Q}_{ji}^{\mathrm{II}}$. Finding the best quantizer in terms of ultimate network utility (e.g., in terms of sum-rate or sum-energy-efficiency) does not appear to be straightforward ($\star$). We present two possible quantization schemes in this section.

A possible, but generally sub-optimal approach, is to determine a quantizer which *minimizes distortion*. The advantage of such approach is that it is possible to express the quantizer and it leads to a scheme which is independent of the network utility ; this may be an advantage when the utility is unknown or changing. A possible choice for the quantizer $\mathcal{Q}_i^{\mathrm{II}}$ is to use the conventional version of the Lloyd-Max algorithm (LMA) [12]. However, this algorithm assumes perfect knowledge of the information source to be quantized (here this would amount to assuming the channel estimate to be noiseless) and no noise between the quantizer and the dequantizer (here this would amount to assuming perfect knowledge of the RS power). The authors of [76] proposed a generalized version of the Lloyd-Max algorithm for which noise can be present both at the source and the transmission but the various noise sources are assumed to verify standard assumptions (such as independence of the noise and the source), which are not verified in the setting under investigation ; in particular, the noise in Phase I is the estimation noise, which is correlated with the transmitted signal. Deriving the corresponding generalized Lloyd-Max algorithm can be checked to be a challenging task, which is left as an extension of the technical solutions proposed here ($\star$). Rather, we will provide here a special case of the generalized Lloyd-Max algorithm, which is very practical in terms of computational complexity and required knowledge.

The version of the Lloyd-Max algorithm we propose will be referred to as *ALMA (advanced Lloyd-Max algorithm)*. ALMA corresponds to the special case (of the most generalized version mentioned previously) in which the algorithm assumes noise on the transmission but not at the source (although the source can be effectively noisy). This setting is very well suited to scenarios where the estimation noise due to Phase I is negligible or when local CSI can be acquired reliably by some other mechanism. In the numerical part, we can observe the improvements of the proposed ALMA with respect to the conventional LMA. Just like the conventional LMA, ALMA aims at minimizing

distortion by iteratively determining the best set of representatives and the best set of cells (which are intervals here) when one of the two is fixed. The calculations for obtaining the optimal representatives and partitions are given in Appendix A for both the special case of no source noise as well as for the general case. Solving the general case can be seen from Appendix A to be computationally challenging.

To comment on the proposed algorithm which is given by the pseudo-code of Algorithm 1, a few notations are in order. We denote by $q \in \{1, ..., Q\}$ the *iteration index* (where $Q$ is the upper bound on the number of iterations) and define $R = 2^{N_{\text{II}}}$. For each channel gain estimate $\widetilde{g}_{ji}$ to be quantized, we denote by $\underline{v}_{ji} = \left\{v_{ji,1}^{(q)}, ..., v_{ji,R}^{(q)}\right\}$ the set of *representatives* and by $\left\{u_{ji,1}^{(q)}, ..., u_{ji,R+1}^{(q)}\right\}$ (with $u_{ji,1}^{(q)} = 0$ and $u_{ji,R+1}^{(q)} = \infty$) the set of *interval bounds* which defines how the set $\widetilde{g}_{ji}$ lies in (namely $[0, +\infty)$) is partitioned. At each iteration, the choice of the set of representatives or intervals aims at minimizing the end-to-end distortion $\mathbb{E}|\widetilde{g}_{ji} - g_{ji}|^2$. This minimization operation requires some statistical knowledge. Indeed, the probability that the dequantizer decodes the representative $v_{ji,r}^{(q)}$ given that $v_{ji,n}^{(q)}$ has been transmitted needs to be known ; this probability is denoted by $\pi_{ji}(r|n)$ and constitutes one of the inputs of Algorithm 1. The second input of Algorithm 1 is the p.d.f. of $g_{ji}$ which is denoted by $\phi_{ji}$. The third input is given by the initial choice for the quantization intervals that is, the set $\left\{u_{ji,1}^{(0)}, ..., u_{ji,R+1}^{(0)}\right\}$. Convergence of ALMA to a global minimum point is not guaranteed and finding sufficient condition for global convergence is known to be non-trivial. However, local convergence is guaranteed ; an elegant and general argument for this can be found in [30]. Conducting a theoretical analysis in which global convergence is tackled would constitute a significant development of the present analysis ($\star$), which is here based on typical and realistic simulation scenarios.

At this point two comments are in order. First, through (3.20)-(3.21), it is seen that ALMA relies on some statistical knowledge which might not always be available in practice. This is especially the case for $\pi_{ji}$ and $\gamma_{ji}$ since the knowledge of channel distribution information (CDI, i.e., $\phi_{ji}$) is typically easier to be obtained. The CDI may be obtained by storing the estimates obtained during past transmissions and forming empirical means (possibly with a sliding window). If the CDI is time-varying, a procedure indicating to the terminals when to update the statistics might be required. Second, if we regard Phase II as a classical communication process, then the amount of information sent by the source is maximized when the source signal is uniformly distributed. It turns out minimizing the (end-to-end) distortion over Phase II does not involve this. Motivated by these two observations we provide here a second quantization scheme, which is simple but will be seen to perform quite well in the numerical part. We will refer to this quantization scheme as *maximum entropy quantizer (MEQ)*. For MEQ, the quantization interval bounds are fixed once and for all according to :

$$\forall r \in \{1, ..., R\}, \forall (j, i) \in \{1, ..., K\}^2, \ \int_{u_{ji,r}}^{u_{ji,r+1}} \phi_{ji}(g_{ji}) \mathrm{d}g_{ji} = \frac{1}{R}. \tag{3.22}$$

The representative of the interval $[u_{ji,r}, u_{ji,r+1}]$ is denoted by $v_{ji,r}$ and is chosen to be its centroid :

$$v_{ji,r} = \frac{\displaystyle\int_{u_{ji,r}}^{u_{ji,r+1}} g_{ji}\phi_{ji}(g_{ji}) \mathrm{d}g_{ji}}{\displaystyle\int_{u_{ji,r}}^{u_{ji,r+1}} \phi_{ji}(g_{ji}) \mathrm{d}g_{ji}}. \tag{3.23}$$

**Inputs :** $\pi_{ji}$, $\phi_{ji}\left(g_{ji}\right)$, $\left\{u_{ji,1}^{(0)},...,u_{ji,R+1}^{(0)}\right\}$
**Outputs :** $\left\{u_{ji,1}^{\star},...,u_{ji,R+1}^{\star}\right\}$, $\left\{v_{ji,1}^{\star},...,v_{ji,R+1}^{\star}\right\}$
**Initialization :** Set $q=0$. Initialize the quantization intervals according to $\left\{u_{ji,1}^{(0)},...,u_{ji,R+1}^{(0)}\right\}$. Set $u_{ji,r}^{(-1)}=0$ for all $r\in\{1,...,R\}$.
**while** $\max_r||u_{ji,r}^{(q)}-u_{ji,r}^{(q-1)}||>\delta$ *and* $q<Q$ **do**
Update the iteration index : $q\leftarrow q+1$.
For all $r\in\{1,2,..,R\}$ set

$$v_{ji,r}^{(q)}\leftarrow\frac{\sum_{n=1}^{R}\pi_{ji}\left(r|n\right)\int_{u_{ji,n}^{(q-1)}}^{u_{ji,n+1}^{(q-1)}}g_{ji}\phi_{ji}(g_{ji})\mathrm{d}g_{ji}}{\sum_{n=1}^{R}\pi_{ji}\left(r|n\right)\int_{u_{ji,n}^{(q-1)}}^{u_{ji,n+1}^{(q-1)}}\phi_{ji}(g_{ji})\mathrm{d}g_{ji}}. \tag{3.20}$$

For all $r\in\{2,3,..,R\}$ set

$$u_{ji,r}^{(q)}\leftarrow\frac{\sum_{n=1}^{R}\left[\pi_{ji}\left(n|r\right)-\pi_{ji}\left(n|r-1\right)\right]\left(v_{ji,n}^{(q)}\right)^{2}}{2\sum_{n=1}^{R}\left[\pi_{ji}\left(n|r\right)-\pi_{ji}\left(n|r-1\right)\right]v_{ji,n}^{(q)}}. \tag{3.21}$$

**end**
$\forall r\in\{2,...,R\}$, $u_{ji,r}^{\star}=u_{ji,r}^{(q)}$, $u_{ji,1}^{\star}=0$ and $u_{ji,R+1}^{\star}=\infty$
$\forall r\in\{1,...,R\}$, $v_{ji,r}^{\star}=v_{ji,r}^{(q)}$

**Algorithm 1:** Advanced Lloyd-Max algorithm (ALMA)

We see that each representative has the same probability to occur, which maximizes the entropy of the quantizer output, hence the proposed name. To implement MEQ, only the knowledge of $\phi_{ji}$ is required. Additionally, the complexity involved is very low.

**Power modulation :** To inform the other transmitters about its knowledge of local CSI, Transmitter $i$ maps the $K$ labels of $N_{\mathrm{II}}$ bits produced by the quantizer $Q_i^{\mathrm{II}}$ to a sequence of power levels $(p_i(T_{\mathrm{I}}+1),p_i(T_{\mathrm{I}}+2),\ldots,p_i(T_{\mathrm{I}}+T_{\mathrm{II}}))$. Any one-to-one mapping might be used a priori. Although the new problem of finding the best mapping for a given network utility arises here and constitutes a relevant direction to explore ($\star$), we will not only develop this here. Rather, our main objective here is to introduce this problem and illustrate it clearly for a special case which is treated in the numerical part. To this end, assume Phase II comprises $T_{\mathrm{II}}=2$ time-slots, $K=2$ users, and that the users only exploit $L=2$ power levels during Phase II say $\mathcal{P}=\{P_{\min},P_{\max}\}$. Further assume $1-$bit quantizers, which means that the quantizers $\mathcal{Q}_{ji}^{\mathrm{II}}$ produce binary labels. For simplicity, we assume the same quantizer $\mathcal{Q}$ is used for all the four channel gains $g_{11}$, $g_{12}$, $g_{21}$, and $g_{22}$ : if $g_{ij}\in[0,\mu]$ then the quantizer output is denoted by $g_{\min}$ ; if $g_{ij}\in(\mu,+\infty)$ then the quantizer output is denoted by $g_{\max}$. Therefore a simple mapping scheme for Transmitter 1 (whose objective is to inform Transmitter 2 about $(g_{11},g_{21})$) is to choose $p_1(T_{\mathrm{I}}+1)=P_{\min}$ if $\mathcal{Q}(g_{11})=g_{\min}$ and $p_1(T_{\mathrm{I}}+1)=P_{\max}$ otherwise ; and $p_1(T_{\mathrm{I}}+2)=P_{\min}$ if $\mathcal{Q}(g_{21})=g_{\min}$ and

$p_1(T_{\mathrm{I}}+2) = P_{\max}$ otherwise. Therefore, depending on the p.d.f. of $g_{ij}$, the value of $\mu$, the performance criterion under consideration, a proper mapping can chosen. For example, to minimize the energy consumed at the transmitter, using the minimum transmit power level $P_{\min}$ as much as possible is preferable ; thus if $\Pr(\mathcal{Q}(g_{11}) = g_{\min}) \geq \Pr(\mathcal{Q}(g_{11}) = g_{\max})$, the power level $P_{\min}$ will be associated with the minimum quantized channel gain that is $\mathcal{Q}(g_{11}) = g_{\min}$.

**Power level decoding :** For every time-slot $t \in \{T_{\mathrm{I}}+1, ..., T_{\mathrm{I}}+T_{\mathrm{II}}\}$ the power levels are estimated by Transmitter $i$ as follows

$$\widetilde{\underline{p}}_{-i}(t) \in \arg \min_{\underline{p}_{-i} \in \mathcal{P}^{K-1}} \left| \sum_{j \neq i} p_j \widetilde{g}_{ji} - (\widetilde{\omega}_i(t) - p_i(t)\widetilde{g}_{ii} - \sigma^2) \right|, \tag{3.24}$$

where $\underline{p}_{-i} = (p_1, .., p_{i-1}, p_{i+1}, .., p_K)$. As for every $j$, $\widetilde{g}_{ji}$ is known at Transmitter $i$, the above minimization operation can be performed. It is seen that exhaustive search can be performed as long as the number of tests, which is $L^{K-1}$, is reasonable. For this purpose, one possible approach is to impose the number of power levels which are exploited over Phase II to be small. In this respect, using binary power over Phase II is not only relevant regarding complexity issues but also in terms of robustness against the various possible sources of noise. As for **the number of interfering users** using the same channel (meaning operating on the same frequency band, at the same period of time, in the same geographical area), it **will typically be small and does not exceed** 3 **or** 4 **in real wireless systems**. More generally, this shows that the proposed technique can accommodate more than 4 users in total ; For example, if we have 12 bands, having $48 = 12 \times 4$ users would be manageable by applying the proposed technique for each band. As our numerical results indicate, using (3.24) as a decoding rule to find the power levels of the other transmitters generally works very well for $K = 2$. When the number of users is higher, each transmitter needs to estimate $K-1$ power levels with only one observation equation, which typically induces a non-negligible degradation in terms of symbol error rate. In this situation, Phase II can be performed by scheduling the activity of all the users, such that only 2 users are active at any given time-slot in Phase II. Once all pairs of users have exchanged information on their channel states, Phase II is concluded.

*Remark 1 (required number of time-slots).* The proposed technique typically requires $K + K = 2K$ time-slots for the whole exploration phase (Phases I and II). It therefore roughly require the same amount of resources as IWFA, which indeed needs about $2K$ or $3K$ SINR samples to converge to Nash equilibrium. While channel acquisition may seem to take some time, please note that regular communication is uninterrupted and occurs in parallel. As already mentioned, the context in which the proposed technique and IWFA are the most suited is a context where the channel is constant over a large number of time-slots, which means that the influence of the exploration phase on the average performance is typically negligible. Nonetheless, some simulations will be provided to assess the optimality loss induced by using power levels to convey information.

*Remark 2 (extension to the multi-band scenario).* As explained in the beginning of this chapter, Phases I and II are described for the single-band case, mainly for clarity reasons. Here, we briefly explain how to adapt the algorithm when there are multiple bands. In Phase I, the only difference exists in choosing the training matrix. With say $S$ bands to transmit, for each band $s \in \{1, ..., S\}$, the training matrix $\mathbf{P}_{\mathrm{I}}^s$ has to fulfill the constraint

$\sum_{s=1}^{S} p_i^s(t) \leq P_{\max}$ where $p_i^s$ is the power Transmitter $i$ allocates to band $s$. In Phase II, each band performs in parallel like the single-band case. Since there are power constraints for each transmitter, the modulated power should satisfy $\sum_{s=1}^{S} p_i^s(t) \leq P_{\max}$.

*Remark 3 (extension to the multi-antenna case).* To perform operation such as beamforming, the phase information is generally required. The proposed local CSI estimation techniques (namely, for Phase I) do not allow the phase information or the direction information to be recovered ; Therefore, another type of feedback should be considered for this. However, if another estimation scheme is available or used for local CSI acquisition and that scheme provides the information phase, then the techniques proposed for local CSI exchange (namely, for Phase II) can be extended. An extension which is more in line with the spirit of the manuscript is given by a MIMO interference channel for which each transmitter knows the interference-plus-noise covariance matrix and its own channel. This is the setup assumed by Scutari et al in their work on MIMO iterative water-filling [15].

*Remark 4 (type of information exchanged).* One of the strengths of the proposed exchange procedure is that **any kind** of information can be exchanged. However, since SINR or RSSI is used as the communication channel, this has to be at a low-rate which is given by the frequency at which the power control levels are updated and the feedback samples sent.

## 3.5 Local CSI exchange with continuous power levels (Continuous Power Modulation)

In this section, we discuss a solution to exploit continuous power levels whenever they are allowed under certain conditions : local CSI is well estimated and the RSSI quality is good. Then we can devise a much simpler solution by using *continuous* power modulation (CPM). The technique proposed here differs from the preceding section since here quantizing local CSI is not necessary and decoding scheme can thus be simpler and more efficient in the continuous case. Apart from the notations in Sec 2.2, here the channel gain $g_{ij}$ is assumed to lie in the interval $[g_{ij}^{\min}, g_{ij}^{\max}]$. The key feature of the proposed technique is to adjust the power level of Transmitter $i$ on time-slot $t \in \{1, ..., T\}$ as the linear combination of the channel gains to be exchanged :

$$p_i(t) = \sum_{j=1}^{K} \overline{a}_{ji}(t) \widetilde{g}_{ji} \tag{3.25}$$

where

$$\overline{a}_{ji}(t) = a_{ji}(t) \frac{P_{\max}}{g_{ji}^{\max}}, \; a_{ji}(t) \geq 0, \; \sum_{j=1}^{K} a_{ji}(t) = 1. \tag{3.26}$$

Therefore, the power levels used during the exploration phase conveys information about local CSI. It turns out that local CSI information can be recovered, provided the interference is observed either through RSSI or SINR feedback. Here we consider RSSI feedback, which has the advantage of directly leading to linear estimators. As defined in Sec 2.2,

the RS power at Receiver $i$ on time-slot $t$ writes as follows :

$$\omega_i(t) = \sum_{j=1}^{K} g_{ji} p_j(t) + \sigma^2 \tag{3.27}$$

where $\sigma^2$ is the receive noise variance. But in a real wireless system the RS power is quantized and transmitted through a noisy feedback channel (the corresponding quantizer and channel will be specified in Sec. 2.6). Thus Transmitter $i$ has only access to an observed or a noisy version of $\omega_i(t)$, which is denoted by $\widetilde{\omega}_i(t)$. To facilitate and make more accurate the local CSI exchange procedure, the used power levels during the exploration phase are imposed to follow a time-sharing rule. This means that during the exploration phase the power level of Transmitter $i$, is chosen either to follow (3.25) or to be zero. Assuming time-sharing for the exploration phase, Transmitter $j$ is only active when $t \in \{t_j + 1, t_j + 2, \ldots, t_j + K\}$ with $t_j := j(K-1)$ . The observed RS power at Transmitter $i$ when Transmitter $j$ is active expresses as :

$$\begin{aligned} \widetilde{\omega}_i^j(t) &= \omega_i^j(t) + z_{i,1}^j(t) \\ &= g_{ji} p_j(t) + \sigma^2 + z_{i,1}^j(t) \\ &= \widetilde{g}_{ji} p_j(t) + \sigma^2 + z_{i,1}^j(t) + z_{i,2}^j(t) \\ &= \widetilde{g}_{ji} p_j(t) + \sigma^2 + z_i^j(t) \end{aligned} \tag{3.28}$$

where $z_{i,1}^j(t) = \widetilde{\omega}_i^j(t) - \omega_i^j(t)$ and $z_{i,2}^j(t) = (g_{ji} - \widetilde{g}_{ji})\, p_j(t)$. By substituting $p_j(t)$ in (3.28) by its expanded version (3.25), it follows that the sequence of RS powers observed by Transmitter $i$ when Transmitter $j$ is active, expresses as :

$$\underline{\widetilde{\omega}}_i^j = \mathbf{P}^j \underline{\widetilde{g}}_j \widetilde{g}_{ji} + \underline{z}_i^j + \sigma^2 \underline{1} \tag{3.29}$$

where $\underline{\widetilde{\omega}}_i^j = (\widetilde{\omega}_i^j(t_j{+}1), ..., \widetilde{\omega}_i^j(t_j{+}K))^{\mathrm{T}}$, $\underline{\widetilde{g}}_j = (\widetilde{g}_{1j}, ..., \widetilde{g}_{Kj})^{\mathrm{T}}$, $\underline{z}_i^j = (z_i^j(t_j{+}1), ..., z_i^j(t_j{+}K))^{\mathrm{T}}$, $\underline{1} = (1, 1, ..., 1)^{\mathrm{T}}$, and

$$\mathbf{P}^j = P_{\max} \begin{pmatrix} \frac{a_{1j}(t_j+1)}{g_{1j}^{\max}} & \cdots & \frac{a_{Kj}(t_j+1)}{g_{Kj}^{\max}} \\ \vdots & \vdots & \vdots \\ \frac{a_{1j}(t_j+K)}{g_{1j}^{\max}} & \cdots & \frac{a_{Kj}(t_j+K)}{g_{Kj}^{\max}} \end{pmatrix}. \tag{3.30}$$

This means that when $j$ is broadcasting from time $t_j{+}1$ to $t_j{+}K$, the sequence of transmit powers it uses (as a column vector), over the $K$ time slots, is given by $\mathbf{P}^j \underline{\widetilde{g}}_j$. Finally, the local CSI estimate $\widetilde{g}_j$ is estimated at Transmitter $i$ as :

$$\underline{\widetilde{g}}_j^i = \frac{\mathbf{P}^{j\,-1}}{\widetilde{g}_{ji}} \left( \underline{\widetilde{\omega}}_i^j - \sigma^2 \underline{1} \right). \tag{3.31}$$

where $\widetilde{g}_{kj}^i$ denotes the estimate of the channel $g_{kj}$ by transmitter $i$. Of course, writing the above implicitly assumes that the coefficients $a_{ji}$ are chosen properly. Note that more advanced estimators such as the minimum mean square error (MMSE) or maximum likelihood (ML) estimators might be used but here, low complexity is prioritized. Normal requirements in terms of local CSI and RSSI qualities are the targeted operating conditions for the proposed technique. Once a global CSI estimate is available, it becomes

possible for Transmitter $i$, $i \in \{1, ..., K\}$, to maximize a common network performance criterion under the form

$$u(p_1, ..., p_K; \widetilde{\mathbf{G}}^i), \tag{3.32}$$

$\widetilde{\mathbf{G}}^i = \left[\underline{\widetilde{g}}_1^i \cdots \underline{\widetilde{g}}_K^i\right]$ being the global channel matrix estimate (this setup has been coined for distributed CSI and studied in [31]).

Compared to the local CSI exchange technique with discrete power levels, the CPM has two distinguishing technical features. First, the transmit power during the exploration phase is continuous. Thus, the proposed technique can be seen as a complementary technique for scenarios in which discrete power levels are not allowed. Additionally, the continuous power is chosen in a very specific manner, namely to be the linear combination of the channel gains. Second, only one transmitter is active at a time during the local CSI exchange phase, which makes the estimation procedure simple, but it is observed to be very efficient via simulations. To understand the underlying problem let us consider a special case $K = 3$ and Transmitter 1. When three users are active at a time and $g_{31} >> g_{21}$ it becomes difficult to recover $p_2$ from $\omega_1(t) = g_{11}p_1(t) + g_{21}p_2(t) + g_{31}p_3(t) + \sigma^2$. One drawback for only activating one transmitter at a time appears if only SINR feedback is available instead of RSSI feedback. In the presence of SINR feedback, at least two users have to be active at a time to allow information exchange in the power domain.

If one assumes that the number of required observations has to be equal to the number of unknowns to estimate, the local CSI exchange technique of [14] requires $K(K-1)$ time-slots. During this CSI exchange phase, regular communication occurs in parallel, but with potentially high interference. Under the same assumption, the technique proposed here requires $T = K^2$ time-slots for the exchange phase since each transmitter has $K$ channel gains to be exchanged and only one user is active at a time (regular communication is effectively time-division multiple access). For $K$ being respectively equal to 2, 3, and 4, this corresponds to an additional cost in terms of time-slots of 100%, 50%, and 33%. Indeed, the number of effectively interfering users using the same channel (meaning operating on the same frequency band, at the same period of time, in the same geographical area) will typically be small in practice and not exceed 3 or 4, which makes the number of time-slots of the exploration phase reasonable.

## 3.6 Numerical Performance Analysis

In this section, as a first step (Sec. 3.6.1), we start with providing simulations which result from the combined effects of Phases I and II. To make a coherent comparison with IWFA, the network utility will be evaluated without taking into account a cost possibly associated with the exploration or training phases (i.e., Phases I and II for the proposed scheme or the convergence time for IWFA). The results are provided for a reasonable scenario of small cell networks which is similar to those already studied in other works (see e.g., [32] for a recent work). As a second step (Sec. 3.6.2 and 3.6.3), we study special cases to better understand the influence of each estimation phase and the different parameters which impact the system performance.

### 3.6.1 Global performance analysis : a simple small cell network scenario

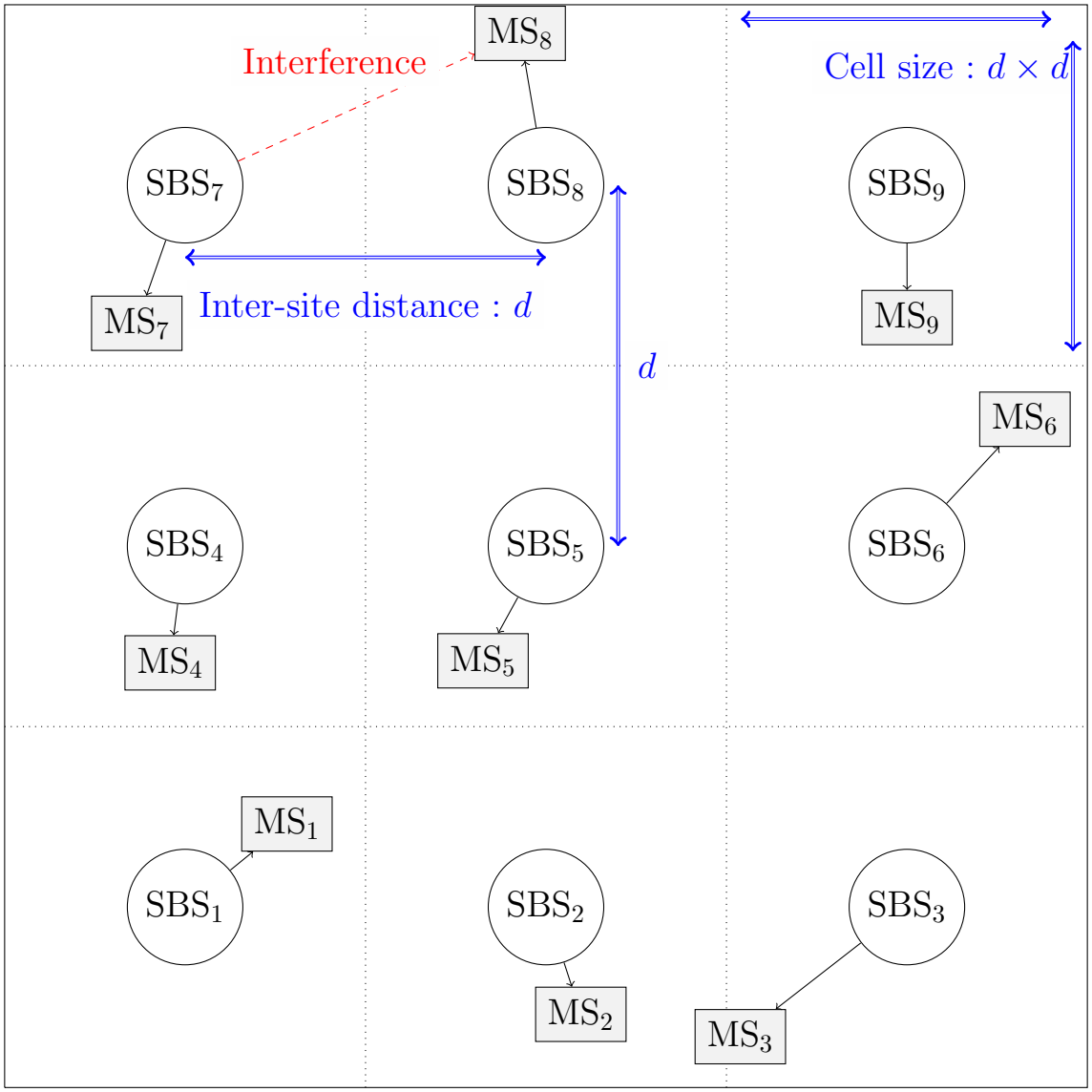


FIGURE 3.3 – Small cell network configuration assumed in Sec. 3.6.1

As shown in Fig. 2.3, the considered scenario assumes $K = 9$ small cell base stations with maximal transmit power $P_{\max} = 30$ dBm. One or two bands are assumed, depending on the scenario considered. In this subsection, discrete power modulation is used to exchange local CSI and only two users are active at any given time-slot in Phase II. One user per cell is assumed, which corresponds to a possible scenario in practice (see e.g., [32][33][34]). We also use this setup to be able to compare the proposed scheme with IWFA whose performance is generally assessed for the most conventional form of the interference channel, namely, $K$ transmitter-receiver pairs. The normalized receive noise power is $\sigma^2 = 0$ dBm. This corresponds to SNR(dB) = 30 where the *signal-to-noise ratio*

is defined by

$$\mathrm{SNR(dB)} = 10\log_{10}\left(\frac{P_{\max}}{\sigma^2}\right). \tag{3.33}$$

Here and in all the simulation section, we set the SNR to 30 dB by default. RS power measurements are quantized uniformly in a dB scale with $N = 8$ bits and the quantizer input dynamics or range in dB is $[\mathrm{SNR(dB)}-20, \mathrm{SNR(dB)}+10]$. The DMC $\Gamma$ is constructed with error probability $\epsilon$ to the two nearest neighbors, i.e., for the symbols $\mathrm{w}_1 < \mathrm{w}_2 < \cdots < \mathrm{w}_M$ (with $M = 2^N$), $\Gamma(\mathrm{w}_i|\mathrm{w}_j) = \epsilon$ if $|i-j| = 1$ and $\Gamma(\mathrm{w}_i|\mathrm{w}_j) = 0$ if $|i-j| > 1$. In this subsection $\epsilon = 1\%$; the quantity $\epsilon$ will be referred to as the *feedback channel symbol error rate* (FCSER). For all $(i,j)$ and $s$ ($s$ always being the band index) the channel gain $g_{ij}^s$ on band $s$ is assumed to be exponentially distributed namely, its p.d.f. writes as $\phi_{ij}^s(g_{ij}^s) = \frac{1}{\mathbb{E}[g_{ij}^s]}\exp\left(-\frac{g_{ij}^s}{\mathbb{E}[g_{ij}^s]}\right)$; this corresponds to the well-known Rayleigh fading assumption. Here, $\mathbb{E}(g_{ij}^s)$ models the path loss effects for the link $ij$ and depends of the distance as follows : $\mathbb{E}(g_{ij}^s) = \left(\frac{d_0}{d_{ij}}\right)^2$ where $d_{ij}$ is the distance between Transmitter $i$ and Receiver $j$ and $d_0 = 5$ m is a normalization factor. The normalized coordinates of the mobile stations $\mathrm{MS}_1, ..., \mathrm{MS}_9$ are respectively given by : $(3.8, 3.2)$, $(7.9, 1.4)$, $(10.2, 0.7)$, $(2.3, 5.9)$, $(6.6, 5.9)$, $(14.1, 9.3)$, $(1.8, 10.6)$, $(7.1, 14.6)$, $(12.5, 10.7)$; the real coordinates are obtained by multiplying the former by the ratio $\frac{\mathrm{ISD}}{d_0}$, ISD being the inter site distance. In this subsection, the system performance is assessed in terms of sum-rate, the *sum-rate* being given by :

$$u^{\text{sum-rate}}(\underline{p}_1, ..., \underline{p}_K; \mathbf{G}) = \sum_{i=1}^{K}\sum_{s=1}^{S}\log(1 + \mathrm{SINR}_i^s(\underline{p}_1, ..., \underline{p}_K; \mathbf{G})). \tag{3.34}$$

where $\underline{p}_i = (p_i^1, ..., p_i^S)$ represents the power allocation vector of Transmitter $i$, $\mathrm{SINR}_i^s$ is the SINR at Receiver $i$ in band $s$ and expresses as $\mathrm{SINR}_i^s = \dfrac{g_{ii}^s p_i^s}{\sigma^2 + \sum\limits_{j\neq i} g_{ji}^s p_j^s}$.

Fig. 3.4a, represents the average sum-rate against the ISD. The sum-rate is averaged over $10^4$ realizations of the channel gain matrix $\mathbf{G}$ and the *inter site distance* is the distance between two neighboring small base stations. Three curves are represented. The top curve corresponds to the performance of the sequential best-response dynamics applied to the sum-rate (referred to as *Team BRD*) in the presence of perfect global CSI. The curve in the middle corresponds to Team BRD which uses the estimate obtained by using the most simple association proposed in this chapter namely, LSPD for Phase I and the $2-$bit MEQ for Phase II. The LSPD estimator uses $K$ time-slots and the $K-$dimensional identity matrix $\mathbf{P}_{\mathrm{I}} = P_{\max}\mathbf{I}_K$ for the training matrix. The $2-$bit MEQ uses binary power control ($L = 2$) and $2K$ time-slots to send the information, i.e., $\underline{g}_i$); this corresponds to the typical number of time-slots IWFA needs to converge. At last, the bottom curve corresponds to IWFA using local CSI estimates provided by Phase I. It is seen that about 50% of the gap between IWFA and Team BRD with perfect CSI can be bridged by using the proposed estimation procedure. When the interference level is higher, the gap becomes larger. Fig. 3.4b depicts exactly the same scenario as Fig. 3.4a except that only one band is available to the small cells i.e., $S = 1$. Here the gap can be bridged at about 65% when using Team BRD with the proposed estimation procedure.

In this subsection, some choices have been made : a diagonal training matrix and the LSPD estimator has been chosen for Phase I and the MEQ has been chosen for Phase II.

The purpose of the next subsections is to explain these choices, and to better identify the strengths and weaknesses of the proposed estimation procedures.

### 3.6.2 Comparison of estimation techniques for Phase I

In Phase I, there are two main issues to be addressed : the choice of the estimator and the choice of the training matrix $\mathbf{P}_{\mathrm{I}}$. To compare the LSPD and MMSEPD estimators, we first consider the estimation SNR (ESNR) as the performance criterion to compare them. The *estimation SNR* of Transmitter $i$ is defined here for the case $S = 1$ and is given by :

$$\mathrm{ESNR}_i = \frac{\mathbb{E}[\|\mathbf{G}\|^2]}{\mathbb{E}[\|\mathbf{G} - \widetilde{\mathbf{G}}_i\|^2]}. \tag{3.35}$$

where $\|.\|^2$ stands for the Frobenius norm and $\widetilde{\mathbf{G}}_i$ is the global channel estimate which is available to Transmitter $i$ after Phases I and II. In this subsection, we always assume a perfect exchange in Phase II to conduct the different comparisons. This choice is made to isolate the impact of Phase I estimation techniques on the estimation SNR and the utility functions which are considered for the exploitation phase. After extensive simulations, we have observed that the gain in terms of ESIR by using the best training matrix (computed by an exhaustive search over all the matrix elements) is found to be either negligible or quite small when compared to the best diagonal training matrix (computed by an exhaustive search over the diagonal elements) ; see e.g., Fig. 3.5 for such a simulation. Therefore, for the rest of this chapter, we will restrict our attention to diagonal training matrices for reducing the computational complexity without any significant performance loss. To conclude about the choice of the training matrix, we assess the impact of using power levels to learn local CSI instead of using them to optimize the performance of Phase I. For this, we compare in Fig. 3.6 the scenario in which a diagonal training matrix is used to learn local CSI, with the scenario in which the best training matrix in the sense of the expected sum-rate (over Phase I). Global channel distribution information is assumed to be available in the latter scenario. The corresponding choice is feasible computationally speaking for small systems.

Fig. 3.7 represents for $K = 2$, $S = 1$, and $\mathrm{SNR(dB)} = 30$, the estimation SNR (in dB) against the signal-to-interference ratio (SIR) in dB SIR(dB) which is defined here as

$$\mathrm{SIR(dB)} = 10\log_{10}\left(\frac{\mathbb{E}(g_{11})}{\mathbb{E}(g_{21})}\right) = 10\log_{10}\left(\frac{\mathbb{E}(g_{22})}{\mathbb{E}(g_{12})}\right). \tag{3.36}$$

The three curves in red solid lines represent the MMSEPD estimator performance while the three curves in blue dashed line represent the LSPD estimator performance. The performance gap between MMSEPD and LSPD depends on the quality of the RSSI at the transmitters. When RS power measurements are quantized with $N = 8$ bits and the feedback channel symbol error rate is $\epsilon = 1\%$, the gap in dB is very close to 0. Using MMSEPD instead of LSPD becomes much more relevant in terms of ESNR when the quality of feedback is degraded. Indeed, for $N = 2$ bits and $\epsilon = 10\%$, the gap is about 5 dB. Note that having a very small number of RSSI quantization bits and therefore significant feedback quality degradation may also occur in classical wireless systems where the feedback would be binary such as an ACK/NACK feedback. Indeed, an ACK/NACK feedback can be seen as the result of a $1-$bit quantization of the RSSI or SINR. The

proposed technique might be used to coordinate the transmitters just based on this particular and rough feedback. Even though the noise on the RSSI is correlated with the signal and is not Gaussian, we observe that MMSEPD and LSPD (which can be seen as a zero-forcing solution) perform similarly when the noise becomes negligible. At last note that the ESNR is seen to be independent of the SIR ; this can be explained by the used training matrix, which is diagonal.

The above comparison is conducted in terms of ESNR but not in terms of final utility. To assess the impact of Phase I on the exploration phase, two common utility functions are considered namely, the sum-rate and the *sum-energy-efficiency* (sum-EE) which is defined as :

$$u^{\text{sum-EE}}(\underline{p}_1, ..., \underline{p}_K; \mathbf{G}) = \sum_{i=1}^{K} \frac{\sum_{s=1}^{S} f(\text{SINR}_i^s(\underline{p}_1, ..., \underline{p}_K; \mathbf{G}))}{\sum_{s=1}^{S} p_i^s}. \tag{3.37}$$

where the same notations as in (3.34) are used ; $f$ is an efficiency function which represents the packet success rate or the probability of having no outage. Indeed, the utility function $u^{\text{sum-EE}}$ corresponds to the ratio of the packet success rate to the consumed transmit power and has been used in many papers (see e.g., [3][35][36][37][38]). Here we choose the efficiency function of [35] : $f(x) = \exp\left(-\frac{c}{x}\right)$ with $c = 2^r - 1 = 1$, $r$ being the spectral efficiency. Fig. 3.8 depicts for $K = 2$, $S = 1$, $N = 2$, $\epsilon = 10\%$ the *average relative utility loss* $\Delta u$ in % against the SIR in dB. The average relative utility loss in % is defined by

$$\Delta u(\%) = 100\mathbb{E}\left[\frac{u(\underline{p}_1^\star, ..., \underline{p}_K^\star; \mathbf{G}) - u(\widetilde{\underline{p}}_1^\star, ..., \widetilde{\underline{p}}_K^\star; \mathbf{G})}{u(\underline{p}_1^\star, ..., \underline{p}_K^\star; \mathbf{G})}\right]. \tag{3.38}$$

where $u(\underline{p}_1^\star, ..., \underline{p}_K^\star; \mathbf{G})$ is the best sum-utility which can be attained when every realization of $\mathbf{G}$ is known perfectly. The latter is obtained by performing exhaustive search over 100 values equally spaced in $[0, P_{\max}]$ and this for each draw of $\mathbf{G}$ ; the average is obtained from $10^4$ independent draws of $\mathbf{G}$. The utility $u(\widetilde{\underline{p}}_1^\star, ..., \widetilde{\underline{p}}_K^\star; \mathbf{G})$ is also obtained with exhaustive search but by using either the LSPD or MMSEPD estimator and assuming Phase II to be perfect. Fig. 3.8 shows that even under severe conditions in terms observing the RS power at the transmitter, the MMSEPD and LSPD estimators have the same performance in terms of sum-rate. This holds even though the gap in terms of ESNR is 5 dB (see Fig. 3.7). Note that the relative utility loss is about 3% showing that the sum-rate performance criterion is very robust against channel estimation errors. When one considers the sum-EE, the relative utility loss becomes higher and is the range $15\% - 20\%$ and the gap between MMSEPD and LSPD becomes more apparent this time and equals about 5%. The observations made for the special setting considered here have been checked to be quite general and apply for more users, more bands, and other propagation scenarios : unless the RSSI is very noisy or when only an ACK/NACK-type feedback is available, the MMSEPD and LSPD estimators perform quite similarly. Since the MMSEPD estimator requires more knowledge and more computational complexity to be implemented, the LSPD estimator seems to be the best choice when the quality of RSSI is good as it is in current cellular and Wifi systems.

To conclude this subsection, we provide the counterpart of Fig. 3.6 for phase II in Fig. 3.9. The scenario in which a diagonal training matrix is used to exchange local CSI,

with the scenario in which power control is to maximize the expected sum-rate (over Phase II). But here, the expectation is not taken over local CSI since it is assumed to be known. The corresponding choice is feasible computationally speaking for small systems.

### 3.6.3 Comparison of quantization techniques for discrete power modulation

In this subsection, we assume Phase I to be perfect. Again, this choice is made to isolate the impact of Phase II estimation techniques on the estimation SNR and the utility functions which are considered for the exploitation phase. When $L = 2$ and we quantize with 1-bit, we map the smallest representative of the quantizer to the lowest power and the largest to the highest power level in $\mathcal{P}$ and the other element. If $L > 2$, the power levels belong to the set $\left\{0, \frac{1}{L-1}P_{\max}, \frac{2}{L-1}P_{\max}, ..., P_{\max}\right\}$ are picked and the representatives are mapped in the order corresponding to their value. In Phase II, the most relevant techniques to be determined is the quantization of the channel gains estimated through Phase I.

For $K = 2$ users, $S = 1$ band, $L = 2$ power levels, and SNR(dB) = 30, Fig. 3.10 provides ESNR(dB) versus SIR(dB) for the three channel gain quantizers mentioned in this chapter : ALMA, LMA, and MEQ. The three quantizers are assumed to quantize the channel gains with only 1 bit. Since only two power levels are exploited over Phase II, this means that the local CSI exchange phase (Phase II) comprises $K$ time-slots. The three top curves of Fig. 3.10 correspond to $N = 8$ RS power quantization bits and $\epsilon = 1\%$ while the three bottom curves correspond to $N = 2$ bits and $\epsilon = 10\%$. First of all, it is seen that the obtained values for ESNR are much lower than for Phase I. Even in the case where $N = 8$ and $\epsilon = 1\%$, the ESNR is around 10 dB whereas it was about 40 dB for Phase I. This shows that the limiting factor for the global estimation accuracy will come from Phase II ; additional comments on this point are provided at the end of this subsection. Secondly, Fig. 3.10 shows the advantages offered by the proposed ALMA over the conventional LMA.

Fig. 3.11 depicts for $K = 2$, $S = 1$, $N = 8$, $\epsilon = 1\%$ the average relative utility loss $\Delta u$ in % against the SIR in dB for ALMA and MEQ. The two bottom (resp. top) curves correspond to the sum-rate (resp. sum-EE). The relative utility loss is seen to be comparable to the one obtained for Phase I. Interestingly, MEQ is seen to induce less performance losses than ALMA, showing that the ENSR or distortion does not perfectly reflect the need in terms optimality for the exploration phase. This observation partly explains why we have chosen MEQ in Sec. 3.6.1 for the global performance evaluation ; many other simulations (which involve various values for $K$, $N$, $S$, $\epsilon$, etc) not provided here confirm this observation.

An important comment made previously is that Phase II constitutes the bottleneck in terms of estimation accuracy for the final global CSI estimate available for the exploitation phase. Here, we provide more details about this limitation. Indeed, even when the quality of the RSSI is good, the ESNR only reaches 10 dB and even increasing the quantization bits by increasing the power modulation levels or time slots used does not improve the ESNR as demonstrated by the following figures.

For $N = 8$ RS power quantization bits and $\epsilon = 1\%$, SNR(dB) = 30, Fig. 3.12a shows

the ESNR versus the number of channel quantization bits used by MEQ. It is seen that the ESNR reaches a maximum whether a high interference scenario (SIR(dB) = 0) or a low interference scenario (SIR(dB) = 10) is considered. In Fig. 3.10, the ESNR was about 9 dB when the 1−bit MEQ is used and the SIR equals 0 dB. Here we retrieve this value and see that the ESNR can reach 13 dB when the 4−bit MEQ is implemented, meaning that 16 power levels are used in Phase II. Now, when the SIR is higher, using the 2−bit MEQ is almost optimal. If the RSSI quality degrades, then using only 1 or 2 bits for MEQ is always the best configuration.

Another approach would be to increase the number of channel gain quantization bits and still only use two power levels over Phase II by increasing the number of time-slots used in Phase II. Fig. 3.12b assumes exactly the same setup as Fig. 3.12a but here it represents the ESNR as a function of the number of time-slots used in Phase II. Here again, an optimal number of time-slots appears for the same reason as for Fig. 3.12a. Both for Fig. 3.12a and Fig. 3.12b, one might wonder why the ESNR is better when the interference is high. This is due to the fact that when the interference is very low, the decoding operation of the power levels of the others becomes less reliable. The existence of maximum points in Fig. 3.12a and Fig. 3.12b precisely translates the tradeoff between the channel gain quantization noise and power level decoding errors.

### 3.6.4 Comparison between Continuous power modulation and Discrete power modulation

In this subsection, we chose the parameters $g_{ij}^{\min} = 0.01\mathbb{E}(g_{ij})$, $g_{ij}^{\max} = 5\mathbb{E}(g_{ij})$ (when $i \neq j$) and $\mathbb{E}(g_{ii}) = 1$, with $\mathbb{E}(g_{ij})$ determined by the SIR indicated. The channel gain dynamics $\frac{g_{ij}^{\max}}{g_{ij}^{\min}}$ is thus equal to 27 dB, which is a quite typical value in real systems. The ESNR is obtained by averaging over $10^4$ realizations for the channel matrix, the channel gains being chosen independently and according to an exponential law $\phi_{ij}(g_{ij}) = \frac{1}{\mathbb{E}(g_{ij})} \exp\left(-\frac{g_{ij}}{\mathbb{E}(g_{ij})}\right)$ (that is, Rayleigh fading is assumed). The local CSI estimates are assumed to be perfectly known.

**Influence of the choice of the parameters $a_{ij}(t)$.** First, we study the impact of the choice of the matrix $\mathbf{P}^j$ on the ESNR. Denote by $\mathbf{A}^j$ the matrix whose entries are the coefficients $a_{ij}(t)$ for all $t \in \{t_j + 1, \ldots, t_j + K\}$, i.e.,

$$\mathbf{A}^j = \begin{pmatrix} a_{1j}(t_j+1) & \ldots & a_{Kj}(t_j+1) \\ \vdots & \vdots & \vdots \\ a_{1j}(t_j+K) & \ldots & a_{Kj}(t_j+K) \end{pmatrix}. \tag{3.39}$$

Interestingly, for typical scenarios, the particular choice $\mathbf{A}^j = \mathbf{I}$ only induces a quite small performance loss with respect to the optimal choice e.g., measured in terms of ESNR. In this respect, we perform simulations to compare the ENSR obtained by choosing the best possible $\mathbf{A}^j$ over that of choosing $\mathbf{A}^j = \mathbf{I}$, for all $j$. For $S = 1$, $K = 2$, $N = 8$, $\varepsilon = 1\%$, SNR(dB) = 30, and SIR(dB) = 10 our comparison has shown that choosing the best matrix only provides marginal improvements. Indeed, for typical values for the SIR (say above 5 dB), estimating the cross-channel gains reliably lead to matrices which are quite similar to the identity matrix; otherwise, the influence of the cross-channel gains

in the sum (1) or in the RS power might be dominated by that of the direct channel. Therefore, for the rest of this section, we will choose $\mathbf{A}^j = \mathbf{I}$ for all $j$, as this choice results in a very low complexity technique and guarantees the invertibility of the power matrix in (7).

**Continuous power modulation Versus Discrete power modulation** We compare the performance in terms of sum-rate between the continuous power modulation and the discrete power modulation in Fig. 3.13. We consider the parameters $K = 4$ (number of users), $S = 2$ bands, perfect *local* CSI estimate and SIR(dB) = 10. The RSSI feedback is assumed to be with $N = 8$ bits and $\varepsilon = 0.01$. We compare the performance measured by the sum-rate using CSI exchange using our proposed scheme, of CPM, with that of : 1) perfect global CSI (ideal case) ; 2)local CSI exchange using a discrete power modulation based on Lloyd-Max quantization (as in [14]) with 2 or 16 quantization levels ; 3) the iterative water-filling algorithm (IWFA). When global CSI is available (perfect or otherwise), we implement a *team best response dynamics (BRD)*[3] to select the power control, where each transmitter uses the CSI available for the BRD. In the case of IWFA, no exchange of local CSI is required (no phase II), but there is a time taken for the algorithm to converge. This figure demonstrates the performance improvement offered by our proposed modulation technique in terms of sum-rate, and we can observe that the team-BRD with CPM achieves a sum-rate that is very close to that with perfect global CSI (which is the ideal case).

Fig. 3.14 represents the ESNR in dB against the SIR in dB and assumes a similar setting to Fig. 3.13 except that here, SNR(dB) = 30, $K = 2$ users and $S = 1$ bands. Three scenarios are considered : $(N, \varepsilon) = (8, 1\%)$, $(N, \varepsilon) = (4, 5\%)$, and $(N, \varepsilon) = (1, 5\%)$. The first scenario corresponds to typical conditions in terms of quality for the RSSI, while the two others correspond to quite severe conditions. The scenario with only one RS power quantization bit can be seen as a scenario with an ACK/NACK feedback. For each scenario, two schemes are compared : the scheme with continuous power levels and the one with discrete power modulation which relies on channel gain quantization (here with 1 or 4 bits), discrete power modulation with $L$ levels and lattice decoding. In Fig. 3.14 we compare with the case of $L = 2$.

Fig. 3.14 clearly shows that the CPM provides a performance in terms of ESNR, which is independent of the SIR level ; this is one of the effects of using time-sharing in the exploration phase. When the quality of the RSSI is good, it is seen that the proposed technique provides a very significant gain in terms of ESNR ; the gain ranges from 10 dB to 25 dB, depending on the SIR level. It is only when the RSSI quality is severely degraded (namely, when $(N, \varepsilon) = (1, 5\%)$) that the proposed technique does not perform well when compared to the discrete power modulation when using $L = 2$ (as seen in Fig. 3.14).

3. Team BRD for sum-rate with power control implies that each transmitter iteratively updates its best transmit power given the other transmit powers until all the powers converge. Since global CSI is available, each transmitter can do this offline by assuming an arbitrary initial power vector and with perfect global CSI, all transmitters will converge to the same equilibrium.

## 3.7 Conclusion

First, we would like to remind a few comments about the scope and originality of this chapter. One of the purposes of this chapter is to show that the sole knowledge of the received power or SINR feedback is sufficient to recover global CSI. The proposed technique comprises two phases. Phase I allows each transmitter to estimate local CSI. Obviously, if there already exists a dedicated feedback or signalling channel which allows the transmitter to estimate local CSI, Phase I may be skipped. But even in the latter situation, the problem remains to know how to exchange local CSI among the transmitters. Phase II proposes a completely new solution for exchanging local CSI, namely using power modulation (discrete or continuous). Discrete power modulation is based in particular on a robust quantization scheme of the local channel gains. Therefore it is robust against perturbations on the received power measurements ; it might even be used for $1-$bit RSSI which would correspond to an ACK/NACK-type feedback, showing that even a rough feedback channel may help the transmitters to coordinate. When the RSSI quality is good and local CSI is well estimated, continuous power modulation performs very well. Note that the proposed technique is general and can be used to exchange and kind of information and not only local CSI.

Second, we summarize here a few observations of practical interest. For Phase I, two estimators have been proposed for Phase I : the LSPD and the MMSEPD estimators. Simulations show that using the MMSEPD requires some statistical knowledge and is more complex, but is well motivated when the RS power is quantized roughly or the feedback channel is very noisy. Otherwise, the use of the LSPD estimator is shown to be sufficient. During Phase II, transmitters exchange local CSI by encoding it onto their power level and using interference as a communication channel. For discrete power modulation, three estimation schemes are provided which are in part based on one of the two quantizers ALMA and MEQ ; the quantizers are computed offline but are exploited online. MEQ seems to offer a good trade-off between complexity and performance in terms of sum-rate or sum-energy-efficiency. In contrast with Phase I in which the estimation SNR typically reaches 40 dB for good RS power measurements, the estimation SNR with discrete power modulation is typically around 10 dB. To improve the quality of local CSI exchange, the continuous power modulation scheme is proposed and it is shown to perform very well under normal conditions in terms of RSSI quality. In Phase III, having global CSI, each transmitter can apply the BRD to the sum-utility instead of applying it to an individual utility as IWFA does, resulting in a significant performance improvement as seen from our numerical results.

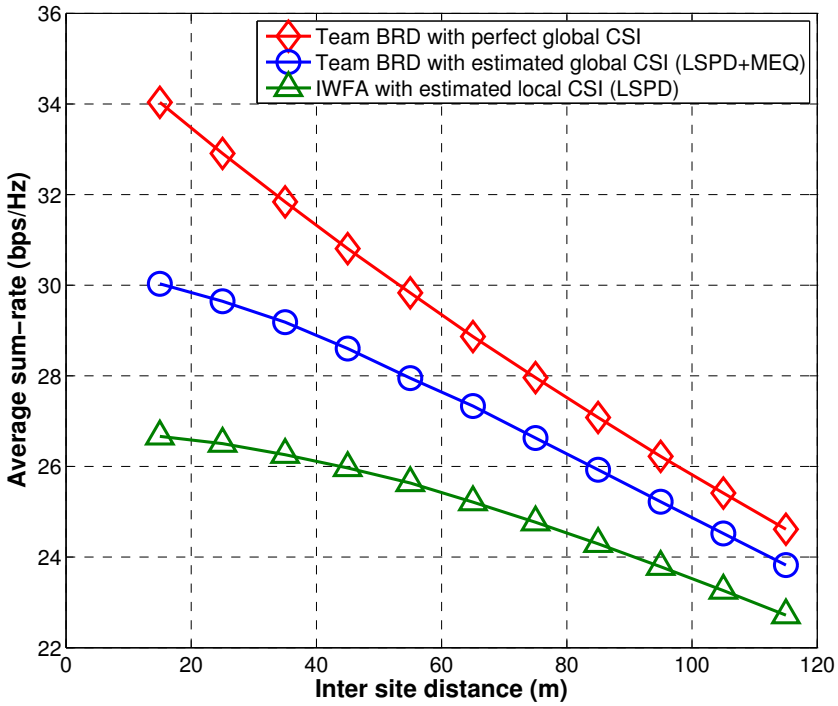


(a) $S = 2$

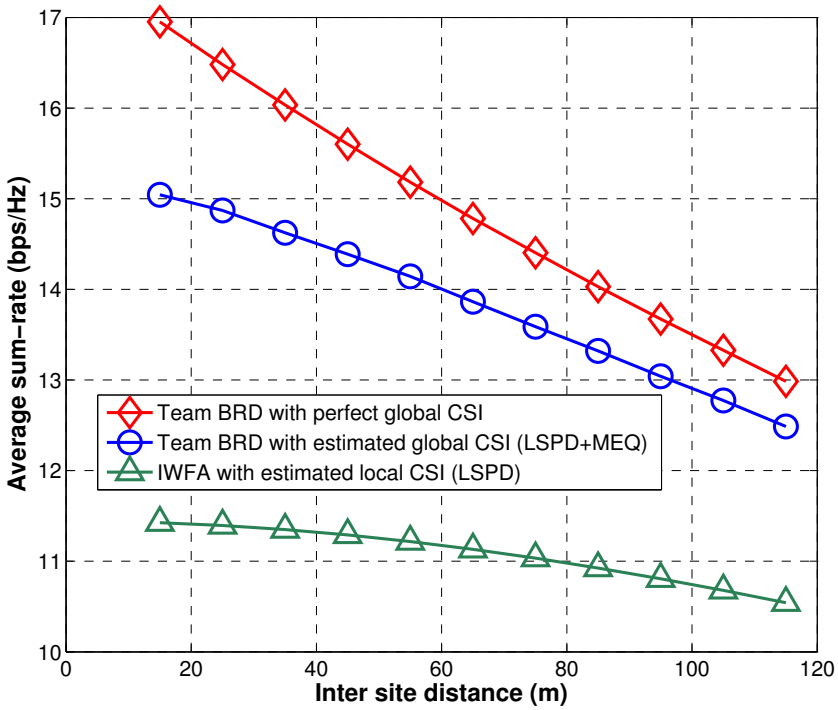


(b) $S = 1$

FIGURE 3.4 – The above curves are obtained in the scenario of Fig. 4 in which $K = 9$ transmitter-receiver pairs, SNR(dB) $= 30$, the FCSER is given by $\epsilon = 0.01$, $N = 8$ quantization bits for the RSSI, and $L = 2$ power levels. Using the most simple estimation schemes proposed in this chapter namely LSPD and MEQ can bridge the gap between the IWFA and the team BRD with perfect CSI, about 50% when $S = 2$ and about 65% when $S = 1$.

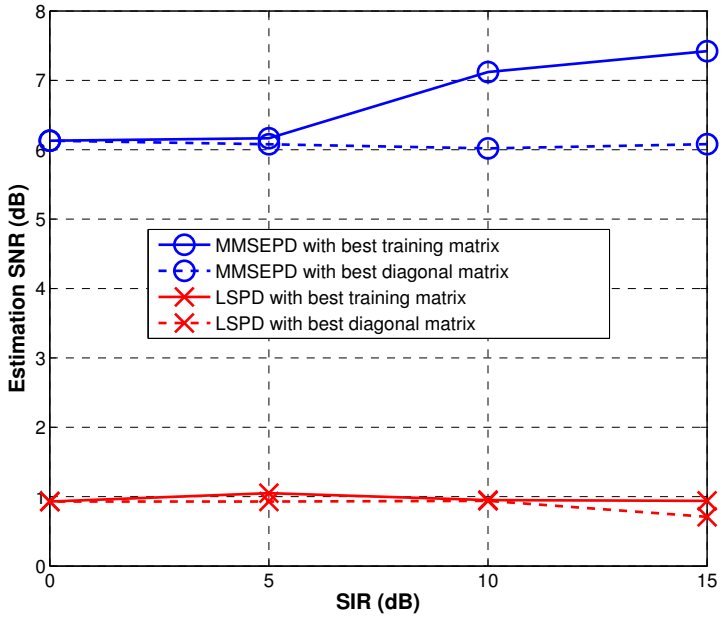


FIGURE 3.5 – Scenario : $K = 2$, $S = 1$, and SNR(dB) $= 30$, $\epsilon = 0$, $N = 2$ quantization bits. Using a diagonal training matrix typically induces a small performance loss in terms of ESNR even in worst-case scenarios.

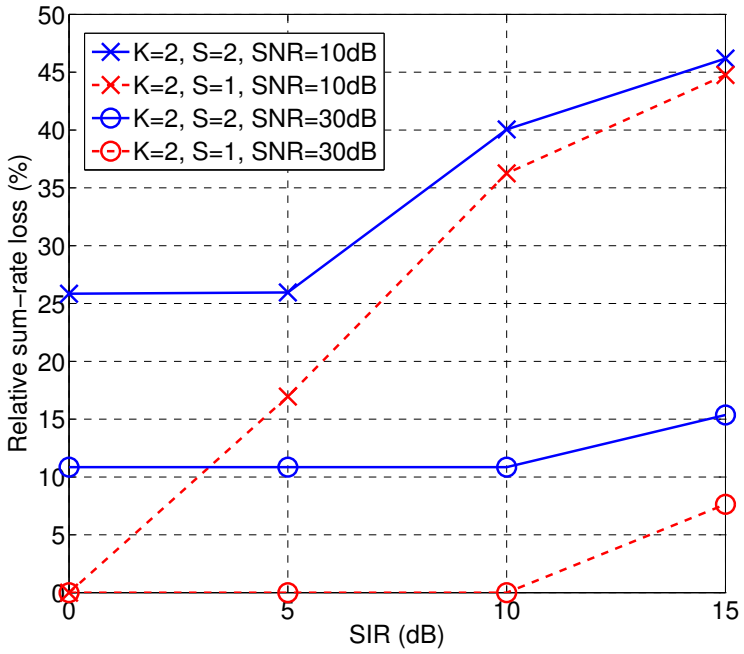


FIGURE 3.6 – Optimality loss induced in Phase I when using power levels to learn local CSI instead of maximizing the expected sum-rate. This loss may be influential on the average performance when the number of time-slots of the exploitation phase is not large enough.

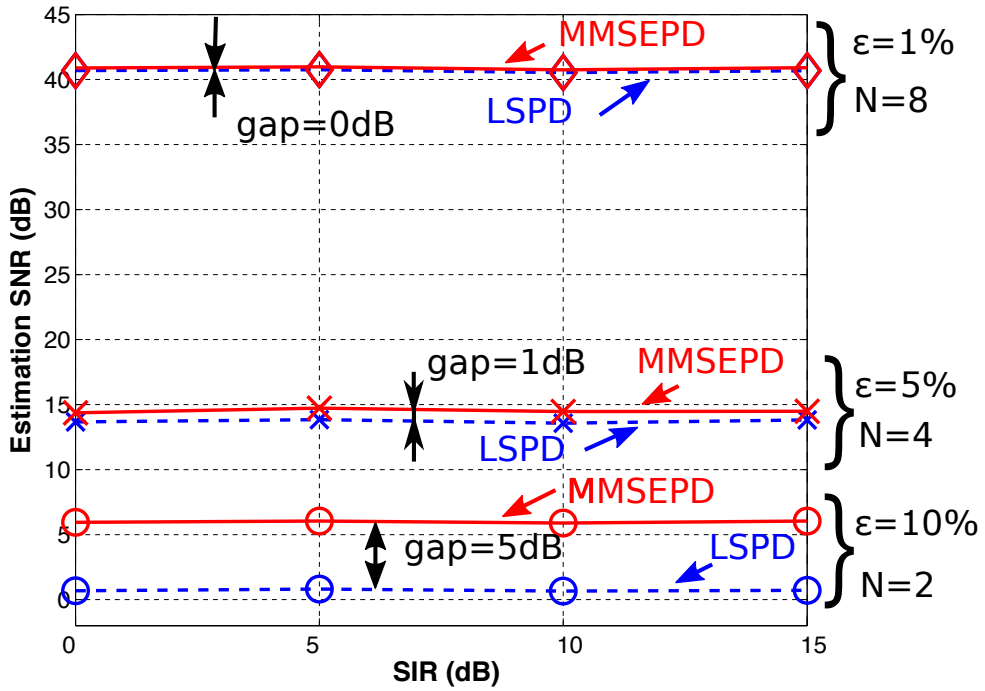


FIGURE 3.7 – Using MMSEPD instead of LSPD in Phase I becomes useful in terms of ESNR when the RSSI quality becomes too rough (bottom curves).

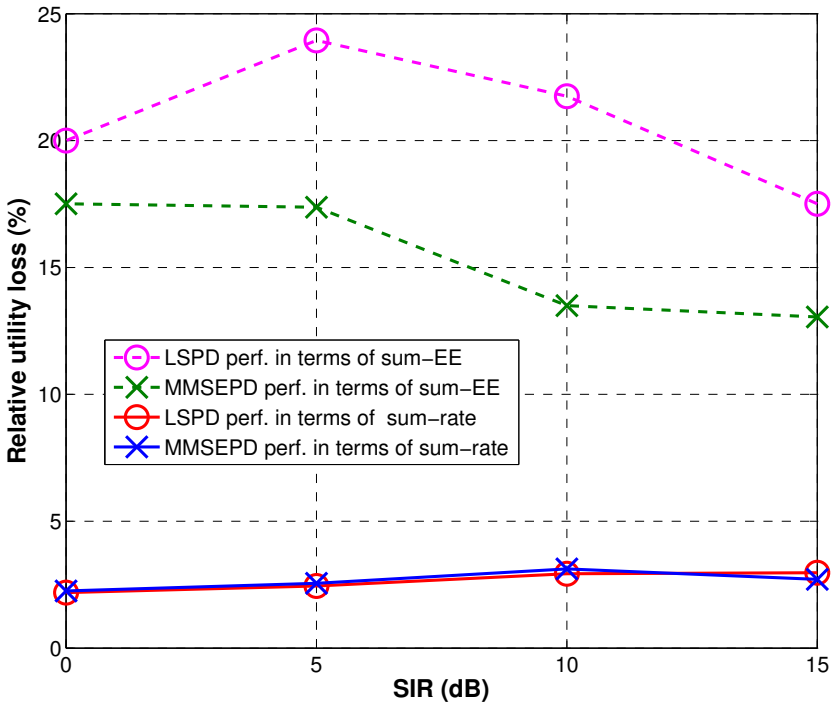


FIGURE 3.8 – The figure provides the relative utility loss under quite severe conditions in terms of RSSI quality ($N = 2$, $\epsilon = 10\%$).

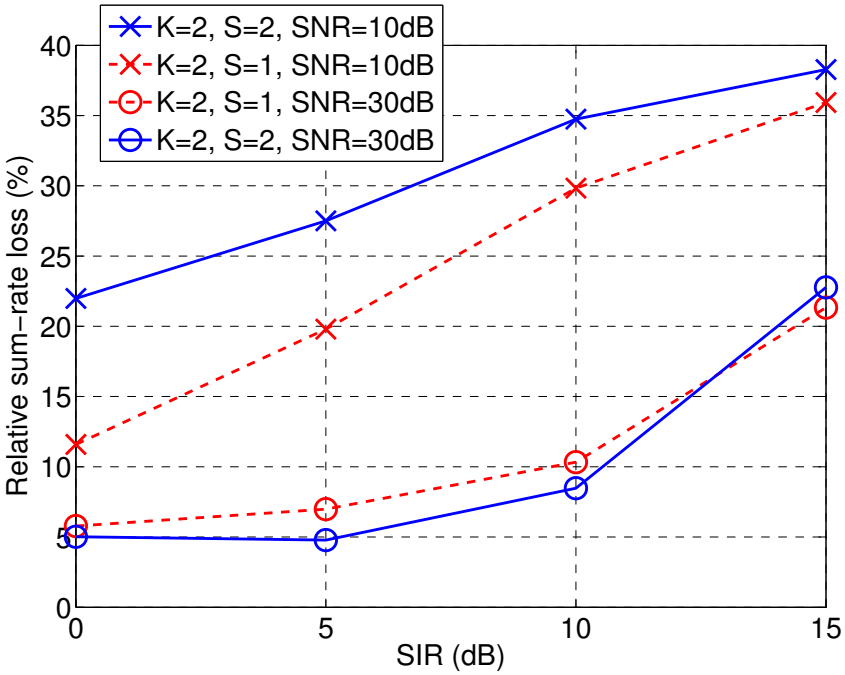


FIGURE 3.9 – Optimality loss induced in Phase II when using power levels to exchange local CSI instead of maximizing the expected sum-rate. This loss may be influential on the average performance when the number of time-slots of the exploitation phase is not large enough.

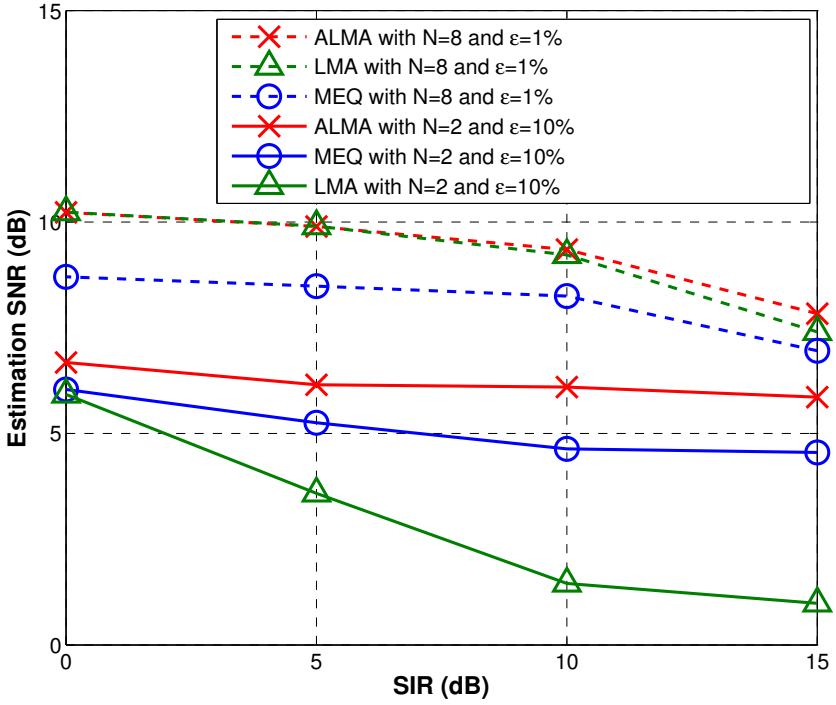


FIGURE 3.10 – Performance measured by ESNR considering good (three top curves) and bad (three bottom curves) RSSI quality conditions.

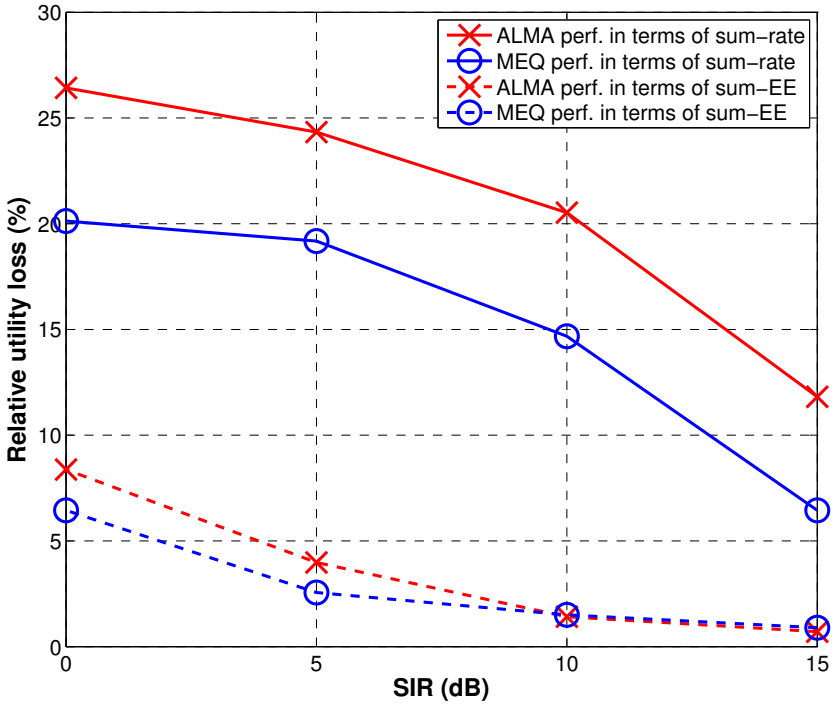


FIGURE 3.11 – Performance measured by relative utility loss, with utility being the sum-EE or sum-rate.

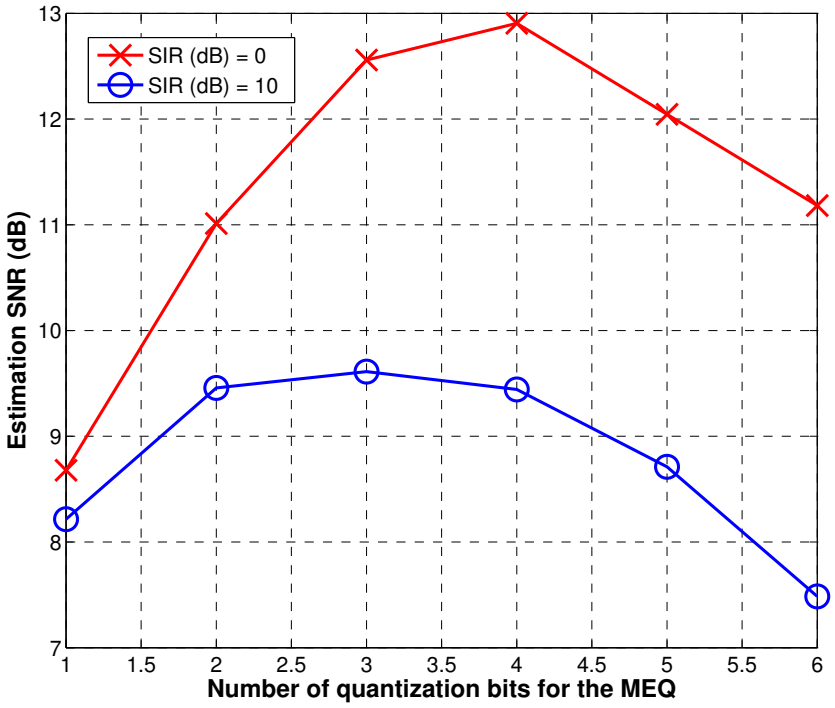


(a) ESNR against quantization bits used in MEQ.

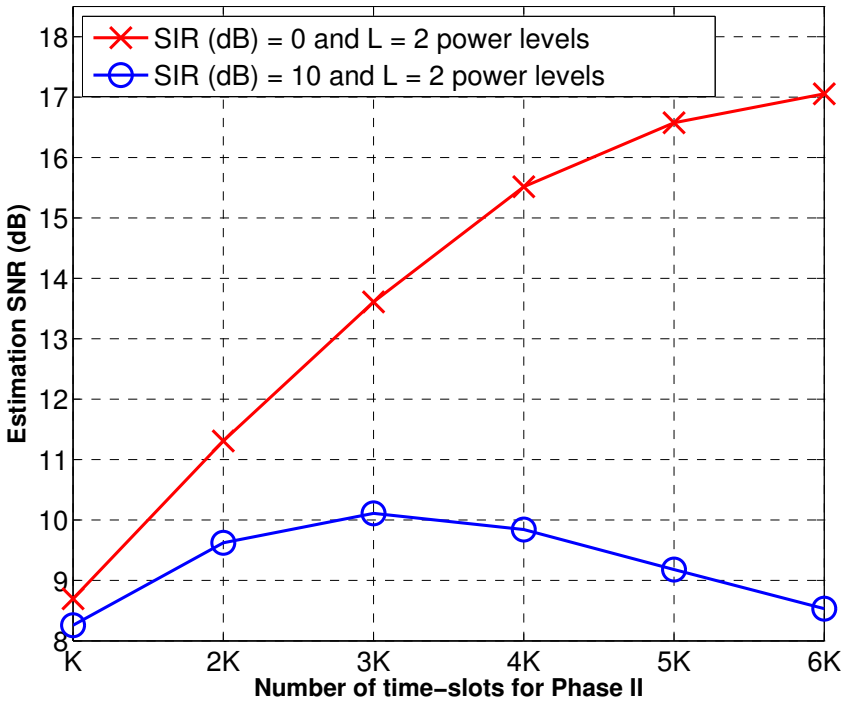


(b) ESNR against $T_{\mathrm{II}}$

FIGURE 3.12 – The power level decoding scheme proposed in this chapter is simple and has the advantage of being usable for the SINR feedback instead of RSSI feedback. However, the proposed scheme exhibits a limitation in terms of coordination ability when the inference is very low. The consequence of this is the existence of a maximum ESNR for Phase II. Here we observe that despite increasing the number of quantization bits or time slots used, the ESNR is bounded.

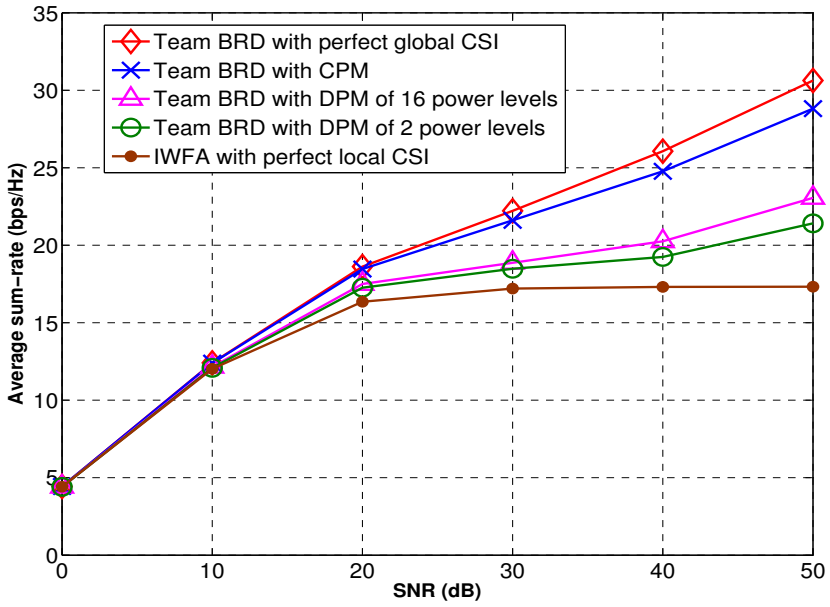


FIGURE 3.13 – Comparison of average sum-rate between CPM with DPM. We observe that CPM results in an average sum-rate that is very close to the ideal case of perfect global CSI.

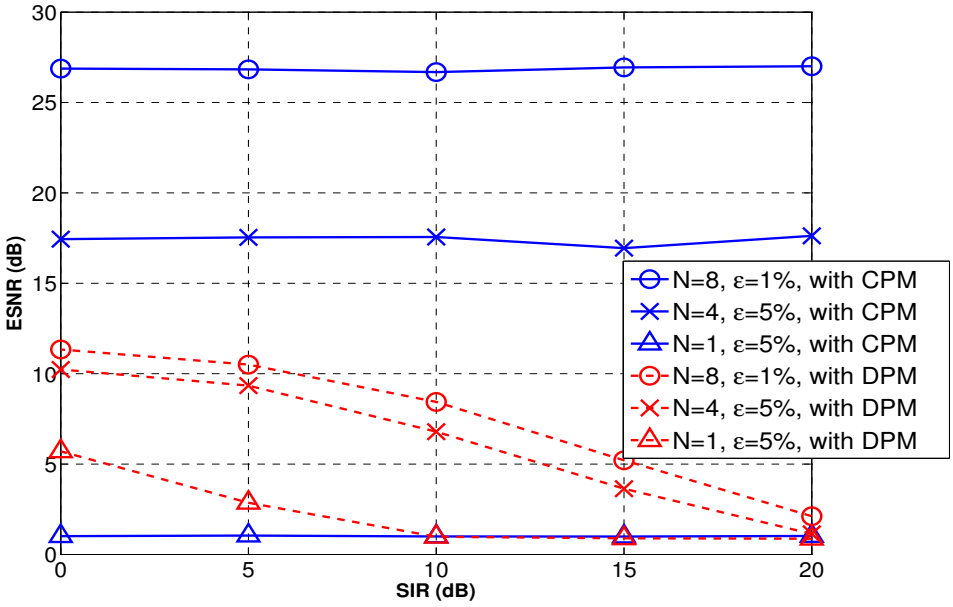


FIGURE 3.14 – ESNR against SIR. Using continuous power modulation to exchange local CSI appears to be a relevant choice when the RSSI quality is good or even medium. Under severe conditions (e.g., when only an ACK/NACK-type feedback is available for estimating the channel), quantizing the channel gains and power modulating the corresponding labels with discrete power levels is more appropriate.

# 4

# Efficient distributed power control in interference networks

The goal of this chapter is to contribute to finding power control strategies which exploit as well as possible the available information about the global channel state ; the available information considered here for the considered scenarios is mainly local and may be noisy. Differing from the technique proposed in the last section, which can acquire global channel state information by using power modulation, a framework on power control based on local information is proposed here. As a suited way of measuring the global efficiency of a power control scheme is to use the average utility region, we first tackle the problem of characterizing the feasible utility region. We provide the average utility region characterization for any power control problem for which the channel state is i.i.d. and the observation structure is memoryless. Second, the corresponding theorem is exploited to obtain an iterative algorithm which provides memoryless and stationary power control strategies (strategies therefore boil down to **one-shot** decision functions). Although the proposed algorithm is not proved to be optimal in terms of weighted sum-utility, many simulations show that it performs very well for classical utility functions (e.g., the sum energy-efficiency, the sum-rate, the sum-goodput). Aside from **team power control** policies, we also propose a selfish power control scheme. Indeed we study a multi-band interference network in the presence of multiple utility functions. One of the key insights we have found is that restricting the choices in terms of allowed power allocation vectors for the transmitters may be beneficial for both the individual and network performance, proving a Braess paradox. This result justifies a posteriori that using discrete action spaces instead of continuous action spaces may be a better choice for the performance. This also partly justifies why the iterative algorithm we propose to compute the one-shot decision functions has been assuming discrete action sets. This argument comes in addition to other arguments given in previous works such as [41] (binary power control) which shows that using small alphabets might induce zero or small optimality loss when compared to continuous alphabets.

## 4.1 Motivation and state of the art

Many modern wireless networks tend to become distributed. This is already the case of Wifi networks which are distributed decision-wise ; for example, each access point performs channel or band selection without the assistance of a central or coordinating node. As another example, small cells networks, which are envisioned to constitute one of the key components to implement the ambitious roadmap set for 5G networks [1][42][43], will need to be largely distributed ; distributedness is one way of dealing with complexity and signalling issues induced by the large number of small base stations and mobile stations. In this chapter, we consider wireless interference networks that are distributed both decision-wise and information-wise. More specifically, each transmitter has to perform a power control or resource allocation task by itself and by having only access to partial information of the network state.

When inspecting the literature on distributed power control (see e.g.,[2]), one can conclude that while the derived power control scheme is effectively distributed decision-wise and information-wise, it is not globally efficient. A natural and important question arises : is it because the considered power control scheme is not good enough or does it stem from intrinsic limitations such as information availability ? To the authors' knowledge, this question has not been addressed formally. One of the goals of the this chapter is precisely to provide a framework that allows one to derive the limiting performance of power control with partial information and therefore to be able to measure the efficiency of a given power control scheme. To reach this goal we resort to recent results that bridges the gap between decision theory and information theory [8]. We exploit these results to characterize the limiting performance in terms of long-term utility region, each transmitter being assumed to have its own utility function. The performance characterization is then exploited in a constructive manner to determine power control strategies and more specifically one-shot decision functions that is, functions that allow the transmitter to choose its power based on a single observation about the global channel state. To be concrete, if Transmitter $i$ knows an estimate $\widehat{g}_{ii}$ of the channel gain of the link between Transmitter $i$ and Receiver $i$, the decision function writes under the form $f_i(\widehat{g}_{ii})$. For example, in the famous work on energy-efficient power control [44], the obtained distributed decision function is of the form $f_i(x) = \frac{1}{x}$. Remarkably, our approach allows one to obtain decision functions which perform much better globally e.g., when measured in terms of sum energy-efficiency.

The developed approach mainly relies on two key assumptions : the global channel state is assumed to be i.i.d., which is a quite common assumption. The transmit power and channel state are assumed to be discrete. The latter assumption is less common and is supported by several strong arguments. First, assuming the transmit power to be discrete is of practical interest since there exist wireless communication standards in which the power can only be decreased or increased by step and in which quantized wireless channel state information (CSI) is used (see e.g., [31][45]) ; additionally, if the transmitter task is to perform band or channel selection, which is a special instance of power control, the transmitter action set is again intrisically discrete. Second, the argument is mathematical ; it is well known from the coding theorem literature [46] that the performance characterization for the continuous case follows as a special case of the discrete case. Third, quite remarkably, imposing the transmitters to use a reduced action space may be beneficial both for the network and individual performance ; simulations provided in this chapter shows that the very interesting result obtained in [41] is in fact

more general ; in [41], the authors show that binary power control may be optimal or generate a very small performance loss compared to the continuous case. In this respect, the authors have shown in [47] that using one-shot decision functions which are step functions may be optimal when the utility function is chosen to be the Shannon sum-rate. One of the important contributions of the present work can be seen as a generalization of such a result to arbitrary utility functions.

Apart from the system performance, we also consider a distributed network where transmitters perform individual or local maximization operations. However, it is not clear whether allowing them to use more channels will lead to a better global performance. Providing elements of response to this question is precisely the purpose of the Sec. 3.6. To address the raised issue, we exploit one of the classical models of interference networks which is the parallel interference channel (PIC). This model represents a communication scenario in which several transmitter-receiver pairs communicate through a common set of orthogonal channels. While the problem of distributed power allocation in PICs has attracted a lot of attention from the communications community (the corresponding line of works was to a large extent pioneered by [48]), the problem of distributed channel selection in PICs has only been treated analytically in a relatively very small number of papers. The closest works to this chapter are [49][50]. In [49], the authors focus on the Nash equilibrium existence and uniqueness problems of the following power allocation and channel selection [1] games : the considered PIC is assumed to comprise two transmitter-receiver pairs and two channels ; for each channel realization, each transmitter chooses its power allocation vector or selects its channel in order to "maximize" its individual data rate. The problem of comparing the global performance of the two scenarios in terms of power allocation policies is not tackled. In [50], the equilibrium analysis is treated in detail in the case of the parallel multiple access channel, which is a special case of the PIC. The problem of comparing the global performance in terms of sum-rate of distributed power allocation with the one of channel selection is introduced but not developed. Motivated by the practical importance of this comparison, the aim of the present work is to provide more general analytical and simulation results in PIC. Our interesting results provide a better understanding on how to use the spectrum in interference networks.

## 4.2 Problem statement

The wireless system under consideration comprises $K \geq 2$ pairs of interfering transmitters and receivers which can operate over $B \geq 1$ non-overlapping bands. The power Transmitter $i \in \{1, ..., K\}$ allocates to band $b \in \{1, ..., B\}$ is denoted by $p_i^b$, $p_i^b$ being subject to classical power limitations : $p_i^b \leq P_{\max}$ and $\sum_{b=1}^{B} p_i^b \leq P$, with $P_{\max} \leq P$. In the setup under study, the quantities of interest for Transmitter $i$ to control its *power vector*

$$p_i = (p_i^1, ..., p_i^B) \tag{4.1}$$

are given by the channel gains of the different links between the transmitters and receivers. The channel gain of the link between Transmitter $i \in \{1, ..., K\}$ and Receiver $j \in \{1, ..., K\}$ for band $b \in \{1, ..., B\}$ is denoted by $g_{ij}^b = |h_{ij}^b|^2$, where $h_{ij}^b$ may typically be the realization of a complex Gaussian random variable, if Rayleigh fading is conside-

1. Note that selecting a channel corresponds to allocating all the available power to a single channel.

red. Each channel gain is assumed to obey a classical block-fading variation law whose probability density function is given by : $f^n_{k\ell}(x) = \frac{1}{\gamma^n_{k\ell}} \exp\left(-\frac{x}{\gamma^n_{k\ell}}\right)$ and channel realizations are assumed to be i.i.d. from block to block . Transmitter $i$, $i \in \{1, ..., K\}$, can update its power vector $p_i$ from block to block. To update its power, each transmitter has a certain knowledge of the global channel state, which is defined as follows. The *global channel state* is given by the following $K^2-$dimensional vector which comprises all channel gains :

$$a_0 = (g^1_{11}, ..., g^B_{11}, g^1_{12}, ..., g^B_{12}, ..., g^1_{KK}, ..., g^B_{KK}). \tag{4.2}$$

In full generality, Transmitter $i$ is assumed to have partial CSI. The knowledge available at Transmitter $i$ is represented by the signal $s_i$. In this chapter, the power vectors $p_i$, the global channel state $a_0$, and the signals or available *partial information* $s_i$ are assumed to lie in discrete sets : $\forall i \in \{1, ..., K\}, \mathbf{p_i} \in \mathcal{A_i}$ and $s_i \in \mathcal{S}_i$ where $|\mathcal{A}_i| < \infty$ and $|\mathcal{S}_i| < \infty$. More specifically, the signal $s_i$ is assumed to be the output of a discrete memoryless channel $\mathrm{P}(S_i = s_i | A_0 = a_0) = \Gamma_i(s_i|a_0)$ [46], where $A_0$ and $S_i$ and respectively represent the random variables used to model the channel state variations and the partial information available to Transmitter $i$ [2]. The full or perfect global CSI at Transmitter $i$ corresponds to $s_i = a_0$. The case where only perfect individual CSI is available is given by $s_i = (g^1_{ii}, ..., g^B_{ii})$. The signal $s_i$ may also be a noisy estimate of $(g^1_{ii}, ..., g^B_{ii})$ : $s_i = (\widehat{g}^1_{ii}, ..., \widehat{g}^B_{ii})$.

By denoting $t$ the block index, the purpose of Transmitter $i$ is therefore to tune the power vector $p_i(t)$ for block $t$ by exploiting its knowledge about the channel state that is, the signal $s_i(t)$. More precisely, we assume that Transmitter knows $s_i$ at time $t$ but also the past realizations of it namely, $s_i(1), ..., s_i(t-1)$, the transmission being assumed to start at block $t = 1$ and to stop at block $t = T$. In its general form, the *power control strategy* of Transmitter $i$ is a sequence of functions which is denoted by $f_i = (f_{i,t})_{1 \le t \le T}$ and defined by :

$$\begin{array}{rccc} f_{i,t} & : & \mathcal{S}_i^t & \longrightarrow & \mathcal{A}_i \\ & & (s_i(1), s_i(2), ..., s_i(t)) & \longmapsto & p_i(t). \end{array} \tag{4.3}$$

The three main issues addressed in this chapter are as follows. First, we characterize the achievable performance in terms of long-term utility region when the block or *instantaneous utility* is a function of the form $u_i(a_0, p_1, ..., p_K)$. The *long-term utility* of Transmitter $i$ is defined by :

$$U_i(f_1, ..., f_K) = \lim_{T \to +\infty} \frac{1}{T} \sum_{t=1}^{T} \mathbb{E}\big[u_i(a_0(t), p_1(t), ..., p_K(t))\big] \tag{4.4}$$

whenever the above limit exists. The presence of the expectation operator is required in general (it can be omitted when a law of large numbers is available) since the channel is random and every power vector is a function of it. In general the channel is a random process $A_0(1), ..., A_0(T)$ but since we assume the channel gains to be i.i.d., the notation can be simplified by only using a single random variable $A_0$. The corresponding probability distribution is the *global channel state distribution* and is denoted by $\rho_0$ in the sequel. The second issue we want to address in this chapter is to determine power control strategies which only use the available local information while performing as well as possible in terms of a global utility e.g., in terms of sum-utility $\sum_{i=1}^K U_i$. The last issue to be addressed is

2. To avoid any ambiguity where there is any, we use capital letters to refer to random processes or variables. In particular, $A_i$ **is used to represent the random process of** $p_i$.

the selfish power control to maximize the individual bit-rate of each transmitter in a distributed way, which can be seen as the performance comparison at equilibrium with different action profiles.

## 4.3 Limiting performance characterization of power control with partial information

While many power control schemes using partial CSI are available in the literature, very often it is not possible to know whether the available information is exploited optimally by the considered power control scheme. While the problem of optimality is in general a very important and challenging problem, it turns out to be solvable in important scenarios such as the scenario under investigation in this chapter. Indeed, an important message of the present work is that, under the made assumptions, information theory tools can be used to fully characterize the limiting theoretical performance of the power control strategies. The two key assumptions which are made for this are as follows : (i) The channel state $a_0(t)$ is i.i.d. ; (ii) The observation structure which defines the partial observation $s_i$ is memoryless. Assuming (i) and (ii), the following theorem provides the utility region characterization for any power control problem under the form specified by [8]. For the sake of clarity we will use the following notations : $a = (a_0, p_1, ..., p_K)$ and $s = (s_1, ..., s_K)$ ; $\Gamma$ stands for the conditional probability $\mathrm{P}_{S|A_0}$, $S$ being the random variable used to model the vector of individual signals available to the transmitters ; $V$ is an auxiliary variable as used in coding theorems [46] and its role will be commented a little further ; the notation $\Delta_K$ will refer to the *unit simplex* of dimension $K$ : $\Delta_K = \left\{ (x_1, ..., x_K) \in \mathbb{R}^K : \forall i \in \{1, ..., K\}, x_i \geq 0; \sum_{i=1}^{K} x_i = 1 \right\}$.

**Theorem 4.3.1.** *Assume the system has $M$ constraints, which are related to the functions of the form $u^{(m)}(a_0, p_1, \ldots, p_K)$ where $m \in \{1, \ldots, M\}$. Let $\lambda = (\lambda_1, ..., \lambda_K) \in \Delta_K$ and $w_\lambda = \sum_{i=1}^{K} \lambda_i u_i$. Define the $(K+1)-$uplet of probability distributions $\left( Q^\lambda_{A_1|S_1,V}, ..., Q^\lambda_{A_K|S_K,V}, Q^\lambda_V \right)$ as the solution of the following optimization problem*

$$\max_{P_{A_1|S_1,V}, ..., P_{A_K|S_K,V}, P_V} W_\lambda \left( P_{A_1|S_1,V}, ..., P_{A_K|S_K,V}, P_V \right) \tag{4.5}$$

$$\text{s.t.} \, \forall m \in \{1, \ldots, M\}, \; U^{(m)} \left( P_{A_1|S_1,V}, ..., P_{A_K|S_K,V}, P_V \right) \geq C_m \tag{4.6}$$

*where*

$$\begin{aligned} &W_\lambda \left( P_{A_1|S_1,V}, ..., P_{A_K|S_K,V}, P_V \right) = \\ &\textstyle\sum_{a,s,v} \rho_0(a_0) \Gamma(s|a_0) P_V(v) \prod_{i=1}^{K} P_{A_i|S_i,V}(p_i|s_i, v) w_\lambda(a_0, p_1, ..., p_K) \end{aligned} \tag{4.7}$$

$$\begin{aligned} &U^{(m)} \left( P_{A_1|S_1,V}, ..., P_{A_K|S_K,V}, P_V \right) = \\ &\textstyle\sum_{a,s,v} \rho_0(a_0) \Gamma(s|a_0) P_V(v) \prod_{i=1}^{K} P_{A_i|S_i,V}(p_i|s_i, v) u^{(m)}(a_0, p_1, ..., p_K) \end{aligned} \tag{4.8}$$

*$P_V$ being the distribution of some auxiliary variable $V \in \mathcal{V}$ verifying the Markov chain $V-(A_0,A_1,...,A_K)-(S_1,...,S_K)$. Then, when $T \to +\infty$, the Pareto frontier $\overline{\mathcal{U}}$ of the long-term utility region associated with the constraints is given by :*

$$\overline{\mathcal{U}} = \left\{ (U_1,...,U_K) \in \mathbb{R}^K : U_i = \sum_{a,s,v} Q^{\lambda}(a,s,v) u_i(a_0,p_1,...,p_K),\ \lambda \in \Delta_K \right\} \tag{4.9}$$

*with* $Q^{\lambda}(a,s,v) = \rho_0(a_0)\Gamma(s|a_0)Q_V^{\lambda}(v)\prod_{i=1}^{K} Q^{\lambda}_{A_i|S_i,V}(p_i|s_i,v)$.

**Proof :** First of all, we show that the power control strategies of the different users $f_1,...,f_K$ intervene in the long-term utility only through the joint probability over $\mathcal{A}_0 \times ...\mathcal{A}_K$. Therefore, characterizing the long-term utility region is equivalent to characterizing the set of achievable or implementable joint probability distribution. We have that :

$$U_i(f_1,...,f_K) \tag{4.10}$$

$$= \lim_{T\to+\infty} \frac{1}{T} \sum_{t=1}^{T} \mathbb{E}\left[u_i(A_0(t),A_1(t),...,A_K(t))\right] \tag{4.11}$$

$$= \lim_{T\to+\infty} \frac{1}{T} \sum_{t=1}^{T} \sum_{a_0,...,p_K} P_t(a_0,...,p_K) u_i(a_0,...p_K) \tag{4.12}$$

$$= \sum_{a_0,...,p_K} u_i(a_0,...,p_K) \lim_{T\to+\infty} \frac{1}{T} \sum_{t=1}^{T} P_t(a_0,...,p_K) \tag{4.13}$$

where $P_t(a_0,...,p_K)$ is the joint probability induced by the power control strategy profile $f_1,...,f_K$ at time $t$ and we use here again capital letters for the random processes to clearly distinguish between the random process $A_i(t)$ and its realization $p_i$. Therefore, a utility $\mu_i$ is achievable if and only if it writes as

$$\mu_i = \sum_{a_0,p_1,...,p_K} Q(a_0,p_1,...,p_K) u_i(p_1,...,p_K) \tag{4.14}$$

and there exists a power control strategy profile $(f_1,...,f_K)$ such that

$$\lim_{T\to\infty} \frac{1}{T} \sum_{t=1}^{T} P_t(a_0,...,p_K) = Q(a_0,...,p_K). \tag{4.15}$$

Second, we show that the long-term utility region is necessarily convex, whatever the instantaneous utility functions under consideration. As a consequence, as indicated by 4.9 the Pareto frontier can be obtained by maximizing the long-term weighted utility $W_\lambda$. Assume that there exists a power control strategy profile $(f_1,...,f_K)$ which allows to reach a point $(\mu_1,...,\mu_K)$ of the long-term utility region. Then, there exists a joint distribution $Q$ which is implementable. Similarly, we consider another power control strategy profile $(f'_1,...,f'_K)$ which insures that $(\mu'_1,...,\mu'_K)$ can be reached and that there exists an implementable $Q'$. By using $100\alpha$ % of the time the strategy profile $(f_1,...,f_K)$ and

$100\alpha' = 100(1-\alpha)$ % of the time the strategy profile $(f'_1, ..., f'_K)$ it follows that the convex combination $Q'' = \alpha Q + \alpha' Q'$, $\alpha + \alpha' = 1$, $\alpha \geq 0$, $\alpha' \geq 0$, is also implementable. Therefore the point $(\mu_1", ..., \mu_K")$, $\mu_i" = \alpha\mu_i + \alpha\mu'_i$ can be attained.

As the last step of the proof, we exploit the coding theorem of [8] which states that a joint probability distribution $Q(a_0, p_1, ..., p_K)$ is implementable if and only if it writes as :

$$Q(a) = \rho_0(a_0) \sum_{s,v} \Gamma(s|a_0) P_V(v) \prod_{i=1}^{K} P_{A_i|S_i,V}(p_i|s_i, v) \tag{4.16}$$

where $V$ is any random variable which verifies the Markov chain $V - (A_0, A_1, ..., A_K) - (S_1, ..., S_K)$.■

To better understand Theorem 3.3.1 and its proof, let us comment on it in detail.

The first comment which can be made is that the long-term utility region Pareto frontier characterization relies on the use of an auxiliary random variable $V$. The presence of such variables is very common in coding theorems. For example, the capacity region of degraded broadcast channels is parameterized by auxiliary variables ; for one transmitter and two receivers, only one auxiliary variable suffices. In the latter case, the auxiliary variable can be interpreted for instance as a degree of freedom the transmitter has for allocating the available resource between the two transmitters [46]. In general, auxiliary random variables have to be considered as parameters which allow one to describe a set of points and therefore constitute before all a purely mathematical tool. Their operational meaning is generally given by the achievability part of the coding theorem. As far as Theorem 3.3.1 is concerned, the achievability part mainly corresponds to the general coding theorem given in [8]. In a power control setting, $V$ may be seen as a coordination random variable or a lottery which allows one to generate a coordination key. To be more concrete, consider a single-band interference channel with two transmitters and two receivers. The idea is to exchange a coordination key offline which consists of a sequence of realizations $v(1), ..., v(T)$ of a (Bernouilli) binary random variable : $V \sim \mathcal{B}(\tau)$, $\tau \in [0, 1]$. Then, online, a possible rule for the transmitters might be as follows : if $v(t) = 1$, Transmitter 1 transmits and if $v(t) = 0$, Transmitter 1 transmits. We see that in this simple example, $V$ would act as a time-sharing variable which would allow to manage interference even if the transmitters have no knowledge at all about the channel (i.e., $s_i = const.$). Then, by optimizing the Bernoulli probability $\tau$, one can obtain better performance than transmitting at full (or constant) power. Note that the full power operation point would be obtained by applying the iterative water-filling algorithm (IWFA) to a single-band interference network where Transmitter $i$ wants to maximize the utility $u_i = \log(1 + \text{SINR}_i)$, $\text{SINR}_i$ being the signal-to interference-plus-noise ratio.

The second comment we would like to make on Theorem 3.3.1 is that the achievable utility region can be described only by its Pareto frontier. This result follows from the fact that the long-term utility region is convex, as shown throughout the proof. This explains the presence of the vector $\lambda$. The vector allows one to move along the Pareto frontier $\overline{\mathcal{U}}$.

The third comment we will make here is that the power control strategy only intervenes in the long-term utility through its behavior in terms of conditional probability $P_{A_i|S_i,U}$ that is, the (conditional) frequency at which a given power vector $p_i$ is used.

The fourth comment concerns the alphabet $V$ lies in, namely $\mathcal{V}$. Indeed, it is possible to cover all the feasible utility region by choosing the size of $\mathcal{V}$ according to the next

theorem. In particular, Theorem 3.3.1 is of particular interest when it comes to solving the optimization problem, which in turn allows to determine the feasible points. We show that there is an upper bound for the alphabet size $\mathcal{V}$, beyond which one can always attain the feasible regions .

**Theorem 4.3.2.** *(Range for the cardinality of $\mathcal{V}$) Any implementable distribution $Q$ (Defined by [8]) can be achieved by selecting the auxiliary random variable $V$ satisfying $|\mathcal{V}| \leq |\mathcal{A}| \cdot |\mathcal{S}| - 1$, where $|\mathcal{A}| = \prod_{i=0}^{K} |\mathcal{A}_i|$ and $|\mathcal{S}| = \prod_{i=1}^{K} |\mathcal{S}_i|$.*

**Proof :** See Appendix B.

According to this theorem, the auxiliary random variable is upper bounded by $|\mathcal{A}|\cdot|\mathcal{S}|-1$. Hence, it is not necessary to choose the auxiliary variable $V'$ with $|V'| \geq |\mathcal{A}| \cdot |\mathcal{S}| - 1$ since the additional cardinality can not bring any improvements to the implementable distribution $Q$, and consequently no improvements to the system performance.

The last comment is about the necessity of the auxiliary variable. As described before, the auxiliary variable can be the coordination key among the users. However, the auxiliary variable is not always useful to the system performance. According to the following theorem, it can be checked that the auxiliary variable will not change the Pareto frontier $\overline{\mathcal{U}}$ under certain conditions.

**Theorem 4.3.3.** *(Sufficient condition for omiting $V$) Define $\widehat{W}_\lambda\left(P_{A_1|S_1}, ..., P_{A_K|S_K}\right)$, a special case of $W_\lambda\left(P_{A_1|S_1,V}, ..., P_{A_K|S_K,V}, P_V\right)$ and $\widehat{U}_c^{(m)}\left(P_{A_1|S_1}, ..., P_{A_K|S_K}\right)$, a special case of $U_c^{(m)}\left(P_{A_1|S_1,V}, ..., P_{A_K|S_K,V}, P_V\right)$, which corresponds to auxiliary variable $V$ assumed constant, as follows*

$$\begin{aligned}&\widehat{W}_\lambda\left(P_{A_1|S_1}, ..., P_{A_K|S_K}\right) = \\ &\textstyle\sum_{a,s} \rho_0(a_0)\Gamma(s|a_0)\prod_{i=1}^{K} P_{A_i|S_i}(p_i|s_i) w_\lambda(a_0, p_1, ..., p_K)\end{aligned} \tag{4.17}$$

$$\begin{aligned}&\widehat{U}^{(m)}\left(P_{A_1|S_1}, ..., P_{A_K|S_K}\right) = \\ &\textstyle\sum_{a,s,v} \rho_0(a_0)\Gamma(s|a_0)\prod_{i=1}^{K} P_{A_i|S_i}(p_i|s_i) u^{(m)}(a_0, p_1, ..., p_K)\end{aligned} \tag{4.18}$$

*Suppose* $\left(P^\lambda_{A_1|S_1}, ..., P^\lambda_{A_K|S_K}\right) = \underset{\left(P_{A_1|S_1}, ..., P_{A_K|S_K}\right)}{\arg\max} \widehat{W}_\lambda\left(P_{A_1|S_1}, ..., P_{A_K|S_K}\right)$. *Then for every $V$, the sufficient condition for* $\left(Q^\lambda_{A_1|S_1,V}, ..., Q^\lambda_{A_K|S_K,V}\right) = \left(P^\lambda_{A_1|S_1}, ..., P^\lambda_{A_K|S_K}\right)$ *is*

$$\forall m \in \{1, \ldots, M\}, \quad \widehat{U}^{(m)}\left(P^\lambda_{A_1|S_1}, ..., P^\lambda_{A_K|S_K}\right) \geq C_m \tag{4.19}$$

**Proof :** Firstly, $W_\lambda\left(P_{A_1|S_1,V}, ..., P_{A_K|S_K,V}, P_V\right)$ can be rewritten as :

$$\begin{aligned}&W_\lambda\left(P_{A_1|S_1,V}, ..., P_{A_K|S_K,V}, P_V\right) \\ &= \textstyle\sum_v P_V(v) \sum_{a,s} \rho_0(a_0)\Gamma(s|a_0)\prod_{i=1}^{K} P_{A_i|S_i,V}(p_i|s_i, v) w_\lambda(a_0, p_1, ..., p_K) \\ &\leq \textstyle\sum_v P_V(v) \widehat{W}_\lambda\left(P^\lambda_{A_1|S_1}, ..., P^\lambda_{A_K|S_K}\right) \\ &= \widehat{W}_\lambda\left(P^\lambda_{A_1|S_1}, ..., P^\lambda_{A_K|S_K}\right)\end{aligned} \tag{4.20}$$

with the equality if $\left(P_{A_1|S_1,V},...,P_{A_K|S_K,V}\right)=\left(P^{\lambda}_{A_1|S_1},...,P^{\lambda}_{A_K|S_K}\right)$.

Secondly,knowing $\widehat{U}_c^{(m)}\left(P^{\lambda}_{A_1|S_1},...,P^{\lambda}_{A_K|S_K}\right)\geq C_m$, if $\left(P_{A_1|S_1,V},...,P_{A_K|S_K,V}\right)=\left(P^{\lambda}_{A_1|S_1},...,P^{\lambda}_{A_K|S_K}\right)$, it can be checked that

$$U_c^{(m)}\left(P_{A_1|S_1,V},...,P_{A_K|S_K,V},P_V\right)\geq C_m \tag{4.21}$$

According to the equality condition and (4.21), it can be concluded that $\left(Q^{\lambda}_{A_1|S_1,V},...,Q^{\lambda}_{A_K|S_K,V}\right)=\left(P^{\lambda}_{A_1|S_1},...,P^{\lambda}_{A_K|S_K}\right)$. ■

Additionally, from this theorem, it can be found that the auxiliary variable will not bring any improvements to the Pareto frontier $\overline{\mathcal{U}}$ when there is no constraints since the sufficient conditions can be always fulfilled.

## 4.4 Proposed power control strategies

Even though the coding theorem establishes the capacity region of a network, designing practical coding schemes which attain the limiting performance is not evident. There is no general recipe to find a power control scheme which allows one to operate arbitrarily close to a point of the utility region established through Theorem 3.3.1. To be able to provide practical power control schemes, we propose to focus on a special class of power control schemes. We will restrict our attention to memoryless and stationary power control strategies, which amounts to finding good one-shot decision functions. A strategy is *memoryless* in the sense that it does not exploit the past realizations of the signal $s_i$ ; it is therefore a sequence of functions which writes as $f_{i,t}(s_i(t))$. Additionally, we assume it is *stationary* which means that the function $f_{i,t}$ does not depend on time, which ultimately means that a power control strategy boils down to a single function $f_i(s_i(t))$ ; the latter function will be referred to as a *decision function*. In fact, considering that the power level, vector, or matrix of a transmitter only depends on the current realization of the channel, and this in a stationary manner, is a very common and practical scenario in the wireless literature. As advocated by recent works (see e.g., [53] for the MIMO case), the problem of finding one-shot decision functions with partial information and which perform well in terms of global performance is still a challenging problem. Remarkably, one of our observations is that Theorem 3.3.1 can be exploited in a constructive way that is, it can be exploited to find good decision functions. This is precisely the purpose of this section.

The key observation we make is as follows. The functional $W_\lambda$ is a multilinear function of its arguments which are conditional probability distributions $P_{A_1|S_1,V},...,P_{A_K|S_K,V},P_V$ (see [8]). Since $W_\lambda$ is multilinear, its maximum points are on the vertices of the unit simplex [54]. The important consequence of this is that optimal condition probabilities boil down to functions $f_1(s_1,v),...,f_K(s_K,v)$. The key idea is to solve the corresponding optimization problem to determine these functions and use them as candidates for power control decision functions. But finding a low-complexity numerical technique to determine the optimal functions is left as a challenging extension of the present work. Instead, we propose a suboptimal optimization technique which has a lower complexity and relies on the use of the sequential best-response dynamics (see e.g., [55][17])

To apply the sequential best-response dynamics to $W_\lambda$ we rewrite it by isolating the sum w.r.t. $s_i$ i.e., the observation of Transmitter $i$ :

$$W_\lambda = \sum_{a_0,s,v} \rho_0(a_0)\Gamma(s|a_0)w_\lambda(a_0, f_1(s_1, v), ..., f_K(s_K, v)) \tag{4.22}$$

$$= \sum_{a_0,s_i,v} \Gamma_i(s_i|a_0) \sum_{s_{-i}} \Gamma_{-i}(s_{-i}|a_0)w_\lambda(a_0, f_1(s_1, v), ..., f_K(s_K, v)) \tag{4.23}$$

where : $s_{-i} = (s_1, ..., s_{i-1}, s_{i+1}, ..., s_K)$ represents the vector comprising all observations of the transmitters other than agent $i$ ; the condition probability $\Gamma_{-i}$ is given by

$$\Gamma_{-i}(s_{-i}|a_0) = \sum_{s_i} \Gamma(s|a_0). \tag{4.24}$$

To describe the proposed iterative algorithm, it is convenient to introduce the following auxiliary quantity :

$$\begin{aligned}\omega(s_i, p_i, v) = \sum_{a_0,v} \Bigg[ \rho_0(a_0)\Gamma(s_i|a_0) \sum_{s_{-i}} \Gamma_{-i}(s_{-i}|a_0)\times \\ w_\lambda(a_0, f_1(s_1, v), ..., f_{i-1}(s_{i-1}, v), p_i, f_{i+1}(s_{i+1}, v), ..., f_K(s_K, v)))\Bigg] .\end{aligned} \tag{4.25}$$

The sequential best-response dynamics procedure consists in updating one variable at a time, the variables being the decision functions here. Denoting an algorithm iteration as iter, the auxiliary quantity $\omega$ at iteration iter writes as :

$$\begin{aligned}\omega^{\text{iter}}(s_i, p_i, v) = \sum_{a_0,v} \rho_0(a_0)\Gamma(s_i|a_0) \sum_{s_{-i}} \Gamma_{-i}(s_{-i}|a_0) \\ w_\lambda(a_0, f_1^{\text{iter}}(s_1, v), .., f_{i-1}^{\text{iter}}(s_{i-1}, v), p_i, f_{i+1}^{\text{iter}-1}(s_{i+1}, v), .., f_K^{\text{iter}-1}(s_K, v))).\end{aligned} \tag{4.26}$$

By assuming the knowledge of the utility function $w_\lambda$, the alphabets $\mathcal{A}_0, \mathcal{A}_1, ..., \mathcal{A}_K$, $\mathcal{S}_1, ..., \mathcal{S}_K$, the probability distribution of the channel $\rho_0$, the observed signals $\Gamma$, and an initial choice for the decision functions $f_1^{\text{init}}, ..., f_K^{\text{init}}$ Algorithm 1 can be implemented. The proposed algorithm should be implemented offline, whereas the obtained decision functions are designed to be exploited online. Therefore, even though the decision function determination operation requires the knowledge of the different alphabets, the channel statistics, the observation signal statistics, and the initial decision functions, Transmitter $i$ only needs $s_i$ and $v$ to tune (online) its power vector. Typically, the former operation might be performed offline by a base station while the online operations would be executed by the transmitters.

The classical issue is whether this iterative algorithm converges. For clarity, we state the following convergence result under the form of a proposition.

**Proposition 4.4.1.** *Algorithm 1 always converges.*

**Proof :** The result can be proved by induction or by calling for an exact potential game property [56]. Indeed, since the underlying game is a strategic-form game with a common utility $W_\lambda$, it is trivially an exact potential game, which ensures convergence.■

**inputs** : $\forall i \in \{0, ..., K\},\ \mathcal{A}_i;\ \forall i \in \{1, ..., K\},\ \mathcal{S}_i$
$w_\lambda,\ \rho_0,\ \Gamma$
$\forall i \in \{1, ..., K\},\ f_i^{\text{init}}$
**outputs:** $\forall i \in \{1, ..., K\},\ f_i^\star$

Initialization : $f_i^0 = f_i^{\text{init}},\ \ \text{iter} = 0$

**while** $\exists i : f_i^{\text{iter}-1} - f_i^{\text{iter}} \geq \epsilon\ \ AND\ \ \text{iter} \leq \text{iter}_{\max}\ \ \ OR\ \ \ \text{iter} = 0$ **do**
  iter = iter + 1;
  **foreach** $i \in \{1, \ldots, K\}$ **do**
    **foreach** $s_i \in \mathcal{S}_i$ **do**
      $f_i^{\text{iter}}(s_i, v) = \arg\max_{p_i} \omega_i^{\text{iter}}(s_i, p_i, v)$ using (4.26);
    **end**
  **end**
**end**
Final update : $\forall i \in \{1, ..., K\},\ f_i^\star = f_i^{\text{iter}}$

**Algorithm 2:** Proposed decentralized algorithm for finding decision functions for the transmitters

Obviously, there is no guarantee for global optimality and only local maximum points for $W_\lambda$ are reached in general by implementing Algorithm 1. Quantifying the optimality gap is known to be a non-trivial issue related to the problem of determining a tight bound of the price of anarchy [57][17]. Two comments can be made. First, if the algorithm is initialized by the best state-of-the art decision functions, then it will lead to new decision functions which perform at least as well as the initial functions. Second, many simulations performed for a large variety of scenarios have shown that the optimality gap seems to be relatively small for classical utility functions used in the power control literature.

## 4.5 Energy-efficient team power control

In this section we shall analyze the problem for a particular utility function ; namely energy-efficient team power control. For this analysis, we shall assume that there is no constraint about quality of service to simplify the discussion. In this case, according to Theorem 3.3.3, the auxiliary variable is not useful to determine the Pareto frontier. Therefore we shall omit it in this section. The energy efficiency utility function in single band scenario ($B = 1$) is defined as

$$w_\lambda(a_0, p_1, ..., p_K) = \sum_{i=1}^{K} \frac{\exp\left(-\frac{\sigma^2 + \sum_{j \neq i} g_{ji} p_j}{g_{ii} p_i}\right)}{p_i} \tag{4.27}$$

For illustration purposes, we assume the case where the power limitation is always met, i.e. $P_{\max}$ is sufficient large.

As the setup, consider each transmitter knows the local CSI perfectly from the observations, namely $s_i = g_{ii}$. Consequently the conditional probability $\Gamma_i$ becomes a determi-

nistic function (discrete Dirac function). Hence, (4.23) can be rewritten as

$$W_\lambda = \sum_{a_0} \rho_0(a_0) w_\lambda(a_0, f_1(g_{11}), ..., f_K(g_{KK})) \tag{4.28}$$

Additionally, define the signal-to-interference ratio (SIR) as follows :

$$\mathrm{SIR}_{\max} = \max_{i,j,j\neq i} \left( \frac{\mathbb{E}(g_{ii})}{\mathbb{E}(g_{ji})} \right) \tag{4.29}$$

$$\mathrm{SIR}_{\min} = \min_{i,j,j\neq i} \left( \frac{\mathbb{E}(g_{ii})}{\mathbb{E}(g_{ji})} \right) \tag{4.30}$$

We assume the expectation for direct channels $\mathbb{E}(g_{ii})$ to be fixed and we study the function $f_i(g_{ii})$ for the asymptotic cases : $\mathrm{SIR}_{\max} \to 0$ and $\mathrm{SIR}_{\min} \to \infty$.

**Proposition 4.5.1.** *When* $\mathrm{SIR}_{\max} \to 0$*, the optimal function* $f_i(g_{ii})$ *to maximize* $W_\lambda$ *can be expressed as :*

$$f_i(g_{ii}) = \begin{cases} 0 & \text{if } g_{ii} < \lambda_i \\ \frac{\sigma^2}{g_{ii}} & \text{if } g_{ii} \geq \lambda_i \end{cases} \tag{4.31}$$

*where* $\lambda_i$ *is the positive threshold.*

**Proof :** This claim can be proved in 2 steps. As a first step, we will prove that only 2 power control strategies can be chosen for optimal performance.
It is important to note that if there exists interference for user $i$, its own utility, i.e. $\frac{\exp\left(-\frac{\sigma^2+\sum_{j\neq i} g_{ji}p_j}{g_{ii}p_i}\right)}{p_i}$ will be zero for every $p_i$. Moreover, if there is no interference for user $i$, $p_i$ will be selected to maximize its own utility, i.e. $p_i = \frac{\sigma^2}{g_{ii}}$. To find the optimal $f_i(g_{ii})$, assume $\rho_0(a_0) = \rho_i(g_{ii})\rho_{-i}(a_{0,-i}|g_{ii})$ where $a_{0,-i} = (g_{11}, g_{12}, ..., g_{i,i-1}, g_{i,i+1}, ..., g_{KK})$, then (4.28) can be rewritten as :

$$\begin{aligned} W_\lambda &= \sum_{a_0} \rho_0(a_0) w_\lambda(a_0, f_1(g_{11}), ..., f_K(g_{KK})) \\ &= \sum_{g_{ii}} \rho_i(g_{ii}) \sum_{a_{0,-i}} \rho_{-i}(a_{0,-i}|g_{ii}) w_\lambda(a_0, f_1(g_{11}), ..., f_K(g_{KK})) \\ &= \sum_{g_{ii}} \rho_i(g_{ii}) \theta_i\left(g_{ii}, f_i(g_{ii})\right) \end{aligned} \tag{4.32}$$

where $\theta_i\left(g_{ii}, f_i(g_{ii})\right) = \sum_{a_{0,-i}} \rho_{-i}(a_{0,-i}|g_{ii}) w_\lambda(a_0, f_1(g_{11}), ..., f_K(g_{KK}))$. Denote as the interference of user $i$

$$I_i = \sum_{j\neq i} g_{ji} p_j \tag{4.33}$$

Knowing that $g_{ji}$ follows the exponential distribution, it can be checked that

$$\lim_{\mathbb{E}(g_{ji})\to\infty} \Pr(g_{ji} < \infty) = 0 \tag{4.34}$$

If $I_i \neq 0$, cross channel gain $g_{ji} \to \infty$ almost surely, it can be checked that

$$w_\lambda(a_0, ..., f_i(g_{ii}) > 0, ...) \to 0 \quad \text{a.s.} \tag{4.35}$$

Otherwise, when $I_i = 0$

$$w_\lambda(a_0, ..., f_i(g_{ii}) > 0, ...) = \frac{\exp\left(-\frac{\sigma^2}{g_{ii}p_i}\right)}{p_i} \tag{4.36}$$

Hence, we can conclude that

$$\theta_i\left(g_{ii}, f_i(g_{ii}) = \frac{\sigma^2}{g_{ii}}\right) \geq \theta_i\left(g_{ii}, f_i(g_{ii}) > 0\right) \quad \text{a.s.} \tag{4.37}$$

Therefore, $f_i(g_{ii}) = \frac{\sigma^2}{g_{ii}}$ dominates other positive actions almost surely. The optimal action for user $i$ thus belongs to the set $\{0, \frac{\sigma^2}{g_{ii}}\}$.
In the second step, we prove that there exists an unique threshold between the two actions. Define the difference between the utility of 2 actions as :

$$\Delta(g_{ii}) = \theta_i\left(g_{ii}, f_i(g_{ii}) = 0\right) - \theta_i\left(g_{ii}, f_i(g_{ii}) = \frac{\sigma^2}{g_{ii}}\right) \tag{4.38}$$

Then three following conditions can be easily checked :

$$\frac{\partial\Delta(g_{ii})}{g_{ii}} < 0 \quad \forall g_{ii} > 0 \tag{4.39}$$

$$\lim_{g_{ii}\to 0} \Delta(g_{ii}) > 0 \tag{4.40}$$

$$\lim_{g_{ii}\to \infty} \Delta(g_{ii}) < 0 \tag{4.41}$$

Hence, we can conclude that there exists one unique threshold $\lambda_i$ such that $\Delta(g_{ii} = \lambda_i) = 0$, $\Delta(g_{ii}) > 0$ if $g_{ii} < \lambda_i$ and $\Delta(g_{ii}) < 0$ if $g_{ii} > \lambda_i$. ■

**Proposition 4.5.2.** *When* $\mathrm{SIR}_{\min} \to \infty$*, the optimal function* $f_i(g_{ii})$ *to maximize the* $W_\lambda$ *is* $f_i(g_{ii}) = \frac{\sigma^2}{g_{ii}}$.

**Proof :** Since the interference is negligible here, each user $i$ will choose the action which maximizes its own utility, leading to the optimal solution $f_i(g_{ii}) = \frac{\sigma^2}{g_{ii}}$. ■

When the SIR is moderate, the threshold policy of the form (4.31) can not be proved to be optimal. However, it will be shown through simulations that it still achieve good performance with low computational complexity. When the complexity of the algorithm is prohibitive, the threshold policy can be an alternative solution.

## 4.6 Selfish spectrally efficient power allocation

In this section, we shall consider the case where transmitter receiver pair $i$ tries to maximize its own utility $u_i$ based on local information only. Compare to Sec. 3.5, the scenarios considered in this section has three distinguishing features : 1) We are not considering a team framework anymore but a scenario with possibly non-aligned utility functions ; 2) We consider instantaneous utility functions instead of considering expected

utility functions. This can be seen as a special case of the problem discussed in Sec. 3.2 by assuming $\lambda_k = 1$ for Transmitter $k$ and $s_k = g_k$ (local CSI of Transmitter $k$) without considering the auxiliary variable ; 3) The several utility functions aim at maximizing spectral efficiency but not energy efficiency.

This choice can be motivated by many arguments but we will just mention a few of them. Note that even if there were a central node that could control the whole vector $p = (p_1^1, ..., p_1^B, ..., p_K^1, ..., p_K^B)$ and would have global channel state information (CSI) $g = (g_1, ..., g_K)$ with $g_k = (g_{1k}^1, ..., g_{Kk}^1, ..., g_{1k}^B, ..., g_{Kk}^B)$, it wouldn't be able to perform the direct maximization of the sum-utility w.r.t. $p$. Indeed, the corresponding problem is very difficult from an optimization point of view, but also from a computational point of view if exhaustive search over partitioned spaces is performed, which can be seen from the algorithm proposed in last section. Therefore, there is a high interest in considering individual utilities with partial or local control of the variables.

For a classical optimization problem which involves a single function and full control of its variables, the notion of optimality is clear. However, in the presence of multiple decision makers that have partial control of these variables, the very meaning of optimality is unclear. Indeed, the optimal decision for transmitter $k$ depends on the decisions made by the other transmitters. This is one of the reasons why other solution concepts than optimality need to be considered in such a setting. A fundamental solution concept is the notion of Nash point or equilibrium. As very well illustrated by the iterative water-filling algorithm (IWFA) [48], which converges to a Nash equilibrium (NE), one of the major assets of the NE is that it may be implemented with local knowledge only and reached through low complexity iterative or learning procedures (see e.g., [17]). This is why we consider, in this section, the performance of the network at equilibrium. The procedures or algorithms to reach NE are not addressed here. Before introducing an NE, we first define explicitly the strategic-form games.

The strategic-form game of interest consists of a triplet : the set of decision makers corresponding to $\mathcal{K}$ here ; their strategy sets that contain all their possible choices and are the power allocation sets ; and their utility functions that depend on their own choices but also on the others' choices and are defined here below. We consider three different scenarios with respect to the set of power allocation vectors allowed to each transmitter. The considered utility functions are given by

$$u_k(p; g_k) = \sum_{b=1}^{B} \log_2 \left( 1 + \frac{g_{kk}^b p_k^b}{\sigma^2 + \sum_{\ell \neq k} g_{\ell k}^b p_\ell^b} \right) \tag{4.42}$$

However, to clearly indicate that the power allocation sets and, thus, the domains of $u_k$ are different, we will denote the corresponding utility functions by $v_k^{\mathrm{s}}(p; g_k)$ where $\mathrm{s} \in \{\mathrm{MC}, \mathrm{MT}, \mathrm{SC}\}$ and MC, MT, and SC respectively stands for multi-channel, multi-transmitter, and single-channel scenarios. The single-channel or channel selection scenario corresponds to a network in which every transmitter can use only one channel among $N$ possible ones. Denoting by $P_{\max}$ the maximal transmit power and introducing $p_k = (p_k^1, ..., p_k^N)$, the sets of power allocation vectors are defined as follows :

- $\mathcal{P}_k^{\mathrm{MC}} = \left\{ p_k \in \mathbb{R}^B : p_k^b \geq 0, \sum_{b=1}^{B} p_k^b \leq P_{\max} \right\}$ ;

• $\mathcal{P}_k^{\mathrm{MT}} = \left\{p_k \in \mathbb{R}^B : p_k^b \geq 0, p_k^b \leq P_{\max}\right\}$;
• $\mathcal{P}_k^{\mathrm{SC}} = \{P_{\max}e_1, ..., P_{\max}e_N\}$ where $(e_1, ..., e_N)$ represents the canonical basis of $\mathbb{R}^B$ (i.e., $e_1 = (1, 0, ..., 0), e_2 = (0, 1, 0, ..., 0)$, etc). An important comment is now in order. The MC and SC scenarios assume a total budget $P_{\max}$ while the MT scenario assumes an $B$ times higher total power budged. In spite of this fact, the latter scenario is of practical importance as well. In WiFi networks, the startup *Codeon* promotes a software solution which allows channel bundling to be implemented by using available USB ports on the access point and user terminals. In such a case, there can be one radio frequency transmitter per channel and there is no additional power constraint on the sum.

Now, let us define an NE for the games under consideration. With a slight abuse of notation, the power vector $p$ is denoted by $p = (p_1, ..., p_K) = (p_k, p_{-k})$.

**Definition 4.6.1** (**Pure Nash Equilibrium**). *Let* $\mathrm{s} \in \{\mathrm{MC}, \mathrm{MT}, \mathrm{SC}\}$. *The power vector* $p = (p_k, p_{-k})$ *is an NE of the strategic form game* $(\mathcal{K}, (\mathcal{P}_k^{\mathrm{s}})_{k\in\mathcal{K}}, (v_k^{\mathrm{s}})_{k\in\mathcal{K}})$, *if for all* $k \in \mathcal{K}$ *and for all* $p_k' \in \mathcal{P}_k^{\mathrm{s}}$

$$v_k^{\mathrm{s}}\left(p_k, p_{-k}; g_k\right) \geq v_k^{\mathrm{s}}\left(p_k', p_{-k}; g_k\right). \tag{4.43}$$

At this point, we can define the different quantities proposed to compare the global performance of an interference network in which transmitters can use several bands simultaneously (i.e., either all transmitters use $\mathcal{P}_k^{\mathrm{MC}}$ or they all use $\mathcal{P}_k^{\mathrm{MT}}$) and another one where using only one band is allowed (i.e., all the transmitters use $\mathcal{P}_k^{\mathrm{SC}}$). We will denote by $w^{\mathrm{s}}(p; g)$ the *sum-utility function* for scenario $\mathrm{s} \in \{\mathrm{MC}, \mathrm{MT}, \mathrm{SC}\}$ .

**Definition 4.6.2** (**Global performance comparison measures**). *Let* $\mathrm{SNR} \triangleq \frac{P_{\max}}{\sigma^2}$. *The four measures under consideration are as follows :*
• $\Pr_g\left[\widetilde{\mathrm{R}}_{\mathrm{s}}\left(\mathrm{SNR}; K; B; g\right) < 1\right]$ *with*

$$\widetilde{\mathrm{R}}_{\mathrm{s}}\left(\mathrm{SNR}; K; B; g\right) = \frac{w^{\mathrm{s}}(\widehat{p}^{\mathrm{s}}(g); g)}{w^{\mathrm{SC}}(\widetilde{p}^{\mathrm{SC}}(g); g)}$$

*where* $\widetilde{p}^{\mathrm{SC}}(g)$ *is the worst NE in terms of sum-utility of the SC game and* $\widehat{p}^{\mathrm{s}}(g)$ *is the best NE of the power allocation game* $s \in \{\mathrm{MC}, \mathrm{MT}\}$ *;*
• $\Pr_g\left[\overline{\mathrm{R}}_{\mathrm{s}}\left(\mathrm{SNR}; K; B; g\right) < 1\right]$ *with*

$$\overline{\mathrm{R}}_{\mathrm{s}}\left(\mathrm{SNR}; K; B; g\right) = \frac{w^{\mathrm{s}}(p^{\mathrm{UPA:s}}; g)}{w^{\mathrm{SC}}(p^{\mathrm{CS}}(g); g)}$$

*where* $p^{\mathrm{CS}}$ *corresponds to the power vector obtained when each transmitter selects its best channel regardless of the other transmitters' decisions and* $p^{\mathrm{UPA:s}}$ *is the power vector obtained when each transmitter allocates the available power uniformly in scenario* $s \in \{\mathrm{MC}, \mathrm{MT}\}$. *Note that the corresponding power vectors do not always correspond to equilibria ;*
•

$$\widetilde{\Gamma}_{\mathrm{s}}\left(\mathrm{SNR}; K; B\right) = \frac{\mathbb{E}_g[w^{\mathrm{s}}(\widehat{p}^{\mathrm{s}}(g); g)]}{\mathbb{E}_g[w^{\mathrm{SC}}(\widetilde{p}^{\mathrm{SC}}(g); g)]}$$

*with the same notations as above ;*
•

$$\overline{\Gamma}_{\mathrm{s}}\left(\mathrm{SNR}; K; B\right) = \frac{\mathbb{E}_g[w^{\mathrm{s}}(p^{\mathrm{UPA:s}}; g)]}{\mathbb{E}_g[w^{\mathrm{SC}}(p^{\mathrm{CS}}(g); g)]}$$

*with the same notations as above.*

The above quantities rely on the equilibrium analysis of the power allocation games under consideration. The corresponding analyses have been conducted in [48][49][50] and will not be detailed here. The main points to be mentioned are as follows. The power allocation game for the scenario MC possesses in general several equilibria [49]. The same observation holds for the channel selection game for scenario SC [50]. This is the reason why the best and worst equilibria are considered. In fact, the metric $\widetilde{\mathrm{R}}_{\mathrm{s}}$ is deliberately in favor of the power allocation game MC. If the best equilibrium of the game in scenario SC is considered, the global performance degradation phenomenon under consideration occurs more frequently ; some numerical results will be provided to illustrate this point. Now, in the power allocation game of scenario MT, there exists a unique Nash equilibrium which corresponds to using full power on each band. Therefore, the equilibrium power allocation policies can be seen as uniform power allocation policies with a power budget of $NP_{\max}$.

To exploit the above measures to prove the existence of scenarios where allowing every transmitter to use several bands instead of one leads to a global performance degradation, without loss of generality, it is assumed that the noise level is the same at all the receivers. The common SNR parameter $\mathrm{SNR} = \frac{P_{\max}}{\sigma^2}$ plays a major role in determining whether using multiple bands instead of one is beneficial in terms of global performance. When the SNR is small, equilibrium power allocation policies in scenarios SC and MC can be proved to coincide.

**Proposition 4.6.3** (**Low SNR regime,** $K$, $B$ **arbitrary**). *For all* $K \geq 2$, $B \geq 2$, *and* $\mathrm{s} \in \{\mathrm{MC}, \mathrm{MT}\}$ *we have that*

$$\lim_{\mathrm{SNR}\to 0} \mathrm{Pr}_g \left[\widetilde{\mathrm{R}}_{\mathrm{s}}\left(\mathrm{SNR}; K; B; g\right) < 1\right] = 0. \tag{4.44}$$

Proposition 4.6.3 translates that the interference is negligible compared to the noise when $\sigma^2 \to \infty$. The transmitters' decisions are no longer interdependent and the power allocation games MC, MT, and SC become classical optimization problems : only the direct channel gains $g^n_{kk}$ matter to transmitter $k$. Since total transmit power is limited to $P_{\max}$ for MC, the rate is maximized by selecting the best band. The SC game also becomes a mere channel selection problem, which means that the distributed power allocation policies of MC and SC coincide at low SNR. On the other hand, for the game MT, the point $p = (P_{\max}, ..., P_{\max}) \in \mathbb{R}^{KB}$ remains the unique Nash equilibrium and its structure does not change with the operating SNR. This equilibrium can be checked to be more sum-rate-efficient than the equilibrium of the SC game, explaining that the above probability vanishes with the SNR.

A natural question is to know what happens when the SNR is high. Do we reach the same conclusion as in the low SNR regime ? Providing the general answer for an arbitrary pair $(K, B)$ seems to be a non-trivial problem, which is left as an extension of this chapter. Rather, we treat here some special cases of interest $B \geq K$ and $K = B = 2$ that provide some useful insight into the general case.

**Proposition 4.6.4** (**High SNR regime,** $K \leq B$). *Consider a symmetric interference channel where* $\forall b$, $\gamma^b_{11} = \gamma^b_{22} = \lambda$, $\gamma^b_{12} = \gamma^b_{21} = \mu$, *and* $\frac{\lambda}{\mu} < \infty$. *Assuming* $K \leq B$, *we have that*

$$\lim_{\mathrm{SNR}\to\infty} \mathrm{Pr}_g \left[\widetilde{\mathrm{R}}_{\mathrm{MC}}\left(\mathrm{SNR}; 2; 2; g\right) < 1\right] = \omega\left(\frac{\lambda}{\mu}\right), \tag{4.45}$$

*with* $\omega(x) \triangleq \left(1 - \frac{1}{(1+x)^2}\right)^2$ *;*

$$\lim_{\mathrm{SNR}\to\infty} \mathrm{Pr}_g \left[\widetilde{\mathrm{R}}_{\mathrm{MT}}\left(\mathrm{SNR}; K; B; g\right) < 1\right] = 1. \tag{4.46}$$

For the scenario MC, it is seen that (in the high SNR regime) allowing the transmitters to water-fill over the $B$ available bands instead of restricting the spectrum use to a single band leads to a global performance degradation with a probability which is not vanishing. The probability of having a performance degradation is seen to be an increasing function of $\frac{\lambda}{\mu}$. It equals to $\frac{9}{16} = 56.25\%$ when the channels gains are i.i.d. (namely, $\lambda = \mu$) and equals about 98% when $(\lambda, \mu) = (1, 0.1)$ ; note that this result holds for high SNR. Simulations will show that, for medium SNRs, the considered probability is in fact decreasing from a certain SNR value, confirming the intuition that under low interference levels water-filling is optimal. The result concerning the potential performance degradation questions the use of algorithms such as the IWFA ; rather, an iterative algorithm which operates with discrete sets may lead to a better global performance. At high SNR, the scenario MT, in which equilibrium consists in using all bands at full power, always performs less than the worst equilibrium of the scenario SC. This is due to the fact the global performance is interference limited in this regime and the MT equilibrium creates more interference than the MC equilibrium, which is already less efficient than the SC equilibrium with a typically high probability. Of course, the fact that the degradation event is likely in scenario MC does not necessarily mean that the average rate is severely degraded, which explains why the expected rate is also considered. This is the purpose of the next proposition.

**Proposition 4.6.5** (**Extreme SNR regimes, expected rates**). *Assume that* $\forall b$, $\gamma_{11}^b = \gamma_{22}^b = \lambda$, $\gamma_{12}^b = \gamma_{21}^b = \mu$, *and* $\frac{\lambda}{\mu} < \infty$. *We have that*

$$\lim_{\mathrm{SNR}\to 0} \widetilde{\Gamma}_{\mathrm{MC}}\left(\mathrm{SNR}; K; B\right) = 1, \ \textit{for arbitrary } K \textit{ and } B; \tag{4.47}$$

$$\lim_{\mathrm{SNR}\to 0} \widetilde{\Gamma}_{\mathrm{MT}}\left(\mathrm{SNR}; K; B\right) = \frac{B}{\sum_{b=1}^{B} \frac{1}{b}}, \ \textit{for arbitrary } K \textit{ and } B; \tag{4.48}$$

$$1 - \omega\left(\frac{\lambda}{\mu}\right) < \lim_{\mathrm{SNR}\to\infty} \widetilde{\Gamma}_{\mathrm{MC}}\left(\mathrm{SNR}; 2; 2\right) < 1 - \frac{1}{2}\omega\left(\frac{\lambda}{\mu}\right) \tag{4.49}$$

*where* $\omega(x)$ *is defined in Proposition 4.6.4 ;*

$$\lim_{\mathrm{SNR}\to\infty} \widetilde{\Gamma}_{\mathrm{MT}}\left(\mathrm{SNR}; KB\right) = 0, \ \textit{for any } K \leq B. \tag{4.50}$$

The first result translates that the equilibrium power allocation policies of the MC and SC scenario coincide in terms of expected rate at low SNR. The second result allows one to quantify to what extent MT equilibrium policies performs better than SC ones. This gain is seen to be independent of $\lambda$ and $\mu$, which is due to the fact that noise dominates the interference and useful or direct channels are identically distributed. The third result shows that equilibrium MC policies necessarily induce a performance degradation and the corresponding loss can be bounded. In a typical case in which the interference power is smaller than the useful signal by 10 dB (e.g., when $(\lambda, \mu) = (1, 0.1)$), we have that

$0.02 < \widetilde{\Gamma}_{\mathrm{s}}(\mathrm{SNR}; 2; 2) < 0.51$. This means that using a multi-channel power allocation scheme instead of a single-channel one leads to dividing the total sum-rate by at least $\frac{1}{0.51} \simeq 2$. The fourth result readily follows from the result of Proposition 4.6.4 concerning the MT scenario.

So far, almost all the provided results concern finite interference networks regarding the number of transmitter-receiver pairs and the number of bands. An important question is whether the exhibited performance degradation phenomenon can be observed in larger networks. Finding the worst and best equilibria in games with large number of players does not seem to be trivial and is left as a significant extension of the present work. Instead, we compare interesting power allocation policies which do not correspond to equilibria in general :

• For the MC scenario : $\forall k \in \mathcal{K}, p_k = \left(\frac{P_{\max}}{B}, ..., \frac{P_{\max}}{B}\right)$.

• For the SC scenario : $\forall k \in \mathcal{K}, p_k = P_{\max} e_{b_k^\star}$ where $b_k^\star = \arg\max_b g_{kk}^b$.

• For the MT scenario : $\forall k \in \mathcal{K}, p_k = (P_{\max}, ..., P_{\max})$. The uniform power allocation policy happens to be the unique equilibrium of the game MT as well.

Assuming these policies and a large interference network, the following result can be proved.

**Proposition 4.6.6** ($K$ **large,** $B$ **finite**). *Assume $K \to \infty$, $B < \infty$ with i.i.d. information channel gains $g_{kk}^b$ and i.i.d interference channel gains $g_{k\ell}^b (k \neq \ell)$. Then for all* $\mathrm{s} \in \{\mathrm{MC}, \mathrm{MT}\}$ *we have that*

$$\lim_{\mathrm{K}\to\infty} \overline{\mathrm{R}}_{\mathrm{s}}(\mathrm{SNR}; K; B; g) = \ell_B = \frac{1}{\sum_{b=1}^{B} \frac{1}{b}} \tag{4.51}$$

*If $K \to \infty$, $B \to \infty$ and $\frac{B}{K} \to 0$, we have that $\ell_B \sim \frac{1}{\log B}$.*

This result allows one to compare the scaling laws of two interference networks which allow only uniform power allocation and channel selection respectively. For $B = 10$, the corresponding ratio equals about 3, showing a significant degradation involved by allowing the transmittenewr to exploit all the available bands. Of course, this result is pessimistic in the sense that interference channels are assumed to have the same average gain as the direct channels. Otherwise, the interference scenario will be less severe. The generalization of Proposition 4.6.6 to the non i.i.d. channel gains may be obtained by using tools from large random matrix theory [58] [59]. It might be argued that the number of transmitter-receiver pairs is taken to be large while not expanding the available spectrum resources. To address this issue another type of asymptotic regimes has to be considered that will not be be tackled here.

## 4.7 Numerical performance analysis

### 4.7.1 Team power control

In this subsection, we first illustrate the influence of auxiliary variable through simulations. More specifically, we demonstrate the theoretical results that under certain conditions, auxiliary variable brings performance improvement. We then analyze the algorithm

proposed in Sec 3.4 in greater detail showing its salient features in wireless applications as well as its limitations. To this effect, we shall mainly concentrate on energy efficiency as the utility function, proposing a novel continuous and scalable power control policy. However our framework is general and can be applied to different problems in wireless communications with distributed resource allocation.

### Simulation setup

Firstly, we shall define the various utilities that we consider in our simulations. Denote as $\mathbf{G}$ the global channel matrix with the entries $g_{ij}$, where $i$ and $j$ being respectively the row and column indices, the utilities sum-energy-efficiency, sum-goodput and sum-rate can be defined respectively as :

$$u^{\mathrm{EE}}(p_1, \ldots, p_K; \mathbf{G}) = \sum_{k=1}^{K} \frac{\exp(-c/\gamma_k)}{p_k} \tag{4.52}$$

$$u^{\mathrm{GP}}(p_1, \ldots, p_K; \mathbf{G}) = \sum_{k=1}^{K} \exp(-c/\gamma_k) \tag{4.53}$$

$$u^{\mathrm{SR}}(p_1, \ldots, p_K; \mathbf{G}) = \sum_{k=1}^{K} \log_2(1+\gamma_k) \tag{4.54}$$

where $\gamma_k = \frac{p_k g_{kk}}{\sigma^2 + \sum_{j \neq k} p_j g_{jj}}$, $\sigma^2$ is the received noise variance and $c = 2^r - 1$ with $r$ being the spectral efficiency. In this chapter, we set $c = 1$ for all simulations.

Algorithm 2 requires the channel realization feedback to be quantized. To this effect, we chose to use maximum entropy quantizer (MEQ). This is to ensure that even in the case of skewed channel statistics, the quantization intervals have uniform probability, thus maximizing the entropy and encoding the most information. More formally, assume $R$ as the size of the quantizer and $\phi_{ii}(g_{ii})$ as the p.d.f. of $g_{ii}$, for MEQ, the quantization interval bounds $u_{ii,r}$ are fixed once and for all according to :

$$\forall r \in \{1, ..., R\}, \forall i \in \{1, ..., K\}, \ \int_{u_{ii,r}}^{u_{ii,r+1}} \phi_{ii}(g_{ii}) \mathrm{d}g_{ii} = \frac{1}{R}. \tag{4.55}$$

The representative of the interval $[u_{ii,r}, u_{ii,r+1}]$ is denoted by $v_{ii,r}$ and is chosen to be its centroid :

$$v_{ii,r} = \frac{\displaystyle\int_{u_{ii,r}}^{u_{ii,r+1}} g_{ii}\phi_{ii}(g_{ii})\mathrm{d}g_{ii}}{\displaystyle\int_{u_{ii,r}}^{u_{ii,r+1}} \phi_{ii}(g_{ii})\mathrm{d}g_{ii}}. \tag{4.56}$$

To implement MEQ, only the knowledge of channel statistics $\phi_{ii}$ is required. Additionally, the complexity involved is very low. In all the simulations, MEQ is implemented to quantize the channel gain unless otherwise stated.

The channel gains are chosen independently and according to an exponential law $\phi_{ij}(g_{ij}) = \frac{1}{\mathbb{E}(g_{ij})} \exp\left(-\frac{g_{ij}}{\mathbb{E}(g_{ij})}\right)$ (that is, Rayleigh fading is assumed). We also assume, for

ease of exposition, that the channel gain statistics (path losses) are symmetric over all the users and $\mathbb{E}(g_{ii}) = 1$.

Unless otherwise stated, we consider the following parameters in our simulations; number of Tx-Rx pairs $K = 2$, the noise variance $\sigma^2 = 1$, $P_{\max} = 2$, SIR $= 5.2dB$, and $\text{card}(\mathcal{G}) = 15$.

**Effects of the auxiliary variables**

In Theorem 3.3.1 we show that the auxiliary variable can be useful in coordination problems when constraints are present. In the problem of power control, a natural constraint to consider would be the quality of service constraint. In our illustration, we consider the utility sum-rate in multi access channel (MAC) scenario, which is a special case of interference channel scenario. The channel between the $i$th transmitter and the receiver is denoted as $g_i$ and the sum-rate can be similarly defined as

$$u_{\text{MAC}}^{\text{SR}}(p_1, \ldots, p_K; g_1, \ldots, g_K) = \sum_{k=1}^{K} u_i \tag{4.57}$$

where

$$u_i(p_1, \ldots, p_K; g_1, \ldots, g_K) = \sum_{k=1}^{K} \log_2(1 + \frac{g_k p_k}{\sigma^2 + \sum_{j \neq k} g_j p_j}) \tag{4.58}$$

All the alphabets are considered to be binary with $P_i \in \{0, P_{max}\}$, $g_i \in \{0.3, 1\}$ and $V \in \{V_1, V_2\}$. The probability for each channel realization is half, namely, for $i \in \{1, 2\}$, $\Pr(g_i = 0.3) = \Pr(g_i = 1) = 50\%$. For the constraints, we considered the asymmetric case where $u_1 \geq 0.45 \times \sum_{k=1}^{K} \log_2(1 + \text{SNR})$ and $u_2 \geq 0.15 \times \sum_{k=1}^{K} \log_2(1 + \text{SNR})$ with $\text{SNR} = \frac{P_{\max}}{\sigma^2}$. For maximizing the utility sum-rate for $K = 2$ transmitters, we show in Fig. 4.1 that having a coordination key can significantly improve the performance, especially at high SNR where coordination becomes important. We plot 2 curves with the auxiliary variable with different probability distributions for the binary alphabet. We chose the probabilities for the benchmark curve with auxiliary variable to be $\Pr(V = V_1) = \Pr(V = V_2) = 50\%$. Additionally, it can be observed that the performance can be improved when optimizing the distribution of the auxiliary variable. With the optimal $V^\star$, the higher sum-energy-efficiency can be achieved when comparing with the performance with the equiprobability auxiliary variable $V$.

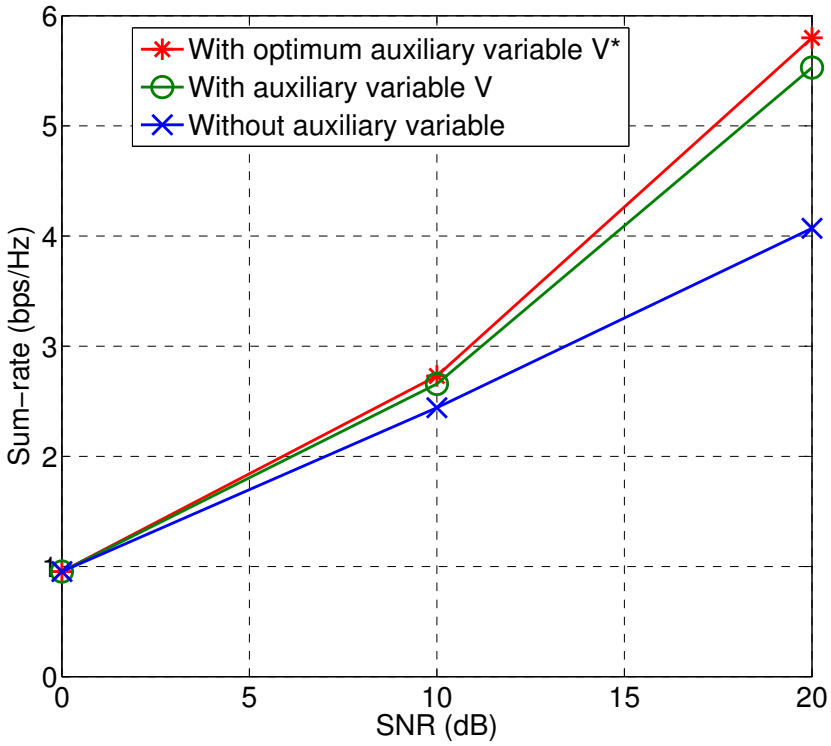


FIGURE 4.1 – Considering the sum-rate utility for $K = 2$ with quality of service constraints, we see a significant performance gain at high SNR. This figure demonstrates the usefulness of the auxiliary variable in improving the coordination performance.

### Analysis of the algorithm

We compare the performance of our distributed algorithm with two references which serve as an upper and a lower bound. For the upper bound, we consider the centralized social optimum given the global CSI. Even though our algorithm uses much less information than the upper bound, we show that we can achieve comparable performances with a distributed algorithm with much lesser complexity.

For the lower bound, we consider Nash Equilibrium. At first glance, this comparison might seem unfair given the fact that Nash equilibrium is arrived at by each transmitter maximizing it's individual utility not the sum-utility. However, given that our algorithm uses only local CSI and is distributed, this is the best state of the art algorithm for comparison.

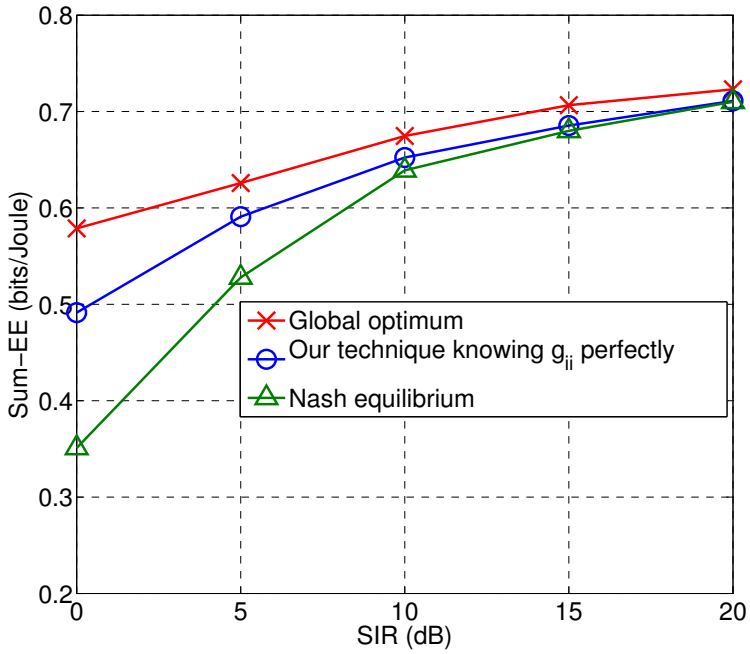


FIGURE 4.2 – Considering the sum-energy for K=2, our technique outperforms the Nash equilibrium at low SIR.

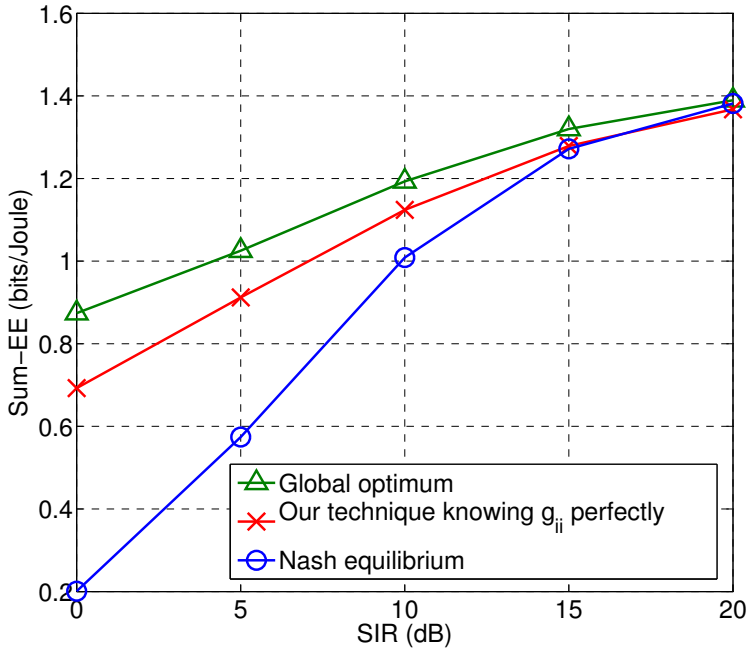


FIGURE 4.3 – Same scenario as Fig. 4.2 but for K=4. We notice similar trends. However the performance gain w.r.t. Nash equilibrium is unsurprisingly higher.

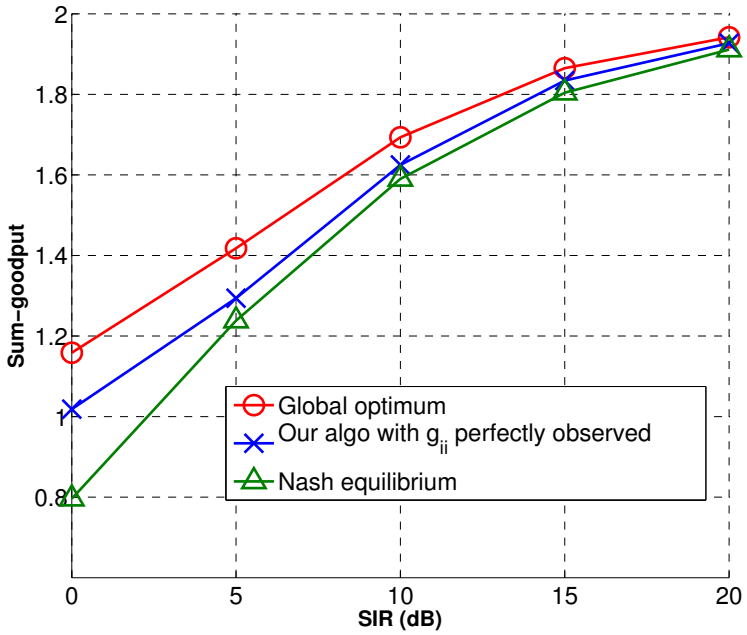


FIGURE 4.4 – Considering the sum-goodput utility, we notice that eventhough our algorithm outperforms Nash equilibrium, the performance gain is not much .

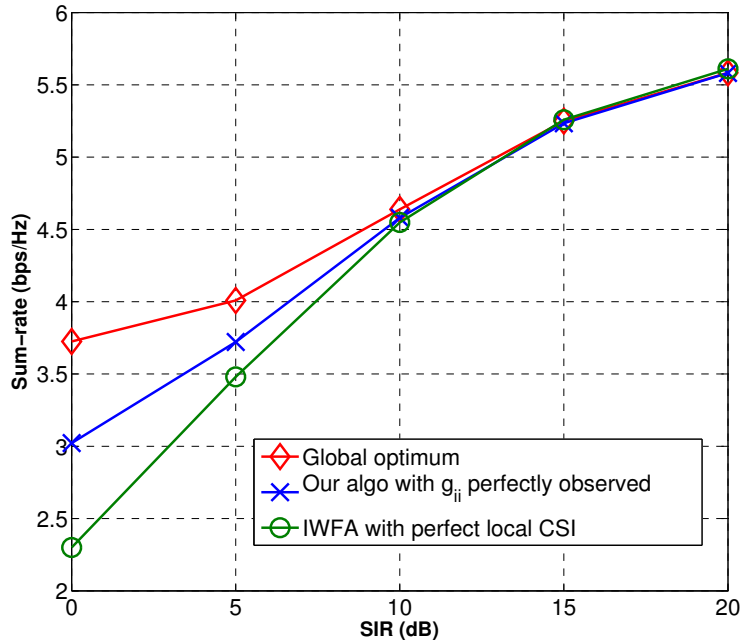


FIGURE 4.5 – Considering the sum-rate utility, we see similar gains as in the case of sum-goodput.

In Figs. 4.2, 4.4 and 4.5, we plot the performance of these three techniques for different utilities, namely sum-energy-efficiency , sum-goodput ($P_{\max} = 1000$) and sum-rate

($P_{\max} = 10$) respectively. The performance of three techniques is evaluated via Monte Carlo simulations. We plot the performance as a function of signal to interference ratio (SIR). As an example, the signal-to interference ratio (SIR) for the case with $K = 2$ transmitters :

$$\mathrm{SIR(dB)} = 10\log_{10}\left(\frac{\mathbb{E}(g_{11})}{\mathbb{E}(g_{21})}\right) = 10\log_{10}\left(\frac{\mathbb{E}(g_{22})}{\mathbb{E}(g_{12})}\right). \tag{4.59}$$

assuming symmetric channel statistics. For intuition, the higher the SIR, the lesser the influence of cross channels.

Figs 4.2 and 4.3 serve as comparison for the same utility (sum-energy) but for different number of transmitters $K = 2$ and $K = 4$. Greater number of transmitters only improves the performance gain w.r.t. the Nash equilibrium.

As expected, we notice that at low SIR, one can obtain significant performance gains with our algorithm as compared to the Nash equilibrium. This is because at low SIR levels, coordination is important to mitigate the strong interference. More importantly, and surprisingly however, our algorithm performs close to the social optimum with much less information available to it. In As a sanity check, we see that for all the three figures, at high SIR, the performance of all the three techniques coincide, since the interference is negligible.

Our algorithm takes into account the feedback noise. To illustrate the effect of noise on the utility region, in Fig. 4.6, we plot the regions for different levels of noise. To parametrize different levels of noise, we define the estimation signal-to-noise ratio (ESNR) for the feedback (prior information) as follows :

$$\mathrm{ESNR}_i = \frac{\mathbb{E}[\mathcal{Q}^2(g_{ii})]}{\mathbb{E}[(\mathcal{Q}(g_{ii}) - \mathcal{Q}(\widetilde{g}_{ii}))^2]}. \tag{4.60}$$

where $g_{ii}$ is the channel gain from transmitter $i$ to receiver $i$, $\widetilde{g}_{ii}$ is the estimated channel gain in the receiver side and $\mathcal{Q}$ is the quantization function.

We also plot the social optimum for reference. Unsurprisingly, we see that the more noisy the feedback, the smaller the utility region becomes. Our algorithm performs only 10 % worse than the centralized social optimum, and even at high noise levels (ESNR=3 dB), the performance gap is less than 20%.

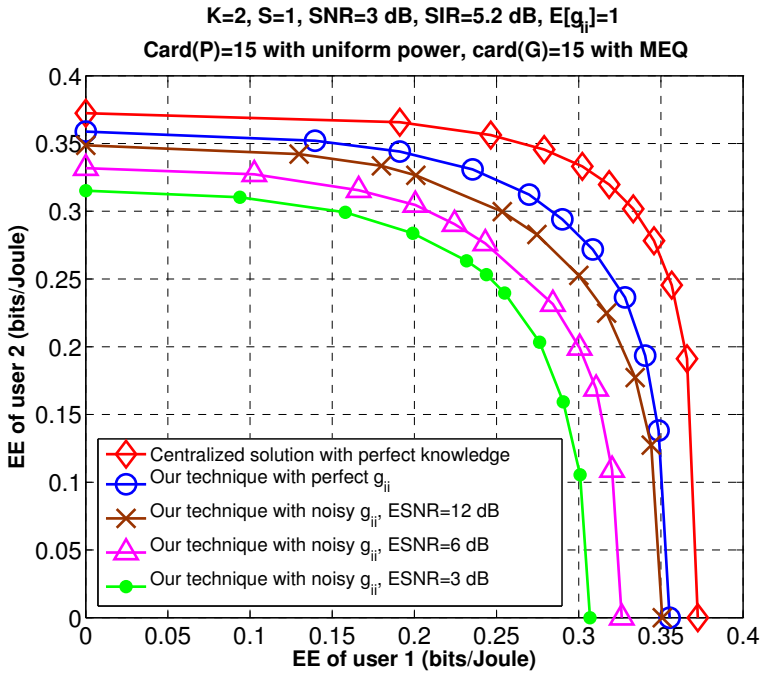


FIGURE 4.6 – The loss induced by our algorithm is less than 10% when the receiver has perfect channel estimate. The loss increases when we have noisy observation but is still less than 20% even at a high noise level.

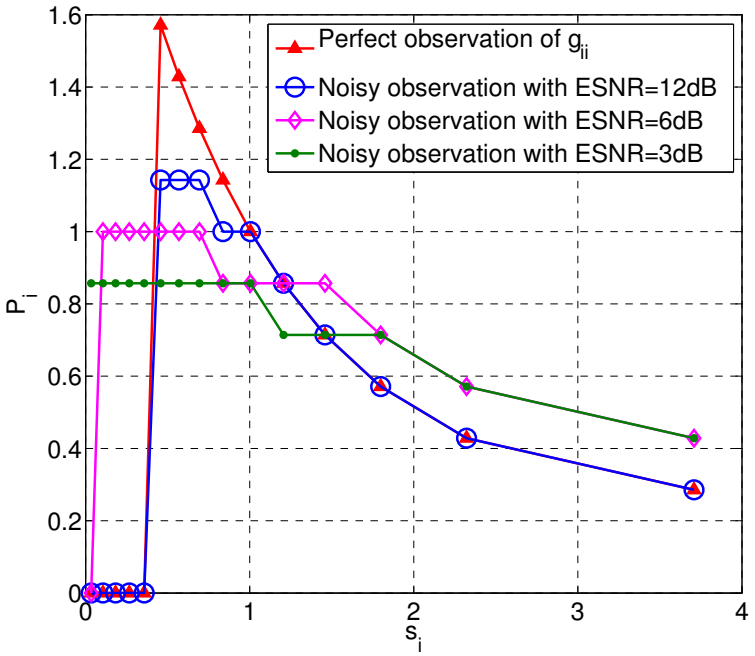


FIGURE 4.7 – The shape of decision function with no noise is a threshold function. At higher noise levels, less power levels will be selected due to the inaccuracy of the information available.

From Fig 4.7, we can gain intuition on the influence of noise on the decision functions found by our algorithm. It can be observed that the power control functions become more uniform at higher noise levels, as the information received is less reliable, and thus transmitters emit at a power level which maximizes the utility after averaging over the uncertainty in observation due to the noise.

The principal drawback of the algorithm for applications in wireless applications is its complexity. Even for the simple problem of power control in an interference channel, if there are $K$ transmitter receiver pairs, the cardinality of the alphabet of global channel states $|\mathcal{A}_0| = |\mathcal{S}_{ij}|^{K^2}$. Since we do an exhaustive search for power control policies for each configuration of the global channel states, our algorithm scales badly w.r.t. number of Tx-Rx pairs.

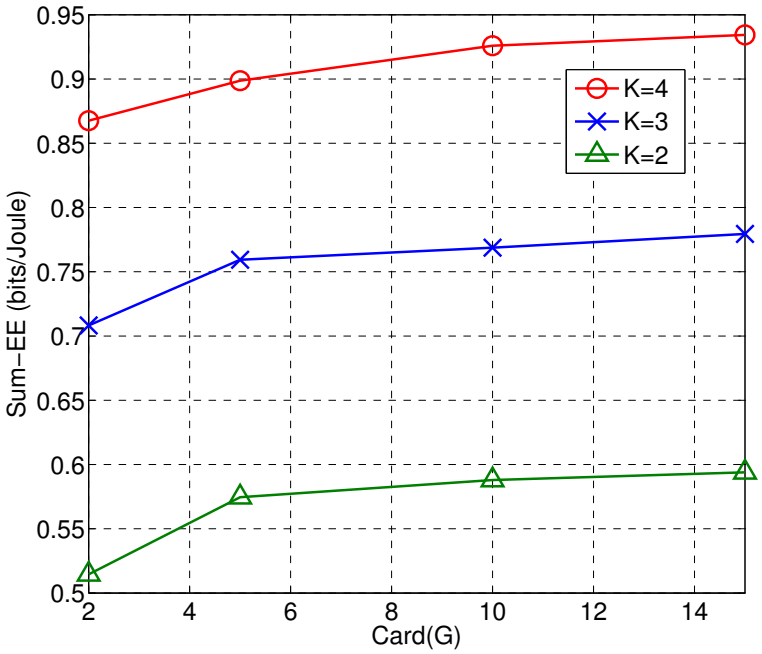


FIGURE 4.8 – The complexity of the algorithm depends highly on the cardinality of G. From this figure, we see that card(G) as less as 10 suffices to achieve good enough performance.

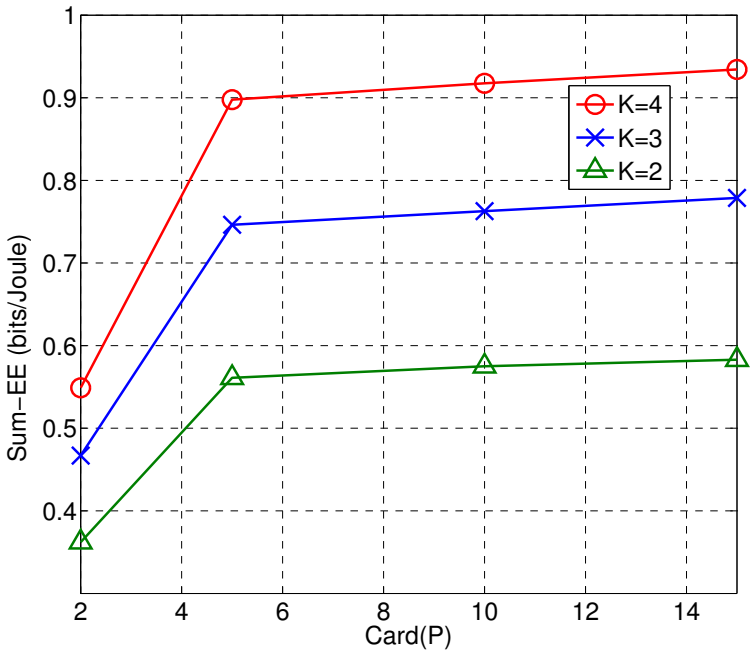


FIGURE 4.9 – While Card(P) is a less important factor in the complexity of the algorithm, we show that one does not require many power levels to get good decision functions.

However, it is not all doom and gloom. The complexity also depends on the cardinality of the power levels, $|\mathcal{P}|$, available for the transmitters. From Figs. 4.9 and 4.8, we see that the required cardinality of P and G to achieve good performances is relatively small. This helps the optimization problem tractable at least for problems with small number of transmitter receiver pairs.

The intuition gained from the small test cases can be used to reduce the search space for optimal power control functions. We illustrate the methodology by treating the case of sum-energy. From Fig 4.7 we see that the decision function in case of no noise has a simple structure. Transmitters either transmit at zero, if the channel is below certain threshold and $\frac{c\sigma^2}{\Omega(g_{ii})}$ otherwise. This continuous power control scheme requires only the threshold to be found for each transmitter instead of finding the decision function for each transmitter. This reduces the search space for the optimization many-fold. We can use the same procedure as our algorithm for finding the thresholds for all transmitters in a distributed fashion.

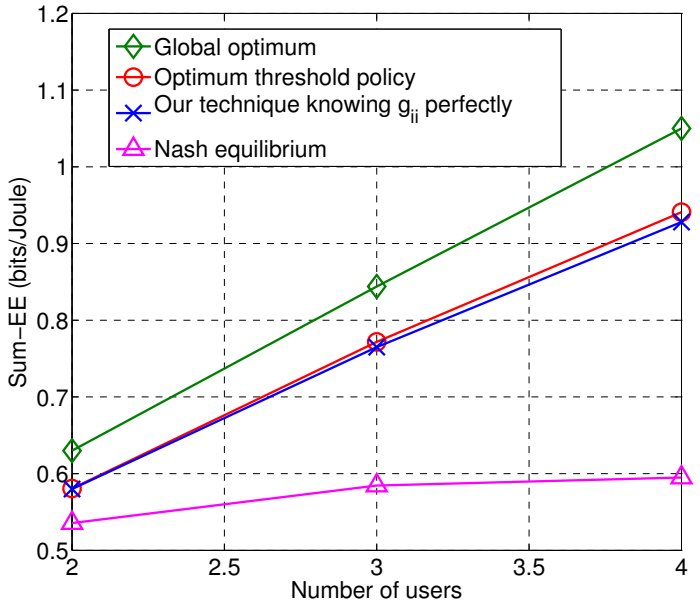


FIGURE 4.10 – In this figure, we compare the performance of the four proposed methods for different number of users. We see that the threshold policy performs comparably to the algorithm. Also, increasing the number of users gives greater performance gain w.r.t. Nash equilibrium

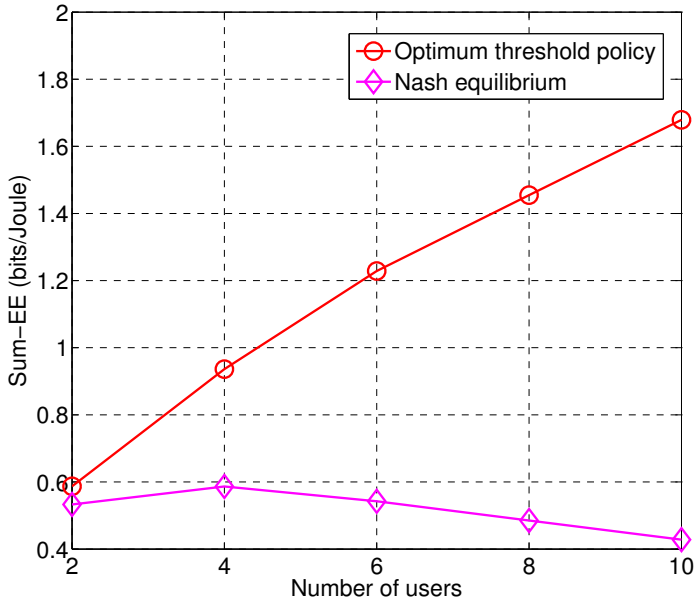


FIGURE 4.11 – The threshold policy is highly scalable and we can thus compare it to Nash equilibrium when number of users are high. The performance difference increases dramatically as number of users increase, thus highlighting the inbuilt coordination in the threshold policy.

To be sure that this reduction of complexity does not entail any performance loss, in Fig. 4.10 we compare the threshold policy with our algorithm for upto 4 transmitters. While this is not a proof that there is no performance loss, it does instill some confidence in our simplification. Moreover since it is a continuous power control scheme, it slightly outperforms the algorithm since there is no loss induced by discretization of P. In Fig. 4.11, we see that while the performance of Nash equilibrium deteriorates with more number of transmitters, the thresholding policy scales very well. This is not surprising as coordination becomes more important when there are many transmitters.

Unfortunately, this step requires intuition which cannot be easily automatized and is not a general procedure. Nonetheless, given the tremendous gains achieved due to this step in reducing the complexity, it is well worth the effort.

### 4.7.2 Selfish power control

In this subsection, we provide simulations for the case where all agents maximize their own utility in a selfish way. We consider three different scenarios corresponding to different action profiles described in Sec. 3.6, namely MC (multi channel), MT (multi transmitter) and SC (single channel). We compare their performances at equilibria. For the analysis, we distinguish different scenarios in terms of the network size ; Finite systems corresponding to upto 4 users - 4 bands and Large systems corresponding to the case when there are more (in orders of magnitude) users and 10 bands.

#### Finite systems : Multi-Channel scenario equilibria vs. Single-Channel scenario equilibria

We consider here that $(K, B) = (2, 2)$ and $(K, B) = (4, 4)$. The direct channels are assumed stronger than the interfering ones : $(\lambda, \mu) = (1, 0.1)$. Our objective is to evaluate the sum-rate performance gap between the MC and SC at equilibrium. Fig. 4.12 and 4.13 respectively represent $\mathrm{Pr}_g\left[\widetilde{\mathrm{R}}_{\mathrm{MC}}\left(\mathrm{SNR}; K; B; g\right) < 1\right]$ and $\widetilde{\Gamma}_{\mathrm{MC}}\left(\mathrm{SNR}; K; B\right)$ as functions of $\mathrm{SNR(dB)} = 10\log_{10}\mathrm{SNR}$. As our analytical results forecast, the probability that the MC equilibrium power allocation policies perform less than the SC ones tends to zero at low SNR and tends to one at high SNR. Fig. 4.12 also shows that this probability increases with SNR. These results are obtained using the IWFA algorithm under the equilibrium uniqueness condition of [48]. Interestingly, the figure allows one to delineate the two regimes in which the multi-channel solution performs better or worse than the SC one : the SNR threshold is about 25 dB. Above this threshold, restricting the choices of the transmitters in terms of using the spectrum is beneficial. For example, as shown in Fig. 4.13, when SNR(dB) = 45 dB (which is a typical value in WiFi systems) the equilibrium MC sum-rate is only 60% of the sum-rate achieved by allowing the transmitters to use a single band only. Since these observations hold for a typical but specific choice $(\lambda, \mu) = (1, 0.1)$, we also study the influence of the ratio $\frac{\lambda}{\mu}$ which represents the relative strength of the useful link compared to interference links. For SNR(dB) = 70 dB and $\lambda = 1$, Fig. 4.14 precisely represents $\mathrm{Pr}_g\left[\widetilde{\mathrm{R}}_{\mathrm{MC}}\left(\mathrm{SNR}; K; B; g\right) < 1\right]$ as function of $\frac{\lambda}{\mu}$ in dB, for $(K, B) = (2, 2)$ and $(K, B) = (4, 4)$. As proved in (4.45) for $(K, B) = (2, 2)$, it can be seen that the probability that MC induces global performance degradation increases

with the latter ratio. In other words, if the interference is relatively weak, the probability of performance degradation will be high. This is also confirmed by simulations for $(K, B) = (4, 4)$. But this holds for very high SNRs. By considering SNR(dB) = 50 dB, Fig. 4.15 shows that the performance degradation vanishes as the interference level decreases. The intuition is that, when the interference is low, the network behaves like a set of independent single-user communications i.e., water-filling over all the available bands is optimal. However, this is not observed for SNR(dB) = 70 dB and higher values for SNR : when $\sigma^2 \to 0$, the interference is not negligible compared to the noise. Other simulations, which are not reported here for obvious space limitations confirm the general tendencies the three commented figures indicate for different $(K, B)$.

**Finite systems : Multi-Transmitter scenario equilibria vs. Single-Channel scenario equilibria**

Here, exactly the same approach as the preceding subsection is conducted by considering the MT scenario instead of MC. The observations concerning $\mathrm{Pr}_g\left[\widetilde{\mathrm{R}}_{\mathrm{MT}}\left(\mathrm{SNR}; K; B; g\right) < 1\right]$ are similar to those made for $\mathrm{Pr}_g\left[\widetilde{\mathrm{R}}_{\mathrm{MC}}\left(\mathrm{SNR}; K; B; g\right) < 1\right]$ and will therefore not be reported here. For $\widetilde{\Gamma}_{\mathrm{MT}}\left(\mathrm{SNR}; K; B\right)$ the behavior is also quite similar to $\widetilde{\Gamma}_{\mathrm{MC}}\left(\mathrm{SNR}; K; B\right)$, as advocated by Fig. 4.16. For $(K, B) = (4, 4)$, it can be seen that : at low SNR, using the multi-transmitter solution allows the sum-rate to be multiplied by about 2 w.r.t. the single-channel solution ; at high SNR, the MT solution sum-rate is divided by about 2 ; for intermediate SNR, the sum-rate performance of the MT and SC are close. At low SNR, the values forecasted by (4.48) are validated. Similarly, when the SNR goes beyond 70 dB, predictions from (4.50) are also observed.

**Large systems : MC/MT Uniform Power Allocation policy vs. Best Channel Selection policy**

We focus here on the expected sum-rate comparison between the UPA (MC setting), the full power $P^{\max}$ in every channel policy (MT setting) and the best channel selection policy (CS setting). Fig. 4.17 represents the expected sum-rates against the number of transmitter-receiver pairs $K$, for the scenario : $B = 10$, SNR = 10 dB, $(\lambda, \mu) = (1, 0.1)$. This figure allows one to have an idea about the network scaling laws under different power allocation policies. Roughly, when the system is not loaded, say for a load which is less than $\frac{K}{B} = \frac{30}{10}$ for the considered simulation setting, using several bands is beneficial for the network sum-rate. Above this threshold, using a single band allows to achieve a significantly better sum-rate performance.

## 4.8 Conclusion

From the analytical point of view, this chapter provides three important contributions. Firstly, it offers a possible framework to fully characterize the performance of distributed power control under (arbitrary) partial information. The limiting performance analysis is conducted in terms of long-term utility region and while we assume the global channel state to be i.i.d. and the observation structure to be memoryless ; one relevant extension

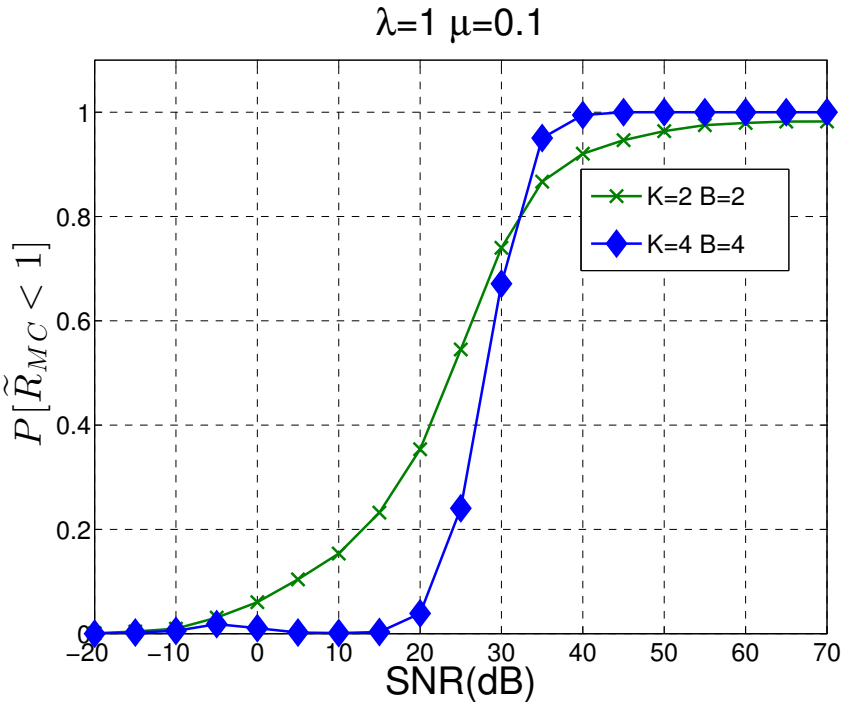


FIGURE 4.12 – Probability that using multiple channels (MC) instead of one (SC) induces a global performance degradation at equilibrium vs. SNR.

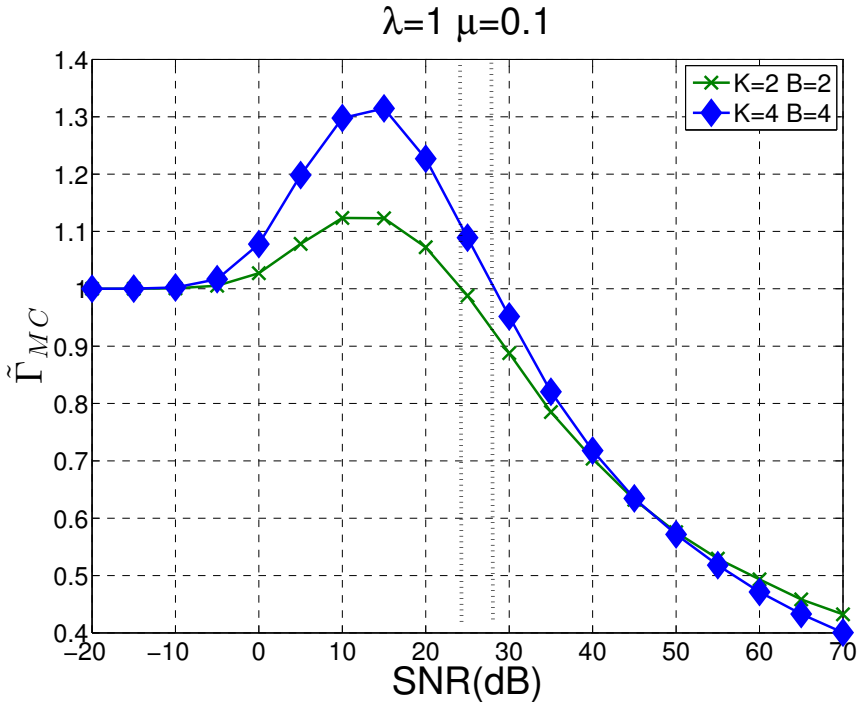


FIGURE 4.13 – Ratio between the expected equilibrium sum-rates in MC and SC scenarios.

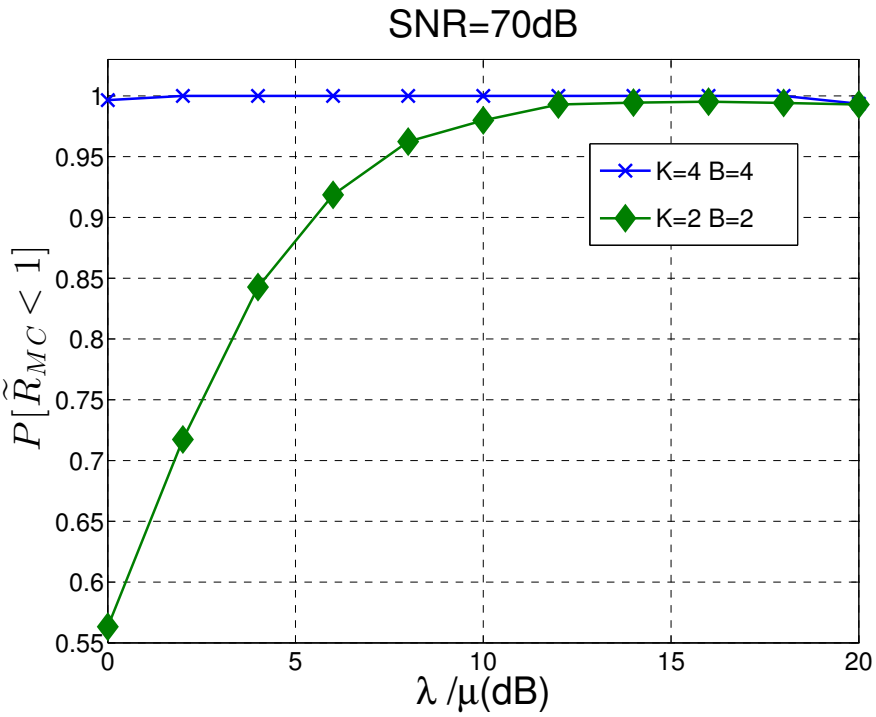


FIGURE 4.14 – Probability that using multiple channels (MC) instead of one (SC) induces a global performance degradation at equilibrium vs. $\frac{\lambda}{\mu}$.

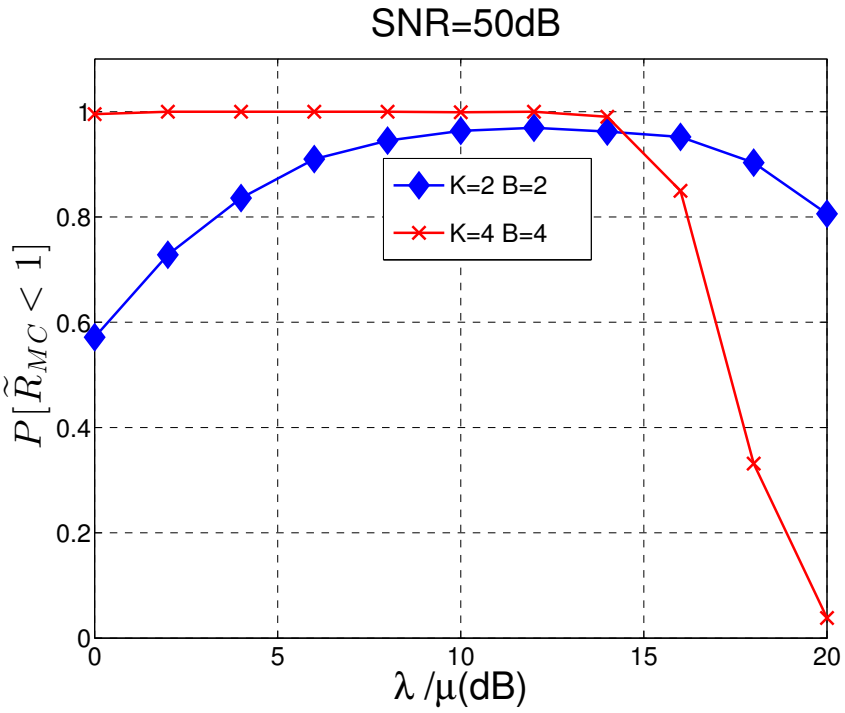


FIGURE 4.15 – Probability that using multiple channels (MC) instead of one (SC) induces a global performance degradation at equilibrium vs. $\frac{\lambda}{\mu}$.

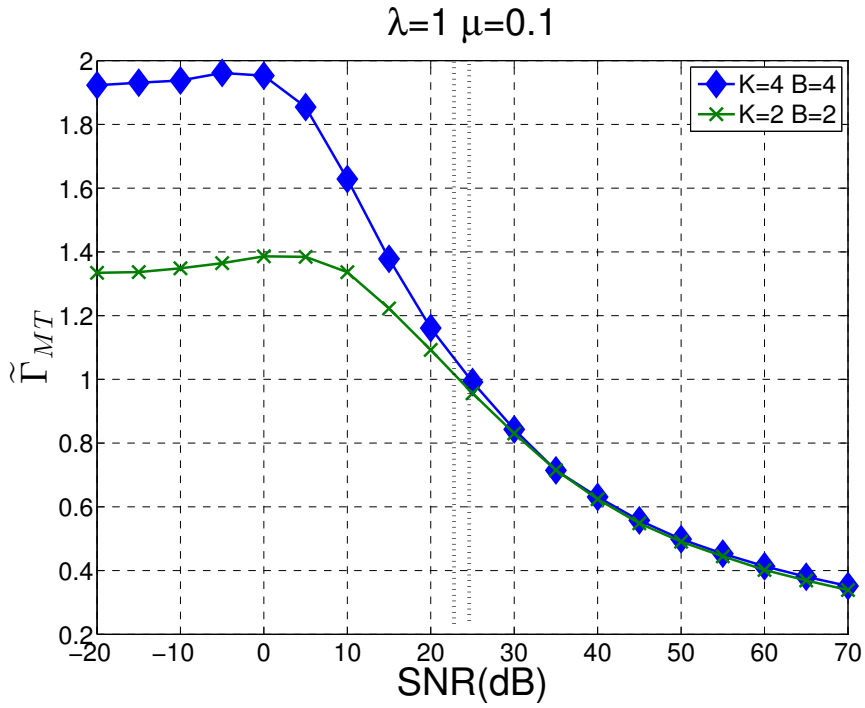


FIGURE 4.16 – Ratio between the expected equilibrium sum-rates in MT and SC scenarios.

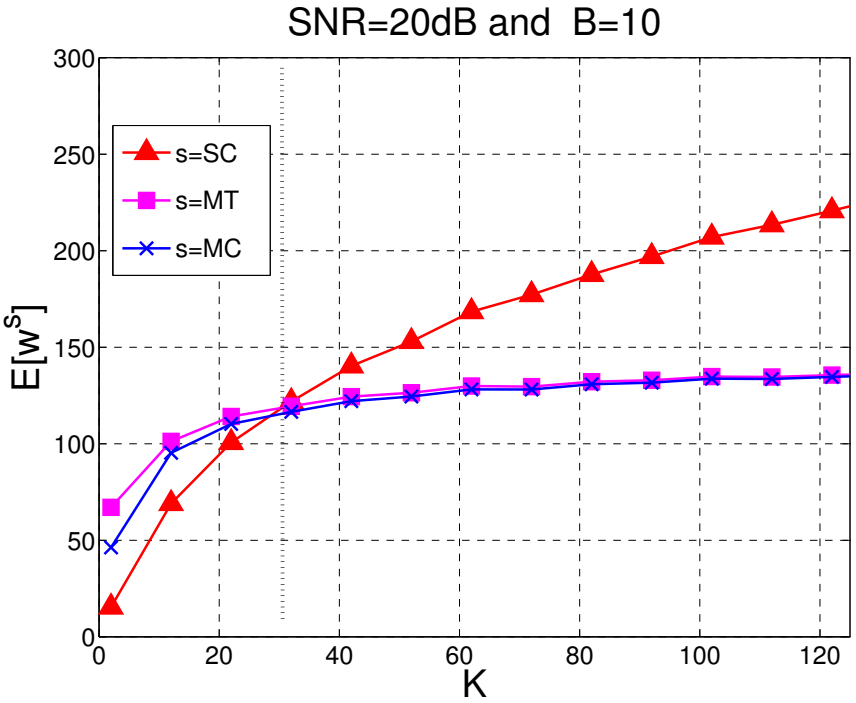


FIGURE 4.17 – Expected sum-rate against the number of users $K$.

is to relax these assumptions e.g., by considering Gauss-Markov processes for the channel variations. Additionally, the analysis is conducted by assuming discrete the various quantities at use such as the transmit power. We have provided several strong motivations for this but the proposed framework might be easily developed to continuous quantities. Now, one of the drawbacks for considering discrete quantities is the computational complexity involved by the determination of good power control strategies. Here also, our work might be improved.

Secondly, considering the numerical performance analysis, the obtained results of the proposed team power control scheme are convincing in the sense that the state of the art power control schemes are outperformed. In particular, our work allows one to determine the shape of good decision functions in a systematic manner, whereas it has been done so far in an empirical manner. And, this, for any utility function. As clearly explained, we have shown how to find good stationary memoryless power control strategies, but when it comes to other channel processes such as Gauss-Markov processes, good strategies might have to be with memory. This conjecture would need to be explored, constituting another technical challenge to be face with.

Finally, in distributed interference networks, it can be seen that allowing individual rate-maximizing transmitters to spread their power over the entire spectrum, as opposed to using a single band, may result in sum-rate performance losses.

# 5

# New connections between power domain feedback and signal domain operations

In this chapter, we show how power domain measurements can be exploited for two well-known signal domain processing techniques, namely opportunistic interference alignment and training-based signal domain channel estimation. As far as interference alignment is concerned, we consider the opportunistic version which was proposed in [9]. In [9], the authors assume that the primary transmitter chooses its precoding matrix to maximize its individual transmission rate while the secondary transmitter exploits the available spatial opportunities. For this, the secondary transmitter aligns its signal to guarantee zero interference at the primary receiver and needs global channel state information (CSI). A crucial problem problem with this technique is that the authors did not provide any technique to acquire the required information about the different channels, knowing that the authors recommend that global CSI be available. In this chapter, we show that global CSI is not required to implement the opportunistic interference alignment of [9]. Indeed we prove that the sole knowledge of the interference-plus-noise covariance matrix feedback at the secondary transmitter is sufficient to implement the technique under consideration ; this assumption has been made e.g., to derive the MIMO version of iterative water-filling algorithm [15]. Now concerning training-based channel estimation, we show that the received power measurements can be used as priors to improve the channel estimation accuracy level significantly. Specifically, we propose a new MMSE and MAP estimators which integrate this prior knowledge. Mean square estimation error can be decreased by about 50% in typical scenarios in terms of SNR and even by assuming a quite small number of available received power measurements.

# 5.1 Implementing opportunistic interference alignment in MIMO cognitive radio networks

## 5.1.1 Motivation and state of the art

To respond to the ever increasing demand for spectrum, recently, cognitive networks have been proposed. Under the cognitive network paradigm, unlicensed wireless users (secondary users) may dynamically access the licensed bands from legacy spectrum holders (primary users), either through negotiations or on an opportunistic basis [60]. In the case of opportunistic access however, it is important that secondary users do not induce any significant degradation of quality of service (QoS). The opportunity for exploitation arises when either the transmissions by the primary users are sporadic, thus allowing the secondary users to exploit the spectrum in between or simply because the primary network has no infrastructure in a particular area, in which case the secondary networks can exploit it at all times.

In the case of dense networks however, the unused spectrums, also referred to as white spaces, might be a rare and ephemeral occurence. Cognitive radio, as originally presented in [61], relies crucially on the availability of such white spaces, failing which the secondary systems generate additional interference while transmitting. One way to mitigate this issue is by using a recently developed solution of interference alignment (IA). In essence, the technique of IA involves constructing signals such that the corresponding interference signal lie in an orthogonal subspace to the signal of interest at receiver. This technique was introduced independently through several articles [62][63]. It has recently become an important tool to study the degrees of freedom of interference channels [63]. IA has been analyzed for feasibility and implementation issues, especially the required channel state information, in [64]. In [9], the technique of IA for cognitive networks was extended for the case of MIMO.

In this section, we present an alternative to the solution given in [9] to re-use the transmit opportunities. The latter solution aims at maximizing the transmission rate of the secondary link without generating interference to the primary link. However, as shown in [9], it is assumed that the secondary user knows the global channel state information (CSI) perfectly, which is not practical in many real wireless systems. Without dedicated feedback or inter-transmitter signaling channels, only the local CSI can be acquired easily by sending pilot symbols [11]. Technically, the approach proposed here distinguishes from [9] by the fact that it relies solely on local CSI and uses power domain feedback, namely covariance matrix [65]. Here we show how to reconstruct the IA scheme as [9] with less information about the channel available at the transmitters.

## 5.1.2 System Model

We consider two unidirectional links simultaneously operating in the same frequency band and producing mutual interference. The first transmitter-receiver pair $(\mathrm{Tx}_1, \mathrm{Rx}_1)$ is the primary link. The pair $(\mathrm{Tx}_2, \mathrm{Rx}_2)$ is an opportunistic link subject to the strict constraint that the primary link must transmit at a rate equivalent to its single-user capacity. Denote by $N_i$ and $M_i$, with $i = 1$ (resp. $i = 2$), the number of antennas at the

primary (resp. secondary) receiver and transmitter, respectively. Each transmitter sends independent messages only to its respective receiver and no cooperation between them is allowed, i.e., there is no message exchange between transmitters. This scenario is known as the MIMO interference channel (IC) [66][67] with private messages. A private message is a message from a given source to a given destination : only one destination node is able to decode it. Indeed, we do not consider the case of common messages which would be generated by a given source in order to be decoded by several destination nodes.

In this section, we assume the channel transfer matrices between different nodes to be fixed over the whole duration of the transmission. The channel transfer matrix from transmitter $j \in \{1,2\}$ to receiver $i \in \{1,2\}$ is an $N_i \times M_j$ matrix denoted by $\boldsymbol{H}_{ji}$ which corresponds to the realization of a random matrix with independent and identically distributed (i.i.d.) complex Gaussian circularly symmetric entries with zero mean and variance 1, which implies

$$\forall (i,j) \in \{1,2\}^2, \quad \text{Trace}\left(\mathbb{E}\left[\boldsymbol{H}_{ji}\,\boldsymbol{H}_{ji}^H\right]\right) = M_j N_i. \tag{5.1}$$

The $L_i$ symbols transmitter $i$ is able to simultaneously transmit, denoted by $x_{i,1}, \ldots, x_{i,L_i}$, are represented by the vector $\boldsymbol{x}_i = (x_{i,1}, \ldots, x_{i,L_i})^T$. We assume that $\forall i \in \{1,2\}$ symbols $x_{i,1}, \ldots, x_{i,L_i}$ are i.i.d. zero-mean circularly-symmetric complex Gaussian variables. In our model, transmitter $i$ processes its symbols using a matrix $\boldsymbol{V}_i$ to construct its transmitted signal $\boldsymbol{V}_i\boldsymbol{x}_i$. Therefore, the matrix $\boldsymbol{V}_i$ is called pre-processing matrix. Following a matrix notation, the primary and secondary received signals, represented by the $N_i \times 1$ column-vectors $\boldsymbol{s}_i$, with $i \in \{1,2\}$, can be written as

$$\begin{pmatrix} \boldsymbol{s}_1 \\ \boldsymbol{s}_2 \end{pmatrix} = \begin{pmatrix} \boldsymbol{H}_{11} & \boldsymbol{H}_{21} \\ \boldsymbol{H}_{12} & \boldsymbol{H}_{22} \end{pmatrix} \begin{pmatrix} \boldsymbol{V}_1\boldsymbol{x}_1 \\ \boldsymbol{V}_2\boldsymbol{x}_2 \end{pmatrix} + \begin{pmatrix} \boldsymbol{n}_1 \\ \boldsymbol{n}_2 \end{pmatrix}, \tag{5.2}$$

where $\boldsymbol{n}_i$ is an $N_i$-dimensional vector representing noise effects at receiver $i$ with entries modeled by an additive white Gaussian noise (AWGN) process with zero mean and variance $\sigma_i^2$, i.e.,$\forall i \in \{1,2\}$, $\mathbb{E}\left[\boldsymbol{n}_i\boldsymbol{n}_i^H\right] = \sigma_i^2\mathbf{I}_{N_i}$. At transmitter $i \in \{1,2\}$, the $L_i \times L_i$ power allocation matrix $\boldsymbol{P}_i$ is defined by the input covariance matrix $\boldsymbol{P}_i = \mathbb{E}\left[\boldsymbol{x}_i\boldsymbol{x}_i^H\right]$. Note that symbols $x_{i,1} \ldots, x_{i,L_i}$, $\forall i \in \{1,2\}$ are mutually independent and zero-mean, thus, the PA matrices can be written as diagonal matrices, i.e., $\boldsymbol{P}_i = \text{diag}\left(p_{i,1}, \ldots, p_{i,L_i}\right)$. Choosing $\mathbf{P}_i$ therefore means selecting a given PA policy. The power constraints on the transmitted signals $\boldsymbol{V}_i\boldsymbol{x}_i$ can be written as

$$\forall i \in \{1,2\}, \quad \text{Trace}\left(\boldsymbol{V}_i\boldsymbol{P}_i\boldsymbol{V}_i^H\right) \leqslant M_i\, p_{i,\max}. \tag{5.3}$$

At receiver $i \in \{1,2\}$, the signal $\boldsymbol{s}_i$ is processed using an $N_i \times N_i$ matrix $\boldsymbol{D}_i$ to form the $N_i$-dimensional vector $\boldsymbol{y}_i = \boldsymbol{D}_i\boldsymbol{s}_i$. All along this section, we refer to $\boldsymbol{D}_i$ as the post-processing matrix at receiver $i$. In [9], it is assumed that the primary terminals (transmitter and receiver) have perfect knowledge of the matrix $\boldsymbol{H}_{11}$ while the secondary terminals have perfect knowledge of all channel transfer matrices $\boldsymbol{H}_{ij}$, $\forall (i,j) \in \{1,2\}^2$. However, this setup is highly demanding in terms of information assumptions. Without inter-transmitter signaling channels, for each transmitter, it is difficult to recover the channel information of other transmitters in MIMO systems. Hence, in our model, we make a more practical assumption here : *the primary terminals (transmitter and receiver) have perfect knowledge of the matrix* $\boldsymbol{H}_{11}$ *and the matrix* $\boldsymbol{H}_{21}$ *while the secondary terminals have perfect knowledge of the matrix* $\boldsymbol{H}_{12}$ *and the matrix* $\boldsymbol{H}_{22}$*, i.e., each user knows its local CSI perfectly.* In fact, there are several technical arguments making this setup relatively

realistic : (a) in some contexts channel reciprocity can be exploited to acquire CSI at the transmitters ; (b) by sending pilot symbols and use feedback channels, the local CSI can be reconstructed (see [11]).

In addition, we propose to use the feedback channel for the secondary user to achieve similar performance as [9] with only local CSI available. Indeed, the feedback, which is the covariance matrix of the received signal for secondary user, can be written as :

$$\boldsymbol{R}_2 = \sigma_2^2 \mathbf{I}_{N_2} + \boldsymbol{D}_2 \boldsymbol{H}_{22} \boldsymbol{V}_2 \boldsymbol{P}_2 \boldsymbol{V}_2^H \boldsymbol{H}_{22}^H \boldsymbol{D}_2^H + \boldsymbol{D}_2 \boldsymbol{H}_{12} \boldsymbol{V}_1 \boldsymbol{P}_1 \boldsymbol{V}_1^H \boldsymbol{H}_{12}^H \boldsymbol{D}_2^H \tag{5.4}$$

### 5.1.3 Opportunistic Interference Alignment

Before presenting the proposed technique, firstly we describe how the primary link operate at its highest transmission rate and the secondary link simultaneously operate at its highest transmission rate without generating interference to the primary link. This problem has been well investigated in [9], in this subsection we list all the obtained results in [9] such that we can better explain our technique in the following subsection.

#### Primary Link Performance

According to the demand of the proposed system model, the primary link must operate at its highest transmission rate in the absence of interference. Hence, following the results in [68] and using our own notation, the optimal pre-processing and post-processing schemes for the primary link are given by the following theorem.

**Theorem 5.1.1.** Let $\boldsymbol{H}_{11} = \boldsymbol{U}_{H_{11}} \boldsymbol{\Lambda}_{H_{11}} \boldsymbol{V}_{H_{11}}^H$ be a singular value decomposition (SVD) of the $N_1 \times M_1$ channel transfer matrix $\boldsymbol{H}_{11}$, with $\boldsymbol{U}_{H_{11}}$ and $\boldsymbol{V}_{H_{11}}$, two unitary matrices with dimension $N_1 \times N_1$ and $M_1 \times M_1$, respectively, and $\boldsymbol{\Lambda}_{H_{11}}$ an $N_1 \times M_1$ matrix with main diagonal $\left(\lambda_{H_{11},1}, \ldots, \lambda_{H_{11},\min(N_1,M_1)}\right)$ and zeros on its off-diagonal. The primary link achieves capacity by choosing $\boldsymbol{V}_1 = \boldsymbol{V}_{H_{11}}$, $\boldsymbol{D}_1 = \boldsymbol{U}_{H_{11}}^H$, $\boldsymbol{P}_1^\star = \operatorname{diag}\left(p_{1,1}^\star, \ldots, p_{1,M_1}^\star\right)$, where

$$\forall n \in \{1, \ldots, M_1\}, \quad p_{1,n}^\star = \left(\beta - \frac{\sigma_1^2}{\lambda_{H_{11}^H H_{11},n}}\right)^+, \tag{5.5}$$

with, $\boldsymbol{\Lambda}_{H_{11}^H H_{11}} = \boldsymbol{\Lambda}_{H_{11}}^H \boldsymbol{\Lambda}_{H_{11}} = \operatorname{diag}\left(\lambda_{H_{11}^H H_{11},1}, \ldots, \lambda_{H_{11}^H H_{11},M_1}\right)$ and the constant $\beta$ (water-level) is set to saturate the power constraint (5.3).

According to Theorem 4.1.1, it is important to note that some of the transmit dimensions can be left unused. Let $m_1 \in \{1, \ldots, M_1\}$ denote the number of transmit dimensions used by the primary user :

$$\begin{aligned} m_1 &\triangleq \sum_{n=1}^{M_1} \mathbb{1}_{]0, M_1 p_{1,\max}]}(p_{1,n}^\star) \\ &= \sum_{n=1}^{M_1} \mathbb{1}_{\left]\frac{\sigma_1^2}{\beta}, +\infty\right[}(\lambda_{H_{11}^H H_{11},n}). \end{aligned} \tag{5.6}$$

Furthermore, it can be checked that

$$1 \leq m_1 \leq \text{rank}(\boldsymbol{H}_{11}^H \boldsymbol{H}_{11}) \tag{5.7}$$

Hence, there are $M_1 - m_1$ left transmit dimensions, which can be used by the secondary user without generating interference to the primary user. In [9], it has been shown how those unused dimensions of the primary system can be seen by the secondary system as opportunities to transmit.

### Pre-processing Matrix of Secondary Link

The objective is first to find a pre-processing matrix $\boldsymbol{V}_2^\star$ that satisfies the interference alignment (IA) condition, which is defined as follows :

**Definition 5.1.2** (IA condition)**.** Let $\boldsymbol{H}_{11} = \boldsymbol{U}_{H_{11}} \boldsymbol{\Lambda}_{H_{11}} \boldsymbol{V}_{H_{11}}^H$ be an SVD of $\boldsymbol{H}_{11}$ and

$$\boldsymbol{R} \;=\; \sigma_1^2 \mathbf{I}_{N_1} + \boldsymbol{U}_{H_{11}}^H \boldsymbol{H}_{21} \boldsymbol{V}_2 \boldsymbol{P}_2 \boldsymbol{V}_2^H \boldsymbol{H}_{21}^H \boldsymbol{U}_{H_{11}}, \tag{5.8}$$

be the covariance matrix of the co-channel interference (CCI) plus noise signal in the primary link. The opportunistic link is said to satisfy the IA condition if its opportunistic transmission is such that the primary link achieves the transmission rate of the equivalent single-user system, which translates mathematically as

$$\begin{aligned} &\log_2 \left| \mathbf{I}_{N_1} + \tfrac{1}{\sigma_1^2} \boldsymbol{\Lambda}_{H_{11}} \boldsymbol{P}_1 \boldsymbol{\Lambda}_{H_{11}}^H \right| = \\ &\log_2 \left| \mathbf{I}_{N_1} + \boldsymbol{R}^{-1} \boldsymbol{\Lambda}_{H_{11}} \boldsymbol{P}_1 \boldsymbol{\Lambda}_{H_{11}}^H \right|. \end{aligned} \tag{5.9}$$

According to [9], to fulfill the IA condition, the pre-processing matrix $\boldsymbol{V}_2^\star$ can be selected as follows :

**Lemma 1** (Pre-processing matrix $\boldsymbol{V}_2^\star$)**.** Let $\boldsymbol{H}_{11} = \boldsymbol{U}_{H_{11}} \boldsymbol{\Lambda}_{H_{11}} \boldsymbol{V}_{H_{11}}^H$ be an ordered SVD of $\boldsymbol{H}_{11}$, with $\boldsymbol{U}_{H_{11}}$ and $\boldsymbol{V}_{H_{11}}$, two unitary matrices of size $N_1 \times N_1$ and $M_1 \times M_1$, respectively, and $\boldsymbol{\Lambda}_{H_{11}}$ an $N_1 \times M_1$ matrix with main diagonal $\left(\lambda_{H_{11},1}, \ldots, \lambda_{H_{11},\min(N_1,M_1)}\right)$ and zeros on its off-diagonal, such that $\lambda_{H_{11},1}^2 \geqslant \lambda_{H_{11},2}^2 \geqslant \ldots \geqslant \lambda_{H_{11},\min(N_1,M_1)}^2$. Let also the $N_1 \times M_2$ matrix $\tilde{\boldsymbol{H}} \triangleq \boldsymbol{U}_{H_{11}}^H \boldsymbol{H}_{21}$ have a block structure,

$$\tilde{\boldsymbol{H}} = \begin{matrix} \\ m_1 \\ N_1 - m_1 \end{matrix} \overset{M_2}{\overbrace{\begin{pmatrix} \tilde{\boldsymbol{H}}_1 \\ \tilde{\boldsymbol{H}}_2 \end{pmatrix}}}. \tag{5.10}$$

The IA condition (Def. 5.1.2) is satisfied independently of the PA matrix $\boldsymbol{P}_2$, when the pre-processing matrix $\boldsymbol{V}_2^\star$ satisfies the condition :

$$\tilde{\boldsymbol{H}}_1 \boldsymbol{V}_2^\star = \mathbf{0}_{m_1 \times L_2}, \tag{5.11}$$

*where $L_2$ is the dimension of the null space of matrix $\tilde{\boldsymbol{H}}_1$.*

**Post-processing Matrix**

Once the pre-processing matrix $\boldsymbol{V}_2$ has been adapted to perform IA, no harmful interference impairs the primary link. However, the secondary receiver undergoes the co-channel interference (CCI) from the primary transmitter. According to [9], the post-processing $\boldsymbol{D}_2^\star$ maximizing the transmission rate of the secondary link can be written as

$$\boldsymbol{D}_2^\star = \left(\boldsymbol{H}_{12}\boldsymbol{V}_{H_{11}}\boldsymbol{P}_1\boldsymbol{V}_{H_{11}}^H\boldsymbol{H}_{12}^H + \sigma_2^2\mathbf{I}_{N_2}\right)^{-\frac{1}{2}} \tag{5.12}$$

## 5.1.4 Coordination scheme to obtain the optimal pre-processing and post-processing matrix for secondary user

In last subsection, we briefly introduced the results obtained in [9]. However, they assume the global CSI, i.e., $\{\boldsymbol{H}_{11}, \boldsymbol{H}_{12}, \boldsymbol{H}_{21}, \boldsymbol{H}_{22}\}$, are known perfectly to the secondary user, which is not practical in real systems. Hence, as described in Section 4.1.2, we make less restrictive assumptions that only the local CSI is known perfectly to the primary user and the secondary user. Based on these new assumptions, we propose a novel scheme to acquire the optimal pre-processing and post-processing matrix for the secondary user when the global channel state information is known only partially to the secondary user. Furthermore, it is assumed that each element in the channel matrix is independent, and thus the channel matrix is fully ranked with probability one. For ease of exposition, we also suppose $M_1 = M_2 = M_c$ and $N_1 = N_2 = N_c$. In this subsection, it will be shown how it is possible to acquire the same pre-processing and post-processing matrix as [9] by exploiting the covariance matrix feedback.

**Acquisition of post-processing matrix for SU**

According to (5.12), the optimal post-processing matrix can be written as :

$$\boldsymbol{D}_2^\star = \left(\boldsymbol{H}_{12}\boldsymbol{V}_{H_{11}}\boldsymbol{P}_1\boldsymbol{V}_{H_{11}}^H\boldsymbol{H}_{12}^H + \sigma_2^2\mathbf{I}_{N_c}\right)^{-\frac{1}{2}} \tag{5.13}$$

Hence, if we can recover the matrix $\boldsymbol{Q} = \left(\boldsymbol{H}_{12}\boldsymbol{V}_{H_{11}}\boldsymbol{P}_1\boldsymbol{V}_{H_{11}}^H\boldsymbol{H}_{12}^H + \sigma_2^2\mathbf{I}_{N_c}\right)$ from the feedback, the optimal post-processing matrix can be acquired easily. Set $\boldsymbol{P}_2 = 0$ and choose an invertible post-processing matrix $\boldsymbol{D}_2$, when the PU transmit with optimal pre-processing matrix $\boldsymbol{V}_{H_{11}}$ and optimal PA matrix $\boldsymbol{P}_1^\star$, the feedback can be rewritten as :

$$\boldsymbol{R}_2 = \sigma_2^2\mathbf{I}_{N_c} + \boldsymbol{D}_2\boldsymbol{H}_{12}\boldsymbol{V}_{H_{11}}\boldsymbol{P}_1^\star\boldsymbol{V}_{H_{11}}^H\boldsymbol{H}_{12}^H\boldsymbol{D}_2^H \tag{5.14}$$

Then the matrix $\boldsymbol{D}_2^\star$ can be obtained by

$$\boldsymbol{D}_2^\star = (\boldsymbol{D}_2^{H^{-1}}\boldsymbol{R}_2\boldsymbol{D}_2^{-1} - \boldsymbol{D}_2^{H^{-1}}\boldsymbol{D}_2^{-1} + \sigma_2^2\mathbf{I}_{N_c})^{-\frac{1}{2}} \tag{5.15}$$

**Acquisition of pre-processing matrix for SU in the scenario $M_c \leq N_c$ (more receiving antennas)**

According to the (5.11), the pre-processing matrix $\boldsymbol{V}_2^\star$ satisfies the condition :

$$\tilde{\boldsymbol{H}}_1\boldsymbol{V}_2^\star = \mathbf{0}_{m_1\times L_2}, \tag{5.16}$$

Therefore, the goal here is to find the null space of $\tilde{\boldsymbol{H}}_1$. Interestingly, as demonstrated by the following proposition, it is not necessary to know $\tilde{\boldsymbol{H}}_1$ to acquire the null space of $\tilde{\boldsymbol{H}}_1$.

**Proposition 5.1.3.** *Assume $\boldsymbol{H}$ is a full row rank matrix and $\boldsymbol{P}$ is a full rank square matrix, then the null space of $\boldsymbol{H}^H\boldsymbol{P}\boldsymbol{H}$ coincides with the null space of $\boldsymbol{H}$.*

**Proof :** Suppose $\boldsymbol{V}$ is the null space of $\boldsymbol{H}$, i.e. $\boldsymbol{H}\boldsymbol{V} = \boldsymbol{0}$. It can be easily checked that

$$\boldsymbol{H}^H\boldsymbol{P}\boldsymbol{H}\boldsymbol{V} = \boldsymbol{0} \tag{5.17}$$

Hence, $\boldsymbol{V}$ is the subset of $\boldsymbol{V}'$, which is the null space of $\boldsymbol{H}^H\boldsymbol{P}\boldsymbol{H}$. If we can show that the dimension of $\boldsymbol{V}$ is the same as the dimension of $\boldsymbol{V}'$, then our claim will be proved.

Note that $\text{rank}(\boldsymbol{A}\boldsymbol{B}) = \text{rank}(\boldsymbol{B})$ when $\boldsymbol{A}$ is a full column rank matrix and $\text{rank}(\boldsymbol{B}\boldsymbol{C}) = \text{rank}(\boldsymbol{B})$ when $\boldsymbol{C}$ is a full row rank matrix. Knowing that $\boldsymbol{H}$ is a full row rank matrix and $\boldsymbol{P}$ is a full rank matrix, it can be obtained that :

$$\text{rank}(\boldsymbol{H}^H\boldsymbol{P}\boldsymbol{H}) = \text{rank}(\boldsymbol{H}) \tag{5.18}$$

Suppose the column number of $\boldsymbol{H}$ is $M$, it can be checked that

$$\begin{aligned} \dim \text{Ker}(\boldsymbol{H}) &= M - \text{rank}(\boldsymbol{H}) \\ &= M - \text{rank}(\boldsymbol{H}^H\boldsymbol{P}\boldsymbol{H}) \\ &= \dim \text{Ker}(\boldsymbol{H}^H\boldsymbol{P}\boldsymbol{H}) \end{aligned} \tag{5.19}$$

Hence, we can conclude that $\boldsymbol{V}$ and $\boldsymbol{V}'$ coincide. ■

According to Proposition 4.1.3, by reconstructing the null space of $\tilde{\boldsymbol{H}}_1^H\boldsymbol{P}\tilde{\boldsymbol{H}}_1$, we can obtain $\boldsymbol{V}_2^\star$ as both the null spaces coincide. To exchange the information between PU and SU, $\tilde{\boldsymbol{H}}_1$ is embedded in the pre-processing matrix of PU. Assume that $M_c \times M_c$ matrix $V_1$ has a block structure,

$$\boldsymbol{V}_1 = \begin{array}{c} \\ M_c \end{array} \overset{\overset{m_1}{\longleftrightarrow}\overset{M_c-m_1}{\longleftrightarrow}}{\begin{pmatrix} \tilde{\boldsymbol{H}}_1^H & \boldsymbol{X}_1 \end{pmatrix}}. \tag{5.20}$$

where the $\boldsymbol{X}_1$ can be any arbitrary matrix.

Note that we can obtain the following inequality with the transmit power defined by (4)

$$p_{1,1}^\star \geq p_{1,2}^\star \geq \cdots \geq p_{1,M_c}^\star \tag{5.21}$$

by choosing the appropriate SVD such that

$$\lambda_{H_{11}^H H_{11},1} \geq \lambda_{H_{11}^H H_{11},2} \geq \cdots \geq \lambda_{H_{11}^H H_{11},M_c} \tag{5.22}$$

Hence, the transmit power matrix of PU has the following block structure :

$$\boldsymbol{P}_1 = \boldsymbol{P}_1^\star = \begin{array}{c} \\ m_1 \\ M_c - m_1 \end{array} \overset{\overset{m_1}{\longleftrightarrow}\overset{M_c-m_1}{\longleftrightarrow}}{\begin{pmatrix} \boldsymbol{P}_{1,11} & \boldsymbol{0} \\ \boldsymbol{0} & \boldsymbol{0} \end{pmatrix}}. \tag{5.23}$$

where $\boldsymbol{P}_{1,11} = \text{diag}(p^{\star}_{1,1}, \ldots, p^{\star}_{1,m_1})$. Knowing (5.20) and (5.23), it can be easily checked that :

$$\boldsymbol{V}_1 \boldsymbol{P}_1 \boldsymbol{V}_1^H = \tilde{\boldsymbol{H}}_1^H \boldsymbol{P}_{1,11} \tilde{\boldsymbol{H}}_1 \tag{5.24}$$

According to Prop. 4.1.3, when $\boldsymbol{P}_{1,11}$ has full rank, knowing $\tilde{\boldsymbol{H}}_1^H \boldsymbol{P}_{1,11} \tilde{\boldsymbol{H}}_1$ is sufficient to reconstruct the null space of $\tilde{\boldsymbol{H}}_1$. Plugging (5.20) and (5.23) into (5.4), and by selecting $\boldsymbol{P_2} = \boldsymbol{0}$, the feedback can be rewritten as :

$$\boldsymbol{R}_2 = \sigma_2^2 \mathbf{I}_{N_c} + \boldsymbol{D}_2 \boldsymbol{H}_{12} \tilde{\boldsymbol{H}}_1^H \boldsymbol{P}_{1,11} \tilde{\boldsymbol{H}}_1 \boldsymbol{H}_{12}^H \boldsymbol{D}_2^H \tag{5.25}$$

Thus, $\tilde{\boldsymbol{H}}_1^H \boldsymbol{P}_{1,11} \tilde{\boldsymbol{H}}_1$ can be calculated by :

$$\tilde{\boldsymbol{H}}_1^H \boldsymbol{P}_{1,11} \tilde{\boldsymbol{H}}_1 = (\boldsymbol{H}_{12}^H \boldsymbol{H}_{12})^{-1} \boldsymbol{H}_{12}^H \boldsymbol{D}_2^{-1} (\boldsymbol{R}_2 - \sigma_2^2 \mathbf{I}_{N_c}) \boldsymbol{D}_2^{H^{-1}} \boldsymbol{H}_{12} (\boldsymbol{H}_{12}^H \boldsymbol{H}_{12})^{-1} \tag{5.26}$$

Since $\boldsymbol{H}_{12}$ and $\boldsymbol{D}_2$ are known to the SU, $\tilde{\boldsymbol{H}}_1^H \boldsymbol{P}_{1,11} \tilde{\boldsymbol{H}}_1$ can be reconstructed by knowing the feedback $\boldsymbol{R}_2$. Consequently the optimal pre-processing matrix $\boldsymbol{V}_2^{\star}$ (null space of $\tilde{\boldsymbol{H}}_1$) can be obtained.

**Acquisition of pre-processing matrix for SU in the scenario $M_c > N_c$ (more transmit antennas)**

In this case, it is impossible to reconstruct the null space by (5.26) since $\boldsymbol{H}_{12}^H \boldsymbol{H}_{12}$ is not invertible when $M_c \geq N_c$. More generally, when we have more transmit antennas, it is impossible to completely reconstruct the $N_c \times M_c$ channel matrix if we have the feedback (covariance matrix of the received signal) just once . However, by using feedbacks from several time-slots, the reconstruction of the null space is feasible. In each time-slot, a part of information of the channel matrix will be exchanged and can be combined by receiving all the information exchanged through the feedback. Therefore, in each time-slot we can reconstruct a part of the channel matrix. Note that $\tilde{\boldsymbol{H}}_1$ can be written as :

$$\tilde{\boldsymbol{H}}_1 = (\tilde{\boldsymbol{h}}_{1,1}, \ldots, \tilde{\boldsymbol{h}}_{1,M_c}) \tag{5.27}$$

where $\tilde{\boldsymbol{h}}_{1,i}$ is the $i$th column vector of $\tilde{\boldsymbol{H}}_1$. Assume $T = N_c - m_1 > 0$, in time-slot $i \in \{1, \ldots, \lceil \frac{M_c - N_c}{T} \rceil\}$, the matrix $\tilde{\boldsymbol{H}}_{1,i}$ is embedded into the pre-processing matrix of PU in the following way :

$$\boldsymbol{V}_1(i) = \begin{array}{r} \\ N_c \\ M_c - N_c \end{array} \overset{\begin{array}{cc} m_1 & M_c - m_1 \end{array}}{\begin{pmatrix} \tilde{\boldsymbol{H}}_{1,i}^H & \boldsymbol{Y}_i \\ \boldsymbol{0} & \boldsymbol{0} \end{pmatrix}}. \tag{5.28}$$

where $\tilde{\boldsymbol{H}}_{1,i} = (\tilde{\boldsymbol{h}}_{1,1+(i-1)T}, \ldots, \tilde{\boldsymbol{h}}_{1,1+(i-1)T+N_c})$ with dimension $m_1 \times N_c$ and $\boldsymbol{Y}_i$ can be any arbitrary matrix with dimensions $N_c \times (M_c - m_1)$. Knowing (5.28) and (5.23), it can be easily checked that :

$$\boldsymbol{V}_1(i) \boldsymbol{P}_1 \boldsymbol{V}_1^H(i) = \begin{array}{r} \\ N_c \\ M_c - N_c \end{array} \overset{\begin{array}{cc} N_c & M_c - N_c \end{array}}{\begin{pmatrix} \tilde{\boldsymbol{H}}_{1,i}^H \boldsymbol{P}_{1,11} \tilde{\boldsymbol{H}}_{1,i} & \boldsymbol{0} \\ \boldsymbol{0} & \boldsymbol{0} \end{pmatrix}}. \tag{5.29}$$

Let the matrix $\boldsymbol{H}_{12}$ have a block structure

$$\boldsymbol{H}_{12} = \begin{array}{c} \\ N_c \updownarrow \end{array} \overset{\overset{N_c}{\longleftrightarrow}\overset{M_c-N_c}{\longleftrightarrow}}{\begin{pmatrix} \boldsymbol{H}_{12,1} & \boldsymbol{H}_{12,2} \end{pmatrix}}. \tag{5.30}$$

Plugging (5.28), (5.23) and (5.30) into (5.4), and selecting $\boldsymbol{P_2} = \boldsymbol{0}$, the feedback in time-slot $i$ can be rewritten as :

$$\boldsymbol{R}_2(i) = \sigma_2^2 \mathbf{I}_{N_c} + \boldsymbol{D}_2 \boldsymbol{H}_{12,1} \tilde{\boldsymbol{H}}_{1,i}^H \boldsymbol{P}_{1,11} \tilde{\boldsymbol{H}}_{1,i} \boldsymbol{H}_{12,1}^H \boldsymbol{D}_2^H \tag{5.31}$$

Thus, $\tilde{\boldsymbol{H}}_{1,i}^H \boldsymbol{P}_{1,11} \tilde{\boldsymbol{H}}_{1,i}$ can be calculated by :

$$\tilde{\boldsymbol{H}}_{1,i}^H \boldsymbol{P}_{1,11} \tilde{\boldsymbol{H}}_{1,i} = \boldsymbol{H}_{12,1}^{-1} \boldsymbol{D}_2^{-1} (\boldsymbol{R}_2(i) - \sigma_2^2 \mathbf{I}_{N_c}) \boldsymbol{D}_2^{H^{-1}} {\boldsymbol{H}_{12,1}^H}^{-1} \tag{5.32}$$

According to proposition 4, the null space of $\tilde{\boldsymbol{H}}_{1,i}$, i.e. $\boldsymbol{V}_{2,i}$, can be obtained by solving $\tilde{\boldsymbol{H}}_{1,i} \boldsymbol{V}_{2,i} = \boldsymbol{0}$. It is important to note that, $\tilde{\boldsymbol{h}}_{1,1}, \ldots, \tilde{\boldsymbol{h}}_{1,m_1}$ are $m_1$ independent vectors with dimension $m_1$. Therefore, the rest of the vectors in $\tilde{\boldsymbol{H}}_1$, $\tilde{\boldsymbol{h}}_{1,m_1+1}, \ldots, \tilde{\boldsymbol{h}}_{1,M_c}$, can be written as the combination of the $m_1$ basis vectors, i.e. $\tilde{\boldsymbol{h}}_{1,1}, \ldots, \tilde{\boldsymbol{h}}_{1,m_1}$. By solving $\tilde{\boldsymbol{H}}_{1,i} \boldsymbol{V}_{2,i} = \boldsymbol{0}$ for every $i \in \{1, \ldots, \lceil \frac{M_c - N_c}{T} \rceil\}$, i.e.

$$[\tilde{\boldsymbol{h}}_{1,1+(i-1)T} \quad \ldots \quad \tilde{\boldsymbol{h}}_{1,1+(i-1)T+N_c}] \boldsymbol{V}_{2,i} = \boldsymbol{0} \tag{5.33}$$

Thus, for every $j \in \{m_1 + 1, \ldots, M_c\}$, $\tilde{\boldsymbol{h}}_{1,j}$ can be rewritten as the sum of the basis vectors :

$$\tilde{\boldsymbol{h}}_{1,j} = a_1^{(j)} \tilde{\boldsymbol{h}}_{1,1} + \cdots + a_{m_1}^{(j)} \tilde{\boldsymbol{h}}_{1,m_1} \tag{5.34}$$

Expressing the above $M_c - m_1$ equalities more succinctly through matrix multiplication :

$$\tilde{\boldsymbol{H}}_1 \begin{pmatrix} a_1^{(m_1+1)} \ldots a_1^{(M_c)} \\ \vdots \quad \vdots \quad \vdots \\ a_{m_1}^{(m_1+1)} \ldots a_{m_1}^{(M_c)} \\ -\boldsymbol{I}_{(M_c-m_1)\times(M_c-m_1)} \end{pmatrix} = 0 \tag{5.35}$$

Thus, the null space of $\tilde{\boldsymbol{H}}_1$ is :

$$\boldsymbol{V}_2^\star = \begin{pmatrix} a_1^{(m_1+1)} \ldots a_1^{(M_c)} \\ \vdots \quad \vdots \quad \vdots \\ a_{m_1}^{(m_1+1)} \ldots a_{m_1}^{(M_c)} \\ -\boldsymbol{I}_{(M_c-m_1)\times(M_c-m_1)} \end{pmatrix} \tag{5.36}$$

### 5.1.5 Numerical performance analysis

As mentioned before, the channel matrix $\boldsymbol{H}_{ji}$ is assumed to be a matrix with independent and identically distributed (i.i.d.) complex Gaussian circularly symmetric entries with zero mean and variance 1. For ease of exposition, we assume each transmitter has the same power constraint and same noise variance, i.e. $p_{1,\max} = p_{2,\max}$ and $\sigma_1 = \sigma_2$. The signal-to-noise ratio (SNR) is defined as

$$\text{SNR} = \frac{M_1 p_{1,\max}}{\sigma_1^2} \tag{5.37}$$

In the simulations, we consider the case with 4 transmit antennas and 4 receive antennas, i.e. $M_1 = M_2 = 4$ and $N_1 = N_2 = 4$.

Firstly, we compare the sum-rate in the following three scenarios :1) The local CSI and the power domain feedback are available ; 2) Only the local CSI is available ; 3) The precoding matrix $V_1$ is used to exchange information with the secondary user (training phase). For the first case, as proved before, the opportunistic interference alignment scheme can be recovered perfectly. Both transmitters can achieve their maximum transmission rate. When we have only the local CSI, the primary user can still transmit at its maximum rate while the secondary user should keep silent to avoid interference with the primary user. As for the training phase, the objective is not to maximize the transmission rate but to exchange information. Fig. 5.1 clearly shows that the sum-rate can be increased by exploiting the feedback. However, as SNR increases, the improvement becomes less significant. This can be explained by the fact that the transmit opportunities for the secondary user will decrease as the power limitation for the primary user is relaxed. Furthermore, it can be seen that during the training phases, exchanging information induces a degradation in sum-rate. Hence, for the proposed scheme, the sum-rate decreases initally during the training phase. This loss can however be recovered since the exchanged information can help exploit the opportunistic interference alignment scheme.

As proved in the analytical part, the training phase for the considered model only lasts for one time-slot. Therefore, it can be predicted that when the coherence time of channel (the duration of a coherence block in which the channel is assumed to be a constant) is long, the average sum-rate over the coherence time will be highly enhanced since the degradation appears only in the first time-slot. Fig. 5.2 illustrates that the improvements in terms of average sum-rate becomes more significant when the coherence time increases. Unsurprisingly, the improvements are mitigated at high SNR since the secondary transmitter has less opportunities to transmit without inducing interference to the primary transmitter.

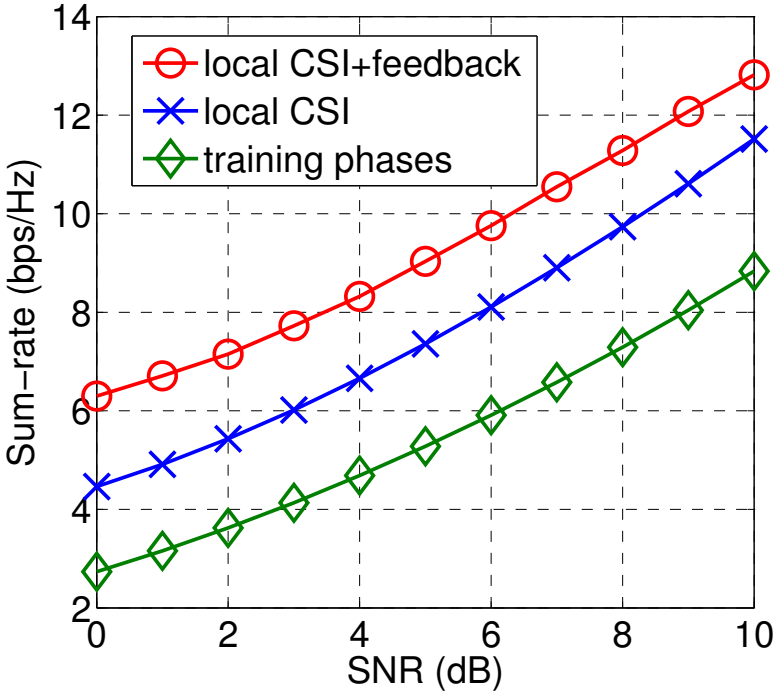


FIGURE 5.1 – Comparison of the performance in terms of sum-rate. In the training phase, the local CSI is embedded into the precoding matrix to exchange information, which induces the sum-rate loss. However, by exploiting the feedback in the training phase, the opportunistic interference alignment scheme can be reconstructed and thus the sum-rate is increased in the following time-slots.

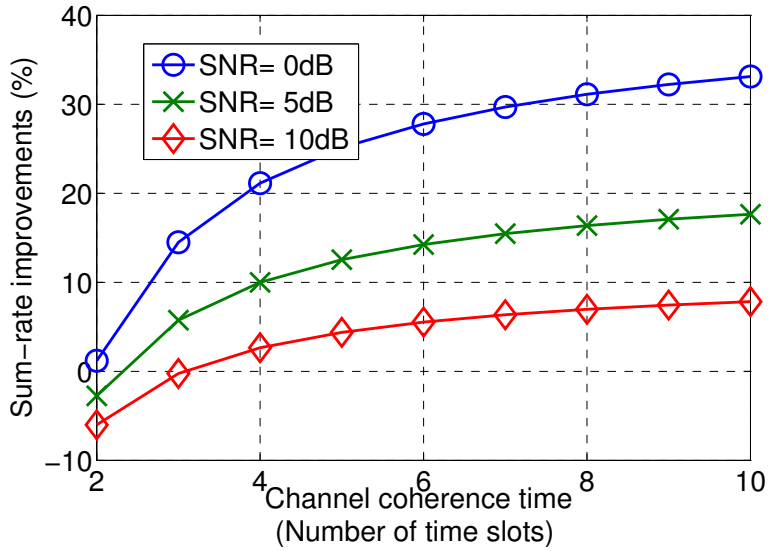


FIGURE 5.2 – Average sum-rate as a function of channel coherence times. When the coherence time is longer, more improvements can be obtained. Furthermore, this gain becomes more significant in low SNR regime.

## 5.2 Improving channel estimation accuracy via power domain feedback in interference networks

### 5.2.1 Motivation and state of the art

The channel information is essential to determine the capacity of system performance in many wireless networks such as orthogonal frequency-division multiplexing (OFDM) and multiple input multiple output (MIMO) (see e.g., [69]). However, the channel information is not perfectly known in practical systems and need to be estimated by sending pilot sequences [11] or using blind channel estimation [70]. Thus the system performance relies on the accuracy level of channel estimation. Improving the quality of channel estimation is a well studied problem for both academic researchers as well as engineers in the communication industry. In the context of interference networks, a precise estimation of the channel between a transmitter and its intended receiver requires coordination between all the interfering transmitters during training phase. Recently in [11][10], it has been shown that the channel state information (CSI) can be acquired by sending pilot symbols and estimating the channel with the minimum mean square error (MMSE) estimator. It turns out that this estimation scheme can be enhanced with power domain feedback, which is the purpose of this section.

In this work, we propose a novel method to improve the channel estimate by exploiting the average received signal strength indicator (RSSI). As the RSSI measurements are an additional source of information on the channel state, they can be used to improve a noisy estimate. For ease of exposition, we focus this section on presenting an improvement on two specific estimators, minimum mean square error (MMSE) estimator and maximum a posteriori (MAP) estimator. We provide a new MMSE estimator which uses RSSI measurements, and show that this results in a better estimate than the classical estimator from [10]. Moreover, a new MAP estimator is proposed to improve the estimation accuracy under the help of RSSI measurements. Finally, we present numerical simulations which indicate distortion improvements of up to 30% using MMSE estimate and up to 50% with a MAP estimate, validating our proposed approach.

### 5.2.2 System Model

We consider an interference network with $K$ single antenna transmitter-receiver pairs. We use $\mathcal{K} := \{1, 2, \ldots, K\}$ to represent the set of transmitters or receivers. The channel state for the duration of a coherence block is assumed to be a constant and is given by $\mathbf{h} \in \mathbb{C}^{K^2}$, which is a $K$ by $K$ matrix with element $h_{ij} \in \mathbb{C}$ denoting the channel from transmitter $i$ to receiver $j$. As a result, the signal received at $j$ is given by

$$y_j = \sum_{i=1}^{K} h_{ij} x_i + z_j \tag{5.38}$$

where $x_i \in \mathbb{C}$ is the signal sent by the $i$-th transmitter and $z_j \in \mathbb{C}$ is the ambient noise at the receiver $j$.

The objective of our scheme is to estimate local channel information, i.e., receiver $j$ must estimate $h_{ij}$ for all $i \in \mathcal{K}$. Let us use $\mathbf{h}_j := (h_{1j}, h_{2j}, \ldots, h_{Kj})^T$ to denote the vector

of local channels at receiver $j$. Classically, this estimate $\hat{\mathbf{h}}_j$ is obtained using pilot signals and training over the signal domain. Assuming that the pilot signals are orthogonal and all use a common maximum power level $P$, and that $\beta$ symbols are used for training per channel, the observation for the receiver used to estimate $\mathbf{h}_j$ is given by

$$\mathbf{s}_j = \sqrt{\beta P}\mathbf{h}_j + \mathbf{z}_j \tag{5.39}$$

where the noise $\mathbf{z}_j \sim \mathcal{CN}(0, N_0\mathbf{I}_K)$. We are interested in estimators (MMSE) of the form

$$\widehat{\mathbf{h}}_j^{\text{MMSE}} = A_j\mathbf{s}_j \tag{5.40}$$

that minimize the expected distortion defined as $\mathbb{E}[|\widehat{\mathbf{h}}_j - \mathbf{h}_j|^2]$. Additionally, we also consider the maximum a posteriori probability (MAP) estimate which is normally obtained by maximizing the a posteriori distribution function, i.e.,

$$\widehat{h}_{ij}^{\text{MAP}} = \arg\max_{h_{ij}} f_{ij}(h_{ij}|\mathbf{s}_j) \tag{5.41}$$

where $f_{ij}(.)$ is the probability distribution function of $h_{ij}$.

In addition to the classical technique which relies solely on $\mathbf{s}_j$ obtained from the training phase to estimate $\mathbf{h}_j$, we also exploit information obtained from the average received signal strength indicator (RSSI). The average signal power received at $j$ for a time slot $t$ can be written as

$$R_{j,t} = \sum_{i=1}^{K} g_{ij}P_i(t) + N_0 \tag{5.42}$$

where $g_{ij} = |h_{ij}|^2$ and $P_i(t) = \mathbb{E}(|x_i(t)|^2)$.

### 5.2.3 Novel estimation technique

For the sake of clarity, we explain our technique in single band scenario. The proposed method can be easily extended to a multi-carrier case as the estimation over each carrier can be done independently. We also assume that the channel stays a constant for a duration of $m$ time slots for which the RSSI is available. In addition to classical channel estimation schemes, we also exploit this RSSI measurements to improve the estimate. Without any loss of generality, we study the channel estimation by a receiver $j$ and assume $\mathbf{h}_j \sim \mathcal{CN}(0, \mathbf{I}_K)$. We first present the improved MMSE estimator.

#### MMSE estimator

If the MMSE estimator is of the form (5.40), minimizing the MMSE can be formulated as the following optimization problem

$$\min_{\mathbf{A}_j} \quad \mathbb{E}_{\mathbf{h}_j,\mathbf{z}_j}[|\mathbf{A}_j\mathbf{s}_j - \mathbf{h}_j|^2] \tag{5.43}$$

By taking the derivative of $\mathbb{E}_{\mathbf{h}_j,\mathbf{z}_j}[|\mathbf{A}_j\mathbf{s}_j - \mathbf{h}_j|^2]$ w.r.t. $\mathbf{A}_j$, the MMSE estimator can be obtained in the following manner :

$$\begin{aligned}
&\frac{\partial \mathbb{E}_{\mathbf{h}_j,\mathbf{z}_j}[|\mathbf{A}_j\mathbf{s}_j - \mathbf{h}_j|^2]}{\partial \mathbf{A}_j} \\
=&\frac{\partial \mathbb{E}_{\mathbf{h}_j,\mathbf{z}_j}[\mathbf{s}_j^{\mathrm{H}}\mathbf{A}_j^{\mathrm{H}}\mathbf{A}_j\mathbf{s}_j - \mathbf{s}_j^{\mathrm{H}}\mathbf{A}_j^{\mathrm{H}}\mathbf{h}_j - \mathbf{h}_j^{\mathrm{H}}\mathbf{A}_j\mathbf{s}_j]}{\partial \mathbf{A}_j} \\
=&\frac{\partial \mathbb{E}_{\mathbf{h}_j,\mathbf{z}_j}\{\mathrm{Tr}[\mathbf{s}_j^{\mathrm{H}}\mathbf{A}_j^{\mathrm{H}}\mathbf{A}_j\mathbf{s}_j - \mathbf{s}_j^{\mathrm{H}}\mathbf{A}_j^{\mathrm{H}}\mathbf{h}_j - \mathbf{h}_j^{\mathrm{H}}\mathbf{A}_j\mathbf{s}_j]\}}{\partial \mathbf{A}_j} \\
=&\mathbf{A}_j^{*}\mathbb{E}_{\mathbf{h}_j,\mathbf{z}_j}[\mathbf{s}_j^{*}\mathbf{s}_j^{\mathrm{T}}] - 2\mathbb{E}_{\mathbf{h}_j,\mathbf{z}_j}[\mathbf{h}_j^{*}\mathbf{s}_j^{\mathrm{T}}]
\end{aligned} \tag{5.44}$$

where $(.)^*$ is the conjugate operator, $(.)^{\mathrm{T}}$ is the transpose operator and $(.)^{\mathrm{H}}$ is the conjugate transpose operator.

The optimum $\mathbf{A}_j^{\mathrm{OPT:0}}$ can be obtained by setting the derivative to zero, i.e.

$$\mathbf{A}_j^{\mathrm{OPT:0}} = \mathbb{E}_{\mathbf{h}_j,\mathbf{z}_j}[\mathbf{h}_j\mathbf{s}_j^{\mathrm{H}}]\mathbb{E}_{\mathbf{h}_j,\mathbf{z}_j}[\mathbf{s}_j\mathbf{s}_j^{\mathrm{H}}]^{-1} \tag{5.45}$$

In the absence of any additional information such as the RSSI, we can simply write

$$\mathbb{E}_{\mathbf{h}_j,\mathbf{z}_j}[\mathbf{h}_j\mathbf{s}_j^{\mathrm{H}}]\mathbb{E}_{\mathbf{h}_j,\mathbf{z}_j}[\mathbf{s}_j\mathbf{s}_j^{\mathrm{H}}]^{-1} = \frac{\sqrt{\beta P}}{\beta P + N_0}\mathbf{I}_K \tag{5.46}$$

This result is well known and has been provided in [11] and [10]. However, if the RSSI is known, then the expectation in (5.45) must be conditioned with respect to this information. The RSSI at time $t$ and receiver $j$ is a random variable $R_{j,t}$ as provided in (5.42). This random variable is observed and takes a realization $r_{j,t}$. Denote by $\mathbf{R}_j^{(m)} = (R_{j,1}, \ldots, R_{j,m})$ the vector of random RSSI observed at $j$ over $m$ time slots and by $\mathbf{r}_j^{(m)} = (r_{j,1}, \ldots, r_{j,m})$ a vector of RSSI realizations. Then, the optimal MMSE estimator knowing $\mathbf{r}_j^{(m)}$ is simply given by

$$\mathbf{A}_j^{\mathrm{OPT:m}} = \mathbb{E}_{\mathbf{h}_j,\mathbf{z}_j|\mathbf{R}_j^{(m)}=\mathbf{r}_j^{(m)}}[\mathbf{h}_j\mathbf{s}_j^{\mathrm{H}}]\mathbb{E}_{\mathbf{h}_j,\mathbf{z}_j|\mathbf{R}_j^{(m)}=\mathbf{r}_j^{(m)}}[\mathbf{s}_j\mathbf{s}_j^{\mathrm{H}}]^{-1} \tag{5.47}$$

Note that

$$\begin{aligned}
r_{j,i} =& \sum_k g_{kj}P_k(i) + N_0 \\
=& \sum_k |h_{kj}|^2 P_k(i) + N_0 \\
=& \mathbf{h}_j^{\mathrm{H}}\mathbf{P}(i)\mathbf{h}_j + N_0
\end{aligned} \tag{5.48}$$

where $\mathbf{P}(i) = \mathrm{diag}(P_1(i), \ldots, P_K(i))$. This results in

$$\mathbf{A}_j^{\mathrm{OPT:m}} = \frac{\sqrt{\beta P}\mathbb{E}_{|\mathbf{R}_j^{(m)}=\mathbf{r}_j^{(m)}}[\mathbf{h}_j\mathbf{h}_j^{\mathrm{H}}]}{\sqrt{\beta P}\mathbb{E}_{|\mathbf{R}_j^{(m)}=\mathbf{r}_j^{(m)}}[\mathbf{h}_j\mathbf{h}_j^{\mathrm{H}}] + N_0\mathbf{I}_K} \tag{5.49}$$

Knowing the optimal estimator, we can calculate the conditional distortion (conditioned to $\mathbf{R}_j^{(m)} = \mathbf{r}_j^{(m)}$) as a result of using the MMSE given by (5.49). This conditional

distortion is denoted by $\mathrm{D}_j(\mathbf{r}_j^{(m)})$ when $m$ RSSI observations are available, and can be evaluated as

$$\mathrm{D}_j(\mathbf{r}_j^{(m)}) = \mathbb{E}_{|\mathbf{R}_j^{(m)}=\mathbf{r}_j^{(m)}}[|\mathbf{A}_j\mathbf{s}_j - \mathbf{h}_j|^2] \tag{5.50}$$

Finally, the real distortion of the estimator with $m$ RSSI measurements can be expressed as :

$$\Delta_{j;m} = \mathbb{E}_{\mathbf{r}_j^{(m)}}[\mathrm{D}_j(\mathbf{r}_j^{(m)})] \tag{5.51}$$

We use $D_j^*$ and $\Delta_{j;m}^*$ to denote the conditonal and real distortions when the estimator used is that given in (5.49), which yields

$$\mathrm{D}_j^*(\mathbf{r}_j^{(m)}) = \sum_{k=1}^{K} \frac{N_0\mathbb{E}_{|\mathbf{R}_j^{(m)}=\mathbf{r}_j^{(m)}}[|h_{kj}|^2]}{\beta P\mathbb{E}_{|\mathbf{R}_j^{(m)}=\mathbf{r}_j^{(m)}}[|h_{kj}|^2] + N_0} \tag{5.52}$$

$$\Delta_{j;m}^* = \mathbb{E}_{\mathbf{r}_j^{(m)}}^*[\mathrm{D}_j^*(\mathbf{r}_j^{(m)})] \tag{5.53}$$

The $\mathbb{E}_{|\mathbf{R}_j^{(m)}=\mathbf{r}_j^{(m)}}[\mathbf{h}_j\mathbf{h}_j^{\mathrm{H}}]$ term in (5.49) is not always easy to evaluate, therefore, we provide details on how such an estimator can be designed in practice. First, it can be easily verified that the non-diagonal elements of $\mathbb{E}_{|\mathbf{R}_j^{(m)}=\mathbf{r}_j^{(m)}}[\mathbf{h}_j\mathbf{h}_j^{\mathrm{H}}]$ equal to zero, i.e.

$$\mathbb{E}_{|\mathbf{R}_j^{(m)}=\mathbf{r}_j^{(m)}}[h_{ij}h_{kj}^*] = 0 \quad (k \neq i) \tag{5.54}$$

Additionally, note that the chain gain $g_{kj} = |h_{kj}|^2$ follows the exponential distribution with expectation 1. Hence, the diagonal elements can be expressed as :

$$\begin{aligned} &\mathbb{E}_{|\mathbf{R}_j^{(m)}=\mathbf{r}_j^{(m)}}[h_{kj}h_{kj}^*] \\ &= \int_{C_m} g_{kj}\exp(-g_{k1} - \cdots - g_{kK})\mathrm{d}g_{k1}\ldots\mathrm{d}g_{kK} \end{aligned} \tag{5.55}$$

where $C_m = \{\mathbf{g}_j | \forall\ 1 \leq i \leq m, \quad \mathbf{g}_j\mathbf{P}(i)\mathbf{1}_K + N_0 = r_{j,i}\}$ with $\mathbf{g}_j = (g_{1j}, \ldots, g_{Kj})$ and $\mathbf{1}_K = (1, \ldots, 1)^{\mathrm{T}}$ of dimension $K \times 1$.

The diagonal elements can be easily evaluated if

1. $g_{kj}$ is known for all $k$, or
2. $g_{kj}$ is known for some $k \in S$, $S \subseteq \mathcal{K}$ and no information other than the statistics in available on $g_{ij}$ with $i = \mathcal{K} \setminus S$.

The second case can be satisfied if the $k$ transmitters for $k \in S$ are the only active transmitters while obtaining the RSSI, and they are active in a time-division multiple access (TDMA) manner, i.e., no two transmitters are active simultaneously. This will allow any receiver $j$ to obtain the measurement $Pg_{kj} + N_0$ for $k \in S$, thereby evaluating $g_{kj}$ easily.

The first case can also be satisfied if all $K$ devices operate in TDMA. However, we might also use techniques like that mentioned in [71], so that each receiver $j$ obtains $g_{kj}$ for all $k$ where all transmitters will use a pre-designed power level that is known to

all receivers in order to obtain $g_{kj}$ from a set of $K$ RSSI measurements (resulting in $K$ equations and $K$ unknowns).

Next, we prove that the performance in terms of the real distortion given in (5.53), for the proposed estimator in (5.49) is at least as good as the classical estimator. We also provide upper and lower bounds for the real distortion. We formalize this result with the following proposition.

**Proposition 5.2.1.** *The distortion resulting from the proposed estimator in (5.49) is a decreasing function of the number of RSSI feedbacks available at any receiver $j$, i.e., $\Delta^*_{j;m} \geq \Delta^*_{j;m+1}$. Additionally, the distortion is lower bounded by a constant*

$$\Delta^*_{j;m} \geq \sum_{k=1}^{K} \mathbb{E}_{h_{kj}} \left[ \frac{N_0 |h_{kj}|^2}{\beta P |h_{kj}|^2 + N_0} \right] \tag{5.56}$$

**Proof :** See Appendix C.

### MAP estimator

Apart from the MMSE estimate, the maximum a posteriori (MAP) estimate is often used to estimate the signal with prior information as well. Here we present the improved MAP knowing the feedback information. With $m$ RSSI measurements given by $\mathbf{r}_j^{(m)}$ available at the $j$-th receiver, the MAP estimate will be now given by

$$\widehat{h}_{ij}^{\text{MAP}} = \arg\max_{h_{ij}} f_{ij}(h_{ij} | \mathbf{s}_j, \mathbf{r}_j^{(m)}) \tag{5.57}$$

when $m = 0$, i.e., no RSSI measurements are available, this becomes the classical MAP, which in the case of training as described in our system model, and $f_{ij}(.)$ according to $h_{ij} \sim C\mathcal{N}(0,1)$, becomes

$$\widehat{h}_{ij}^{\text{MAP}} = \frac{\sqrt{\beta P}}{N_0 + \beta P} s_{ij} \tag{5.58}$$

which coincides with the MMSE when $m = 0$. However, when the RSSI estimates are known, the optimization must be done under the condition that $R_{j,1} = r_{j,1}, \ldots, R_{j,m} = r_{j,m}$, i.e.

$$\begin{aligned} \min_{\mathbf{h}_j} \quad & \frac{(\mathbf{s}_j - \sqrt{\beta P}\mathbf{h}_j)^H (\mathbf{s}_j - \sqrt{\beta P}\mathbf{h}_j)}{N_0} + \mathbf{h}_j^H \mathbf{h}_j \\ \text{s.t.} \quad & \mathbf{h}_j^{\text{H}} \mathbf{P}(k) \mathbf{h}_j + N_0 = r_{j,k}, \ \forall\ k \in \{1, 2, \ldots, m\} \end{aligned} \tag{5.59}$$

This problem can be solved by using Lagrange method. The optimal solution $\widehat{\mathbf{h}}_j^{\text{MAP}}$ can be written as

$$\widehat{\mathbf{h}}_j^{\text{MAP}} = \frac{\sqrt{\beta P}[(1 + \frac{\beta P}{N_0}) I_K + \sum_{n=1}^{m} \lambda_n \mathbf{P}(k)]^{-1}}{N_0} \mathbf{s}_j \tag{5.60}$$

where $\lambda_k$ can be obtained from the constraint

$$\lambda_k (\tilde{\mathbf{h}_j}^H \mathbf{P}(k) \tilde{\mathbf{h}_j} - r_{j,k} + N_0) = 0 \tag{5.61}$$

for all $k \in \{1, 2, \ldots, m\}$. However, there are several solutions for the above set of equations and the complexity is too high to get relevant solutions. Hence, for the sake of simplicity, we assume that by combining the feedbacks (or with channel selection transmission policy), $|h_{nj}|^2$ or $g_{nj}$ can be perfectly known for $n \in S$ where $S \subseteq \mathcal{K}$ and $|S| \leq m$, as explained in the previous subsection. This results in a simpler optimization problem given by

$$\begin{aligned} \min_{\mathbf{h}_j} \quad & \frac{(\mathbf{s}_j - \sqrt{\beta P}\mathbf{h}_j)^H(\mathbf{s}_j - \sqrt{\beta P}\mathbf{h}_j)}{N_0} + \mathbf{h}_j^H \mathbf{h}_j \\ \text{s.t.} \quad & |h_{nj}| = g_{nj}, \ \forall \ n \in S \end{aligned} \tag{5.62}$$

The solution of the simplified problem can be written as :

$$\widehat{\mathbf{h}}_j^{\text{MAP}} = \frac{\sqrt{\beta P}[(1 + \frac{\beta P}{N_0})\mathbf{I}_K + \mathbf{Q}_\lambda]^{-1}}{N_0}\mathbf{s}_j \tag{5.63}$$

$$\frac{\beta P |s_{nj}|^2}{[(N_0 + \beta P) + N_0\lambda_n]^2} = g_{nj} \tag{5.64}$$

where $\mathbf{Q}_\lambda = \text{diag}(q_1, \ldots, q_K)$ with $q_k = \lambda_k$ when $k \in S$ and $q_k = 0$ otherwise. With (5.64), for $n \in S$, we have :

$$\lambda_n = \frac{\pm\sqrt{\dfrac{\beta P |s_{nj}|^2}{g_{nj}}} - (N_0 + \beta P)}{N_0} \tag{5.65}$$

To determine the sign of $\lambda_n$ which minimizes the cost function in (5.63), the optimal $\lambda_n$ can be expressed as :

$$\lambda_n = \frac{\sqrt{\dfrac{\beta P |s_{nj}|^2}{g_{nj}}} - (N_0 + \beta P)}{N_0} \tag{5.66}$$

for all $n \in S$. Therefore, the MAP estimator can be simplified and rewritten as :

$$\widehat{h}_{nj}^{\text{MAP}} = g_{nj}\frac{s_{nj}}{|s_{nj}|} \tag{5.67}$$

for all $n \in S$ and $\widehat{h}_{ij}^{\text{MAP}}$ given by (5.58) when $i \in \mathcal{K} \setminus S$. We use $\Delta_{j;m}^{\text{MAP}*}$ to denote the resulting expected distortion from using the MAP estimator with $m$ RSSI measurements.

### 5.2.4 Numerical performance analysis

As mentioned before, the channel gains statistics are symmetric, i.e. $h_{ij} \sim \mathcal{CN}(0, 1)$. The signal-to-noise ratio (SNR) in the training phase is defined as

$$\text{SNR} = \frac{\beta P}{N_0} \tag{5.68}$$

In the simulations, we fix $N_0 = 1$, $\beta = 1$, $K = 4$ and change the transmit power $P$ to observe the performance at different SNR. Since the classical MMSE coincides with

the classical MAP in our model as seen from (5.46) and (5.57), to compare the distortion with $m$ feedbacks and the distortion without feedback (classical), the reduced distortion is defined as

$$\frac{\Delta^*_{j;0} - \Delta^{\text{MMSE}*}_{j;m}}{\Delta^*_{j;0}} \times 100\%. \tag{5.69}$$

for comparing the new MMSE or

$$\frac{\Delta^*_{j;0} - \Delta^{\text{MAP}*}_{j;m}}{\Delta^*_{j;0}} \times 100\%. \tag{5.70}$$

for comparing the new MAP estimate. For ease of exposition, we assume that from each feedback, we can perfectly reconstruct one channel gain, i.e., with $m$ feedbacks, the transmitter $j$ can acquire $g_{1j}, \ldots, g_{mj}$.

First,, we see the influence of the prior information on the MMSE estimator. We compare the reduced distortion in terms of number of feedbacks with different SNR in Fig. 5.3 . Fig. 5.3 clearly shows that the distortion can be mitigated by using the RSSI measurements and the distortion decreases with more measurements. Interestingly, the reduced distortion is not a monotonic function with respect to SNR. In the low SNR regime, the MMSE estimator doesn't work well since we multiply a constant matrix $\mathbf{A}_j$ to the observation $\mathbf{s}_j$, which is dominated by the noise when SNR is low. Hence, even if we can improve the selection of the $\mathbf{A}_j$ by knowing the RSSI, the distortion can not be reduced much due to the dominant noise level. On the other hand, in the high SNR regime, the classical MMSE estimator is very close to the real channel coefficient, resulting in the classical MMSE performing very close to the best and this results in limited gains. Our technique can bring more improvements (around 20%) in the mid-SNR range close to 0dB.

As a second step, we see the influence of the prior information to the MAP estimator. We compare the reduced distortion in terms of number of feedbacks with different SNR in Fig. 5.4 and also compare the resulting reduced distortion against the new MMSE. Fig. 5.4 clearly shows that the distortion might increase with more RSSI measurements for the MAP estimate as the MAP estimate is not designed to minimize distortion. However, when SNR increases, the RSSI measurements can lead to a significant reduced distortion and it can even outperform the new MMSE. Hence, in terms of the distortion, it is recommended to use the proposed MMSE in the low SNR regime and the proposed MAP in the high SNR regime.

## 5.3 Conclusion

In this chapter, two novel connections between power domain feedback and signal domain operations have been proposed. Firstly, in MIMO cognitive network, depending solely on the local CSI, the opportunistic interference alignment scheme proposed in [9] can be reconstructed by exploiting the interference plus noise covariance matrix feedback. Instead of only allowing the primary user to transmit, the secondary user can transmit and guarantee zero interference to the primary link. Compared to the scheme where only the primary user can transmit at its maximum rate, our proposed technique brings significant

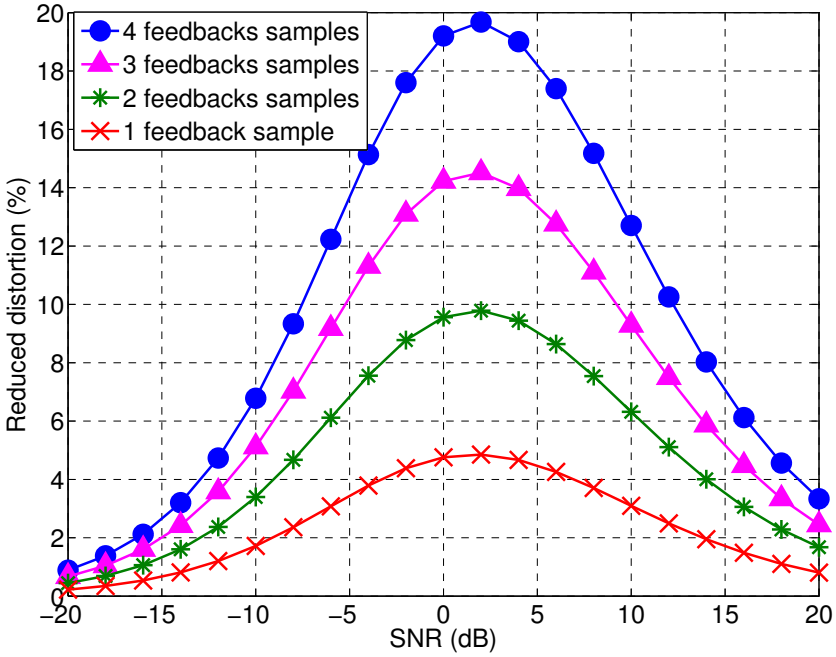


FIGURE 5.3 – More feedbacks we have, more distortion will be mitigated by the proposed MMSE estimator. Our scheme brings more improvements in moderate SNR regime.

improvements in terms of network utility, especially when SNR is not high and the channel coherence time is long.

Secondly, we have provided novel MMSE and MAP estimators for channel estimation in the framework of an interference channel. While classical estimators rely solely on the pilot sequence and training, we also exploit the relevant RSSI measurements available in order to further tune the estimate. Although this information might be hard to exploit in general, we have specified some scenarios where the information available can be easily used in order to improve the quality of estimations. We provide numerical results that validate our approach which show the percentage of reduced distortion when compared to the distortion resulting from the classical estimate.

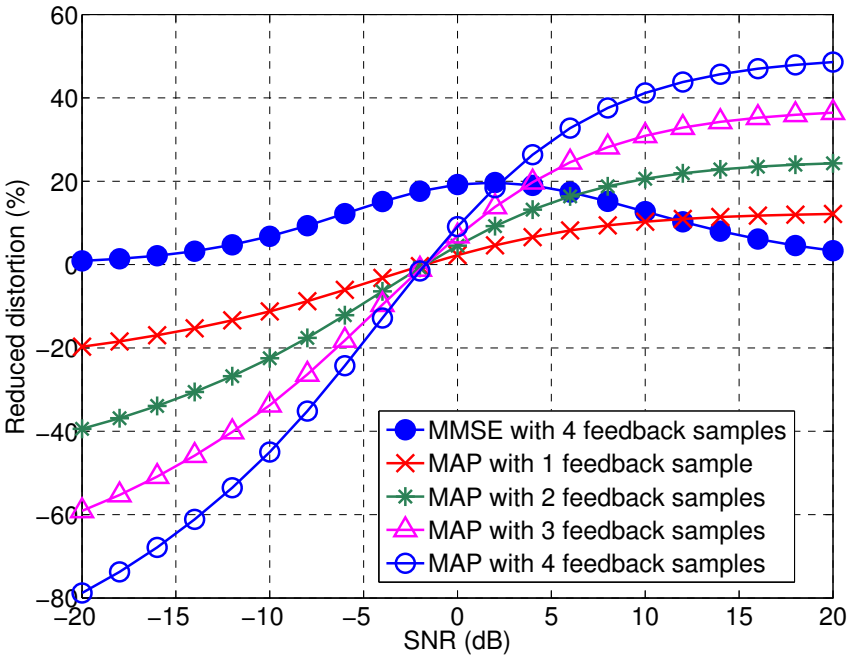


FIGURE 5.4 – In high SNR regime, the proposed MAP can have less distortion than the classical MAP and the proposed MMSE.

# 6

# About the interplay between quantization and utility

In the first part of the chapter, we revisit the problem of quantization by considering an arbitrary choice for the utility function instead of the classical performance criterion namely, the distortion or mean square error. This new and general way of tackling the quantization problem is relevant e.g., for scenarios where the receiver has to quantize channel state information (CSI) and report this imperfect version of the channel to the transmitter which has to maximize a certain utility function. The corresponding maximization operation is necessarily suboptimal since the perfect knowledge of the channel is not available at the transmitter, hence our motivation in making the corresponding optimality loss as small as possible. Implicitly, we assume that the quantizer and dequantizer have the same objective, that is, to maximize the utility function under consideration. Simulations show that using the proposed utility-oriented quantizer allows one to reduce the global optimality loss by 5% instead of 40% when using the classical Lloyd-Max algorithm. In the second part of the chapter, we assume that the transmitter and the receiver have non-aligned utility functions, that is, their interest might be divergent. In the simulations, we exhibit the influence of the bias in terms of utilities on the equilibrium performance of the transmitter and receiver. We have identified a communication scenario which appears in the smart grid area for which this framework is fully relevant. When a consumer has to reveal some information about its need in terms in energy, its interest might be different from the aggregator, energy provider, or operator. For instance, the consumer may want to completely fulfill its energy need whereas, the operator may also want to manage the electricity network or take into account some constraints related to the energy production level. This gives rise to a bias in terms of utility functions and therefore constitutes a communication scenario in presence of diverging interests. For such scenarios, we provide some preliminary results to understand the impact of the bias on the communication. Admittedly, a lot of efforts should be made to understand this tricky communication scenario but our results constitute a first step towards this challenging objective.

# 6.1 Utility-oriented quantization with aligned utility function and application to power control in wireless networks

## 6.1.1 Motivation and state of the art

The primary motivation for formulating the technical problem under consideration in this section comes from resource allocation problems in wireless communications. For this type of problems, quite often, one has to deal with the following situation. A payoff, reward or utility function $f(x;g)$ has to be maximized with respect to the vector $x$ but its parameters (which are represented by the vector $g$) are not perfectly known. In this section, we restrict our attention to the case where what is available to maximize $f$ is a quantized version of the function parameters. Although it has not been addressed from the technical perspective proposed in this section, this scenario is well motivated by numerous papers in the literature of wireless communications (see e.g., [11][72][14]). For instance, it is fully relevant when a transmitter has to perform power allocation by exploiting a quantized version of the channel which is sent by the receiver (through a feedback mechanism) ; in this example, the receiver needs to quantize the channel gains or matrix to meet some constraints e.g., linked to the feedback channel capacity.

The problem we introduce in this section is the design of the quantizer which produces the distorted vector of parameters which is effectively available to maximize the utility function $f$ ; in the power allocation problem which has been mentioned previously, the receiver has to quantize the downlink channel and send it to the transmitter whose role is to perform power allocation based on the quantized channel sent by the receiver. More precisely, we want to minimize the impact of quantization noise on the optimality loss which occurs when using the quantized version of $g$ to maximize the utility function $f$. Of course, this design is performed under a resource constraint which is the number of quantization bits. The design of a quantizer consists in finding a partition and the corresponding representatives. Indeed, the space in which the vector of parameters lies has to be partitioned into cells or regions. For any input $g$ which belongs to a given cell, the quantizer produces the same output $\widehat{g}$, which is called the representative of the considered cell.The maximum number of cells the quantizer can use is given by the total number of bits available for quantizing.

To determine the best quantizer in the sense of minimizing the optimality loss induced by using $\widehat{g}$ instead of $g$, we generalize the well-known Lloyd-Max algorithm (LMA) [12][13]. Indeed, the LMA-based quantizer aims at minimizing the distortion i.e., the mean square error between the source and its reconstructed version. But, note that this design is independent of the use of the quantized quantity. It turns out that the quantizer design might be improved when measured in terms of the final utility of payoff. The original version of the LMA has been generalized in many diverse ways. For instance, it has been generalized to scenarios where the source to be quantized has to be sent through a noisy channel (see e.g., [74][75]) and the source is itself noisy[76]. However, almost always, the performance criterion is the distortion. There exist some other works where a different performance criterion is considered such as [77] where the $L_p-$ norm is considered (instead of the Euclidean norm) or some specific performance criterion such as in [78]

where the goal is to obtain a quantized beamforming vector. More generally, in [79], the author considers the problem of minimizing an arbitrary function of the difference between the actual vector of parameters and its quantized version but, again, this problem does not correspond to the framework of utility-oriented quantization we propose here. Recently, several works like [80] adrress the issue of quantization noise as a primary concern in resource allocation problems. As a result, some new studies like [81], optimize the allocation of quantization bits specifically for sum-rate maximization. However, in these works the goal is not to design the complete quantization scheme for their payoff (i.e., the allocation of bits, partitions and representatives). Finally, some papers study situations where specific control-theoretic performance criteria are optimized (see e.g., [82]) but the quantization problem is not stated in general and not solved by using a generalized version of the LMA. To the best knowledge of the authors, the quantization problem has not been formulated as in the present work.

### 6.1.2 Problem statement

We consider a function $f(x;g) : \mathcal{X} \times \mathcal{G} \to \mathbb{R}$, referred to as the utility function. Both $x \in \mathcal{X}$ and $g \in \mathcal{G}$ may be vectors in general with $\mathcal{X} \subset \mathbb{R}^N$ and $\mathcal{G} \subset \mathbb{R}^K$. The ultimate goal is to maximize $f$ with respect to $x$ while only knowing a quantized version of $g$, which is denoted by $\mathcal{Q}(g)$. Here, the objective is to find a good quantizer namely a quantizer which allows to minimize the impact of quantization on the optimality loss induced by using $\mathcal{Q}(g)$ in the final optimization problem.

A quantizer $\mathcal{Q}$ is given by a partition of $\mathcal{G}$ into cells and their representatives. We denote by $M$ the maximum number of cells. The cells are denoted by $\{\mathcal{C}_1, ..., \mathcal{C}_M\}$ and satisfy $\mathcal{C}_m \subset \mathcal{G}$ such that $\mathcal{C}_1 \cup \mathcal{C}_2 \cup \cdots \cup \mathcal{C}_M = \mathcal{G}$ and $\mathcal{C}_m \cap \mathcal{C}_n = \emptyset$ for any $m \neq n$. The quantization rule is assumed to be as follows : $\mathcal{Q}(g) = r_m$ if $g \in \mathcal{C}_m$ where $m = 1, 2, ..., M$. The conventional approach consists in determining $\mathcal{Q}$ so that the distortion is minimized i.e., to minimize

$$D = \int \phi(g) \|\mathcal{Q}(g) - g\|^2 \mathrm{d}g \tag{6.1}$$

where $\phi$ is the probability density function (p.d.f.) of $g$. The advantage of such an approach is that it may be possible to obtain the quantizer explicitly (namely the representatives and cells) and this leads to a scheme which is independent of the payoff. However, if the payoff is known, it is generally possible to further improve the performance when it is measured in terms of final payoff. Indeed, if one denotes by $F$ the actual maximum of $f$

$$F(g) = \max_x f(x;g) \tag{6.2}$$

and by $\widehat{F}$

$$\widehat{F}(\mathcal{Q}(g)) = \max_x f(x;\mathcal{Q}(g)) \tag{6.3}$$

the level which is effectively attained by only knowing $\mathcal{Q}(g)$ and not $g$, it is relevant to determine $\mathcal{Q}$ through the following relation :

$$\mathcal{Q}^\star \in \arg\min_{\mathcal{Q}} \mathbb{E}_g \|F(g) - \widehat{F}(\mathcal{Q}(g))\|^2. \tag{6.4}$$

The purpose of the next section is precisely to provide results in order to minimize the quantity defined in (6.4). Just as in the LMA, in general there is no guarantee for global

optimality. This classical issue is left as an extension of the present work, the goal here being to focus on what is really novel.

### 6.1.3 General quantization scheme

When $g$ is a $K-$dimensional vector ($K > 1$), finding the cells and the representatives jointly which minimize (6.4) is a highly non-trivial problem. This is the main reason why we take inspiration from classical quantization schemes such as the LMA, in order to search for a scheme that can find the most suitable representatives $\{r_1, ..., r_M\}$ (locally optimal) for a given set of cells $\{\mathcal{C}_1, ..., \mathcal{C}_M\}$, and to find locally optimal cells for a given set of representatives. Once these can be found, we can iteratively solve for $\{r_1, ..., r_M\}$ and $\{\mathcal{C}_1, ..., \mathcal{C}_M\}$, to find a locally optimal solution (not necessarily globally optimal).

Finding the optimal cells for a given set of representatives $\{r_1, ..., r_M\}$, can be done in a manner similar to the classical LMA, and by constructing the partitions that are similar to Voronoi partitions :

$$\mathcal{C}_m = \left\{ g \in \mathbb{R}^K : \left[F(g) - F(r_m)\right]^2 \leq \left[F(g) - F(r_n)\right]^2 \right\} \tag{6.5}$$

where $n \neq m$. Clearly, the motivation for this choice is that instead of the Euclidean distance or distortion of $g$ as taken in the classical Voronoi partition, here we look for the set with the minimum distortion in terms of $F(g)$. On the other hand, finding the optimal representative $r_m$ for a given cell $\mathcal{C}_m$, might not be as straightforward. Indeed, when $g$ is a scalar and $F$ is invertible, and if $\mathcal{C}_m$ is defined by an interval of the form $[t_m, t_{m+1}]$, then the best representative $r_m^\star$ is given by

$$F(r_m^\star) = \frac{\displaystyle\int_{t_m}^{t_{m+1}} \phi(g) F(g) \mathrm{d}g}{\displaystyle\int_{t_m}^{t_{m+1}} \phi(g) \mathrm{d}g}. \tag{6.6}$$

The above result can be shown to be true by differentiating $\mathbb{E}_g(\|F(\widehat{g}) - F(g)\|^2)$ w.r.t $r_m$ in a given cell $\mathcal{C}_m = [t_m, t_{m+1}]$. Since $F$ is invertible, its derivative never vanishes and thus (6.6) can be obtained. Although $F$ is typically an invertible function when $g$ is scalar, this property is generally lost when $g$ becomes a vector and the $K$ elements of $r_m$ can not be recovered from only one equation (1 equation for $K$ unknowns). For this reason, when $g$ is the vector of the form $g = (g_1, g_2, \ldots, g_K)^T$, some assumptions have to be added to make the identification procedure possible. The next result is precisely based on one reasonable assumption which allows identifiability to be possible.

**Assumption 6.1.1** (Decomposability assumption)**.** *The function $F$ can be written as $F = \sum_{k=1}^{K} u_k$ with $u_k : \mathcal{G} \to \mathbb{R}$ and it is such that then the vector function $V(g) := (u_1(g), ..., u_K(g))^{\mathrm{T}}$ is invertible in $\mathcal{C}_m$.*

This assumption is well suited for several applications where the total payoff is the sum of several components, for example, when the payoff is the sum of the rates over each band. Indeed, the function $V$ may not be globally invertible, but our results can be applied to partitions $\mathcal{C}_m$ such that this assumption holds as we will illustrate in Sec. 4. For wireless systems, this sufficient condition is often met due to the monotonicity of most

utility functions; indeed, many utility functions in wireless communications are typically monotonically increasing w.r.t. the signal-to-interference plus noise ratio (SINR).

**Proposition 6.1.2** (Optimal representatives)**.** *If Assumption 6.1.1 holds for a partition* $\mathcal{C}_m$*, with the decomposed invertible function being* $V(g) = (u_1(g), ..., u_K(g))^{\mathrm{T}}$*, then the optimal representative* $r_m^*$ *which minimize* $\mathbb{E}_g(\|V(\widehat{g}) - V(g)\|^2)$ *also minimize* $\mathbb{E}_g(\|F(\widehat{g}) - F(g)\|^2)$ *where* $\widehat{g} = \mathcal{Q}(g)$*, and can be obtained by solving the following system of* $K$ *equations*

$$u_k(r_m^*) = \frac{\displaystyle\int_{\mathcal{C}_m} \phi(g) u_k(g) \mathrm{d}g}{\displaystyle\int_{\mathcal{C}_m} \phi(g) \mathrm{d}g} \tag{6.7}$$

**Proof :** See Appendix D.

The scalar case (6.4) can be obtained by simply setting $K$ to 1. Now, we exploit Proposition 6.1.2 to derive a suitable algorithm to find a utility-oriented quantizer knowing $F$.

**Inputs :** $\phi(g) : \mathbb{R}^K \to \mathbb{R}_{\geq 0}$, $F = \sum_k u_k$ satisfying assumption 6.1.1, $\{r_1^{(0)}, ..., r_M^{(0)}\}$
**Outputs :** $\{r_1^\star, ..., r_M^\star\}$, $\{C_1^\star, ..., C_M^\star\}$
**Initialization :** Set iteration index $q = 0$. Initialize the quantization representatives according to $\{r_1^{(0)}, ..., r_M^{(0)}\}$. Set $r_m^{(-1)} = 0$ for all $m \in \{1, ..., M\}$.
**while** $\displaystyle\sum_{m=1}^{M} (r_m^{(q)} - r_m^{(q-1)})^2 > \delta$ *and* $q < Q$ **do**
  Update the iteration index : $q \leftarrow q + 1$.
  For all $m \in \{1, 2, .., M\}$, update $C_m^q$ from $r_m^{q-1}$ using (6.5).
  For all $m \in \{1, 2, .., M\}$, update
  $r_m^q$ for each partition $C_m^q$ using (6.7).
**end**
$\forall m \in \{1, ..., M\}$, $r_m^\star = r_m^{(q)}$, $t_m^\star = t_m^{(q)}$, $t_{M+1}^\star = +\infty$

**Algorithm 3:** Algorithm to obtain the utility-oriented quantizer

The new quantizer can be summarized by the Algorithm 1. It is also important to note that the LMA can be treated as the first order Taylor approximation of the proposed algorithm, or just a special case in which $F$ is a linear function. Note that Assumption 6.1.1 may not hold over the entire set $\mathcal{G}$, in this case, $\mathcal{G}$ can be partitioned into several sub-regions where each region can be quantized specifically. For example, as seen in the next section, when energy maximization is pursued, solutions are such that only the best channel is picked, in which case just the best channel needs to be quantized and then the minimum number of bits can be allocated to the other channels.

### 6.1.4 Application to typical wireless utility functions

#### Energy-efficiency maximization

In this subsection, we consider a particular utility function, the energy efficiency function, for a multi-band scenario. The quantizers of interest for the transmitter to allocate its

power are given by the channel gains. The channel gain in band $k$ is denoted by $g_k = |h_k|^2$ where $h_k$ may typically be the realization of a complex Gaussian random variable if Rayleigh fading is considered. The power emitted in band $k$ is denoted by $p_k$ and is assumed to be subject to power limitation as : $p_k \geq 0$ and $\sum_{k=1}^{K} p_k \leq P_{\max}$. The K-dimensional column vector formed by the transmit power levels and channel gains will be denoted by $p = (p_1, ..., p_K)^{\mathrm{T}}$ and $g = (g_1, ..., g_K)^{\mathrm{T}}$, respectively. Here we choose the efficiency function of [83], which is defined as

$$f(p,g) = \frac{\sum_{k=1}^{K} e^{\left(-\frac{c\sigma^2}{g_k p_k}\right)}}{\sum_{k=1}^{K} p_k} \tag{6.8}$$

where $\sigma^2$ is the receive noise variance and $c = 2^r - 1$ with $r$ being the spectral efficiency. To find $F$ in the case of energy-efficiency maximization, we first derive the optimal power control policy. This is the purpose of the next proposition.

**Proposition 6.1.3.** *In multi-band scenario, to maximize the system energy-efficiency, the optimal power allocation scheme is*

$$p_k^{\star}(g_k) = \begin{cases} 0 & k \neq \arg\max\limits_i \ g_i \\ \min\left(\frac{c\sigma^2}{g_k}, P_{\max}\right) & k = \arg\max\limits_i \ g_i \end{cases} \tag{6.9}$$

*Démonstration.* The proof is omitted because of the lack of space. □

According to Proposition 6.1.3, to maximize energy-efficiency, the transmitter will only transmit through the best channel. To better estimate the utility at the transmitter side, we can use the vector quantization method proposed in the previous subsection. However, this will entail a high complexity if the number of bands is very large. Since only one band is active in each time-slot, this property can be used to design a special quantization scheme. Firstly, we divide the whole region into $K$ sub-regions $\widehat{\mathcal{C}}_1, ..., \widehat{\mathcal{C}}_K$, where $\widehat{\mathcal{C}}_k = \{g \in \mathbb{R}^K : g_k = \max\limits_i \ g_i\}$. The region $\widehat{\mathcal{C}}_k$ corresponds to the region in which $g_k$ is the best channel. Without loss of generality, we consider the quantization scheme for region $\widehat{C}_k$. If the channel realization belongs to $\widehat{C}_k$, then only band $k$ will be active. It implies that only selection of band $k$ and the value of $g_k$ are useful to improve the energy efficiency. Suppose $\mathcal{Q}(g) = (\widehat{g}_1, ..., \widehat{g}_K)^{\mathrm{T}}$, the first issue can be easily solved by setting the largest element of the representatives in $\widehat{\mathcal{C}}_k$ as $\widehat{g}_k$, i.e. $\max \mathcal{Q}(g \in \widehat{\mathcal{C}}_k) = \widehat{g}_k$. Note that the optimal energy efficiency function in $\widehat{\mathcal{C}}_k$ can be simplified as

$$F(g \in \widehat{\mathcal{C}}_k) = \max_p \ f(p, g \in \widehat{\mathcal{C}}_k) = \frac{e^{\left(-\frac{c\sigma^2}{g_k p_k^{\star}}\right)}}{p_k^{\star}(g_k)}. \tag{6.10}$$

Hence, the second issue, to find the optimal quantized value of $\widehat{g}_k$, can be solved by minimizing $d(\widehat{g}_k)$ defined as

$$d(\widehat{g}_k) = \mathbb{E}_{g_k | g_k \geq g_1, ..., g_k \geq g_K} \left[F(g_k) - F(\widehat{g}_k)\right]^2. \tag{6.11}$$

**Proposition 6.1.4.** *Define the M-level scalar quantizer of $g_k$ transition levels set as $\{t_{k,1}, ..., t_{k,M+1}\}$ and its corresponding representatives set as $\{l_{k,1}, ..., l_{k,M}\}$. Suppose each channel $g_k$ is i.i.d. with p.d.f. $\phi(g_k) = \gamma e^{-\gamma g_k}$. Assume $P_{\max}$ is sufficiently large, for fixed representatives $\{l_{k,m}\}$, the intervals (cells) which minimize $d(\widehat{g}_k)$ can be obtained by*

$$t_{k,m} = \frac{l_{k,m-1} + l_{k,m}}{2} \tag{6.12}$$

*with fixed transition levels $\{t_{k,m}\}$, the optimum representatives to minimize $d(\widehat{g}_k)$ can be obtained by*

$$l_{k,m} = \frac{\displaystyle\int_{t_{k,m}}^{t_{k,m+1}} g(1 - e^{-\gamma g})^{K-1} \gamma e^{-\gamma g} \mathrm{d}g}{\displaystyle\int_{t_{k,m}}^{t_{k,m+1}} (1 - e^{-\gamma g})^{K-1} \gamma e^{-\gamma g} \mathrm{d}g}. \tag{6.13}$$

*Démonstration.* The proof is omitted because of the lack of space. □

Obtaining this scalar quantizer, $d(\widehat{g}_k)$ can be minimized knowing $g_k$ is the best channel. Without loss of generality, we assume that each region $\widehat{\mathcal{C}}_k$ will be divided to M different quantization cells $\{\mathcal{C}_{k,1}, ..., \mathcal{C}_{k,M}\}$. The corresponding representative of the quantization region $\mathcal{C}_{k,m}$ is defined as a K-dimensional vector $r_{k,m} = (r^1_{k,m}, ..., r^K_{k,m})^{\mathrm{T}}$. Based on the results in the previous section, the vector quantization region $\mathcal{C}_{k,m}$ can be expressed as

$$\mathcal{C}_{k,m} = \{g \in \mathbb{R}^K : \ t_{k,m} < g_k \leq t_{k,m+1}\} \cap \widehat{\mathcal{C}}_k. \tag{6.14}$$

The corresponding representative $r_{k,m}$ can be chosen as :

$$r^k_{k,m} = l_{k,m} \tag{6.15}$$

$$r^{k'}_{k,m} = \text{const} < r^k_{k,m} (k' \neq k). \tag{6.16}$$

For the vector quantization of $g$, the quantization region set $\mathcal{C} = \{\mathcal{C}_{1,1}, \mathcal{C}_{1,2}, ..., \mathcal{C}_{K,M}\}$ and the representatives set $r = \{r_{1,1}, r_{1,2}, ..., r_{K,M}\}$ can be found using (6.14)(6.15)(6.16). With this new approach, the complexity of the computation has been considerably reduced.

### Spectral efficiency maximization

Using the same notations as in the previous section, here we consider the following well-known sum-rate function

$$u^{\mathrm{sum-rate}}(p, g) = \sum_{k=1}^{K} \log\left(1 + \mathrm{SINR}_k(p, g)\right) \tag{6.17}$$

where $\mathrm{SINR}_k(p, g) = \frac{g_k p_k}{\sigma^2}$. The optimum power allocation policy is given by the water-filling solution, i.e.,

$$p^\star_k = \left[\mu - \frac{\sigma^2}{g_k}\right]^+ \tag{6.18}$$

where the water level $\mu$ can be obtained by solving $\sum_{k=1}^{K} p_k = P_{\max}$ and the function $[x]^+ = \max(x, 0)$. However, due to the incertitude of the function $[x]^+$, it is difficult to obtain the explicit expression for the function $F(g)$. To express $F(g)$ explicitly, we can firstly divide the whole region to specific partitions for each case corresponding to if $p_k^* = 0$ or not. In each of these partitions, a different quantization scheme must be ideally used for optimal results, as we cannot find $u_k$ satisfying Assumption 6.1.1 for the general channel space. So, we focus on a practically relevant case of high signal-to-noise ratio (SNR) for the purpose of this work. Studying the general case is left as an extension which can be solved by treating each partition (corresponding to $p_k^* = 0$ or not) separately.

In the high SNR case, i.e., when $\frac{P_{\max}}{\sigma^2} \to \infty$ we have $p_k^* > 0$ for all $k$. Further, it can be observed that the sum-rate can be decomposed to individual payoff. Substituting (6.18) into (6.17), the individual payoff can be expressed as follows :

$$\begin{aligned} u_k^{\text{sum-rate}} &= \log(1 + \text{SINR}_k) \\ &= \log\left(1 + g_k \text{SNR} + \sum_{j \neq k} \frac{g_k}{g_j}\right) - \log(2) \end{aligned} \tag{6.19}$$

with $\text{SNR} := \frac{P_{\max}}{\sigma^2}$. This $V = (u_1, u_2, \ldots, u_K)^T$ is clearly invertible w.r.t $g$ satisfying Assumption 6.1.1, and we can therefore directly apply Proposition 6.1.2 and Algorithm 3 to obtain the utility oriented quantizer.

### 6.1.5 Numerical performance analysis

In this section, we present simulation results to illustrate the performance of the proposed quantizer for a single user multi-band scenario. For comparison with the classical LMA, we look at the optimality loss induced by quantization defined as

$$\Delta F(\%) = \mathbb{E}_g \left[ \left| \frac{F(g) - \widehat{F}(\mathcal{Q}(g))}{F(g)} \right| \right] \times 100 \tag{6.20}$$

which we term the relative optimality loss, where expectation is calculated by Monte-Carlo simulations for the channel gain $g$. For all $k$, the channel gain $g_k$ in band $k$ is assumed to be exponentially distributed, namely, its p.d.f. writes $\phi(g_k) = \exp(-g_k)$ ; this corresponds to the well known standard Rayleigh fading assumption. The considered scenario for all simulations is such that the transmit power $P_{\max} = 20$ dBm and a normalized receive noise power $\sigma^2 = 0$ dBm, resulting in SNR= 20 dB.

In Fig. 6.1, the energy-efficiency utility function defined in (6.8) is considered as the utility function $f$ and the relative optimality loss is plotted against the number of quantization bits when the number of bands $K = 16$. Our quantizer is obtained by using the Proposition 6.1.3 we have provided.

In Fig. 6.2 we look at the sum-rate utility function as defined in (6.17). There are two bands available for communication, i.e. $K = 2$. We plot the relative optimality loss induced by quantization w.r.t the number of quantization bits used.

As expected, when the number of bits increases, the relative optimality loss of both quantizers decreases. The proposed quantizer in Sec. 6.1.4 outperforms the classical LM

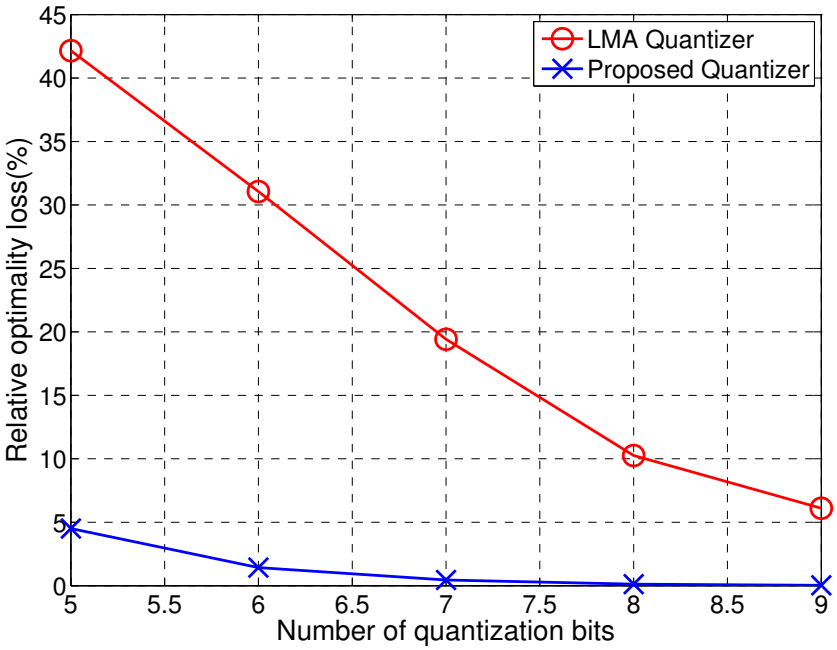


FIGURE 6.1 – Comparison of the performance in terms of final payoff between the conventional paradigm-based quantizer (which aims at minimizing distortion) and the proposed utility-oriented quantizer. The figure represents the relative optimality **energy-efficiency** loss against number of quantization bits. The proposed quantizer results in a relative optimality loss (w.r.t. the case where the channel is known perfectly to the transmitter) of just 5% with 5 quantization bits compared to over 40% when using the classical.

vector quantizer. It is also important to note that the relative optimality loss of our quantizer is very close to 0 when we have more than 7 quantization bits, but the relative optimality loss of LM quantizer still remains significant even with 9 quantization bits. Meanwhile, it can be predicted the novel quantizer will have the same performance as LM quantizer when the number of quantization bits tends to infinity since the relative optimality loss tends to 0 for both quantizer.

Finally, we study the relative optimality loss as a function of the number of bands with a fixed number of quantization bits. The number of quantization bits is set to five for this simulation. Fig. 6.3 illustrates the relative optimality loss against different number of bands. In single band scenario, the proposed quantizer coincides with the LM quantizer as minimizing the relative optimality loss is identical to minimization of distortion. In the multi-band case however, our quantizer achieve a better performance in terms of relative optimality loss and the difference becomes more significant as number of bands increases. Since the number of quantization bits is fixed, the accuracy of each component $\widehat{g}_k$ will degrade as the number of bands increases for the LMA.

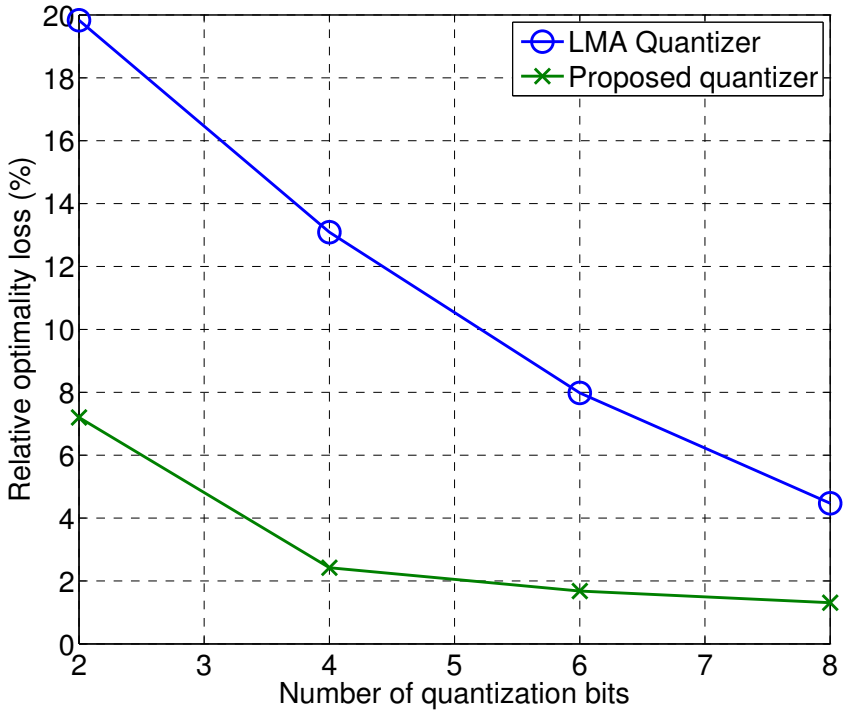


FIGURE 6.2 – Relative optimality **spectral efficiency** loss (sum-rate) based utility against number of quantization bits. The proposed quantizer achieves a better performance and the loss is less than 5% with more than 5 quantization bits.

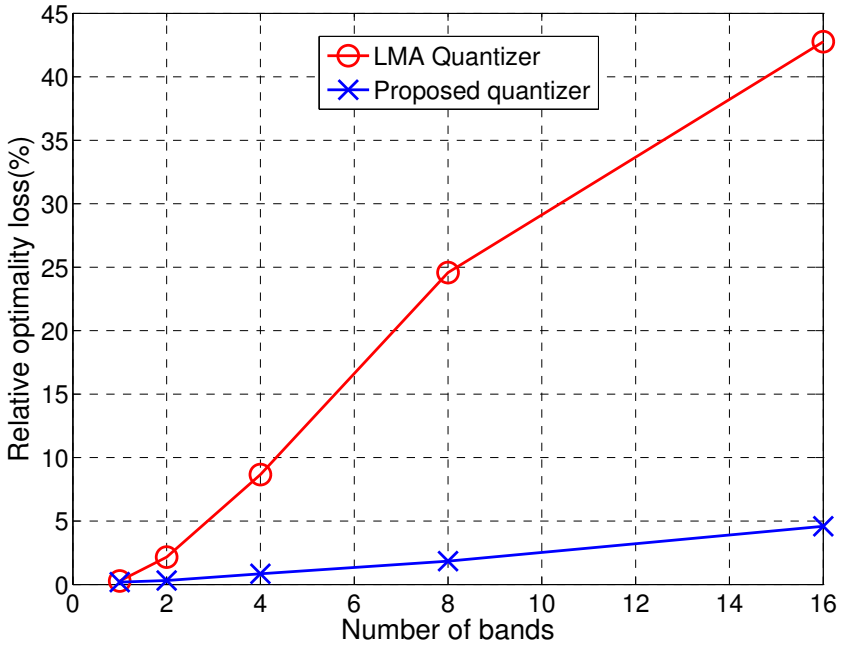


FIGURE 6.3 – Relative optimality energy-efficiency loss against number of bands. The proposed quantizer improves the performance in multi-band scenario and the improvement becomes more significant as the number of bands increases.

## 6.2 Utility-oriented quantization with non-aligned utility function and application to smart grid

### 6.2.1 Motivation and state of the art

Today's electrical infrastructure has been constructed for about a hundred years. While the components of the hierarchical grid are near to the end of their lives, the demand for electricity has gradually increased. To fulfill the increasing demand induced by growing population, a new concept of electric power system, the smart grid, has been proposed in recent years. Smart grid is a term referring to the next generation power grid in which the electricity distribution and management is upgraded by incorporating advanced two-way communications and pervasive computing capabilities for improved control, efficiency, reliability and safety [84][85]. The existing grid is lack of communication capabilities, while a smart power grid infrastructure is full of enhanced sensing and advanced communication and computing abilities [86][87][88][89]. However, in the smart grid it will be more common that the consumer will have to adapt its consumption to production e.g., when an erasure mechanism is implemented or when the energy source is a solar/wind farm. Obviously, the consumer and aggregator (i.e., the entity which takes the decision to which extent to meet the demand) will have diverging objectives in general. As a consequence, it might happen that the consumer reports a demand which is higher than the actual need to be effectively satisfied. Therefore, it is essential to design a point-to-point communication system where the transmitter (or coder) and receiver (or decoder) have diverging objectives. In fact, the classical paradigm in communication systems such as quantization scheme, assumes that the coder and the decoder have a common objective (e.g., to minimize the distortion or symbol error rate). When the consumer and the aggregator have non-aligned goals, the problem of coding needs to be revisited. In this section, we will only make a step into the direction of answering the aforementioned fundamental question.

Specifically, we consider an aggregator whose objective is to satisfy the consumer but also to minimize the operating cost induced by the distribution network. On the other hand, the consumer's ultimate objective is to obtain an amount of power (or energy) as close as possible to its actual need. Based on signal/message received from the consumer about its need in terms of power, the aggregator eventually decides the amount of power effectively allocated to the consumer. One of the purposes of this work is to construct a signaling scheme from the consumer to the aggregator which would allow them to each a consensus or equilibrium about how to communicate in practice (based on a suited communication standard). It turns out that, by considering a simple but realistic model for the aggregator and consumer costs, the problem to be solved is a game whose formulation is related to the problem of strategic information transmission in economics [90] and the one of quantization. Indeed, the problem of strategic information transmission has been introduced in [90] and developed in economics (see e.g., [91] for a recent survey) but not penetrated engineering yet up to a few exceptions [92], which do not consider neither the smart grid application nor the connections with coding/quantization.

### 6.2.2 Problem formulation

Fig. 1 provides several key aspects of the considered problem. We consider a consumer whose objective is to obtain an allocated power which is as close as possible to a desired level denoted by $s \geq 0$. For this purpose, the consumer sends a message $m \in \{1, 2, ..., M\}$ ($M < +\infty$) to the aggregator through a perfect communication channel. Based on the received message, the aggregator effectively provides an amount of power which is denoted by $a \geq 0$. Without loss of generality, it is assumed that $(a, s) \in [0, 1]^2$. The power need $s$ is assumed to follow a distribution $p(s)$ where $p(s)$ is positive and continuous for every $s \in [0, 1]$. One way of mathematically formulating the objective of the consumer, is to consider that he aims at maximizing the following utility function

$$u_{\mathrm{C}}(s, a) = -(s - a)^2 \tag{6.21}$$

With such a model, the consumer both aims at meeting its need in terms of power but also at not exceeding the desired power level, which might for instance induce some unnecessary monetary expenses. This model can also be very well justified when $s$ is interpreted as a desired quantity of energy e.g., for recharging a battery (see, e.g., [93]). Note that here, for the sake of simplicity, we implicitly assume that the energy need corresponds to a need in terms of load or power, which is very realistic when the consumer obtains a constant power transfer rate ; relaxing this assumption can be considered as a possible extension of this work. On the other hand, the aggregator's utility function is assumed to be the weighted sum of the consumer's utility and a utility function related to an operating cost induced by the grid :

$$\begin{aligned} u_{\mathrm{A}}(s, a) &= u_{\mathrm{C}}(s, a) + u_{\mathrm{grid}}(a + \epsilon) \\ &= -(s - a)^2 - bc(a + \epsilon) \end{aligned} \tag{6.22}$$

where $b \geq 0$ represents a weight which translates the importance of the component associated with the grid, $\epsilon$ represents the electric power related to the cost function of aggregator (e.g. circuit power) and $c$ represents the operating cost function which is increasing and convex. More precisely, the grid component can represent a good model of the ageing acceleration factor of a (residential) transformer (see e.g., [94] which justifies why the ageing is accelerated exponentially when operating above its nominal load) as follows :

$$c(a + \epsilon) = e^{a+\epsilon} \tag{6.23}$$

or represent the Joule losses as follows :

$$c(a + \epsilon) = (a + \epsilon)^2 \tag{6.24}$$

Moreover, in the context of strategic information transmission in economics [90], the parameter $b$ is interpreted as a bias which quantifies the divergence of interests between the decision-makers which are the consumer and aggregator here.

One of the contributions of this work is precisely to inspire from the original framework of [90] to design a good/consensus/equilibrium signaling scheme between the consumer and aggregator namely, to determine a good signaling scheme in presence of diverging interests between the coder and decoder. First, the consumer should map its knowledge about its actual power need $s$ into the message sent to the aggregator $m$, which amounts to determining a coding function $f$ defined by :

$$f : \left| \begin{array}{ccc} [0,1] & \to & \{1,2,...,M\} \\ s & \mapsto & m \end{array} \right. . \tag{6.25}$$

Second, the aggregator has to perform the decoding operation by implementing :

$$g : \left| \begin{array}{ccc} \{1,2,...,M\} & \to & [0,1] \\ m & \mapsto & a \end{array} \right. . \tag{6.26}$$

As a first comment note that $f$ and $g$ are deterministic mappings instead of conditional probabilities $q(m|s)$ and $r(a|m)$ ; this choice does not induce any loss in terms of expected utility because $u_{\mathrm{A}}$ and $u_{\mathrm{C}}$ are concave. If $b = 0$ and the power need $s$ is seen as the realization of a random variable whose distribution $p(s)$ is effectively known to the coder and decoder (this corresponds to a particular scenario in terms of beliefs), the problem of determining $f$ and $g$ can be seen as an instance of a scalar quantization problem which is itself a special case of lossy source coding [46]. But, in general $b > 0$ and, even if the distribution $p(s)$ is known to both the coder and decoder, the consequence of this simple difference is that the coder, knowing that the decoder has a different objective, will not maximize its expected utility by revealing its actual need in terms of power. Rather, it will reveal only a degraded version of it and, this, even if $M$ is infinite. As explained in the following section, in general, equilibrium signaling schemes only exploit a fraction of the number of available messages (or bits).

### 6.2.3 Proposed quantization scheme with non-aligned utility functions

In the presence of decision-makers having different utility functions and which can only control some variables of the latter, the very meaning of optimality is unclear and the problem needs to be defined before being solved (see e.g., [17]). In this context, one important solution concept is the Nash Equilibrium (NE), which is a vector of strategies from which no decision-maker or player has anything to gain by changing his own strategy unilaterally. Here, we are in the presence of two players namely, the aggregator and consumer. The strategy of the consumer consists in choosing $f$, which corresponds to choosing a partition of the space of possible power needs i.e., $[0,1]$. With each interval is associated a message $m \in \{1,...,M\}$ intended for the aggregator. The strategy of the aggregator consists in choosing $g$ to generate the action $a_m$, which can be interpreted as choosing a representative of the interval associated with the received message $m$ ; these intervals are denoted by $I_m = [s_m, s_{m+1}]$. Here, the connection with the quantization problem can be established. Typically, the quantization problem consists in minimizing the distortion $\mathbb{E}\left[(s-\widehat{s})^2\right]$ ($\widehat{s} = a$ in our setting), with respect to $f$ and $g$. If $f$ and $g$ are optimized separately, the problem can be interpreted as a game where one player chooses $f$ and the other chooses $g$. Since the cost functions are common and the number of message $M$ is fixed, this defines a potential game [56]. In this type of games, it is known that the iterative procedure consisting in optimizing the cost/utility function w.r.t. $f$ for a fixed $g$, then to optimize it w.r.t. $g$ for the updated $f$, and so on, converges to an NE. This procedure is called the sequential best-response (BR) dynamics in game theory, the BR of a player being the set-valued function which provides the set of strategies which maximize the utility of this player for a given strategy for the other. The Lloyd-Max algorithm precisely implements this procedure and converges to an NE. Indeed, the intersection points between the players' BRs are precisely the NE of the game. In the following paragraphs,

we determine the BRs in the considered setting in which players have different utility functions.

### Best responses for aggregator and consumer

When the aggregator receives a message $m$, it knows that the actual consumer's power need $s$ is in the interval $I_m$ but not its exact value. Therefore, in general, given the knowledge of the message, the aggregator has a certain belief about the power need. With fixed interval $I_m$, the aggregator best-responds to the message by maximizing the expected utility that is,

$$U_{\mathrm{A}}(a,s) = \sum_{m=1}^{M} \int_{s_m}^{s_{m+1}} u_{\mathrm{A}}(a_m, s) p(s) \mathrm{d}s. \tag{6.27}$$

The following proposition provides the expression of the aggregator BR i.e., the best representative of the interval $I_m$.

**Proposition 6.2.1.** *Given a partition scheme $f$ (or $m(s)$), the aggregator's best-response $a_m$ to a message $m$ is :*

$$a_m = \left( \left[ h^{-1} \left( 2 \frac{\int_{s_m}^{s_{m+1}} s p(s) \mathrm{d}s}{\int_{s_m}^{s_{m+1}} p(s) \mathrm{d}s} \right) \right]^+ \right)_{m \in \{1,\dots,M\}}, \tag{6.28}$$

*where*

$$\begin{array}{rccl} h: & [0,1] & \longrightarrow & [bc'(\epsilon), +\infty[ \\ & a & \longmapsto & 2a + bc'(a+\epsilon) \end{array} \tag{6.29}$$

*and* $[x]^+ = \max(x, 0)$.

The above result shows that it is possible to express the aggregator's best action (for a given message) in a simple way. The integral term of the optimal action corresponds to what is called the centroid in quantization. The presence of the function $h^{-1}$ is precisely due to the fact that the coder and decoder have diverging interests. In the extreme case where $b \to 0$ and $\epsilon \to 0$, the optimal action for the aggregator therefore corresponds to the centroid whereas the optimal action is simply 0 when $b \to \infty$ or $\epsilon \to 0$.

The consumer's strategy is to choose a partition of the power need space $[0,1]$ into intervals $I_1, I_2, ..., I_M$ with $I_m = [s_m, s_{m+1}]$. With fixed representatives $a_m$, the optimal partitions can be obtained by maximizing the expected utility that is,

$$U_{\mathrm{C}}(a,s) = \sum_{m=1}^{M} \int_{s_m}^{s_{m+1}} u_{\mathrm{C}}(a_m, s) p(s) \mathrm{d}s. \tag{6.30}$$

The following proposition provides the expression of the aggregator BR i.e., the best representative of the interval $I_m$.

**Proposition 6.2.2.** *Given a aggregator's scheme $g$ (or representatives) , the optimal partition chosen by consumer is :*

$$s_m = \frac{a_{m-1} + a_m}{2} \tag{6.31}$$

Interestingly, according to (6.28), it is possible to have $a_m = 0$ especially when $b$ or $\epsilon$ are large. From (6.31), it can be predicted that some intervals will be degenerated, i.e., $s_m = s_{m+1} = 0$. Therefore, in contrast with a classical quantization problem, the number of messages (or bits) to be used to form the partition are not fixed and can be optimized by the consumer in order to maximize its expected utility function for a given action. This feature constitutes an important technical difference.

These two propositions above completely define the quantization scheme for the problem under investigation (non-aligned utility functions). Indeed, when the consumer chooses a partition of the power need space according to Prop. 5.2.2 and the aggregator chooses the representatives according to Prop. 5.1.1 , we obtain a NE. Inspired from the iterative nature Lloyd-Max algorithm, the sequential best-response (BR) dynamics will be proposed here. The iterative algorithm is given as :

*Initialize the iteration index as* $n = 0$.
*Initialize the partitions as* $\mathcal{S}^{(0)} = (s_1^{(0)}, \ldots, s_{M+1}^{(0)})$ *and the representatives as* $\mathcal{A}^{(0)} = (a_1^{(0)}, \ldots, a_M^{(0)})$.

**while** $\left\|\mathcal{A}^{(n)} - \mathcal{A}^{(n-1)}\right\| > \delta$ *and* $n \leq N$ **do**

Iterate on the iteration index : $n = n + 1$.

***Best-Response of the consumer*** :

$$s_m^{(n)} = \frac{a_{m-1}^{(n-1)} + a_m^{(n-1)}}{2} \tag{6.32}$$

***Best-Response of the aggregator*** :

$$a_m^{(n)} = \left( \left[ h^{-1} \left( 2 \frac{\int_{s_m^{(n)}}^{s_{m+1}^{(n)}} sp(s)\mathrm{d}s}{\int_{s_m^{(n)}}^{s_{m+1}^{(n)}} p(s)\mathrm{d}s} \right) \right]^+ \right) \tag{6.33}$$

**end**

**Algorithm 4:** The proposed procedure to calculate a stable strategic communication system.

*Comments on Algorithm 4* :

- When each agent updates its decision (in (6.32) or (6.33)), the decision of the other is held fixed. Each agent takes the best-response to the current choice of the other. This can be seen as a strategic extension of the Lloyd-Max procedure ;
- Since the consumer and the aggregator update their decision sequentially and not simultaneously, $2 \times n$ updates are needed for $n$ iterations of Algorithm 3 ;
- The order in which the consumer and the aggregator update their action does not matter to obtain convergence (see e.g., [95]). This order has just been chosen here to correspond to the chronology of the problem considered : the consumer sends a message to the aggregator and then the aggregator chooses the representatives ;
- Algorithm 4 can be implemented both in an online and offline fashion. For online communication, a possible protocol to exchange the updated actions between agents can be implemented via an intermediate agent. Alternately, both agents can meet

before physically (offline) and iteratively give their choice to the other (i.e., negotiate) about the communication mechanism. At the end of this "discussion", the obtained communication mechanism can be implemented online ;

### Convergence of Algorithm 4

In contrast with the Lloyd-Max quantization scheme, the convergence of our algorithm cannot be always guaranteed due to the non-aligned utility functions. However, in the following propositions we show some sufficient conditions for Algorithm 4 to converge.

**Proposition 6.2.3.** *If there exists an iteration $k$ such that for every $m \in \{1, \dots, M\}$*

$$a_m^{(k)} \leq a_m^{(k-1)}, \tag{6.34}$$

*Algorithm 4 converges.*

**Proof :** For every $m \in \{1, \dots, M-1\}$, the transition levels can be expressed as :

$$s_m^{(k)} = \frac{a_{m-1}^{(k-1)} + a_m^{(k-1)}}{2} \tag{6.35}$$

$$s_m^{(k+1)} = \frac{a_{m-1}^{(k)} + a_m^{(k)}}{2} \tag{6.36}$$

Knowing $a_m^{(k)} \leq a_m^{(k-1)}$, it can be concluded that $s_m^{(k+1)} \leq s_m^{(k)}$ for every $m \in \{1, \dots, M-1\}$. Thus the representatives can be written as :

$$a_m^{(k)} = (h)^{-1} \left( 2 \frac{\int_{s_m^{(k)}}^{s_{m+1}^{(k)}} sp(s)\mathrm{d}s}{\int_{s_m^{(k)}}^{r_{m+1}^{(k)}} p(s)\mathrm{d}s} \right) \tag{6.37}$$

$$a_m^{(k+1)} = (h)^{-1} \left( 2 \frac{\int_{s_m^{(k+1)}}^{s_{m+1}^{(k+1)}} sp(s)\mathrm{d}s}{\int_{s_m^{(k+1)}}^{s_{m+1}^{(k+1)}} p(s)\mathrm{d}s} \right) \tag{6.38}$$

Note that $(h)^{-1}$ is a non-decreasing function and $\frac{\int_{s_m^{(k)}}^{s_{m+1}^{(k)}} sp(s)\mathrm{d}s}{\int_{s_m^{(k)}}^{s_{m+1}^{(k)}} p(s)\mathrm{d}s} \geq \frac{\int_{s_m^{(k+1)}}^{s_{m+1}^{(k+1)}} sp(s)\mathrm{d}s}{\int_{s_m^{(k+1)}}^{s_{m+1}^{(k+1)}} p(s)\mathrm{d}s}$ because $s_m^{(k+1)} \leq s_m^{(k)}$ and $s_{m+1}^{(k+1)} \leq s_{m+1}^{(k)}$, so $a_m^{(k+1)} \leq a_m^{(k)}$.

Using the same method, it can be obtained that for any iteration $k' > k$, the representatives and transition levels are monotonically non-increasing, i.e.

$$a_m^{(k'+1)} \leq a_m^{(k')} \tag{6.39}$$

$$r_m^{(k'+1)} \leq r_m^{(k')} \tag{6.40}$$

Knowing that these two parameters are monotonically non-increasing and always positive, the Algorithm 4 converges. ■

From the proposition above, if the representatives are non-increasing in a certain iteration $k$, the convergence can be assured. However, it is difficult to evaluate the value of representatives at a later iteration. It might be tractable for the first few iterations. Nonetheless, if one chooses the initial partitions and representatives in a clever fashion, the convergence of the quantization algorithm can be guaranteed. The following proposition shows that the solution obtained through Lloyd-Max algorithm guarantees convergence for our algorithm

**Proposition 6.2.4.** *When the solution of the classical Lloyd-Max algorithm (aims at minimizing* $\sum_{m=1}^{M} \int_{s_m}^{s_{m+1}} (s - a_m)p(s)\mathrm{d}s$*) is chosen as the initial point, the Algorithm 4 converges.*

**Proof :** With the classical Lloyd-Max quantizer, it is important to note that :

$$s_m^{\mathrm{LM}} = \frac{a_{m-1}^{\mathrm{LM}} + a_m^{\mathrm{LM}}}{2} \tag{6.41}$$

$$a_m^{\mathrm{LM}} = \frac{\int_{s_m^{\mathrm{LM}}}^{s_{m+!}^{\mathrm{LM}}} sp(s)\mathrm{d}s}{\int_{s_m^{\mathrm{LM}}}^{s_{m+1}^{\mathrm{LM}}} p(s)\mathrm{d}s} \tag{6.42}$$

Set $a_m^{(0)} = a_m^{\mathrm{LM}}$. In the first iteration, the transition levels can then be calculated by

$$s_m^{(1)} = \frac{a_{m-1}^{\mathrm{LM}} + a_m^{\mathrm{LM}}}{2} = s_m^{\mathrm{LM}} \tag{6.43}$$

The corresponding representatives can be obtained by :

$$\begin{aligned} & 2a_m^{(1)} + bc'(a_m^{(1)} + \epsilon) \\ =& 2\frac{\int_{s_m^{(1)}}^{s_{m+1}^{(1)}} sp(s)\mathrm{d}s}{\int_{s_m^{(1)}}^{s_{m+1}^{(1)}} p(s)\mathrm{d}s} \\ =& 2\frac{\int_{s_m^{\mathrm{LM}}}^{s_{m+1}^{\mathrm{LM}}} sp(s)\mathrm{d}s}{\int_{s_m^{\mathrm{LM}}}^{s_{m+1}^{\mathrm{LM}}} p(s)\mathrm{d}s} \\ =& 2a_m^{(0)} \end{aligned} \tag{6.44}$$

Note that since $bc'(a_m^{(1)} + \epsilon)$ is non-negative, it can be concluded that for every $m \in \{1, \ldots, M\}$

$$a_m^{(1)} \leq a_m^{(0)} \tag{6.45}$$

According to Prop. 5.2.3, the Algorithm 4 converges. ■

### 6.2.4 Numerical performance analysis

In the simulations, we consider a special case of the cost function for the aggregator, i.e. the Joule loss, as follows :

$$c(a + \epsilon) = (a + \epsilon)^2 \tag{6.46}$$

| $b$ \ $\epsilon$ | $10^{-7}$ | $10^{-6}$ | $10^{-5}$ | $10^{-4}$ | $10^{-3}$ | $10^{-2}$ | $10^{-1}$ |
|---|---|---|---|---|---|---|---|
| $10^{-3}$ | 250 | 228 | 193 | 157 | 120 | 84 | 49 |
| $10^{-2}$ | 84 | 73 | 61 | 50 | 38 | 27 | 15 |
| $10^{-1}$ | 26 | 23 | 20 | 16 | 12 | 9 | 5 |
| 0.5 | 13 | 11 | 9 | 8 | 6 | 4 | 2 |
| 1 | 10 | 8 | 7 | 6 | 5 | 3 | 2 |

TABLE 6.1 – maximal size of a partition of equilibrium according to the aggregator's utility margin $\epsilon$ and the weight on grid cost $b$. *The bigger the bias $b$ between utility functions, the smaller the number of non-degenerated cells at equilibrium and the less communication resources (quantization bits) are used.*

For the sake of simplicity, we assume the consumer's power need is distributed uniformly over $[0, 1]$. Firstly, we would like to investigate the maximum size at the equilibrium for the partitions for different biases $\epsilon$ and $b$.

In Tab. 6.1, we note that for higher values of $\epsilon$ and $b$, i.e. when the consumer and the aggregator have more diverging utilities, the size of the partitions are small. This is intuitive as they have less interest in exchanging information with each other and thus having more partitions is not required. Also, we see that $b$ has a greater influence than $\epsilon$. This can be explained by the fact that $b$ has a multiplicative influence to the utility, as opposed to $\epsilon$ which only has an additive influence.

In Fig. 6.4, we study the utility of the consumer with respect to the bias $b$. We initialize the algorithm with k cells for all cases under investigation to isolate the effect of this parameter. We plot three curves corresponding to different $\epsilon$. Unsurprisingly, the utility of consumer decreases as the bias $b$ increases or $\epsilon$ increases, since the aggregator utility is less aligned to satisfying the consumer need.

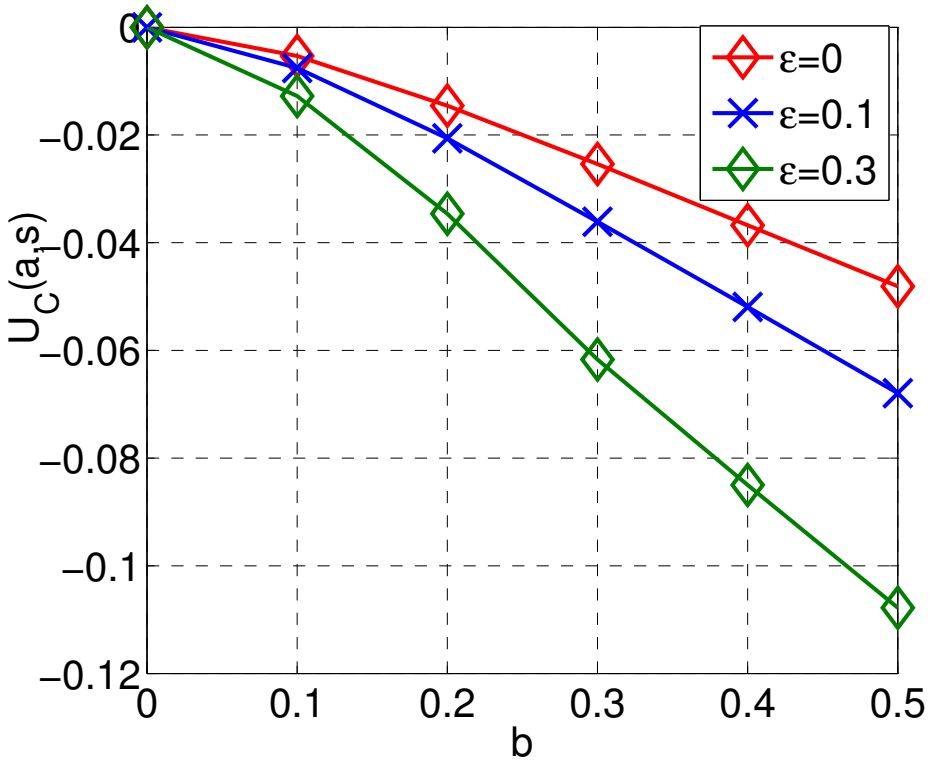


FIGURE 6.4 – More difference between utility functions of the two agents, more degradation will be brought to the consumer's expected utility.

## 6.3 Conclusion

In this chapter, the classical problem of quantization is revisited. We consider the following two problems : the utility functions of the coder and decoder are same or different.

In the first case, instead of designing a quantizer that minimizes distortion or minimum mean square error (MMSE), the relevance of the quantized parameters for the exploitation is considered. This approach is fully relevant in problems such as power control since the transmitter, often has access only to an estimate or quantized version of the parameters (e.g., the channel gains). To effectively determine a good utility-oriented quantizer in the vector case, we make some sufficient but reasonable assumptions on the utility function (such as the decomposability assumption) and resort to a suboptimal iterative algorithm. The benefit from implementing the proposed utility-oriented quantization approach is illustrated with the problem of energy-efficient and spectral efficient power control problem. Significant gains can be obtained in terms of payoff especially when the number of bits decreases. Extending the proposed iterative algorithm to obtain the global optimum solution for a given class of utility functions constitutes a challenging but very important extension.

The second model which is exploited in the second section goes beyond the quantization aspects and the new connections established between [90] and quantization. However, this leads to new technical challenges which concern the general problem of source and channel coding when the coders and decoders have different performance criteria. The si-

mulations show that more the difference between the coder's objective and the decoder's objective, more the degradation that is induced in their individual performance.

# 7

# Conclusions and Perspectives

## 7.1 Conclusions

In this manuscript, our primary objective is to investigate the power control/allocation problems in decentralized interference networks. Two novel techniques (in Chapter 2 and Chapter 3 respectively) are proposed to tackle this issue. One is to exploit the RSSI/SINR to reconstruct the global CSI and consequently seek the power control scheme with global CSI. Another is to provide a framework that allows one to derive the limiting performance of power control with partial information.

More precisely, in Chapter 2 it is shown that the sole knowledge of the received power or SINR feedback is sufficient to recover global CSI. The proposed technique comprises two phases. Phase I allows each transmitter to estimate local CSI. Obviously, if there already exists a dedicated feedback or signaling channel which allows the transmitter to estimate local CSI, Phase I may be skipped. But even in the latter situation, the problem remains to know how to exchange local CSI among the transmitters. Phase II proposes a completely new solution for exchanging local CSI, namely using power modulation (discrete or continuous). Discrete power modulation is based in particular on a robust quantization scheme of the local channel gains. Therefore it is robust against perturbations on the received power measurements ; it might even be used for $1-$bit RSSI, which corresponds to an ACK/NACK-type feedback. This demonstrates that even a rough feedback channel may help the transmitters to coordinate better. When the RSSI quality is good and local CSI is well estimated, continuous power modulation performs very well. Note that the proposed technique is general and can be used to exchange any kind of information and not just local CSI. To the best of our knowledge, in all the power control schemes available in the literature, power levels have never been exploited to exchange information ; therefore, in our setting, interference becomes a communication channel which allows the transmitter to manage it. One of the key novel features of the proposed technique is that the SINR or RSSI feedback is exploited as an implicit

channel the transmitters can use to exchange (low-rate) information. It is essential to understand that in the literature power levels are adapted to the channel but not used to embed information as we do in the manuscript. This is a completely novel approach to distributed power control.

Chapter 3 offers a possible framework to fully characterize the performance of distributed power control under partial information. The limiting performance analysis is conducted in terms of long-term utility region and while we assume the global channel state to be i.i.d. and the observation structure to be memory-less. The proposed framework is shown to be relevant in diverse scenarios of interference networks for finding optimal power control functions. More specifically, the power control functions considered here depends only on local CSI, thus having the merit of being implementable in a completely decentralized manner. Also, the solutions obtained take channel gain estimation noise into account. All the above features illustrate the generality of our approach in tackling problems of power control for maximizing sum-utility functions. Apart from maximizing sum-utility, selfish spectrally efficient power allocation is also studied in Chapter 3. From analytic and numerical results, we provide some conditions, under which allowing selfish transmitters to spread their power over the entire spectrum, as opposed to using a single band, may induce sum-rate performance losses.

As shown in Chapter 2 and 3, the exploitation of feedbacks may bring large improvements in interference networks. In Chapter 4, we present two more methods to utilize power domain feedbacks for signal domain operations. First, in MIMO cognitive networks, relying solely on the local CSI, the interference alignment scheme can be rebuilt by exploiting the power domain feedback. We investigate the case with more transmit antennas and the case with more receiving antennas and therefore propose two different approaches to recover the optimal pre-processing matrix for the secondary user, which guarantees the transmission of the secondary link without generating the interference to the primary link. The second method is studied for the problem of channel estimation in interference networks. We have provided novel MMSE and MAP estimators for channel estimation in the framework of an interference channel. While classical estimators rely solely on the pilot sequence and training, we also exploit the relevant RSSI measurements available in order to further tune the estimate. Although this information might be hard to exploit in general, we have specified some scenarios where the information available can be easily used in order to improve the quality of estimations. We provide numerical results that validate our approach which show the percentage of reduced distortion when compared to the distortion resulting from the classical estimate.

The last major issue that has been considered is in developing a quantization scheme which takes the final use of the quantized quantity into account, namely, utility-oriented quantization. This is presented in Chapter 5 where we study the quantization scheme in two scenarios : the coder and decoder have aligned utility functions or non-aligned utility function. Firstly we investigate the case with aligned utility functions. Instead of considering the distortion or minimum mean square error to design the quantizer, the final use of the quantized parameters is considered. This approach is fully relevant in problems such as power control since the transmitter has often only access to an estimate or quantized version of the parameters (e.g., the channel gains). To effectively determine a good utility-oriented quantizer in the vector case, we make some sufficient but reasonable sufficient conditions on the utility function (such as the decomposability assumption) and resort to a suboptimal iterative algorithm. The benefit from implementing the proposed

utility-oriented quantization approach is illustrated with the problem of energy-efficient and spectral efficient power control problem. Significant gains can be obtained in terms of payoff especially when the number of bits is small. Extending the proposed iterative algorithm to obtain the global optimum solution for a given class of utility functions constitutes a challenging but very important extension. Secondly, we consider the scenario that the consumer and the aggregator have different objectives in smart grid networks. An algorithm has been proposed to obtain a stable information exchange mechanism. Several sufficient conditions have been given for the convergence of the algorithm. Numerically, it is shown that the different objective between consumer and aggregator will induce degradation to both agents. Furthermore, when the difference becomes more significant, the degradation will be more severe.

## 7.2 Perspectives

- Regarding the local CSI exchange scheme proposed in Chapter 2, we recall that our technique concerns the single antenna scenario. Thus, a natural extension would be do the same in the case of MIMO interference networks. The first challenge is that the proposed techniques for Phase I do not allow the phase information or the direction information to be recovered. **However**, if another estimation scheme is available or used for local CSI acquisition and that scheme provides the information phase, then it can be exchanged by using Phase II. This means that global CSI with phase information becomes available. Indeed, one of the strengths of the proposed Phase II is that it allows **any kind of information** to be exchanged, local CSI being the choice made in the present work. All of this means that to address the problem of beamforming in MIMO interference channels, either a more complete feedback should be used or the existence of a local CSI with phase information should be assumed. In the latter case, the manuscript provides an interesting solution for exchanging the corresponding information. Now, another extension which is still challenging but more in line with the spirit of the manuscript is given by a MIMO interference channel for which each transmitter knows the interference-plus-noise covariance matrix and its own channel. This is the setup assumed by Scutari et al in their work on MIMO iterative water-filling [15]. Last possible track for the MIMO extension is to assume the existence of a filter (and even a pre-filter at the transmitter) e.g., an MMSE filter. Then, the notion of SINR per flow might be exploited to develop the framework we propose in the manuscript.
- In Chapter 3, we consider a special case, namely single-band energy efficient power control. It can be seen analytically and numerically that the decision function is similar to the shape of a threshold function. An interesting extension is to consider the multi-band energy efficient power allocation problem and find the form of the decision function.
- In Section 4.1, it is proved that the opportunistic interference alignment schemes can be reconstructed by using the partial channel state information and exploiting the power domain feedback. However, it can be seen that this leads to sum-rate degradation during the training phase (the phase with predetermined precoding matrix, which aims at exchanging information). Therefore, extending the proposed technique to minimize the transmission rate loss while guaranteeing the informa-

tion exchange constitutes an interesting topic. Furthermore, in a MIMO cognitive network with relaxed interference constraints (e.g., the interference from the secondary user upper bounded by a strictly positive constant), or more generally, the MIMO interference network, designing an interference alignment scheme should be a challenging but significant extension.

- In Section 4.2, it is shown that training based channel estimation can be enhanced by exploiting RSSI feedback in SISO interference networks. When considering the channel estimation in MIMO systems, extending our proposed technique to exploit the power domain feedback, e.g. SINR or interference-plus-noise covariance matrix, may bring more insights to the latest wireless networks.
- In Section 5.1, we proposed a quantization scheme taking into account the effect of the quantization on the final utility. In our work, the decided action (transmit power in our scenarios) can be explicitly expressed when the quantized quantity is known. However, in many systems, e.g. power control in multi-user interference networks, the connection between the quantized quantity (channel gain) and the decision (transmit power) can be solely expressed implicitly. Therefore, how to exploit the implicit connection and consequently design the utility-oriented quantization scheme needs to be investigated further in the future. Some learning algorithms might be useful to this extension.

# A

# Calculations for ALMA

As defined in the main text, $\widetilde{g}_{ji}^{k} \in \{v_{ji,1}, ..., v_{ji,R}\}$ and the p.d.f. of $\widetilde{g}_{ji}$ is denoted by $\gamma_{ji}$ in general. Note that when $\widetilde{g}_{ji}$ belongs to a discrete set, we can replace the integrals and $\gamma_{ji}$ with a sum and discrete probability function without any significant alteration to our results and calculations. Denoting the p.d.f of $g_{ji}$ by $\phi_{ji}$, the distortion between $g_{ji}$ and $\widetilde{g}_{ji}^{k}$ can be written as

$$\mathbb{E}[\left(g_{ji} - \widetilde{g}_{ji}^{k}\right)^2] = \sum_{r=1}^{R} \int\limits_{x,\widetilde{x}\in\mathbb{R}_{\geq 0}} \Pr\left(\widetilde{g}_{ji}^{k} = v_{ji,r} | \widetilde{g}_{ji} = \widetilde{x}\right) \gamma_{ji}\left(\widetilde{x}|x\right) \phi_{ji}\left(x\right) \left(x - v_{ji,r}\right)^2 \mathrm{d}x\mathrm{d}\widetilde{x} \tag{A.1}$$

which is the distortion observed by transmitter $k$ when transmitter $i$ communicates $g_{ji}$ in Phase II. As the transmitter $i$ estimates $g_{ji}$ as $\widetilde{g}_{ji}$, the quantization operation $Q_i^{\mathrm{II}}$ is performed resulting in $\widetilde{g}_{ji}$ being quantized into a certain representative $v_{ji,n}$, if $\widetilde{g}_{ji} \in [u_{ji,n}, u_{ji,n+1})$. Given that the transmitter $i$ operates at a power level corresponding to $v_{ji,n}$, the transmitter $k$ will decode $v_{ji,r}$ with a probability $\pi(r|n)$ as defined in Section IV. Now we can expand the term $\Pr\left(\widetilde{g}_{ji}^{k} = v_{ji,r} | \widetilde{g}_{ji} = \widetilde{x}\right)$ in the following manner.

$$\begin{aligned}\Pr\left(\widetilde{g}_{ji}^{k} = v_{ji,r} | \widetilde{g}_{ji} = \widetilde{x}\right) &= \sum_{n=1}^{R} \Pr\left(\widetilde{g}_{ji}^{k} = v_{ji,r} | Q_i^{\mathrm{II}}(\widetilde{g}_{ji}) = v_{ji,n}\right) \Pr\left(Q_i^{\mathrm{II}}(\widetilde{g}_{ji}) = v_{ji,n} | \widetilde{g}_{ji} = \widetilde{x}\right) \\ &= \sum_{n=1}^{R} \pi(r|n) \Pr\left(Q_i^{\mathrm{II}}(\widetilde{g}_{ji}) = v_{ji,n} | \widetilde{g}_{ji} = \widetilde{x}\right)\end{aligned} \tag{A.2}$$

where we know

$$\Pr\left(Q_i^{\mathrm{II}}(\widetilde{g}_{ji}) = v_{ji,n} | \widetilde{g}_{ji} = \widetilde{x}\right) = \begin{cases} 1 & \text{if } \widetilde{x} \in [u_{ji,n}, u_{ji,n+1}) \\ 0 & \text{if } \widetilde{x} \notin [u_{ji,n}, u_{ji,n+1}) \end{cases} \tag{A.3}$$

Substituting (A.3) and (A.2) in (A.1), we get

$$\mathbb{E}[\left(g_{ji}-\widetilde{g}_{ji}^{k}\right)^{2}]=\sum_{n=1}^{R}\sum_{r=1}^{R}\pi_{ji}\left(r|n\right)\int_{x=0}^{\infty}\int_{\widetilde{x}=u_{ji,n}}^{u_{ji,n+1}}\gamma_{ji}\left(\widetilde{x}|x\right)\phi_{ji}\left(x\right)\left(x-v_{ji,r}\right)^{2}\mathrm{d}x\mathrm{d}\widetilde{x}. \tag{A.4}$$

For fixed transition levels $u_{ji,n}$, the optimum representatives $v_{ji,r'}$ are obtained by setting the partial derivatives of the distortion $E[\left(g_{ji}-\widetilde{g}_{ji}^{k}\right)^{2}]$, with respect to $v_{ji,r'}$, to zero. That is

$$\frac{\partial\mathbb{E}[\left(g_{ji}-\widetilde{g}_{ji}^{k}\right)^{2}]}{\partial v_{ji,r'}}=\sum_{n=1}^{R}\pi_{ji}\left(r'|n\right)\int_{x=0}^{\infty}\int_{\widetilde{x}=u_{ji,n}}^{u_{ji,n+1}}2\gamma_{ji}(\widetilde{x}|x)\phi_{ji}(x)\left(x-v_{ji,r'}\right)\mathrm{d}x\mathrm{d}\widetilde{x}=0$$

which results in

$$v_{ji,r'}=\frac{\sum_{n=1}^{R}\pi_{ji}\left(r'|n\right)\int_{x=0}^{\infty}\int_{\widetilde{x}=u_{ji,n}}^{u_{ji,n+1}}x\gamma_{ji}(\widetilde{x}|x)\phi_{ji}(x)\mathrm{d}\widetilde{x}\mathrm{d}x}{\sum_{n=1}^{R}\pi_{ji}\left(r'|n\right)\int_{x=0}^{\infty}\int_{\widetilde{x}=u_{ji,n}}^{u_{ji,n+1}}\gamma_{ji}(\widetilde{x}|x)\phi_{ji}(x)\mathrm{d}\widetilde{x}\mathrm{d}x}. \tag{A.5}$$

For fixed representatives $v_{ji,r}$, the optimum transition levels $u_{ji,n'}$ are obtained by setting the partial derivatives of the distortion $E[\left(g_{ji}-\widetilde{g}_{ji}^{k}\right)^{2}]$ with respect to $u_{ji,n'}$, to zero. We use the second fundamental theorem of calculus, i.e., $\frac{\mathrm{d}}{\mathrm{d}x}\int_{a}^{x}f(t)\mathrm{d}t=f(x)$ to obtain $u_{ji,n'}$ for all $n'\in\{2,..,R\}$ as

$$\frac{\partial\mathbb{E}[\left(g_{ji}-\widetilde{g}_{ji}^{k}\right)^{2}]}{\partial u_{ji,n'}}=\sum_{r=1}^{R}(\pi_{ji}\left(r|n'-1\right)-\pi_{ji}\left(r|n'\right))\int_{0}^{\infty}\gamma_{ji}(u_{ji,n'}|x)\phi_{ji}(x)\left(v_{ji,r}-x\right)^{2}\mathrm{d}x=0 \tag{A.6}$$

with $u_{ji,1}=0$ and $u_{ji,R+1}=\infty$ as the boundary conditions. Solving the above conditions is very difficult as the variable to solve is inside the integral as an argument of $\gamma$. Therefore we consider the special case where $\gamma_{ji}(\widehat{x}|x)=\delta(x-\widehat{x})$ where $\delta$ is the Dirac delta function which is 0 at all points except at 0 and whose integral around a neighborhood of 0 is 1. This corresponds to the case where the channel is perfectly estimated after phase I. This directly transforms (A.5) to (3.20) of the ALMA, and we can simplify (A.6) into

$$0=\sum_{r=1}^{R}\left[\pi_{ji}\left(r|n'-1\right)-\pi_{ji}\left(r|n'\right)\right]\phi_{ji}(u_{ij,n'})\left(v_{ji,r}-u_{ij,n'}\right)^{2} \tag{A.7}$$

We have $\sum_{r=1}^{R}\left[\pi_{ji}\left(r|n'-1\right)-\pi_{ji}\left(r|n'\right)\right]\left(u_{ij,n'}\right)^{2}=0$ since $\sum_{r=1}^{R}\pi_{ji}\left(r|n'\right)=1$, resulting in

$$u_{ij,n'}=\frac{\sum_{r=1}^{R}\left[\pi_{ji}\left(r|n'-1\right)-\pi_{ji}\left(r|n'\right)\right]v_{ji,r}^{2}}{2\sum_{r=1}^{R}\left[\pi_{ji}\left(r|n'-1\right)-\pi_{ji}\left(r|n'\right)\right]v_{ji,r}} \tag{A.8}$$

which is (3.21) used in the ALMA. ■

# B

# Proof of Theorem 3.3.2

The proof is based on the following lemma ([51][52]).

*Support Lemma.* Let $\mathcal{X}$ be a finite set and $V$ be an arbitrary set. Let $\mathcal{P}$ be a connected compact subset of pmfs on $\mathcal{X}$ and $p(x|v) \in \mathcal{P}$, indexed by $v \in \mathcal{V}$, be a collection of (conditional) pmfs on $\mathcal{X}$. Suppose that $g_j(\pi)$, $j = 1, ..., d$, are real-valued continuous functions of $\pi \in \mathcal{P}$. Then for every $V \sim F(v)$ defined on $\mathcal{V}$, there exists a random variable $V' \sim p(v')$ with $|\mathcal{V}'| \leq d$ and a collection of conditional pmts $p(x|v') \in \mathcal{P}$, indexed by $v' \in \mathcal{V}'$, such that for $j = 1, ..., d$,

$$\int_{\mathcal{V}} g_j(p(x|v))dF(v) = \sum_{v' \in \mathcal{V}'} g_j(p(x|v'))p(v') \tag{B.1}$$

We now show how this lemma is used to bound the cardinality of auxiliary random variables. Suppose $\mathcal{X} = \mathcal{A} \cdot \mathcal{S}$, which refers to the joint action and joint state (observation) profiles. The corresponding $\mathcal{P}$ will be a connected compact subset of pmfs on $\mathcal{A} \cdot \mathcal{S}$ and $p(p_1, ..., p_K, s_1, ..., s_K|v) \in \mathcal{P}$, indexed by $v \in \mathcal{V}$, be a collection of (conditional) pmfs on $\mathcal{A} \cdot \mathcal{S}$. Note that $\prod_{i=1}^{K} P_{A_i|S_i,V}(p_i|s_i, v)$ is a special case of the general probability $P_{A_1,...,A_K|S_1,...,S_K,V}(p_1, ..., p_K|s_1, ..., s_K, v)$ (when the general probability is separable, we get the product of individual probability) and the probability can be rewritten as :

$$\begin{aligned} &P_{A_1,...,A_K|S_1,...,S_K,V}(p_1, ..., p_K|s_1, ..., s_K, v) \\ =&\frac{P_{A_1,...,A_K,S_1,...,S_K|V}(p_1, ..., p_K, s_1, ..., s_K|v)}{P_{S_1,...,S_K|V}(s_1, ..., s_K|v)} \end{aligned} \tag{B.2}$$

Hence, $\prod_{i=1}^{K} P_{A_i|S_i,V}(p_i|s_i,v)$ can be expressed by $\pi \in \mathcal{P}$. Denoting $j_q$ as the quotient of $j$ over $K$, consider the following $|\mathcal{A}|-1$ continuous functions on $\mathcal{P}$ :

$$g_j(\pi) = \frac{\pi(j)}{\sum_{i=j_q+1}^{i=j_q+K} \pi(i)} \qquad j = 1, ..., |\mathcal{A}| \cdot |\mathcal{S}| - 1 \tag{B.3}$$

Clearly, these $|\mathcal{A}| \cdot |\mathcal{S}| - 1$ functions are continuous. According to the support lemma, for every $V \sim F(v)$ defined on $\mathcal{V}$, for the distribution $Q(a)$, there exist a $V \sim F(v)$ with $|\mathcal{V}| \leq |\mathcal{A}| \cdot |\mathcal{S}| - 1$ such that

$$\begin{aligned} Q(a) &= \rho_0(a_0) \sum_{s,v} \Gamma(s|a_0) P_V(v) \prod_{i=1}^{K} P_{A_i|S_i,V}(p_i|s_i,v) \\ &= \rho_0(a_0) \sum_{s,v'} \Gamma(s|a_0) P'_V(v') \prod_{i=1}^{K} P_{A_i|S_i,V'}(p_i|s_i,v') \end{aligned} \tag{B.4}$$

# C

# Proof of Proposition 4.2.1

Define the conditional p.d.f. of $r_{j,m+1}$ knowing $\mathbf{r}_j^{(m)}$ as $f(r_{j,m+1}|\mathbf{r}_j^{(m)})$, the distortion with $m+1$ feedbacks can be rewritten as :

$$\begin{aligned}
&\Delta^*_{j;m+1}\\
=&\mathbb{E}_{\mathbf{r}_j^{(m+1)}}[\mathrm{D}_j^*(\mathbf{r}_j^{(m+1)})]\\
=&\mathbb{E}_{\mathbf{r}_j^{(m)}}[\int_{r_{j,m+1}} f(r_{j,m+1}|\mathbf{r}_j^{(m)})\mathrm{D}_j^*(\mathbf{r}_j^{(m+1)})\mathrm{d}r_{j,m+1}]\\
=&\sum_{k=1}^{K}\mathbb{E}_{\mathbf{r}_j^{(m)}}[\int_{r_{j,m+1}} \frac{f(r_{j,m+1}|\mathbf{r}_j^{(m)})}{\frac{\beta P}{N_0}+\frac{1}{\mathbb{E}_{|\mathbf{R}_j^{(m+1)}=\mathbf{r}_j^{(m+1)}}[|h_{kj}|^2]}}\mathrm{d}r_{j,m+1}]
\end{aligned} \tag{C.1}$$

Denote the p.d.f. of $\mathbf{R}_j^{(m+1)}=\mathbf{r}_j^{(m+1)}$ as $f_{m+1}(\mathbf{r}_j^{(m+1)})$ and the p.d.f. of $\mathbf{R}_j^{(m)}=\mathbf{r}_j^{(m)}$ as $f_m(\mathbf{r}_j^{(m)})$, then it can be checked that

$$\frac{f(r_{j,m+1}|\mathbf{r}_j^{(m)})}{f_{m+1}(\mathbf{r}_j^{(m+1)})}=\frac{1}{f_m(\mathbf{r}_j^{(m)})} \tag{C.2}$$

Assume the p.d.f. of $\mathbf{h}_j$ is $\phi_j(\mathbf{h}_j)$, note that for every $k \in \{1, \ldots, K\}$, we have

$$\begin{aligned}
&\int_{r_{j,m+1}} f(r_{j,m+1}|\mathbf{r}_j^{(m)})\mathbb{E}_{|\mathbf{R}_j^{(m+1)}=\mathbf{r}_j^{(m+1)}}[|h_{kj}|^2]\mathrm{d}r_{j,m+1} \\
=&\int_{r_{j,m+1}} \frac{f(r_{j,m+1}|\mathbf{r}_j^{(m)}) \int_{\mathbf{R}_j^{(m+1)}=\mathbf{r}_j^{(m+1)}} |h_{kj}|^2\phi_j(\mathbf{h}_j)\mathrm{d}\mathbf{h}_j}{f_{m+1}(\mathbf{r}_j^{(m+1)})}\mathrm{d}r_{j,m+1} \\
=&\frac{\int_{r_{j,m+1}} \int_{\mathbf{R}_j^{(m+1)}=\mathbf{r}_j^{(m+1)}} |h_{kj}|^2\phi_j(\mathbf{h}_j)\mathrm{d}\mathbf{h}_j\mathrm{d}r_{j,m+1}}{f_m(\mathbf{r}_j^{(m)})} \\
=&\frac{\int_{\mathbf{R}_j^{(m)}=\mathbf{r}_j^{(m)}} |h_{kj}|^2\phi_j(\mathbf{h}_j)\mathrm{d}\mathbf{h}_j}{f_m(\mathbf{r}_j^{(m)})} \\
=&\mathbb{E}_{|\mathbf{R}_j^{(m)}=\mathbf{r}_j^{(m)}}[|h_{kj}|^2]
\end{aligned} \tag{C.3}$$

Additionally, it can be checked from (5.52) that $\mathrm{D}_j(\mathbf{r}_j^{(m+1)})$ is a concave function with respect to $\mathbb{E}_{|\mathbf{R}_j^{(m+1)}=\mathbf{r}_j^{(m+1)}}[|h_{kj}|^2]$. According to (C.3) and the concavity, it can be obtained that :

$$\begin{aligned}
&\int_{r_{j,m+1}} \frac{f(r_{j,m+1}|\mathbf{r}_j^{(m)})N_0\mathbb{E}_{|\mathbf{R}_j^{(m+1)}=\mathbf{r}_j^{(m+1)}}[|h_{kj}|^2]}{\beta P\mathbb{E}_{|\mathbf{R}_j^{(m+1)}=\mathbf{r}_j^{(m+1)}}[|h_{kj}|^2]+N_0}\mathrm{d}r_{j,m+1} \\
\leq&\frac{N_0\mathbb{E}_{|\mathbf{R}_j^{(m)}=\mathbf{r}_j^{(m)}}[|h_{kj}|^2]}{\beta P\mathbb{E}_{|\mathbf{R}_j^{(m)}=\mathbf{r}_j^{(m)}}[|h_{kj}|^2]+N_0}
\end{aligned} \tag{C.4}$$

which yields

$$\begin{aligned}
&\Delta_{j;m+1}^* \\
\leq&\sum_{k=1}^{K} \mathbb{E}_{\mathbf{r}_j^{(m)}}[\frac{N_0\mathbb{E}_{|\mathbf{R}_j^{(m)}=\mathbf{r}_j^{(m)}}[|h_{kj}|^2]}{\beta P\mathbb{E}_{|\mathbf{R}_j^{(m)}=\mathbf{r}_j^{(m)}}[|h_{kj}|^2]+N_0}] \\
=&\Delta_{j;m}^*
\end{aligned} \tag{C.5}$$

$\Delta_m^*$ will decrease when more useful prior information is acquired. Hence, when all the channel gains can be obtained from the feedback, the distortion will be minimized. According to (5.52), by knowing all the channel gain, the distortion of the MMSE estimator can be expressed as $\sum_{k=1}^{K} \mathbb{E}_{h_{kj}}\left[\frac{N_0|h_{kj}|^2}{\beta P|h_{kj}|^2+N_0}\right]$, which is therefore the lower bound on $\Delta_{j;m}^*$.

# D

# Proof of Proposition 5.1.2

For a given quantization region $\mathcal{C}_m$, the gradient of $\mathbb{E}_g(\|V(\widehat{g}) - V(g)\|^2)$ with respect to $r_m$ can be written as :

$$\begin{aligned}
&\nabla \mathbb{E}_g(\|V(\widehat{g}) - V(g)\|^2) \\
=&\frac{\partial \mathbb{E}_g(\|V(\widehat{g}) - V(g)\|^2)}{\partial r_m} \\
=&\int_{\mathcal{C}_m} \phi(g) \frac{\partial \|V(r_m) - V(g)\|^2}{\partial r_m} \mathrm{d}g \\
=&\int_{\mathcal{C}_m} \phi(g) J_V(r_m) \frac{\partial \|V(r_m) - V(g)\|^2}{\partial V(r_m)} \mathrm{d}g \\
=&\int_{\mathcal{C}_m} 2\phi(g) J_V(r_m) [V(r_m) - V(g)] \mathrm{d}g
\end{aligned} \tag{D.1}$$

where $J_V$ is the Jacobian matrix of $V$ evaluated at $r_m$, i.e.,

$$J_V(r_m) = \begin{bmatrix} \frac{\partial u_1}{g_1}(r_m) & \dots & \frac{\partial u_1}{g_K}(r_m) \\ \vdots & \vdots & \vdots \\ \frac{\partial u_K}{g_1}(r_m) & \dots & \frac{\partial u_K}{g_K}(r_m) \end{bmatrix}. \tag{D.2}$$

At the local minimum, we must have the gradient of $\mathbb{E}_g(\|V(\widehat{g}) - V(g)\|^2)$, become zero. Since, we assume that $V(\cdot)$ is invertible in $\mathcal{C}_m$, we can use the inverse function theorem to conclude that $J_V(r_m)$ is invertible at all points in $\mathcal{C}_m$. As a result, we have

$$\int_{\mathcal{C}_m} \phi(g)[V(r_m) - V(g)]\mathrm{d}g = 0. \tag{D.3}$$

Hence, the optimum representatives can be obtained as

$$V(r_m) = \frac{\displaystyle\int_{\mathcal{C}_m} \phi(g) V(g) \mathrm{d}g}{\displaystyle\int_{\mathcal{C}_m} \phi(g) \mathrm{d}g} \tag{D.4}$$

which is equivalent to

$$u_k(r_m) = \frac{\int_{\mathcal{C}_m} \phi(g) u_k(g) \mathrm{d}g}{\int_{\mathcal{C}_m} \phi(g) \mathrm{d}g} \tag{D.5}$$

which must hold for all $k = 1, 2, ..., K$. Taking the sum of (D.5) with respect to $k$, we have

$$\sum_{k=1}^{K} u_k(r_m) = \frac{\sum_{k=1}^{K} \int_{\mathcal{C}_m} \phi(g) u_k(g) \mathrm{d}g}{\int_{\mathcal{C}_m} \phi(g) \mathrm{d}g} \tag{D.6}$$

Knowing $F(g) = \sum_{k=1}^{K} u_k(g)$, the optimum representatives to minimize $\mathbb{E}_g(\|V(\widehat{g}) - V(g)\|^2)$ satisfy the following condition

$$F(r_m) = \frac{\int_{\mathcal{C}_m} \phi(g) F(g) \mathrm{d}g}{\int_{\mathcal{C}_m} \phi(g) \mathrm{d}g} \tag{D.7}$$

which is the expression to minimize the payoff gap $\mathbb{E}_g(\|F(\widehat{g}) - F(g)\|^2)$. This implies that minimizing the quantity $\mathbb{E}_g(\|V(\widehat{g}) - V(g)\|^2)$ implies minimizing $\mathbb{E}_g(\|F(\widehat{g}) - F(g)\|^2)$, which concludes our proof.

# Bibliographie


[1] J. Hoydis, M. Kobayashi, and M. Debbah, "Green Small-Cell Networks," *IEEE Vehicular Technology Magazine*, vol. 6, no. 1, pp. 37–43, Mar. 2011.

[2] M. Chiang, "Geometric programming for communication systems", Short monograph in Foundations and Trends in Communications and Information Theory, vol. 2, no. 1-2, pp. 1-154, Aug. 2005.

[3] F. Meshkati, M. Chiang, H. V. Poor and S. C. Schwartz. "A game-theoretic approach to energy-efficient power control in multicarrier CDMA systems". *IEEE Journal on Selected Areas in Communications*, 24(6) :1115–1129, Jun. 2006.

[4] R. Radner, "Team decision problems", The Annals of Mathematical Statistics, 1962.

[5] P. Cuff, H. H. Permuter, and T. M. Cover, "Coordination capacity", *IEEE Trans. on Information Theory*, vol. 56, no. 9, pp. 4181-4206, 2010.

[6] W. Yu, G. Ginis,and J. M. Cioffi, "Distributed multiuser power control for digital subscriber lines", IEEE J. Sel. Areas Commun., Vol. 20, No. 5,pp. 1105–1115, June 2002.

[7] P. Mertikopoulos, E. V. Belmega, A. Moustakas, and S. Lasaulce, "Distributed Learning Policies for Power Allocation in Multiple Access Channels", IEEE Journal of Selected Areas in Communications (JSAC), Vol. 30, No. 1, pp. 96–106, Jan. 2012.

[8] B. Larrousse, S. Lasaulce, and M. Wigger, "Coordination in State-Dependent Distributed Networks", IEEE Proc. of the Information Theory Workshop (ITW), Jerusalem, Israel, Apr.-May 2015,

[9] S. Medina Perlaza, N. Fawaz, S. Lasaulce, and M. Debbah, "From Spectrum Pooling to Space Pooling : Opportunistic Interference Alignment in MIMO Cognitive Networks", IEEE Trans. On Signal Processing, Vol. 58, No. 7, pp. 3728–3741 Jul. 2010.

[10] V. H. Poor, An introduction to signal detection and estimation. Springer Science and Business Media, 2013.

[11] G. Caire, N. Jindal, , M. Kobayashi, and N. Ravindran, "Multiuser MIMO achievable rates with downlink training and channel state feedback", IEEE Transactions on Information Theory, 56(6), pp.2845-2866, 2010.

[12] S. Lloyd, "Least squares quantization in PCM", IEEE transactions on information theory, 28(2), 129-137,1982.

[13] J. Max, "Quantizing for minimum distortion." IRE Transactions on Information Theory, 6(1), 7-12, 1960.

[14] V. S. Varma, S. Lasaulce, C. Zhang and R. Visoz. "Power modulation : Application to inter-cell interference coordination," in *IEEE EUSIPCO*, Sep. 2015.

[15] G. Scutari, D. P. Palomar and S. Barbarossa. "The MIMO iterative waterfilling algorithm," *IEEE Trans. Signal Process.*, 57(5) :1917–1935, May 2009.

[16] L. Rose, S. Lasaulce, S. M. Perlaza and M. Debbah. "Learning equilibria with partial information in decentralized wireless networks," *IEEE Commun. Mag.*, 49(8) :136–142, Aug. 2011.

[17] S. Lasaulce and H. Tembine. *Game Theory and Learning for Wireless Networks : Fundamentals and Applications*. Academic Press, Waltham, MA, 2011.

[18] S. Stańczak, M. Wiczanowski and H. Boche. "Distributed utility-based power control : Objectives and algorithms." *IEEE Trans. Signal Process.*, 55(10) :5058–5068, Oct. 2007.

[19] J. Schreck, P. Jung and S. Stańczak. "Compressive rate estimation with applications to device-to-device communications," *arXiv preprint arXiv :1504.07365*, 2015.

[20] B. Larrousse and S. Lasaulce. "Coded power control : Performance analysis," in *Proc. IEEE Int. Symp. Information Theory*, Jul. 2013, pp. 3040–3044.

[21] B. Larrousse, S. Lasaulce and M. Bloch. "Coordination in distributed networks via coded actions with application to power control," *arXiv preprint arXiv :1501.03685*, 2015.

[22] A. J. G. Anandkumar, A. Anandkumar, S. Lambotharan and J. A. Chambers. "Robust rate maximization game under bounded channel uncertainty," *IEEE Trans. Vehicular Tech.*, 60(9) :4471–4486, Nov. 2011.

[23] P. Coucheney, B. Gaujal and P. Mertikopoulos. "Distributed optimization in multi-user MIMO systems with imperfect and delayed information," in *Proc. IEEE Int. Symp. Information Theory*, Jun. 2014.

[24] S. Sesia, I. Toufik and M. Baker. *LTE, The UMTS Long Term Evolution : From Theory to Practice*. Wiley Publishing, 2009.

[25] S. Lasaulce, V. S. Varma and R. Visoz. "Technique de coordination d'émetteurs radio fondé sur le codage des niveaux de puissance d'émission," *Patent NO : 1361885*, Nov. 2013.

[26] S. Lasaulce, P. Loubaton, E. Moulines and S. Buljore. "Training-based channel estimation and de-noising for the UMTS TDD mode," in *IEEE Vehicular Tech. Conf.*, Oct. 2001, pp. 1908-1911.

[27] M. A. Maddah-Ali, A. S. Motahari, and A. K. Khandani, "Communication Over MIMO X Channels : Interference Alignment, Decomposition, and Performance Analysis", IEEE Trans. on Info. Theory, 54(8) :3457-3470.

[28] S. Lasaulce, P. Loubaton, E. Moulines, and S. Buljore, "Training-based channel estimation and de-noising for the UMTS-TDD mode", IEEE Proc. of the Vehicular Technology Conference (VTC), Vol. 3, pp. 1908–1911, Atlantic City, USA, Oct. 2001.

[76] B. Djeumou, S. Lasaulce and A. G. Klein. "Practical quantize-and-forward schemes for the frequency division relay channel," *EURASIP Journal on Wireless Communications and Networking*, 2007 :2, Oct. 2007.

[30] O. Beaude, B. Larrousse and S. Lasaulce. "Crawford-Sobel meet Lloyd-Max on the grid," In *IEEE International Conference on Acoustics, Speech and Signal Processing*, Florence, Italy, May 2014, pp. 6127-6131.

[31] P. De Kerret and D. Gesbert, "Degrees of freedom of the network MIMO channel with distributed CSI," *IEEE Trans. on Information Theory*, vol. 58, no. 12, pp. 6806–6824, 2012.

[32] S. Samarakoon, M. Bennis, W. Saad, M. Debbah and M. Latva-aho. "Ultra dense small cell networks : Turning density into energy efficiency," *arXiv preprint arXiv :1603.03682*, 2016.

[33] A. L. Moustakas and N. Bambos. "Power optimization on a random wireless network," in *Proc. IEEE Int. Symp. Information Theory*, Jul. 2013, pp. 844–848.

[34] A. L. Moustakas, P. Mertikopoulos and N. Bambos. "Power optimization in random wireless networks," *arXiv preprint arXiv :1202.6348*, 2015.

[35] E. V. Belmega and S. Lasaulce. "Energy-efficient precoding for multiple-antenna terminals," *IEEE Trans. Signal Process.*, 59(1) :329–340, Jan. 2011.

[36] S. Buzzi, G. Colavolpe, D. Saturnino and A. Zappone. "Potential games for energy-efficient power control and subcarrier allocation in uplink multicell OFDMA systems," *IEEE J. Sel. Topics in Signal Process.*, 6(2) :89–103, Apr. 2012.

[37] G. Bacci, L. Sanguinetti, M. Luise and H. V. Poor. "A game-theoretic approach for energy-efficient contention-based synchronization in OFDMA systems," *IEEE Trans. Signal Process.*, 61(5) :1258–1271, Mar. 2013.

[38] M. Haddad, O. Habachi, P. Wiecek and Y. Hayel. "Spectral efficiency of energy efficient multicarrier systems," *ACM SIGMETRICS Performance Evaluation Review*, 42(2) :24–26, Sep. 2014.

[39] B. Matthiesen, A. Zappone and E. A. Jorswieck. "Resource allocation for energy-efficient 3-way relay channels," IEEE Trans. Wireless Commun., 14(8) :4454–4468, Aug. 2015.

[40] G. Bacci, E. V. Belmega, P. Mertikopoulos and L. Sanguinetti. "Energy-Aware Competitive Power Allocation in Heterogeneous Networks with QoS constraints," IEEE Trans. Wireless Commun., 14(9) :4728–4742, Sep. 2015.

[41] A. Gjendemsjø, D. Gesbert, G. E. Øien, and S. G. Kiani, "Binary power control for sum rate maximization over multiple interfering links", IEEE Transactions on Wireless Communications, no. 7, Aug. 2008.

[42] M. Bennis, M. Simsek, A. Czylwik, W. Saad, S. Valentin, and M. Debbah, (2013). "When cellular meets WiFi in wireless small cell networks", IEEE communications magazine, 51(6), 44-50, 2013.

[43] H. Zhang, C, Jiang, N. C. Beaulieu, X. Chu, X. Wang, and T. Q. Quek, "Resource allocation for cognitive small cell networks : A cooperative bargaining game theoretic approach", IEEE Transactions on Wireless Communications, 14(6), 3481-3493, 2015.

[44] D. Goodman, and N. Mandayam, "Power control for wireless data", IEEE Personal Communications, 7(2), 48-54, 2000.

[45] A. Papadogiannis, E. Hardouin, and D. Gesbert, "Decentralising multicell cooperative processing : A novel robust framework", EURASIP Journal on Wireless Communications and Networking, no.1, 2009.

[46] T. M. Cover, and J. A. Thomas, Elements of information theory, John Wiley and Sons, 2012.

[47] P. De Kerret, S. Lasaulce, D. Gesbert, and U. Salim, "Best-response team power control for the interference channel with local CSI", IEEE International Conference on Communications (ICC), pp. 4132-4136, 2015.

[48] W. Yu, G. Ginnis and J. Cioffi, "Distributed multiuser power control for digital subscriber lines," *IEEE J. Sel. Areas Commun.*, vol. 20, no. 5, pp. 1105-1115, Jun. 2002.

[49] L. Rose, S. M. Perlaza, and M. Debbah, "On the Nash equilibria in decentralized parallel interference channels," *IEEE Intl. Conf. on Communications (ICC)*, pp. 1–6, Kyoto, Japan, Jun. 2011.

[50] S. M. Perlaza, S. Lasaulce, and M. Debbah, "Equilibria of channel selection games in parallel multiple access channels," *EURASIP J. on Wireless Commun. and Networking*, vol. 2013, no. 15, pp. 1–23, Jan. 2013.

[51] R. Ahlswede, and J. Korner, "Source coding with side information and a converse for degraded broadcast channels", IEEE Transactions on Information Theory, 21(6), 629-637, 1975.

[52] A. Wyner, and J. Ziv, "The rate-distortion function for source coding with side information at the decoder", IEEE Transactions on information Theory, 22(1), 1-10, 1976.

[53] P. De Kerret, and D. Gesbert, "Quantized Team Precoding : A robust approach for network MIMO under general CSI uncertainties", IEEE 17th International Workshop In Signal Processing Advances in Wireless Communications (SPAWC), 2016.

[54] J. W. Milnor, and D. Husemoller, Symmetric bilinear forms, (Vol. 60, p. 61). Berlin Heidelberg New York : Springer, 1973.

[55] E. Maskin, and J. Tirole, "A theory of dynamic oligopoly, II : Price competition, kinked demand curves, and Edgeworth cycles", Econometrica : Journal of the Econometric Society, 571-599, 1988.

[56] D. Monderer, and L. S. Shapley, Potential games. Games and economic behavior, 14(1), 124-143, 1996.

[57] C. Papadimitriou, "Algorithms, games, and the internet", Proceedings of the thirty-third annual ACM symposium on Theory of computing. ACM, 2001.

[58] R. Couillet, and M. Debbah, "Random matrix methods for wireless communications," Cambridge University Press, Sep. 2011.

[59] J. Dumont, W. Hachem, S. Lasaulce, P. Loubaton and J. Najim, "On the capacity achieving covariance matrix for Rician MIMO channels : an asymptotic approach," *IEEE Trans. Inf. Theory.*, vol. 56, no. 3, pp. 1048-1069, Mar. 2010

[60] N. Devroye, M. Vu, and V. Tarokh, "Cognitive radio networks", IEEE Signal Processing Magazine, 25(6), 2008.

[61] S. Haykin, "Cognitive radio : brain-empowered wireless communications", IEEE journal on selected areas in communications, 23(2), 201-220, 2005.

[62] M. A. Maddah-Ali, A. K. Khandani, and A. S. Motahari, "Communication over X channel : Signalling and multiplexing gain", Department of Electrical and Computer Engineering, University of Waterloo, 2006.

[63] V. Cadambe and S. Jafar, "Interference alignment and degrees of freedom of the $K$-user interference channel", IEEE Transactions on Information Theory, 54(8), 3425-3441, 2008.

[64] S. W. Peters and R. W. Heath, "Interference alignment via alternating minimization", IEEE International Conference on Acoustics, Speech and Signal Processing (ICASSP), 2009.

[65] E. A. Jorswieck, and H. Boche, "Channel capacity and capacity-range of beamforming in MIMO wireless systems under correlated fading with covariance feedback", IEEE Transactions on Wireless Communications, 3(5), 1543-1553, 2004.

[66] S. Vishwanath, and S. A. Jafar, "On the capacity of vector Gaussian interference channels". In IEEE Information Theory Workshop, pp. 365-369, 2004.

[67] X. Shang, B. Chen, and M. J. Gans, "On the achievable sum rate for MIMO interference channels", IEEE Transactions on Information Theory, 52(9), 4313-4320, 2006.

[68] E. Telatar, "Capacity of Multi ?antenna Gaussian Channels", Eur. Trans. Telecommunication, vol. 10, no. 6, pp. 585-596, Nov. 1999.

[69] Y. Li, "Simplified channel estimation for OFDM systems with multiple transmit antennas", IEEE Transactions on Wireless Communications, 1(1), 67-75, 2002.

[70] B. Muquet, M. De Courville, and P. Duhamel, "Subspace-based blind and semi-blind channel estimation for OFDM systems", IEEE Transactions on signal processing, 50(7), 1699-1712, 2002.

[71] C. Zhang, V. Varma, S. Lasaulce, and R. Visoz, "Interference coordination via power domain channel estimation", IEEE Transactions on Wireless Communications, Vol. 16, No. 10, Oct. 2017.

[72] M. Kontouris, R. De Francisco, D. Gesbert, D. Slock and T. Salzer, "Efficient metrics for scheduling in MIMO broadcast channels with limited feedback." 2007 IEEE International Conference on Acoustics, Speech and Signal Processing-ICASSP'07. Vol. 3. IEEE, 2007.

[73] S. Lloyd, "Least squares quantization in PCM." IEEE transactions on information theory, 28(2), 129-137, 1982.

[74] A. Kurtenbach and P. Wintz. "Quantizing for noisy channels." IEEE Transactions on Communication Technology, 17(2), 291-302, 1969.

[75] N. Farvardin, "A study of vector quantization for noisy channels." IEEE Transactions on Information Theory, 36(4), 799-809, 1990.

[76] B. Djeumou, S. Lasaulce and A. G. Klein. "Practical quantize-and-forward schemes for the frequency division relay channel," *EURASIP Journal on Wireless Communications and Networking*, 2007 :2, Oct. 2007.

[77] L. Wang, N. Piotto and D. Schonfeld. "Boosting quantization for L p norm distortion measure." 2012 IEEE Statistical Signal Processing Workshop (SSP), IEEE, 2012.

[78] C. R. Murthy and B. D. Rao. "A vector quantization based approach for equal gain transmission." IEEE Global Telecommunications Conference, 2005.

[79] J. G. Proakis, *Digital Communications*, 4th ed. New York : McGrawHill, Inc., 2001.

[80] A. D. Dabbagh and D. J. Love, "Multiple antenna MMSE based downlink precoding with quantized feedback or channel mismatch", IEEE Transactions on communications, 56(11), 2008.

[81] R. Bhagavatula and R. W. Heath, "Adaptive limited feedback for sum-rate maximizing beamforming in cooperative multicell systems", IEEE Transactions on Signal Processing, 59(2), 800-811, 2011.

[82] F. Ceragioli and C. De Persis. "Discontinuous stabilization of nonlinear systems : Quantized and switching controls." Systems and Control Letters, 56(7), 461-473, 2007.

[83] E. V. Belmega and S. Lasaulce, "Energy-efficient precoding for multiple-antenna terminals." IEEE. Transactions on Signal Processing, 59(1), 329-340, 2011.

[84] H. Farhangi, "The path of the smart grid", IEEE power and energy magazine, 8(1), 2010.

[85] S. M. Amin, and B. F. Wollenberg, "Toward a smart grid : power delivery for the 21st century", IEEE power and energy magazine, 3(5), 34-41, 2005.

[86] M. H. U. Ahmed, M. G. R. Alam, R. Kamal, C. S. Hong, and S. Lee, "Smart grid cooperative communication with smart relay", Journal of Communications and Networks, 14(6), 640-652, 2012.

[87] A. Brooks, E. Lu, D. Reicher, C. Spirakis, and B. Weihl, "Demand dispatch", IEEE Power and Energy Magazine, 8(3), 20-29, 2010.

[88] D. Niyato, L. Xiao, and P. Wang, "Machine-to-machine communications for home energy management system in smart grid", IEEE Communications Magazine, 49(4), 2011

[89] W. Wang, Y. Xu, and M. Khanna, "A survey on the communication architectures in smart grid", Computer Networks, 55(15), 3604-3629, 2011.

[90] V. P. Crawford, and J. Sobel, "Strategic information transmission", Econometrica : Journal of the Econometric Society, pp. 1431-1451, 2007.

[91] J. Sobel, Signaling games. Encyclopedia of Complexity and System Science, Springer, 2007. Chicago

[92] V. Kavitha, E. Altman, R. El-Azouzi, and R. Sundaresan, "Opportunistic scheduling in cellular systems in the presence of noncooperative mobiles", IEEE Transactions on Information Theory, 58(3), 1757-1773, 2012.

[93] P. Tulpule, V. Marano, and G. Rizzoni, "Effects of different PHEV control strategies on vehicle performance" In American Control Conference (ACC), 2009.

[94] IEC, Loading guide for Oil-Immersed Power Transformers, No. 60354, IEC, 2011. 12. 02.

[95] D. P. Bertsekas, Dynamic programming and optimal control, Vol. 1, no. 2. Belmont, MA : Athena scientific, 1995.

ÉCOLE DOCTORALE
Sciences et technologies de l'information et de la communication (STIC)

**Titre:** Caractérisation des performances limites des jeux non-coopératifs avec observation imparfaite. application à la téléphonie mobile 5G

**Mots clés:** allocation de ressource, théorie des jeux, optimization distribuée, communication sans fil, estimation

**Résumé** Une grande partie des résultats rapportés dans cette thèse est basée sur une observation qui n'a jamais été faite pour les communications sans fil et le contrôle de puissance en particulier: les niveaux de puissance d'émission et plus généralement les matrices de covariance peuvent être exploitées pour intégrer des informations de coordination. Les échantillons de rétroaction dépendants des interférences peuvent être exploités comme canal de communication. Premièrement, nous montrons que le fameux algorithme itératif de remplissage d'eau n'exploite pas suffisamment l'information disponible en termes d'utilité-somme. En effet, nous montrons que l'information globale d'état de canal peut être acquise à partir de la seule connaissance d'une rétroaction de type SINR. Une question naturelle se pose alors. Est-il possible de concevoir un algorithme de contrôle de puissance distribué qui exploite au mieux les informations disponibles? Pour répondre à cette question, nous dérivons la caractérisation de la région d'utilité pour le problème considéré et montrons comment exploiter cette caractérisation non seulement pour mesurer l'efficacité globale, mais aussi pour obtenir des fonctions de contrôle de puissance à un coup globalement efficaces.

Motivés par le succès de notre approche sur les réseaux d'interférences mono bande et multibande, nous nous sommes demandé si elle pourrait être exploitée pour les réseaux MIMO. Nous avons identifié au moins un scénario très pertinent. En effet, nous montrons que l'alignement d'interférence opportuniste peut être implémenté en supposant seulement une rétroaction de covariance d'interférence plus bruit à l'émetteur secondaire. Puis, dans le dernier chapitre, nous généralisons le problème de la quantification, la motivation étant donnée par certaines observations faites dans les chapitres précédents. Premièrement, nous supposons que le quantificateur et le déquantificateur sont conçus pour maximiser une fonction d'utilité générale au lieu de la fonction de distorsion classique. Deuxièmement, nous supposons que le quantificateur et le déquantificateur peuvent avoir des fonctions d'utilité différentes. Cela soulève des problèmes techniques non triviaux, notre revendication est de faire un premier pas dans la résolution d'eux.

**Université Paris-Saclay**
Espace Technologique / Immeuble Discovery
Route de l'Orme aux Merisiers RD 128 / 91190 Saint-Aubin, France

ÉCOLE DOCTORALE
Sciences et technologies de l'information et de la communication (STIC)

**Title:** Characterization of the limit performances of non cooperative games with imperfect observation: application to 5G

**Keywords:** Ressource allocation, game theory, distributed optimization, wireless communication, estimation

**Abstract :** A large part of the results reported in this thesis is based on an observation which has never been made for wireless communications and power control in particular: transmit power levels and more generally transmit covariance matrices can be exploited to embed information such as coordination information and available interference-dependent feedback samples can be exploited as a communication channel. First, we show that the famous iterative water-filling algorithm does not exploit the available information sufficiently well in terms of sum-utility. Indeed, we show that global channel state information can be acquired from the sole knowledge of an SINR-type feedback. A natural question then arises. Is it possible to design a distributed power control algorithm which exploits as well as possible the available information? To answer this question, we derive the characterization of the utility region for the considered problem and show how to exploit this characterization not only to measure globally efficiency but also to obtain globally efficient one-shot power control functions.

Motivated by the success of our approach for single-band and multi-band interference networks, we asked ourselves whether it could be exploited for MIMO networks. We have identified at least one very relevant scenario. Indeed, we show that opportunistic interference alignment can be implemented by only assuming interference-plus-noise covariance feedback at the secondary transmitter. Then, in the last chapter, we generalize the problem of quantization, the motivation for this being given by some observations made in the previous chapters. First, we assume that the quantizer and de-quantizer are designed to maximize a general utility function instead of the conventional distortion function. Second, we assume that the quantizer and de-quantizer may have different utility functions. This raises non-trivial technical problems, our claim is to make a very first step into solving them.

**Université Paris-Saclay**
Espace Technologique / Immeuble Discovery
Route de l'Orme aux Merisiers RD 128 / 91190 Saint-Aubin, France